OPPORTUNITIES TO IMPROVE AFTERTREATMENT THERMAL MANAGEMENT AND SIMPLIFY THE AIR HANDLING ARCHITECTURES OF HIGHLY EFFICIENT DIESEL ENGINES INCORPORATING VALVETRAIN FLEXIBILITY

A Dissertation

Submitted to the Faculty

of

Purdue University

by

Mrunal C. Joshi

In Partial Fulfillment of the

Requirements for the Degree

of

Doctor of Philosophy

May 2020

Purdue University

West Lafayette, Indiana

THE PURDUE UNIVERSITY GRADUATE SCHOOL
STATEMENT OF DISSERTATION APPROVAL

Dr. Gregory M. Shaver, Chair

School of Mechanical Engineering

Dr. Peter H. Meckl

School of Mechanical Engineering

Dr. Robert P. Lucht

School of Mechanical Engineering

Dr. John H. Lumkes Jr

School of Agricultural and Biological Engineering

Approved by:

Dr. Nicole Key

Head of the School Graduate Program

To my parents.

ACKNOWLEDGMENTS

Purdue has been like a second home to me. I would like to very sincerely thank Prof. Greg Shaver for giving me numerous opportunities to grow as an engineer and researcher. I can doubtlessly say that working with Dr. Shaver's group on the VVA has been the most enjoyable and professionally valuable experience. I attribute my academic progresses to the support and patience from Dr. Shaver. I am also thankful to our research collaborators at Cummins Inc. and Eaton for their technical guidance and for sponsoring the project.

I would like to acknowledge my research colleagues for teaching me invaluable lessons related to engine testing, course work, career and life. A few engine-heads need a special call out: Dheeraj Gosala, for being a great mentor/friend and an example of sheer brilliance, and for immensely helping me become a better engine researcher - I have learnt a lot working with such a hard-working and dedicated person; and Cody Allen, an extremely sharp engineer and a caring friend, thank you for great conversations that shaped many career decisions and helped me become a better person. I thank Kalen Vos, John Foster, Aswin Ramesh, Chisom Emegoakor, Alex Taylor, Soumya Nayyar, Matt VanVoorhis and Troy Odstricil for fun times dealing with VVA gremlins. I have immensely enjoyed working and learning with Sharon Zhang, Justin Rhines, Miles Droege, Brady Black, Shubham Ashta, Nishad Damle and Shveta Dhamankar. I thank Vaidehi Hoshing, a hard-working researcher, for also being a stead-fast friend and a source of inspiration.

I also thank the shop and administrative staff at Herrick Labs for helping me countless number of times without which progress would have been much more difficult. Thank you Donna and Cindy for being friendly and caring; thank you to David Meyer, Bob Brown, Frank Lee, Ryan Thayer and Ron Evans for making engine testing a smoother experience.

Thank you also to Eric Holloway for being a role model of time management and management of deliverables. I have learnt more from Eric than he realizes and I hope to carry those learnings with me throughout.

I thank Dr. James McCarthy, Jr. at Eaton for being instrumental in gaining valuable experiences in technical public speaking while being a source of critical career advice.

A big thank you to Matt Fox, Ashish Vora, Gerard Reynolds and others in the group at Tesla for making my internship an outright awesome experience and for giving me new perspectives.

Most importantly, I am eternally indebted to my parents for their immense support and love. I could not have reached here without their blessings. I sincerely thank Rashmi and Sai for their support.

I cannot express in words how grateful I am for this journey of learning and growing at Purdue.

TABLE OF CONTENTS

Page

LIST OF TABLES

LIST OF FIGURES

Figure Page

Figure Page

ABBREVIATIONS

ATS	Aftertreatment system
BSFC	Brake Specific Fuel Consumption
BTE	Brake Thermal Efficiency
CAC	Charge Air Cooler
CCE	Closed Cycle Efficiency
DOC	Diesel Oxidation Catalyst
DPF	Diesel Particulate Filter
ECM	Engine Control Module
EEVO	Early Exhaust Valve Opening
EFGT	Emulated Fixed Geometry Turbocharger Turbine
EGR	Exhaust Gas Recirculation
EOT	Engine Outlet Temperature
ETV	Exhaust Throttle Valve
FGT	Fixed Geometry Turbine Turbocharger
FMEP	Friction Mean Effective Pressure
GHG	Greenhouse Gas
GIMEP	Gross Indicated Mean Effective Pressure
GSI	Generic Serial Interface
iEGR	Internal EGR
LIVC	Late Intake Valve Closing
LEVO	Late Exhaust Valve Opening
LFE	Laminar Flow Element
LVDT	Linear Variable Differential Transformer
ME	Mechanical Efficiency

NIMEP	Net Indicated Mean Effective Pressure
NOx	Oxides of Nitrogen
NVO	Negative Valve Overlap
OCE	Open Cycle Efficiency
PM	Particulate Matter
PMEP	Pumping Mean Effective Pressure
SCR	Selective Catalytic Reduction
TOT	Turbine Outlet Temperature
UHC	Unburnt Hydrocarbons
VGT	Variable Geometry Turbine Turbocharger
VVA	Variable Valve Actuation

NOMENCLATURE

2CF	Two cylinders firing operation
3CF	Three cylinders firing operation
Stay-warm phase	Engine operation with the objective to maintain desired elevated ATS temperature
Warm-up phase	Engine operation with the objective to heat a cold ATS up to desired temperature

ABSTRACT

Joshi, Mrunal C. Ph.D., Purdue University, May 2020. Opportunities to Improve Aftertreatment Thermal Management and Simplify the Air Handling Architectures of Highly Efficient Diesel Engines Incorporating Valvetrain Flexibility. Major Professor: Dr. Gregory M Shaver.

In an effort to reduce harmful pollutants emitted by medium and heavy duty diesel engines, stringent emission regulations have been imposed by the Environmental Protection Agency (EPA) and the California Air Resources Board (CARB). Effective aftertreatment thermal management is critical for controlling tail pipe out levels of NOx and soot, while improved fuel efficiency is also necessary to meet greenhouse gas emissions standards and customer expectations. Engine manufacturers have developed and implemented several engine and non-engine based techniques for emission reduction, a few examples being: exhaust gas recirculation (EGR), use of delayed in-cylinder injections, exhaust throttling, electric heaters and hydrocarbon dosers. This work elaborates the use of variable valve actuation strategies for improved aftertreatment system (ATS) thermal management of a modern medium-duty diesel engine while presenting opportunities for simplification of engine air handling architecture.

Experimental results at curb idle demonstrate that exhaust valve profile modulation enables effective ATS warm-up without requiring exhaust manifold pressure (EMP) control. Early exhaust valve opening with internal exhaust gas recirculation (EEVO+iEGR) resulted in 8% lower fuel consumption and reduction in engine out emissions. Late exhaust valve opening with internal EGR in the absence of EMP control was able to reach exhaust temperature of 287°C, without a penalty in fuel consumption or emissions compared to conventional thermal management. LEVO

combined with EMP control could reach turbine outlet temperature of nearly 460°C at curb idle.

LEVO was studied at higher speeds and loads to assess thermal management benefits of LEVO in the absence of EMP control, with an observation that LEVO can maintain desirable thermal management performance up to certain speed/load conditions, and reduction in exhaust flow rate is observed at higher loads due to the inability of LEVO to compensate for loss of boost associated with absence of EMP control.

Cylinder deactivation (CDA) combined with additional valvetrain flexibility results in low emission, fuel-efficient solutions to maintain temperatures of a warmed-up ATS. Late intake valve closing, internal EGR and early exhaust valve opening were studied with both three cylinder and two cylinder operation. Some of these strategies showed additional benefits such as ability to use earlier injections, elimination of external EGR and operation in the absence of exhaust manifold pressure control. Three cylinder operation with LIVC and iEGR is capable of reaching exhaust temperatures in excess of 230°C with atleast 9% lower fuel consumption than three cylinder operation without VVA. Three cylinder operation with early exhaust valve opening resulted in exhaust temperature of nearly 340°C, suitable for extended idling operation. Two cylinder operation with and without the use of valve train flexibility also resulted in turbine outlet temperature relevant for extended idling (and low load operation), while reducing fuel consumption by 40% compared to the conventional thermal management strategy.

A study comparing the relative merits of internal EGR via reinduction and negative valve overlap (NVO) is presented in order to assess trade-offs between fuel efficient stay-warm operation and engine out emissions. This study develops an understanding of the optimal valve profiles for achieving reinduction/NVO and presents VVA strategies that are not cylinder deactivation based for fuel efficient stay-warm operation. Internal EGR via reinduction is demonstrated to be a more fuel efficient strategy for

ATS stay-warm. An analysis of in-cylinder content shows that NOx emissions are more strongly affected by in-cylinder O_2 content than by method of internal EGR.

1. INTRODUCTION

1.1 Motivation

The planet's surface temperature has risen by nearly 1.62°F since the late nineteenth century. One of the primary culprits for this development is increased emissions of greenhouse gases (CO_2, methane, oxides of nitrogen to name a few) due to industrialization and human activity. Figure 1.1 show data for increased levels of CO_2 in the atmosphere. Controlling these emissions by implementation of appropriate constraints on contributing human activities is critical to prevent further increase in global temperatures.

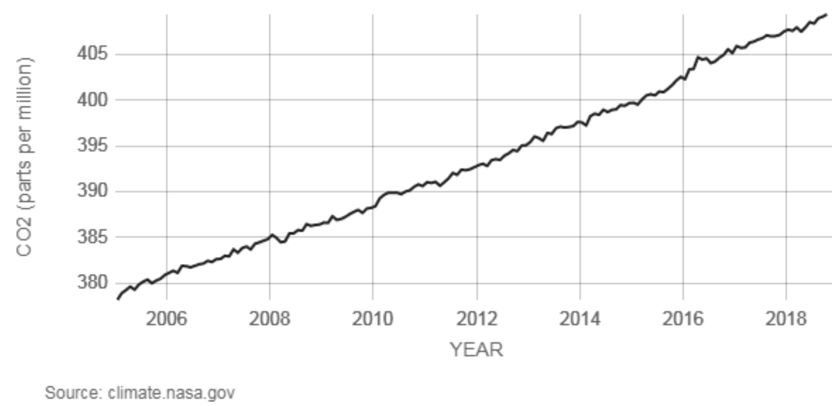

Fig. 1.1. Globally, CO_2 emissions have increased by nearly 8% within a span of 13 years [1].

Figure 1.2 shows that 28% of the total greenhouse gas emissions in 2016 were from the transportation sector. A further analysis showed that light duty vehicles contributed to 60% of the GHG emissions, while medium and heavy duty trucks contributed to 23% of the total GHG emissions. Reducing the carbon footprint of the transportation sector can greatly help in controlling GHG emission levels in the future, and this fact has driven major strides in improving fuel efficiency of vehicles - more than 70% of which will still use internal combustion engines in 2050 [2]. In addition to reducing the carbon consumption of IC engines, reduction in levels of other pollutants like NOx, unburnt hydrocarbons and particulate matter is also critical for ensuring a clean and safe environment for us.

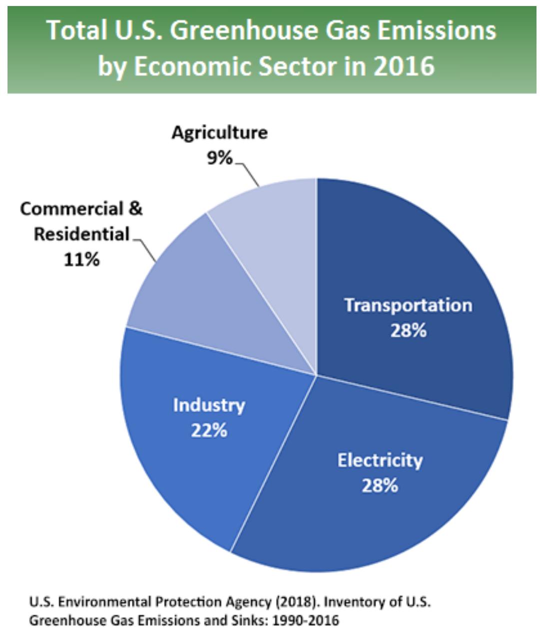

Fig. 1.2. Breakdown of greenhouse gas emissions in the atmosphere by sector. Transportation sector contributes greatly to these GHG emissions [2].

Driven by these factors, the Environmental Protection Agency (EPA) has proposed stricter constraints on emissions from IC engines. The EPA and the National Highway Traffic Safety Administration (NHTSA) have jointly published Phases 1 and 2 of GHG regulations for medium and heavy duty vehicles and engines. Phase 1 became effective in November 2011, and at the time, was projected to result in reduction of CO_2 by 270 million metric tonnes [3]. Phase 2 was published in October 2016. This phase shares the same underlying objective of reducing GHG emissions and also encompasses other entities like requirements for improved aerodynamic drag in trailers and provisions for gliders and race cars. An estimated savings of 1.1 billion metric tonnes of CO_2 can be made due to the two phases of GHG regulations [4]. Figure 1.3 shows the estimated reduction in CO_2 on implementation of the GHG phases.

Other pollutants that are regulated by the EPA include NOx, particulate matter and non-methane unburnt hydrocarbons. Medium and heavy duty diesel engines certified to 2010 emission mandates are required to meet 0.2 g/bhp-hr NOx, 0.01 g/bhp-hr of soot and 0.14 g/bhp-hr of non-methane unburnt hydrocarbons. Significant reduction in NOx emission limits from current values are anticipated in future regulation limits [5].

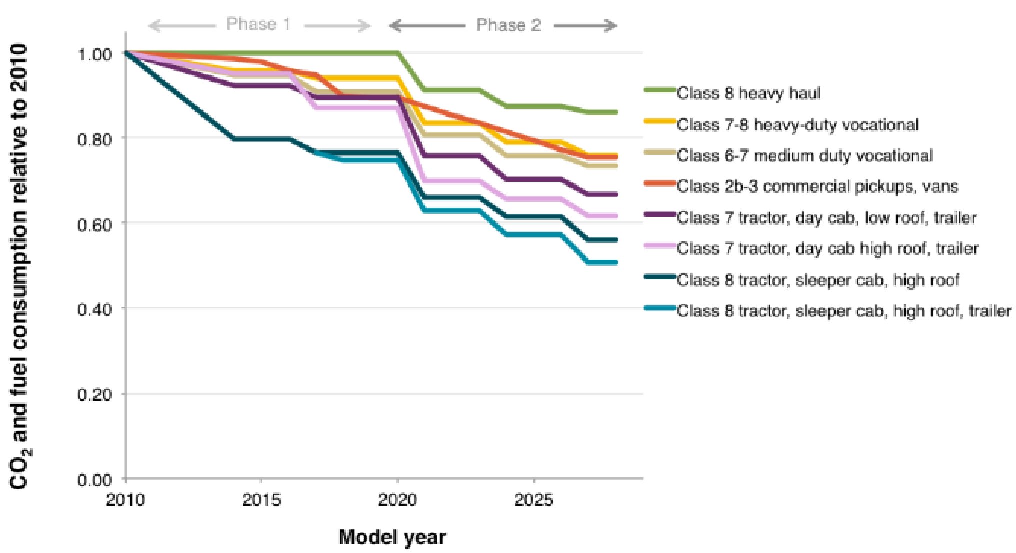

Fig. 1.3. Estimates of reduction in GHG emissions due to the Phases 1 and 2 of the GHG emissions reduction plan.

1.2 Emission Reduction via Effective Aftertreatment Thermal Management

The steep reduction in NOx and PM emission regulation limits in 2010 played a critical role in driving engine manufacturers to rely on additional techniques for emissions control, one such critical technique being the extensive use of an aftertreatment system. Use of exhaust gas recirculation became popular to meet desired NOx levels, along with which use of VGT became commonplace for improved control over amount of EGR. Increased use of EGR led to increase in engine out levels of soot, which necessitated the use of diesel particulate filters. It was found that excessive use of EGR affected fuel consumption, therefore many engine manufacturers decided to use ammonia based selective catalytic converter systems, in addition to EGR, for NOx control [6]. With the increased reliance on aftertreatment systems, a challenge arose to ensure efficient operation of these systems.

1.2.1 Description of Diesel Aftertreatment System

A typical diesel engine aftertreatment consists of a diesel oxidation catalyst (DOC), a diesel particulate filter (DPF) and a selective catalytic reduction (SCR) system. A pump and injector for diesel exhaust fluid is also a part of the system. Figure 1.4 shows a schematic of an engine configuration equipped with an aftertreatment system.

The functions of a DOC include oxidization of unburnt hydrocarbons in the exhaust stream, conversion of fuel injected during an active regeneration event to heat and conversion of NO in the exhaust to NO_2. The DOC requires temperature in the range of 200°C to 250°C for effective operation, and generally relies on the exhaust temperature for 'light-off'. Conversion of NO to NO_2 by the DOC plays an important role in passive regeneration of the diesel particulate filter and can help to reduce the frequency of active regeneration. NO_2 reacts with carbon (soot particles) in the presence of O_2 to form CO_2 and NO. Thus, for passive regeneration, presence of sufficient O_2 in the exhaust stream is also critical. This is less of a concern in lean-operating diesel engine combustion.

The diesel particulate filter uses a honeycomb structure [7] to trap particulate matter. Soot accumulated in the DPF can be cleaned by active regeneration or passive regeneration. Active regeneration requires higher temperature than passive regeneration, and involves oxidation of fuel to 'burn' the soot to form ash. Active regeneration consumes additional fuel, and can last for up to an hour depending on the size of the engine and the level of cleaning required. Active regeneration also leads to ash being accumulated in the DPF (due to presence of lubricant-based content in the exhaust stream), which can hinder the ability of the DPF to trap particulate matter. The most common method of ridding the DPF of ash is physical cleaning of the DPF.

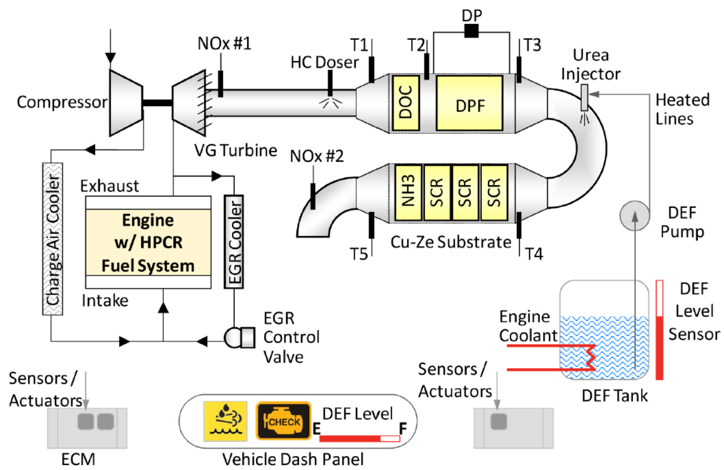

Fig. 1.4. Architecture of an aftertreatment system for a 2013 on-highway vehicle.

The selective catalytic reduction system reduces NOx emissions by acting as a catalyst for the reactions between ammonia and oxides of nitrogen. The conversion efficiency of the SCR is heavily dependent on the temperature of the catalyst (amongst other factors such as exhaust flow rate and mixing) and one of the primary goals of engine operation is to ensure that the SCR stays at desired temperature [8] for most of the engine operation. The SCR requires temperatures above 250°C for efficient NOx conversion [9, 10]. Newer SCR systems can have improved conversion efficiencies at lower exhaust temperatures.

1.2.2 Aftertreatment Thermal Management - ‘Get-hot’ and ‘Stay-warm’ Phases

Maintaining aftertreatment system (ATS) temperatures to desired values involves the use of thermal management strategies. There are two phases of thermal management for a diesel engine ATS system - a ‘warm-up’ phase, where the objective is to increase ATS temperature (for example, during cold starts) to desired values as quickly as possible, without as much concern for fuel consumption; and a ‘stay-warm’ phase where the objective is to maintain the ATS temperature to desirable values, while being as fuel efficient as possible.

Reaching desired ATS temperature as quickly as possible during a cold start (or the ‘get-hot’ phase) can be achieved by using both in-cylinder and non in-cylinder techniques. Multiple, delayed injections can be used to control engine out NOx and soot emissions [11–14] along with use of EGR. Electric heaters in the aftertreatment system have also been considered for rapid warm-up [15]. An aftertreatment system placed closer to the engine (or turbine outlet) can result in faster warm-up due to reduction in heat loss to the environment through the exhaust pipes, while placing the various components of the ATS closer to each other can also be beneficial [16, 17]. Exhaust valve profile modulation can also be used for accelerated ATS warm-up via strategies like early exhaust valve opening [18, 19]. Many of these techniques tend to incur a fuel consumption penalty - a trade-off that is essential to meet the desired emission limits.

Once the ATS has reached desired operating temperatures, it is equally important to maintain those temperature in order to ensure high conversion efficiency. This is the ‘stay-warm phase’, and can be implemented by the use of the same strategies that were used to warm-up the ATS, or by the use of more fuel efficient strategies. Engine down speeding and cylinder deactivation are examples of the same [20–22]. Both these strategies utilize the concept of reduced air flow rate leading to slower cool down of a warmed-up ATS, a method classified as the ‘air path’ method for

ATS thermal management in [23]. Strategies that reduce air flow are more desirable for maintaining ATS temperatures, especially at low load operating conditions [24]. Another technique to reduce air flow at low load operating condition is use of intake valve modulation, which with sufficiently elevated TOT, can be an effective for 'stay-warm' phase of ATS thermal management [25, 26].

1.3 Contributions to Research Project

1.3.1 Study of Sharper Valve Profiles

The author co-led a study with Dheeraj Gosala to understand impacts of varying rates of valve actuation using simulations in GT-Power. This study was carried out at 1200 RPM/3.8 bar BMEP. Opening and closing slopes of intake and exhaust valves were varied. Up to 11.7% better fuel consumption was observed (due to reduced throttling losses across a sharper exhaust valve opening slope), along with reduction in air flow rate. In another case using sharp closing of exhaust valve and sharp opening of the intake valve, 6.5% reduction in fuel consumption was observed with 9% reduction in air flow rate. Reduction in air flow rate was due to increase in overlap between the valves. Results of this study are not discussed in this document.

1.3.2 Study of iEGR via Reinduction, NVO and Boot Valve Profiles

In this simulation study carried out by the author in GT-Power, performance of iEGR via different techniques was evaluated and compared at 800 RPM/1.3 bar BMEP. Internal EGR via reinduction and boot profiles resulted in higher fuel efficiency than iEGR via NVO (and stock fuel efficient operation), with higher exhaust temperatures, 20% lower fuel consumption and decrease in exhaust flow rate. This study formed the basis of experimental analysis discussed in detail in Chapter 5, with the difference that boot profiles could not be implemented on the engine due to lack of interference pistons.

The author mentored undergraduate research assistant Nachiket Vatkar for a GT-Power simulation study of another internal EGR technique, namely, exhaust-stroke based intake re-filling, where the intake valve is opened during the exhaust stroke. Results of this study are not discussed here.

1.3.3 Cylinder Deactivation (CDA) for Fuel-Efficient Stay-warm Operation

The author led on-engine screening and data analysis, with Dheeraj Gosala, to demonstrate 3.4% reduction in fuel consumption over the HD-FTP by using cylinder deactivation. This strategy also led to significant reductions in engine out NOx and soot at steady state operation at 800 RPM/1.3 bar BMEP. The results of this study were discussed by the author in a Master's Thesis in 2017. The author assisted Cody Allen and Dheeraj Gosala with dyno pattern development and engine testing for implementing the above CDA strategy over low-load drive cycles such as the Drayage cycle. Results of the low-load study are not discussed here.

The author led further exploration of CDA with other flexible valve train strategies for significant reductions in fuel consumption; along with other benefits including the option to operate with earlier injection timings and in the absence of exhaust manifold pressure control. Late intake valve closing, internal EGR via NVO and early exhaust valve opening were combined with three cylinder operation and two cylinder operation. Significant improvements in exhaust temperatures were obtained, with exhaust temperatures close to 340°C achieved using three cylinder operation with EEVO at idle. These results are described and analyzed further in Chapter 4.

The author led GT-power simulations for a novel VVA stay-warm strategy, half-bank variable compression ratio (VCR), where in late intake valve closing along with delayed injections and large quantities of external EGR are used in three of the six cylinders. Compared to optimized three cylinder stay-warm operation, this strategy was predicted to have similar exhaust temperature, 13% lower exhaust flow rate and

1% higher fuel consumption. The author mentored undergraduate research assistant Nishad Damle in further analysis of this strategy. Results of this study are not discussed here.

1.3.4 Improved Aftertreatment Thermal Management Using Exhaust Valve Modulation

The author led the study of exhaust valve modulation for aftertreatment thermal management in the absence of exhaust manifold pressure control at curb idle. A precursor to this study was a simulation study in GT-Power to evaluate exhaust valve profiles with the most potential for achieving the target. With the target of achieving similar/improved thermal management than conventional operation, desired valve profiles were developed for late exhaust valve opening and experimental testing was done at idle for meeting desired performance while constraining engine out emissions. A result of this study was the highest exhaust temperature ever achieved at idle on this engine using the VVA, with significantly bounded soot emissions. The results corresponding to this study are discussed in Chapter 3. The author also led LEVO testing at off idle conditions in the absence of EMP control, and the results of this study are discussed in Chapter 4.

The author assisted Dheeraj Gosala and Cody Allen with on-engine experimental screening, data analysis and strategy improvement for using early exhaust valve opening with negative valve overlap for faster aftertreatment warm-up at 800 RPM/1.3 bar BMEP. Results of this study are not discussed here.

1.3.5 Assistance With Development of Statement of Work for Variable Valve Actuation in Spark Ignited (SI) Natural Gas (NG) Engine

The author carried out an extensive literature review for heavy-duty SI NG engine operation and used diesel engine VVA knowledge to propose VVA strategies that can potentially resolve challenges related to heady duty SI NG engine operation. This influenced the statement of work for the upcoming research project in collaboration with industry sponsor Cummins Inc. Results of this study are not discussed here.

1.3.6 Diesel Engine Two Stroke Operation

The author assisted Kalen Vos and John Foster with developing two stroke valve profiles in Simulink, and carrying out experimental testing and analysis for this study at 800 RPM/1.3 bar BMEP. Results of this study are not discussed here.

The author co-mentored undergraduate research assistant Sirish Srinivasan in a GT-Power simulation study for fired 2-stroke operation. This study predicted improvements in exhaust temperature for faster aftertreatment thermal management. Results of this study are not discussed here.

1.3.7 Study of High Speed Idle Operation for Improved Aftertreatment Thermal Management

The author assisted Kalen Vos with experimental testing and analysis for steady state and drive cycle operation with elevated idle speeds for faster ATS warm-up. Results of this study are not discussed here.

1.3.8 Assessing VVA Benefits of Functionality During Diesel Engine Operation Without Exhaust Manifold Pressure Control

The author assisted Kalen Vos and Aswin Ramesh with experimental testing and analysis for this study. Results of this study are not discussed here.

1.4 Outline of Dissertation

1. This chapter (Chapter 1) motivates the study and development of techniques for medium and heavy duty engines to reduce greenhouse gas emissions and other

harmful pollutants. A brief description of the diesel aftertreatment system is presented. Contributions by the author to the research project are stated.

2. Chapter 2 – This chapter discusses details of the experimental test-bed, along with instrumentation for data collection. Frequently used data analysis methodologies are discussed.

3. Chapter 3 – This chapter demonstrates the ability of exhaust valve profile modulation to achieve desired/improved ATS thermal management at curb idle (800 RPM/1.3 bar BMEP). Experimental results for steady state operation with early and late exhaust valve opening are discussed, especially in the absence of exhaust manifold pressure (EMP) control. The warm-up potential of LEVO combined with EMP control is also discussed.

4. Chapter 4 – Late exhaust valve opening is studied at off-idle conditions, namely 1000 RPM and 1200 RPM, at loads up to 10 bar BMEP to assess the thermal management potential of LEVO in the absence of exhaust manifold pressure control at these operating conditions.

5. Chapter 5 – Performance of cylinder deactivation combined with flexible valvetain strategies such as LIVC, EEVO and iEGR via NVO is studied. These strategies demonstrate improvement in the trade-off between fuel consumption and turbine outlet temperature (TOT), while enabling other benefits like lower emissions, earlier injection timings and reduced dependence on exhaust manifold pressure control.

6. Chapter 6 – Performance of internal EGR achieved via reinduction and iEGR via negative valve overlap is compared for fuel-efficient stay-warm operation. This chapter presents effective non-CDA based stay-warm solutions capable of low engine out NOx levels. Sensitivity of iEGR quantity and performance to valve timings and lift is explored.

7. Chapter 7 – A summary of the work discussed in this document is presented here.

8. Chapter 8 – Recommendations for future work are stated in this chapter.

2. EXPERIMENTAL TEST-SETUP AND METHODOLOGY FOR ANALYSIS

2.1 Experimental Test Set-up

The experimental test setup consists of a camless inline 6 cylinder diesel engine, which meets 2010 EPA emission targets. Figure 2.1 shows a schematic of the engine. The engine is equipped with a high pressure common rail system, a variable geometry turbine (VGT) turbocharger, and uses higher pressure external EGR for NOx control. EGR valve position and VGT position are electronically controlled by the ECM and mechanically actuated. The combustion air is air-to-water cooled in the charge air cooler. This schematic also shows the locations for certain stock sensors. Intake

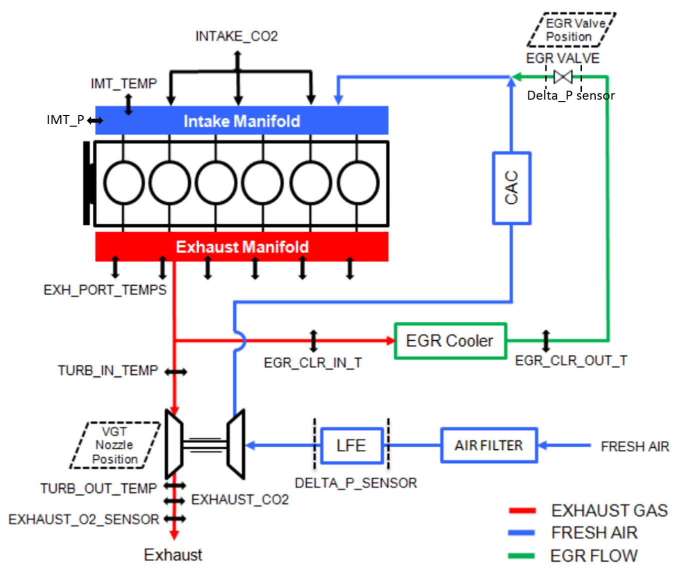

Fig. 2.1. Schematic of the engine in the experimental test set up.

manifold temperature and pressure are used for estimating charge flow (by the ECM). EGR flow is estimated using the measured differential pressure across the EGR valve and the orifice equation for the valve. Exhaust O_2 sensor measures the amount of oxygen content in the exhaust gas, which has utility to monitor DPF regeneration.

Consistent boundary conditions for engine operation are maintained by using temperature and humidity controlled combustion air and controlled ambient temperature.

The engine is also equipped with an aftertreatment system (ATS) consisting of the DOC, DPF and SCR. All three catalysts are instrumented with thermocouples for temperature measurement.

In addition to the stock sensors mentioned above, temperature measurements are available at other relevant locations (for example, engine coolant and oil temperatures) via thermocouples. Relevant pressure measurements are obtained using pressure transducers. This set up also has the capability to measure in-cylinder pressure for all cylinders. In-cylinder pressures are acquired for each of the six-cylinders using Kistler 6067C and AVL QC34C pressure transducers through an AVL 621 Indicom module.

Fresh air flow into the engine is measured using a laminar flow element. Fuel flow is measured gravimetrically using a Cybermetrix Cyrius Fuel Subsystem (CFS) unit. Intake and exhaust CO_2 concentrations are measured using the Cambustion NDIR500 analyzer, allowing for calculation of EGR fraction. A Cambustion fNOx400 fast analyzer is used to measure NOx concentration, along with the stock engine outlet NOx sensor. CO_2 and NOx concentrations are also measured using California Analytical Instruments NDIR600 and HCLD600 analyzers, respectively. Unburnt hydrocarbons are measured using a CAI HFID600 analyzer. Soot is measured using an AVL 483 MicroSoot analyzer, which uses a photoacoustic sensing technique to measure soot concentration. All the emissions are currently measured at the engine outlet (with the exception of intake CO_2), with the capability to measure at aftertreatment outlet. Data is monitored and logged through a dSPACE Controldesk interface. Communication between the engine control module (ECM) and the dSPACE system occurs over a generic serial interface (GSI) link which also allows cycle-to-cycle monitoring and control of cylinder-specific fueling and various other engine functions.

A schematic of the Variable Valve Actuation system is shown in Figure 2.2. A high power hydraulic pump is used to supply hydraulic oil at high pressure for actuating valves (four valves per cylinder - two intake and two exhaust). Commands for valve actuation are sent by the controller via powerful amplifiers, which amplify the signals before supplying them to the actuator.

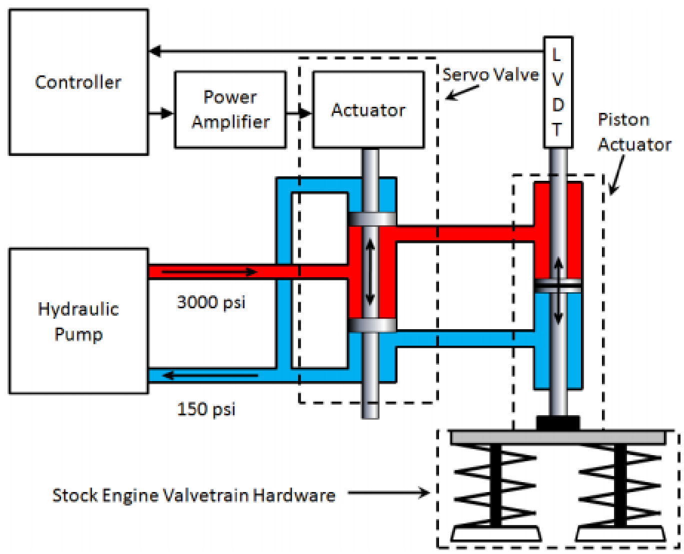

Fig. 2.2. An electronically controlled, hydraulically actuated system is used for valve actuation. Valve positions are measured using LVDT and incorporated into a closed loop controller for accurate valve position control.

The position of the actuator changes depending on the signal, which results in different delta pressure as seen by the piston actuator. This delta pressure results in motion of the valve. Position of the valves is measured using linear variable displacement voltage transformers, where this position is used by the controller for closed loop control of valve position.

The experiments in this work were carried out while strictly following the mechanical constraints in Table 2.1

Table 2.1.
Mechanical constraints during engine operation

Mechanical Parameter	units	limit
Turbine Inlet Temperature	° C	760
Compressor Outlet Temperature	° C	230
Turbo Speed	kRPM	126
Peak Cylinder Pressure	bar	172
Exhaust Manifold Pressure	kPa	500
Pressure Rise Rate	bar/ms	100

2.2 Relevance of the Idle Operating Condition

The curb idle operating condition is an important region of operation for medium and heavy duty engines. The certification for medium and heavy duty engines, the Heavy Duty Federal Test Procedure (HD-FTP) consists of 40% operation at curb idle. Trucks equipped with heavy duty engines spend a considerable amount of time idling, where, in many cases, the idling engine drives auxiliary accessory loads [27]. Trucks that deliver goods at ports spend a large portion of time idling in queues while waiting for their cargo to be loaded or unloaded [28].

The curb idle operating condition is therefore an important consideration for ATS thermal management. Several experimental steady state results in this work therefore focus on operation at 800 RPM/1.3 bar BMEP.

2.3 Cycle Efficiency Analysis

Figure 2.3 shows an example of a plot of in-cylinder pressure against volume on a logarithmic scale. Typically used values of valve opening and closing timing are also shown. In this figure, the closed cycle loop is the part comprising of the compression and the expansion strokes. The open cycle loop is the part of the cycle consisting of the intake and exhaust strokes. The following equations are used to calculate gross indicated mean effective pressure, pumping mean effective pressure and net indicated mean effective pressure.

$$GIMEP = \frac{Area_{ClosedLoop}}{V_d} \tag{2.1}$$

$$PMEP = \frac{Area_{OpenLoop}}{V_d} \tag{2.2}$$

$$NIMEP = GIMEP - PMEP \tag{2.3}$$

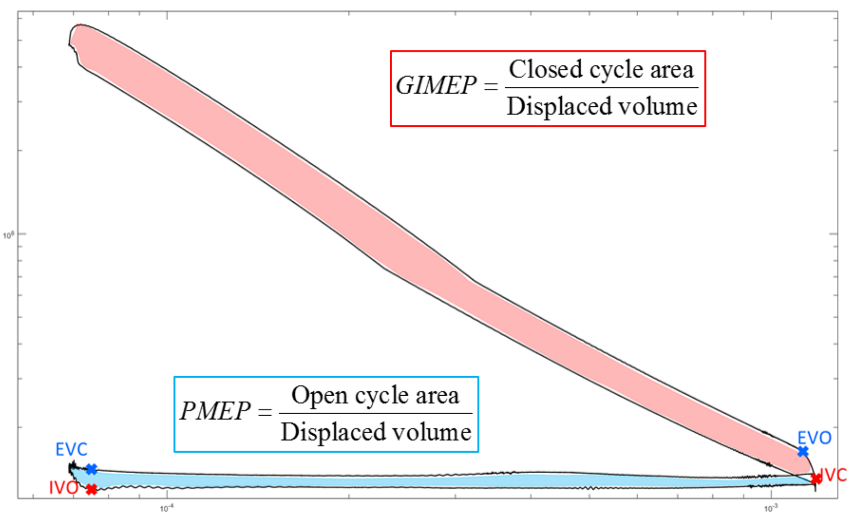

Fig. 2.3. P-V diagram highlighting the conventional definition of closed and open cycle loops.

The brake thermal efficiency can be considered to be constituting of three primary portions – closed cycle efficiency (CCE), open cycle efficiency (OCE) and mechanical efficiency (ME). Closed cycle efficiency captures the efficiency of the combustion process, and is affected by heat loss, in-cylinder dilution, nature of heat release rate and injection timing. Open cycle efficiency is determined by the work done by the piston or on the piston during the gas exchange process. Mechanical efficiency captures losses due to friction and auxiliary losses (for example, fuel pump and oil pump related losses) [8]. The following equations can be used to calculate cycle efficiency values. Brake thermal efficiency is defined as the product of OCE, CCE and ME; and is inversely proportional to fuel consumption.

$$CCE = \frac{GIMEP \times V_d}{m_{fuel} \times LHV_{Diesel}} \tag{2.4}$$

where V_d is the displaced volume, m_{fuel} is the fuel consumption, LHV_{Diesel} is the lower heating value of diesel fuel.

$$OCE = \frac{NIMEP}{GIMEP} \tag{2.5}$$

$$ME = \frac{BMEP}{NIMEP} \tag{2.6}$$

where BMEP is the brake mean effective pressure.

$$BTE = CCE \times OCE \times ME \tag{2.7}$$

2.4 First Law Analysis of Fuel Energy Distribution During Engine Operation

A first law analysis for the engine system can be carried out to study distribution of fuel energy for the various strategies. Figure 2.4 shows a few examples of energy terms utilized in such an energy balance. This section discusses the methodology for carrying out this analysis.

Fuel energy entering the engine is primarily divided into three main energy terms - brake energy, energy of the exhaust stream exiting the engine and losses. Losses can be further identified depending on the source. In-cylinder heat loss, pumping loss and friction loss are examples. Other sources of heat loss include heat loss to the EGR cooler and heat loss to the charge air cooler (CAC). Turbocharger and manifold losses are also contributing terms. The first law analysis used in this work focuses on friction losses, pumping losses, in-cyl heat loss and EGR cooler heat loss. Other contributing terms to losses are not computed individually, but instead grouped as one energy loss term.

Table 2.2 describes the symbols used in equations used for the first law analysis. Equation 2.8 shows a high-level breakdown of fuel energy.

$$\dot{Q}_{fuel} = \dot{W}_{brake} + \dot{Q}_{exh} + \dot{W}_{pumping} + \dot{Q}_{in-cylheatloss} + \dot{W}_{friction} + \dot{Q}_{other} \tag{2.8}$$

Each term of the above equation be computed using the following equations. Equation 2.15 by itself can be considered to be a first law balance for the cylinder. Losses to the manifolds, turbocharger losses and auxiliary losses (oil pump, fuel pump) are lumped as shown in Equation 2.18.

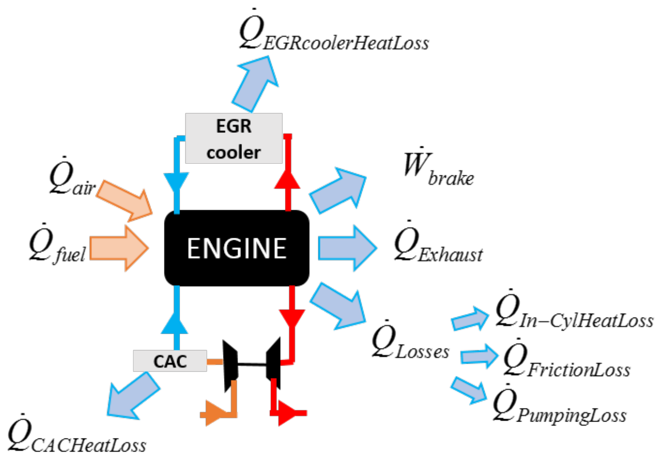

Fig. 2.4. Various sources of losses can be analyzed for the engine system to carry out an energy balance for the engine.

$$\dot{Q}_{fuel} = \dot{m}_{fuel} \times LHV_{Diesel} \tag{2.9}$$

$$\dot{W}_{brake} = T_{brake} \times \frac{2\pi N}{60} \tag{2.10}$$

$$\dot{Q}_{exh} = \dot{m}_{exh} c_{p,exh} \left(T_{exh} - T_{ref}\right) - \dot{m}_{air} c_{p,air} \left(T_{amb} - T_{ref}\right) \tag{2.11}$$

$$\dot{W}_{pumping} = PMEP \times V_d \times \frac{N}{120} \tag{2.12}$$

$$\dot{W}_{indicated} = NIMEP \times V_d \times \frac{N}{120} \tag{2.13}$$

$$\begin{aligned}\dot{Q}_{charge} = {} & \dot{m}_{charge,out} c_{p,charge,out} (T_{ExhManifold} - T_{ref}) \\ & - \dot{m}_{charge,in} c_{p,charge,in} (T_{IntManifold} - T_{ref})\end{aligned} \tag{2.14}$$

$$\dot{Q}_{incyl} = \dot{Q}_{fuel} - \dot{W}_{pumping} - \dot{W}_{indicated} - \dot{Q}_{charge} \tag{2.15}$$

$$\dot{W}_{friction} = FMEP \times V_d \times \frac{N}{120} \tag{2.16}$$

$$\dot{Q}_{EGR} = \dot{m}_{EGR} c_{p,exh} (T_{EGR,in} - T_{EGR,out}) \tag{2.17}$$

$$\dot{Q}_{other} = \dot{Q}_{fuel} - \dot{W}_{brake} - \dot{Q}_{cyl} - \dot{Q}_{EGR} \tag{2.18}$$

Table 2.2.
Description of parameters used for first law analysis

Parameter	Description
c_p	Specific heat constant
$FMEP$	Friction mean effective pressure
LHV_{Diesel}	Lower heating value of diesel
$\dot{m}_{exh}$	Mass flow rate of exhaust
$\dot{m}_{air}$	Mass flow rate of fresh air
$\dot{m}_{fuel}$	Mass flow rate of fuel
$\dot{m}_{charge,in}$	Mass flow rate of charge entering the cylinders
$\dot{m}_{charge,out}$	Mass flow rate of charge exiting the cylinders
N	Engine speed
$NIMEP$	Net indicated mean effective pressure
$PMEP$	Pumping mean effective pressure
$\dot{Q}_{fuel}$	Rate of heat addition due to fuel combustion
$\dot{Q}_{exh}$	Rate of heat transfer to exhaust stream
$\dot{Q}_{in-cylheatloss}$	Rate of heat loss from cylinders
$\dot{Q}_{charge}$	Rate of heat transfer to in-cylinder charge
$\dot{Q}_{EGR}$	Rate of heat transfer from EGR cooler
$\dot{Q}_{other}$	Rate of heat loss due to other sources
T_{brake}	Brake torque of engine
T_{exh}	Temperature of exhaust exiting the turbine
$T_{ExhManifold}$	Temperature of exhaust manifold
T_{EGRin}	Temperature of exhaust gas entering the EGR cooler
T_{EGRout}	Temperature of exhaust gas exiting the EGR cooler
$T_{IntManifold}$	Temperature of intake manifold
T_{ref}	Reference temperature (25°C)
V_d	Displaced volume
W_{brake}	Brake work from the engine
$W_{indicated}$	Brake work from the cylinders
$W_{pumping}$	Pumping work for the cylinders
$W_{friction}$	Friction work

2.5 Normalized Heat Transfer Analysis as a Thermal Management Performance Metric

The temperature of the ATS system is affected by engine operating conditions, mainly, exhaust flow rate and exhaust temperature. The rate of heat transfer between the exhaust gas and the catalyst can be expressed mathematically using the equation shown below [29].

$$q = C \times \dot{m}_{exh}^{\frac{4}{5}} \times (T_{exh} - T_{bed}) \tag{2.19}$$

where $\dot{m}_{exh}$ is the exhaust flow rate at engine outlet, T_{exh} is exhaust temperature at engine outlet, and C is a constant determined based on the convective heat transfer coefficient and the geometric structure of the exhaust piping. See above reference for details of derivation of C. The amount of heat transfer to or from the catalyst at any instant depends on the instantaneous exhaust flow rate, exhaust temperature and catalyst bed temperature. When q is negative, it indicates heat being transferred from the catalyst to the exhaust gas flowing over it.

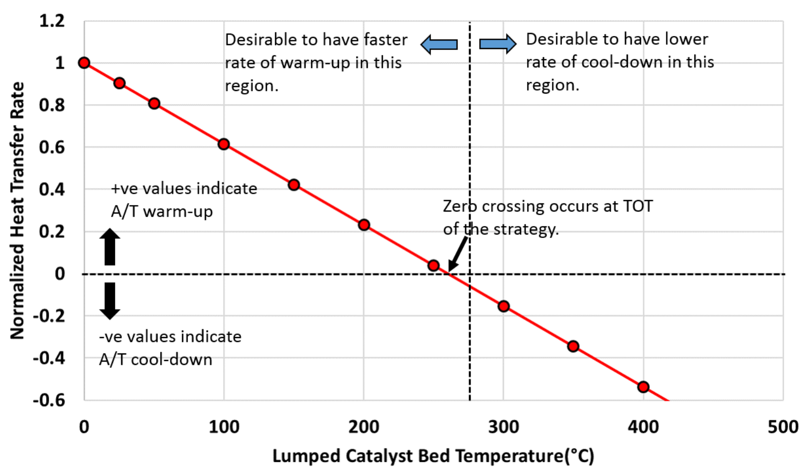

Fig. 2.5. Example of a normalized heat transfer plot.

Positive values of q indicate that the catalyst is gaining heat from the exhaust gas. The heat transfer between the catalyst and the exhaust gas becomes zero when the catalyst and exhaust gas have the same temperature. Exhaust temperature determines the magnitude of the heat transfer from the exhaust gas to the catalyst, while exhaust flow rate dictates how rapidly this heat transfer occurs. Therefore, both high exhaust temperature and high exhaust flow rate are desirable for rapid warm-up of a cold ATS. Figure 2.5 shows an example of a normalized heat transfer plot.

Heat transfer plots obtained using the above equation can give a relative indication of the ability of any strategy to warm-up the ATS. The heat transfer plots so obtained can be normalized with respect to a baseline operating condition with a certain exhaust temperature and exhaust flow rate.

2.6 Summary

This chapter presented an overview of the experimental set-up and described instrumentation used for measuring engine performance. Analysis methodologies used throughout this work were described.

3. EXHAUST VALVE PROFILE MODULATION FOR IMPROVED DIESEL ENGINE CURB IDLE AFTERTREATMENT THERMAL MANAGEMENT

3.1 Literature Review

Aftertreatment system (ATS) warm-up at low loads is a challenge because of the inherently lower exhaust temperatures and exhaust flow rates associated with low-load operation. At the curb idle operating condition of 800 RPM and 1.3 bar BMEP, exhaust temperatures are well below the desired range of 250°C–450°C (which corresponds to highest NOx conversion efficiency of the SCR and oxidation efficiency of the DOC). An effective approach to rapid ATS warm-up is to use techniques to reduce open cycle or closed cycle efficiency, which leads to increase in fuel consumption and hence, exhaust temperatures. Examples of methods to increase exhaust temperatures via reduction in closed cycle efficiency include multiple, delayed in-cylinder injections, hydrocarbon dosers, early exhaust valve opening and use of internal EGR instead of external EGR. Examples of methods to increase exhaust temperatures via reduction in open cycle efficiency include exhaust manifold pressure modulation via various means such as an exhaust throttle valve (ETV) [30] or a variable geometry turbine turbocharger (VGT). Using an ETV is preferred for systems equipped with a fixed geometry turbine (FGT) turbocharger.

Exhaust valve modulation (namely early exhaust valve opening and late exhaust valve opening) have been studied for a gasoline engine in [31] where in LEVO showed benefits in scavenging, but also led to higher pumping losses. EEVO resulted in increase in UHC emissions in this case, an undesirable phenomenon. EEVO was demonstrated to have superior thermal management performance in a medium-duty diesel engine in [18].

3.2 Exhaust Manifold Pressure Control - A Critical Function Served by VGT/ETV

A variable geometry turbine (VGT) turbocharger serves multiple functions over the engine speed and load operating space. Figure 3.1 shows the engine operating space for the engine with the use of stock thermal management calibration. The bubbles in this figure indicate prominent operating spaces over the Heavy Duty Federal Test Procedure (HD-FTP), while the numbers in parentheses indicate the percentage of fuel consumed. The operating space is divided into four primary zones, each of which uses a certain range of VGT actuator position values. The function of the VGT in each zone is briefly mentioned next.

(a) Zone 1 – Zone 1 is primarily low speed and low load operation, where the function of the VGT is exhaust manifold pressure control for aftertreatment thermal management and driving sufficient external EGR.

(b) Zone 2 – At low speeds and medium to high loads, the function of the VGT is to provide boost for desired torque response, while also driving external EGR flow and providing EMP control for thermal management.

(c) Zone 3 – These operating conditions are nearer to the torque curve where the VGT serves the function of providing sufficient boost for desired power requirements. VGT position is optimized to provide sufficient boost without overboosting, which can lead to violation of the peak in-cylinder pressure limit.

(d) Zone 4 – The VGT is used to increase fuel efficiency in this high speed and medium to low load region.

In addition to the above functions, a VGT can also act as an exhaust brake [32].

The focus of this chapter is Zone 1 operating space, specifically the curb idle operating condition of 800 RPM/1.3 bar BMEP. The objective was to study whether exhaust valve modulation can achieve desired aftertreatment thermal management without exhaust manifold pressure control, while also achieving sufficient in-cylinder dilution for NOx control. The use of a VGT for thermal management purposes is a patented application by Cummins Inc [33].

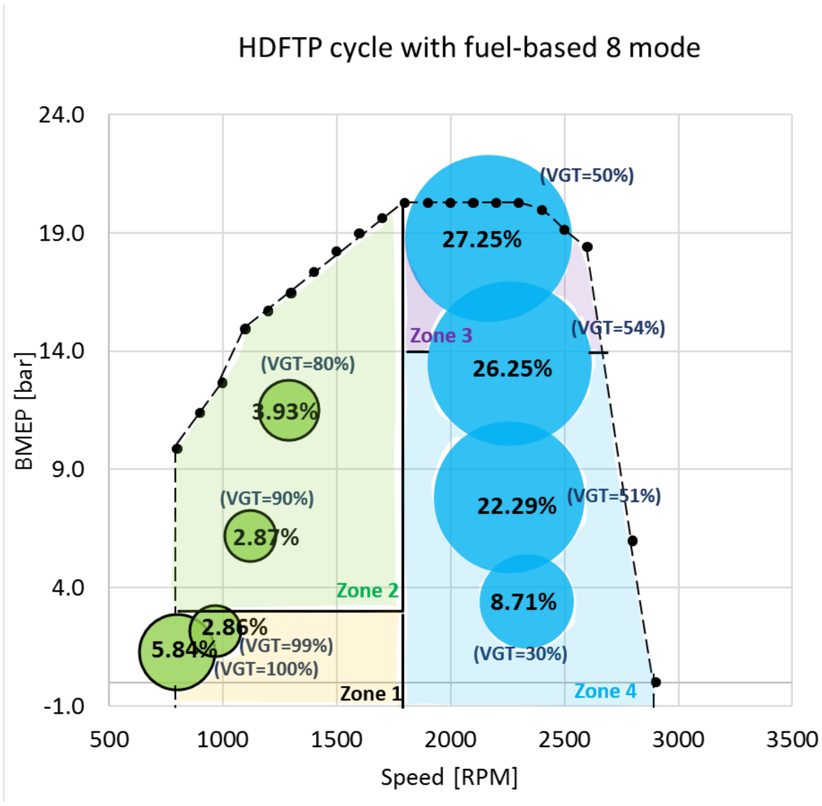

Fig. 3.1. During conventional thermal management operation, different VGT positions are used at different operating conditions of the HD-FTP to optimize power output, emissions and ATS thermal management.

The engine in the experimental setup is equipped with a VGT for exhaust manifold pressure (EMP) control. Absence of EMP control was emulated on the engine by setting the VGT position to 60% closed.

3.3 Exhaust Valve Profile Modulation for ATS Thermal Management at 800 RPM/1.3 bar BMEP Without Requiring Exhaust Manifold Pressure Control

This section discusses experimental results which demonstrate that in the absence of EMP control, exhaust valve profile modulation can enable similar thermal management performance as conventional thermal management operation (which uses EMP control).

3.3.1 Description of Strategies

Various exhaust valve modulation strategies studied at curb idle are described in this section.

Figure 3.2 shows the valve profiles, injections and heat release rates for all the strategies. Injection timings were delayed no further than those used in the conventional thermal management (TM) operation. Rail pressure and EGR valve position were modulated to maintain engine-out emission levels consistent with limits set by baseline operation. Fueling quantities were modulated to meet the desired load of 1.3 bar BMEP.

(a) *Thermal management baseline (TM baseline)* – This is the stock thermal management operation which uses multiple, delayed injections, and elevated exhaust manifold pressure (using maximally shut VGT) to reach engine-outlet temperature and emissions necessary to meet 2010 emission targets. 'TM baseline' results in engine-out NOx levels well below the Certified Clean Idle limit of 30 g/hr [34]. Elevated exhaust manifold pressure also helps to drive sufficient external high pressure EGR for NOx control. Figure 3.2(a) shows the valve profiles, heat release rate and injection timings used. Conventional valve profiles were used. This strategy is the baseline for comparisons of fuel consumption, engine-outlet temperature and emissions.

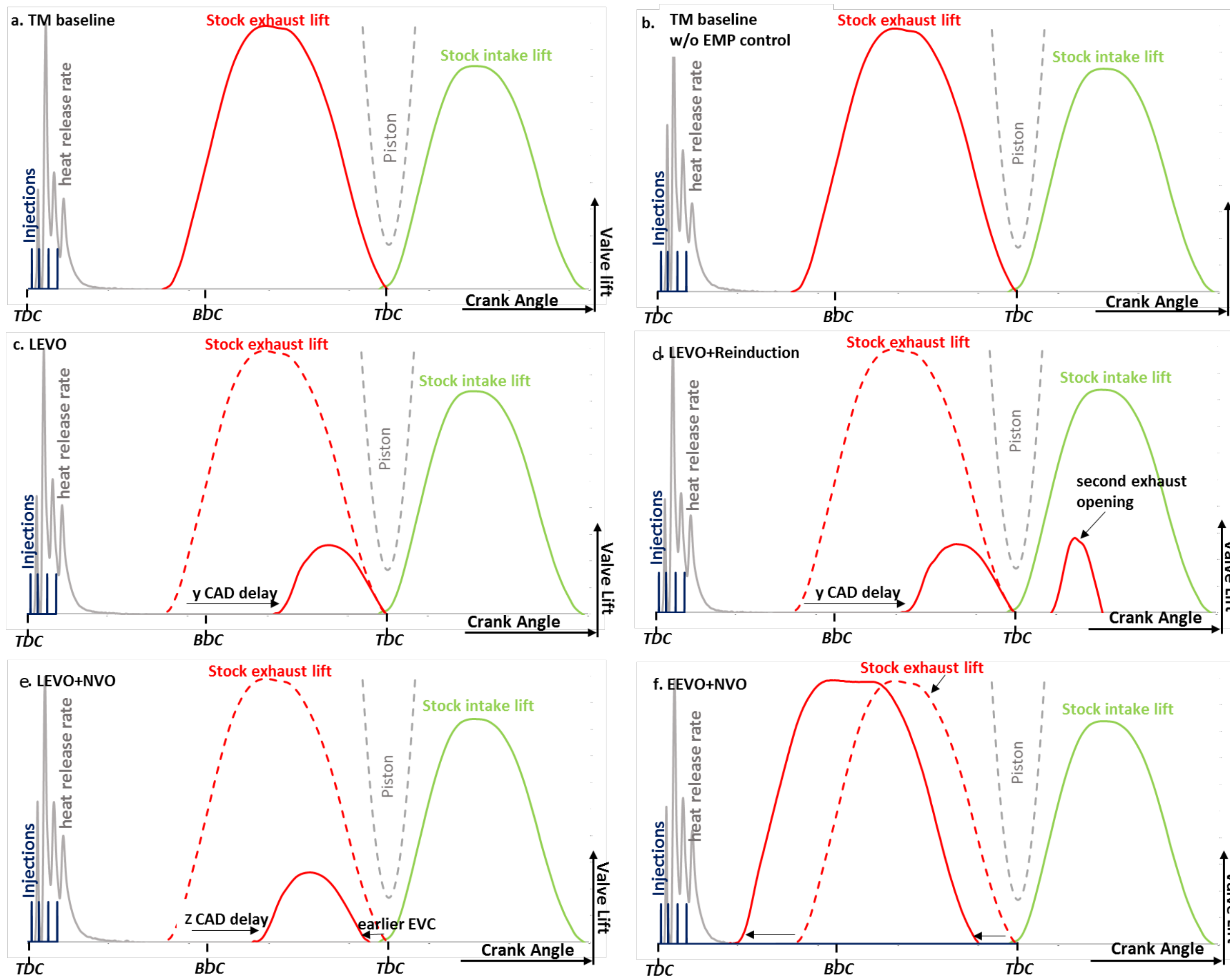

Fig. 3.2. Experimental injections, heat release rates, and exhaust valve profiles for the six strategies at 800 RPM/1.3 bar BMEP. All of these strategies have the same commanded delayed injection timings. (a)'TM baseline' uses four delayed injections (b) 'TM baseline w/o EMP control' also uses four delayed injections, and the same valve profiles as (a), with the added difference of operation without EMP control. (c) 'LEVO' uses delayed opening of the exhaust valve, with the same delayed injections as before, and an emulated FGT operation; (d) 'LEVO+Reinduction' uses LEVO operation combined with a secondary exhaust valve opening during the intake stroke (e) 'LEVO+NVO' is LEVO operation with negative valve overlap via advanced exhaust valve closing and (f) 'EEVO+NVO' uses early exhaust valve opening with negative valve overlap via advanced exhaust valve closing

(b) *TM baseline w/o EMP control* – Strategy to emulate operation without the ability to control EMP, achieved by setting VGT position to a fixed value, while using similar engine operating settings as 'TM baseline'. Stock valve profiles are used here per Figure 3.2(b). This operation is used to highlight the importance of EMP control to the baseline strategy.

(c) *LEVO* – This strategy uses late exhaust valve opening (as shown in Figure 3.2(c)) without EMP control. Exhaust valve opening has been delayed by a considerable amount after BDC. LEVO enabled engine-outlet temperatures via increased pumping work through recompression of exhaust gases, and throttling during the exhaust stroke.

(d) *LEVO+Reinduction* – This strategy uses LEVO in addition to a secondary exhaust valve opening during intake stroke, and no EMP control. Figure 3.2(d) shows the valve profiles, injections and heat release rate for this strategy. The secondary exhaust valve opening serves as a method to achieve internal EGR. External EGR is also used by completely opening the EGR valve. This strategy achieves similar thermal management performance as 'TM baseline', and meets all desired emission constraints.

(e) *LEVO+NVO* – This strategy uses LEVO with negative valve overlap between the exhaust and intake valves, and no EMP control. As shown in Figure 3.2(e), exhaust valve closing (EVC) is advanced from its stock value. The negative valve overlap so realized is a way to achieve internal EGR via trapping, which in conjunction with external EGR, assists with reaching engine-out NOx levels similar to 'TM baseline'. Exhaust valve opening used here is earlier than the previous two LEVO-based strategies.

(f) *EEVO+NVO* – This strategy uses early exhaust valve opening (advanced by 55 CAD w.r.t stock EVO) with internal EGR via NVO, with no EMP control, in order to reach desired engine-outlet temperature. Figure 3.2(f) shows the heat release rate, injections, and the valve profiles used for this strategy. Exhaust valve opening is advanced closer to TDC for elevated engine-outlet temperature. Exhaust valve closing is also advanced, to achieve internal EGR. The intake valve profile is maintained the same as stock profile. This is another VVA based strategy that can achieve similar thermal management performance as 'TM baseline', without requiring EMP control.

Table 3.1 summarizes the VGT and EGR valve position used for the above strategies.

Table 3.1.
Summary of VGT and EGR Positions

Strategy	VGT position	EGR valve position
TM baseline	Maximally shut	Slightly open
TM baseline w/o EMP control	60% shut	Completely open
LEVO	60% shut	Completely open
LEVO+Reinduction	60% shut	Completely open*
LEVO+NVO	60% shut	Completely open*
EEVO+NVO	60% shut	Completely open*

** Also uses internal EGR*

3.3.2 Discussion of Results

Figure 3.3 shows in-cylinder pressure versus volume plots over one engine cycle for each of the above strategies. All of the strategies shown in Figure 3.3 use multiple, delayed injections; and none (except for 'TM baseline') use EMP control. Operation with a maximally shut VGT in 'TM baseline' operation results in a large pumping loop due to higher exhaust manifold pressure. 'TM baseline w/o EMP control' has a smaller pumping loop due to its operation with a less restricted VGT position, and hence exhibits lower exhaust manifold pressure. The differences amongst the

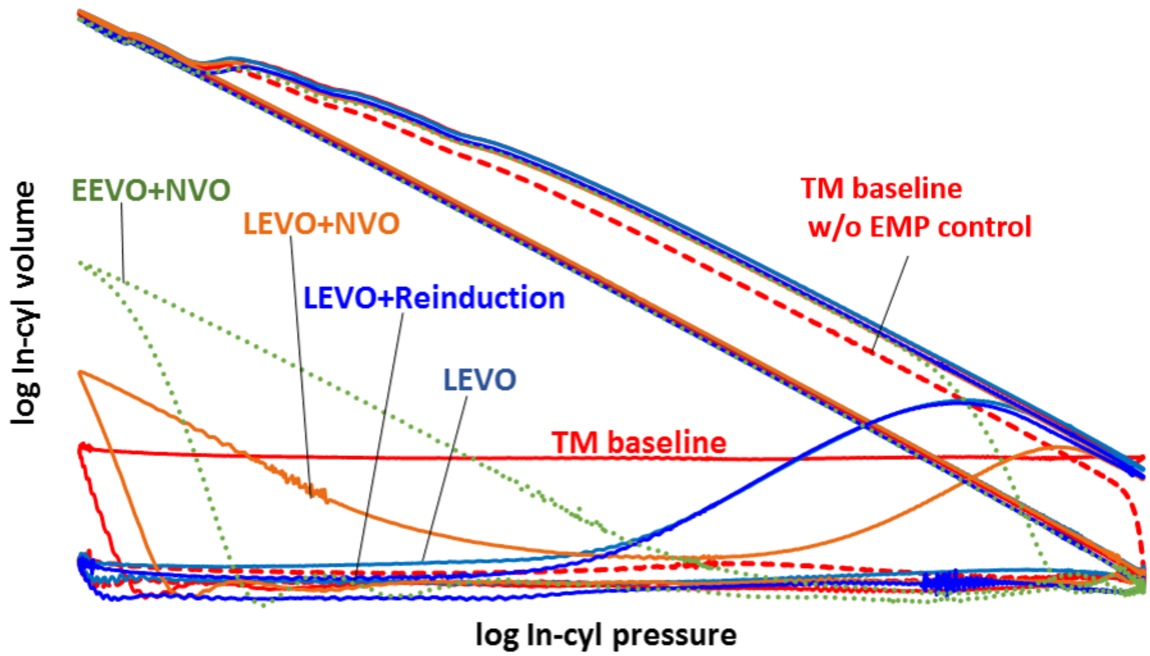

Fig. 3.3. In-cylinder pressure vs volume on a logarithmic scale. i) Maximally shut VGT in 'TM baseline' leads to increased exhaust manifold pressure, and therefore, greater pumping work. ii) 'TM baseline w/o EMP control' has lower EMP and significantly lower pumping work. iii) 'LEVO', 'LEVO+Reinduction' and 'LEVO+NVO' use late exhaust valve opening without EMP control to match the pumping work of 'TM baseline' iv) 'LEVO+NVO' shows recompression at the end of the exhaust stroke due to presence of negative valve overlap. v) Earlier blow down in 'EEVO+NVO' is a result of advanced EVO, while recompression at the end of the exhaust stroke is a result of negative valve overlap.

strategies mainly arise over the pumping loop portion of the cycle. This is because the exhaust valve modulation based strategies described above aim to have similar pumping work as the 'TM baseline' approach, but without requiring elevated exhaust manifold pressure via EMP control (resulting in differences in pumping loops).

The effect of late exhaust valve opening can be seen from the P-V plot as an increase in in-cylinder pressure due to recompression of exhaust gas. The recompression process is nearly polytropic, and retraces the expansion process before the exhaust valve is opened. ‘LEVO’, ‘LEVO+NVO’ and ‘LEVO+Reinduction’ show recompression resulting from late exhaust valve opening. ‘LEVO’ and ‘LEVO+Reinduction’ use the same late exhaust valve opening, and hence show similar in-cylinder pressure during recompression.

‘LEVO+Reinduction’ uses a secondary opening of the exhaust valve during the intake stroke (reinduction), in addition to late exhaust valve opening. In-cylinder pressure is lower for some portion of the intake stroke due to lower intake manifold pressure. In-cylinder pressure during the intake stroke increases further along in the intake stroke due to the reinduction event.

The recompression loop in ‘LEVO+NVO’ is smaller compared to the other LEVO based strategies due to a earlier exhaust valve opening. ‘LEVO+NVO’ also shows additional pumping losses due to recompression at the end of the exhaust stroke because of negative valve overlap and the intake valve opening time close to TDC. Due to such an IVO, recompression work during NVO cannot be recovered.

Advanced EVO in ‘EEVO+NVO’ results in an earlier and faster rate of blow down, while advanced EVC leads to recompression of trapped exhaust gas at the end of exhaust stroke. The large pumping loop is due to the intake valve opening time being close to BDC.

Figure 3.4 compares engine-outlet temperature, exhaust flow rate, cycle efficiencies, turbocharger turbine speed and enthalpy drop across the turbine. ‘TM baseline’ is the conventional thermal management strategy with engine-outlet temperature close to 260°C.

‘TM baseline w/o EMP control’ is obtained by implementing ‘TM baseline’ without EMP control. Figures 3.4(a) and (b) show that with ‘TM baseline w/o EMP control’, engine-outlet temperature and fuel consumption decrease in comparison to ‘TM baseline’. This is due to operation with lower exhaust manifold pressure. This strategy is not consistent with achieving the desired rate of ATS warm-up.

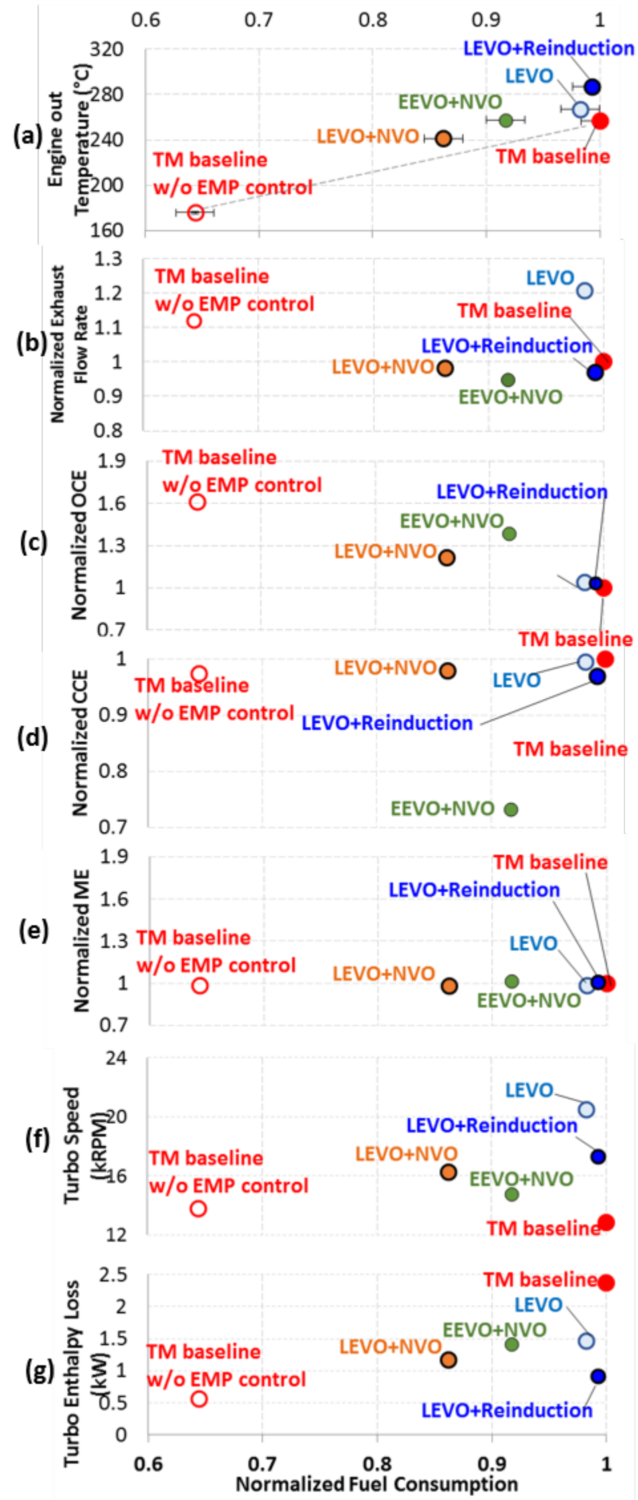

Fig. 3.4. Experimental steady state results at 800 RPM/1.3 bar BMEP.

‘LEVO’ can achieve nearly 10°C higher engine-outlet temperature than ‘TM baseline’ without requiring EMP control (for elevated exhaust manifold pressure), and exhibits no fuel consumption penalty. Throttling losses incurred with ‘LEVO’ are similar to those incurred due to a maximally shut VGT (as in ‘TM baseline’), and as a result, ‘LEVO’ has similar fuel consumption and engine-outlet temperature as the ‘TM baseline’. However, sufficient external EGR cannot be driven due to an inadequate pressure difference between the intake and exhaust manifolds. LEVO is therefore combined with VVA–based internal EGR strategies to meet NOx emission constraints set by the ‘TM baseline’. ‘LEVO+Reinduction’ and ‘LEVO+NVO’ are examples of LEVO operation combined with VVA–based internal EGR strategies.

‘LEVO+Reinduction’ uses the same late exhaust valve opening as ‘LEVO’, in addition to a secondary opening of the exhaust valve during the intake stroke to reinduct exhaust gases from the exhaust manifold. This strategy results in a 30°C higher engine-outlet temperature than ‘TM baseline’, with similar fuel consumption. ‘LEVO+NVO’ uses negative valve overlap to trap in-cylinder residual exhaust gas. This strategy has an earlier exhaust valve opening compared to ‘LEVO’. The result is 17°C and 27°C lower engine-outlet temperature than ‘TM baseline’ and ‘LEVO’, respectively. ‘LEVO+NVO’ has lower engine-outlet temperature and fuel consumption compared to ‘LEVO’ and ‘LEVO+Reinduction’ because it uses an earlier exhaust valve opening and hence, incurs lower pumping losses. ‘EEVO+NVO’ results in very similar engine-outlet temperature as ‘TM baseline’. Earlier EVO results in higher enthalpy at the turbine inlet and helps achieve desired engine-outlet temperature. Negative valve overlap due to advanced exhaust valve closing is used to obtain sufficient dilution for NOx control.

Figure 3.4(b) shows that ‘TM baseline w/o EMP control’ results in higher exhaust flow rate compared to ‘TM baseline’ due to the lower EGR fraction required. Exhaust flow rate increases by nearly 20% with ‘LEVO’ compared to ‘TM baseline’ due to an increase in turbine speed and boost. Exhaust flow rate is observed to decrease when internal EGR strategies are used with LEVO as the amount of exhaust gas used by

‘LEVO+Reinduction’ and ‘LEVO+NVO’ for in–cylinder dilution is greater than that in ‘LEVO’. Operation of LEVO with internal EGR can achieve exhaust flow rates similar to ‘TM baseline’ with all emissions constrained as desired. A slight decrease in exhaust flow rate is seen with ‘EEVO+NVO’. This is a result of a shift in the trade off between increased boost due to higher turbine speed (higher turbine inlet enthalpy due to earlier blow down) and use of internal EGR via NVO.

Figures 3.4(c-e) show normalized values of cycle efficiencies. Figure 3.4(c) shows the improvement in open cycle efficiency obtained with ‘TM baseline w/o EMP control’ compared to ‘TM baseline’. This is due to reduction in exhaust manifold pressure (and pumping losses). Open cycle efficiency decreases for ‘LEVO’, due to recompression and throttling losses across the exhaust valve, where such losses are comparable to losses incurred due to elevated exhaust manifold pressure in ‘TM baseline’. LEVO based strategies therefore have similar open cycle efficiency as ‘TM baseline’. ‘LEVO+NVO’ results in higher open cycle efficiency than ‘LEVO’ and ‘LEVO+Reinduction’ due to an earlier exhaust valve opening. ‘EEVO+NVO’ shows the highest OCE amongst the VVA based strategies. This is because, unlike late EVO, earlier EVO has little to no contributions to OCE. However, OCE is lower compared to ‘TM baseline w/o EMP control’ because of presence of recompressed internal EGR during intake stroke where piston has to work harder to pull charge into the cylinder.

Figure 3.4(d) shows that closed cycle efficiency remains nearly constant between ‘TM baseline’ and ‘TM baseline w/o EMP control’ as these strategies have the same injection timings. ‘LEVO’ results in a very similar CCE as ‘TM baseline’. Lower CCE in ‘LEVO+Reinduction’ and ‘LEVO+NVO’ compared to ‘LEVO’ is a result of using internal–EGR in the former two strategies which results in slightly delayed heat release.

Lower CCE is observed with ‘LEVO+Reinduction than ‘LEVO+NVO’ although both use internal EGR. This is because the amount of internal EGR needed for NOx control is not equal amongst these strategies. Internal EGR achieved via NVO is ‘hotter’ than that achieved via reinduction, and temperature of EGR affects its effectiveness for NOx control. However, ‘LEVO+NVO’ requires lower overall in-cylinder dilution because it has lower fuel consumption than ‘LEVO+Reinduction’, and hence a smaller quantity of fuel combusted per cycle.

‘EEVO+NVO’ shows lower closed cycle efficiency than the other strategies. This is because advanced EVO reduces useful piston work extracted from the combustion products during the expansion stroke.

It is important to note that LEVO based strategies and ‘EEVO+NVO’ use different physical processes to achieve desired the engine-outlet temperature without requiring EMP control. LEVO based strategies achieve similar OCE as that of ‘TM baseline’ operation, while having nearly unchanged CCE and ME. ‘EEVO+NVO’ achieves desired engine-outlet temperature by decreases in both OCE (due to negative valve overlap and IVO timing used) and CCE (due to early EVO).

Figure 3.4(e) shows that mechanical efficiency remains nearly unchanged amongst the various strategies, which is expected because mechanical efficiency is largely a function of speed.

Figure 3.4(f) compares turbocharger turbine speed for the different strategies. An increase in turbine speed is observed from ‘TM baseline’ to ‘TM baseline w/o EMP control’ due to difference in VGT position and increased exhaust flow rate. The increase in turbine speed from ‘TM baseline w/o EMP control’ to the LEVO based strategies is partly an effect of using late exhaust valve opening, due to the rapid expulsion of compressed exhaust gases during the exhaust stroke. The LEVO based strategies have higher fuel consumption than ‘TM baseline w/o EMP control’, which also contributes to higher turbine speed. Decrease in turbine speed from ‘LEVO’ to ‘LEVO+Reinduction’ is due to use of EGR and the subsequent decrease in exhaust flow rate. ‘LEVO+Reinduction’ and ‘LEVO+NVO’ have similar turbine speed, due in part to similar exhaust flow rates.

'EEVO+NVO' has higher turbine speed compared to 'TM baseline w/o EMP control' and 'TM baseline'. This can be accounted to higher turbine inlet exhaust gas enthalpy which arises from an earlier blow–down.

Figures 3.4(g) shows the enthalpy losses across the turbine. 'TM baseline' has the highest enthalpy loss across the turbine due to operation with a maximally shut VGT. Enthalpy drop across the turbine is lower for the strategies which do not use a maximally shut VGT. Lower enthalpy drop across the turbine indicates that a higher fraction of the turbine inlet exhaust energy is available at turbine outlet, and therefore for similar or higher turbine inlet enthalpies as 'TM baseline', can result in higher turbine outlet (or engine-outlet) temperatures.

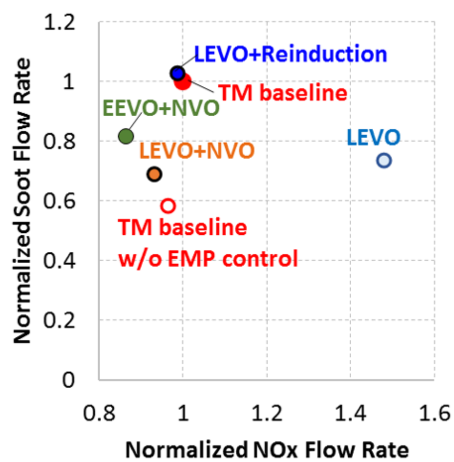

Fig. 3.5. Normalized engine-out NOx and soot emissions.

Figure 3.5 shows normalized engine-outlet soot and NOx flow rate. An effort was made to constrain the emission values to those of 'TM baseline'. 'TM baseline w/o EMP control' could meet the desired NOx constraint due to the lower level of EGR required, which could be achieved with a completely open EGR valve in the absence of EMP control. 'LEVO' does not have EMP control and results in 45% higher engine-out NOx than 'TM baseline' because of the insufficient difference between intake and exhaust manifold pressures, due to which sufficient external EGR cannot be driven even with a completely open EGR valve.

Engine-outlet NOx is still within Certified Clean Idle limit of 30 g/hr for 'LEVO'. The reason that 'TM baseline w/o EMP control' meets desired NOx constraints while 'LEVO' does not is the difference in fuel consumption, and hence the amount of EGR required for each of these strategies. Internal EGR is used with 'LEVO' to increase in-cylinder dilution and achieve desired values of engine-outlet NOx. 'LEVO+Reinduction' and 'LEVO+NVO' can achieve desired NOx values without an increase in engine-outlet soot. 'EEVO+NVO' uses internal EGR via NVO (in addition to external EGR) to reach desired limits for NOx. Unburnt hydrocarbon emissions (not shown) are within desired bounds.

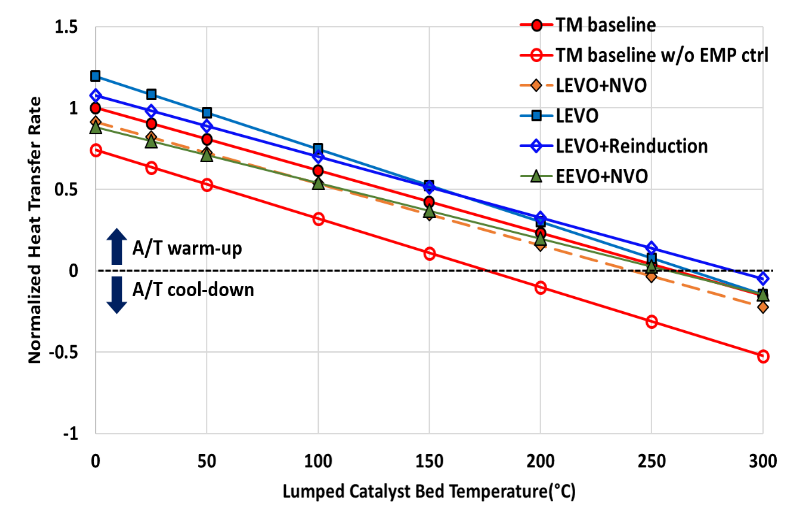

Fig. 3.6. Normalized heat transfer plots for different strategies at 800 RPM/1.3 bar show that without requiring EMP control, VVA based strategies can have very similar ATS warm-up performance compared to 'TM baseline'.

Figure 3.6 shows the normalized heat transfer curves for the different strategies, normalized with respect to 'TM baseline' operation. The catalyst bed temperature range of 0°C to 300°C is considered here as it corresponds to a cold ATS system being heated to temperatures consistent with desirable catalyst conversion efficiency.

It is desirable to have warm-up performance which closely matches, and is better than, that of 'TM baseline' within this catalyst temperature range. Figure 3.6 shows that 'TM baseline w/o EMP control' clearly has worse ATS warm-up potential than 'TM baseline' due to its lower engine-outlet temperature. 'LEVO' and 'LEVO+Reinduction' have slightly improved heat transfer to the catalyst compared to 'TM baseline' as a result of higher exhaust flow rate, and higher engine-outlet temperature, respectively. 'LEVO+NVO' has comparable exhaust flow rate, and lower engine-outlet temperature than 'TM baseline'; while 'EEVO+NVO' has lower exhaust flow rate and comparable engine-outlet temperature than 'TM baseline'. As a result, both these strategies have slightly lower warm-up performance compared to 'TM baseline'. It is important to note that the normalized heat transfer plot is a steady-state approximation of the ATS warm-up potential of any strategy.

A first law analysis of engine operation for the different strategies is shown in Figure 3.7. A breakdown of total fuel energy into brake power, exhaust power, frictional losses, pumping losses, in-cylinder heat losses, heat loss to the EGR cooler and other losses (such as turbine losses, CAC losses and manifold heat/friction loss) is shown. All values have been normalized with respect to the respective 'TM baseline' values.

Brake power is maintained constant for all the strategies because speed and load remain unchanged (800 RPM/1.3 bar BMEP). Exhaust power decreases for 'TM baseline w/o EMP control' compared to 'TM baseline' as the former strategy has significantly lower engine-outlet temperature. 'LEVO' has higher exhaust power than 'TM baseline' in spite of similar engine-outlet temperature - this is accountable to higher exhaust flow rate with 'LEVO'. 'TM baseline' and 'LEVO+NVO' have similar exhaust flow rate, with 'LEVO+NVO' resulting in lower engine-outlet temperature, explaining the difference in exhaust power for these two strategies. 'LEVO+Reinduction' has higher engine-outlet temperature and comparable exhaust flow rate than 'TM baseline', resulting in higher exhaust power in the former. Now, 'TM baseline' and 'EEVO+NVO' have similar engine-outlet temperature, but the former has higher exhaust flow rate, causing it to have higher exhaust power. A similar

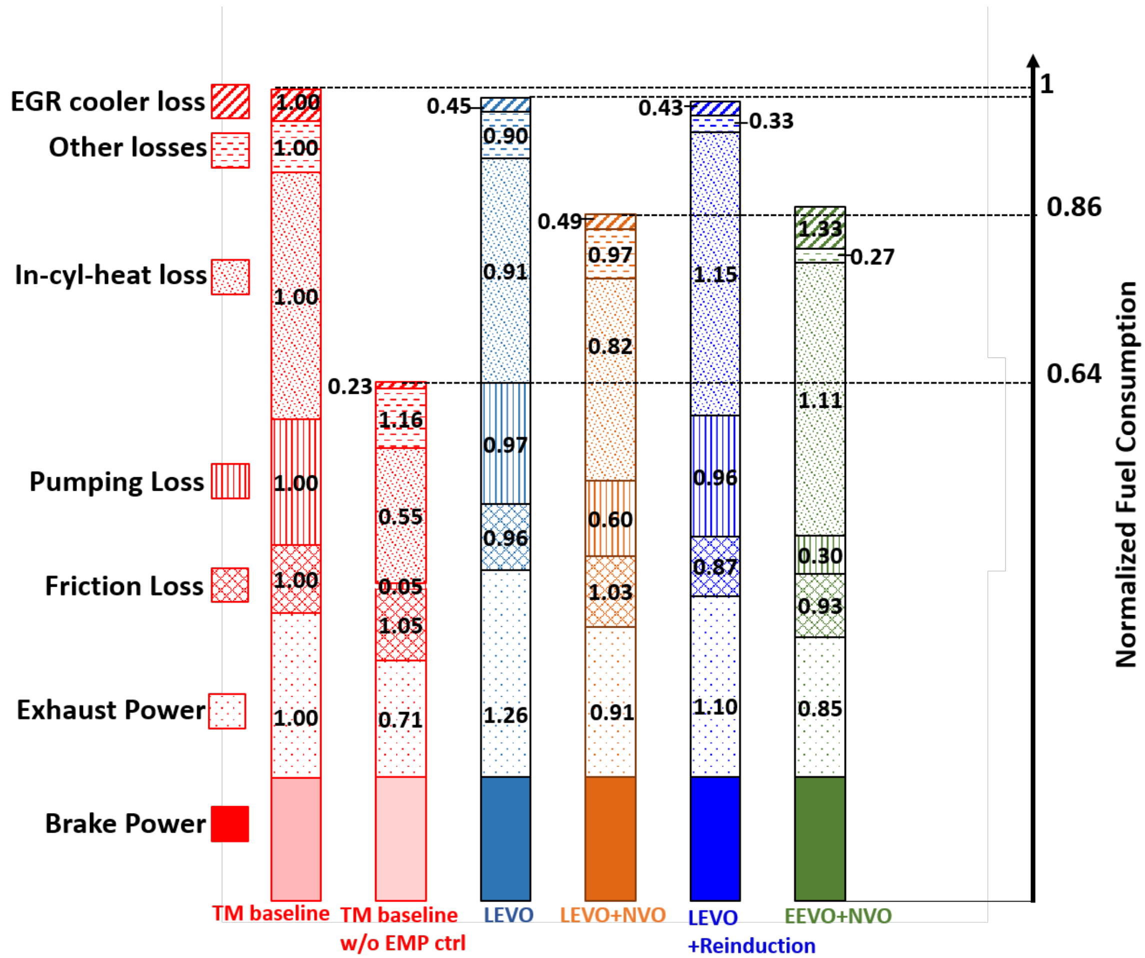

Fig. 3.7. Results of a first law analysis for the different strategies studied above. Similar exhaust power with 'TM baseline', 'LEVO', 'LEVO+Reinduction' and 'LEVO+NVO' is a contributing factor for their similar engine-outlet temperature. 'EEVO+NVO' has lower exhaust power due to lower exhaust flow rate. Frictional losses and pumping losses are comparable for 'TM baseline' and the LEVO based strategies, while being lower for 'EEVO+NVO'. EGR cooler losses are lower for 'LEVO' as sufficient external EGR could not be driven, while they still remain lower for 'LEVO+Reinduction' and 'LEVO+NVO' as these strategies use internal EGR.

reasoning can be used to explain the higher exhaust power with 'LEVO' compared to 'LEVO+NVO'. Combining LEVO operation with internal EGR via reinduction (as in 'LEVO+Reinduction') leads to a decrease in exhaust power compared to 'LEVO', however exhaust power is still higher than 'TM baseline'.

Frictional losses are observed to have small differences amongst the different strategies. 'LEVO+Reinduction' has lower frictional losses compared to other strategies.

'TM baseline w/o EMP control' has lower pumping losses compared to 'TM baseline' because of lower EMP. In general, the LEVO based strategies (except for 'LEVO+NVO') have similar pumping losses compared to 'TM baseline'. This is because 'LEVO' and 'LEVO+Reinduction' use recompression and throttling to achieve similar pumping losses as 'TM baseline'. 'LEVO+NVO' uses a relatively earlier EVO compared to the other LEVO strategies and results in relatively lower pumping losses. In the case of 'EEVO+NVO', the primary detriment to pumping efficiency is not being able to recover the recompression due to NVO on account of IVO close to BDC. Therefore, pumping losses are lower than those of any other exhaust valve profile modulation strategy shown here.

In-cylinder heat loss is higher with 'LEVO+Reinduction' and 'EEVO+NVO' compared to 'TM baseline'. In case of 'LEVO+Reinduction', exhaust gas reinducted during the intake stroke has lost heat to the exhaust manifold/cylinder walls before it is reinducted, which results in higher heat loss. 'EEVO+NVO' shows higher in-cylinder losses due to recompression of trapped exhaust gas which results in heat loss to cylinder walls.

Heat losses to the EGR cooler are directly related to the amount of external EGR used. 'LEVO' cannot reach the same levels of external EGR as 'TM baseline' and has lower EGR cooler heat loss. 'EEVO+NVO' has significantly higher EGR cooler heat loss than 'TM baseline'. This is partly due to the fact that the exhaust gas being recirculated is hotter (due to earlier EVO) and rejects more heat to the cooling circuit.

A key conclusion from this analysis is that 'LEVO+Reinduction' has nearly 50% lower heat loss to the EGR cooler than 'TM baseline', and results in higher engine-outlet temperature than 'TM baseline' while meeting desired NOx and soot constraints.

Table 3.2.
Summary of steady state results at 800 RPM/1.3 bar BMEP comparing ATS warm-up, fuel consumption and engine-out emissions of 'TM baseline' with strategies that use exhaust valve profile modulation and do not require EMP control.

Strategy	TM baseline	LEVO	LEVO+Reinduction	LEVO+NVO	EEVO+NVO
Similar/Better A/T warm-up	–	✓	✓	✓	✓
Lower/Similar Fuel Consumption	–	✓	✓	✓	✓
Lower/Similar Engine out NOx	–	✗	✓	✓	✓
Lower/Similar Engine out soot	–	✓	✓	✓	✓
EMP control not reqd.	✗	✓	✓	✓	✓

Table 3.2 summarizes the performance of the the different strategies studied in this section in comparison to 'TM baseline'.

3.4 Late exhaust valve opening (LEVO) + EMP control for improved ATS thermal management using exhaust manifold pressure control at 800 RPM/1.3 bar BMEP – both with, and without, relaxed engine-outlet emissions

The conventional thermal management strategy, 'TM baseline' uses a maximally shut VGT for exhaust pressure control to achieve engine out temperature of nearly

260°C and to drive external EGR. It also uses multiple, delayed injections. As a consequence of fuel-oil dilution impacts, injections timings delay must be limited. As a result, 'TM baseline' operation cannot be modified to obtain higher engine outlet temperature using conventional actuators without exceeding emission constraints.

This section explores the improvements in thermal management that are possible with the simultaneous use of EMP control and late exhaust valve opening (LEVO). Experimental results show that engine outlet temperatures in excess of 340°C can be achieved using LEVO + EMP control, with constrained engine out emissions and an increase in fuel consumption. It is further demonstrated that with relaxed engine-out emission constraints (primarily soot), late exhaust valve opening can result in superior thermal management.

Prior work has described the effect of early exhaust valve opening and negative valve overlap (AEEVO+NVO) to reach engine outlet temperature in excess of 400°C at 800 RPM/1.3 bar BMEP. This strategy resulted in high levels of engine-outlet soot. The reason for higher engine-outlet soot was theorized to be insufficient duration for post-combustion oxidation of soot, as exhaust valve opening was held relatively close to the top dead center.

As opposed to early exhaust valve opening, late exhaust valve opening allows for sufficient time duration for post-combustion oxidation of soot leading to relatively lower levels of engine-outlet soot. Delaying exhaust valve opening beyond BDC increases the pumping work required by the piston to expel the exhaust gases through the throttled exhaust valve, leading to increased fuel consumption and engine outlet temperature. Therefore, LEVO is a promising strategy for ATS thermal management with an improved trade-off between emissions and engine outlet temperature.

A description of the strategies is outlined next, followed by a discussion of steady state results.

Table 3.3 summarizes the EGR valve and VGT position for the various ATS warm-up strategies studied.

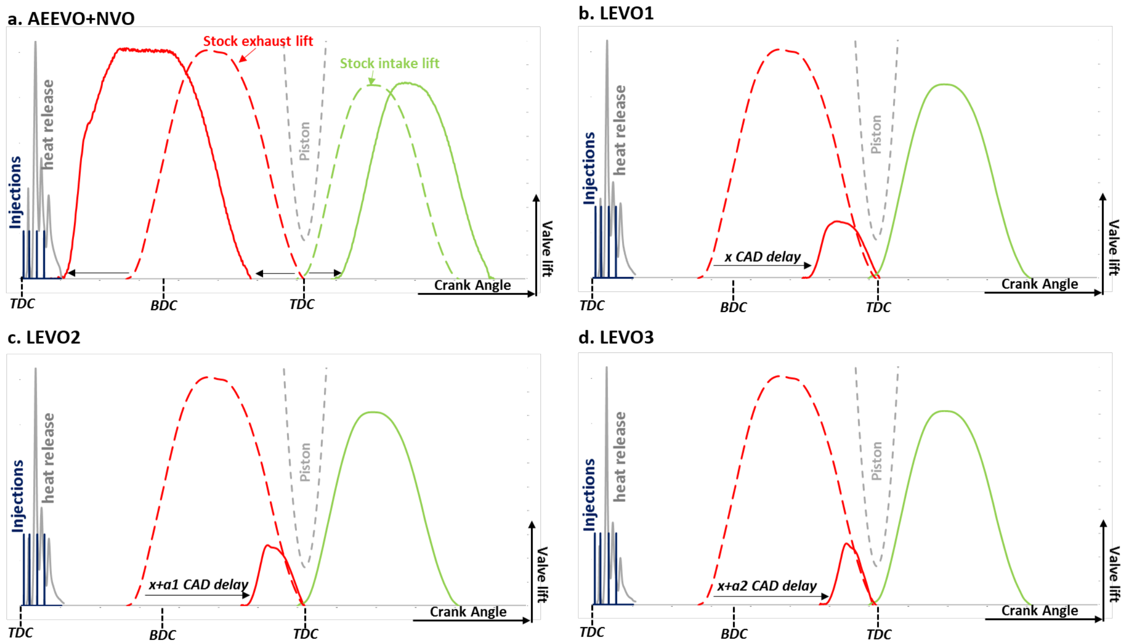

Fig. 3.8. Experimental heat release rates, injector current profiles and valve profiles used for the four ATS warm-up strategies. All strategies have the same commanded late injection profiles. (a) 'AEEVO+NVO' uses aggressively advanced exhaust valve opening, advanced exhaust valve closing along with delayed intake valve opening and closing. (b), (c) and (d) use delayed exhaust valve opening, with the delay increasing progressively for each of these cases (i.e. 0<a1<a2).

Table 3.3.
Summary of VGT and EGR Positions

Strategy	VGT Position	EGR Valve Position
TM baseline	Maximally shut	Slightly open
Modified TM baseline	Maximally shut	Slightly open
AEEVO+NVO	Relatively unrestricted	Completely shut*
LEVO1	Restricted (not maximally shut)	Completely open
LEVO2	Restricted (not maximally shut)	Completely open
LEVO3	Restricted (not maximally shut)	Completely open

**Uses only internal EGR*

3.4.1 Description of Additional Strategies

(a) *AEEVO+NVO [18]* – Aggressive early exhaust valve opening with negative valve overlap or 'AEEVO+NVO' was explored in a prior study, and used early exhaust valve opening (advanced by 100 CAD compared to nominal EVO), and negative valve overlap between the intake and exhaust valves (as shown in Figure 3.8(a)) to achieve higher engine outlet temperature than 'TM baseline'. Intake valve profile was also modulated by delaying IVO and IVC. Multiple, delayed injections were used. This strategy used a relatively unrestricted VGT position, as sufficient internal EGR achieved via NVO eliminated the need to use external EGR. Delayed IVC also assisted with NOx control via reduced ECR. As a result, this strategy did not require EMP control.

(b) *Modified TM baseline* – This strategy is obtained by modifying 'TM baseline' operation by using conventional actuators only (no VVA) to obtain higher engine outlet temperature, albeit with relaxed emission constraints. EGR valve position, rail pressure and fuel injections quantities (not main quantity) are modified.

(c) *LEVO 1, LEVO 2, and LEVO 3* – These strategies use progressively delayed EVO, with EVO delayed by 135 CAD, 150 CAD and 160 CAD respectively, compared to stock EVO timing. The corresponding valve profiles are shown in Figure 3.8(b), (c) and (d), respectively. These strategies also use multiple, delayed injections. Exhaust manifold pressure was controlled as required to drive sufficient external EGR for engine-out NOx control.

3.4.2 Discussion of Results

Figure 3.9 shows the in-cylinder pressure versus volume plot over an engine cycle for each strategy. 'TM baseline' incurs a large pumping loop due to elevated exhaust manifold pressure as a result of oversqueezed VGT. 'AEEVO+NVO' uses an exhaust valve opening that is advanced by 100 CAD compared to stock timing, which results in an early blow down. This strategy also uses advanced exhaust valve closing, and a phased intake valve profile for achieving internal EGR. Intake valve opening and intake valve closing are both delayed as compared to stock timings. 'AEEVO+NVO' also shows lower in-cylinder pressure during compression - this is an effect of using delayed IVC (delayed by 25 CAD compared to stock IVC timing). Delayed IVC leads to reduction in charge (EGR + fresh air) flow as well as the effective compression ratio. Increase in in-cylinder pressure corresponding to advanced exhaust valve closing can be obeserved which results due to recompression of trapped exhayst gas. 'LEVO1', 'LEVO2' and 'LEVO3' use increasingly delayed exhaust valve opening. This results in recompression of the combusted exhaust gas. In-cylinder pressure at the end of the exhaust stroke (close to TDC) increases due to higher exhaust manifold pressure required for driving external EGR.

Figure 3.10(a) shows the trade off between fuel consumption and engine outlet temperature.

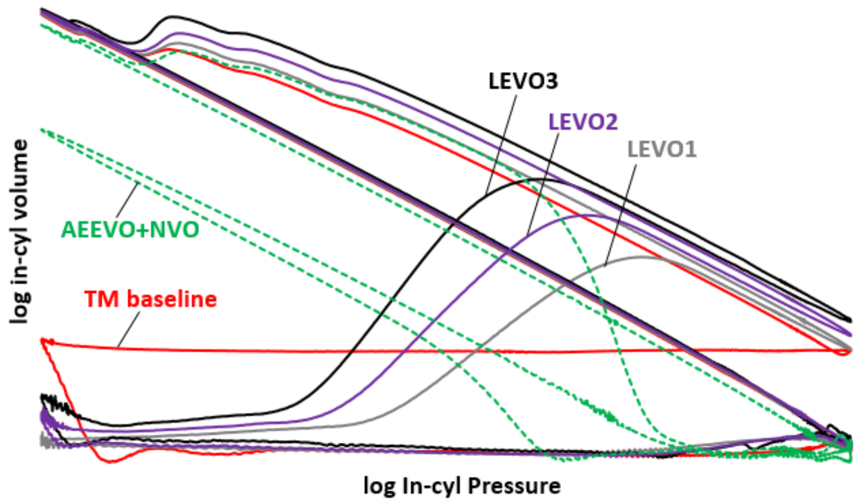

Fig. 3.9. Plot of log pressure-log volume shows that 'TM baseline' has a large pumping loop, which is due to operation with a maximally shut VGT. Earlier EVO in 'AEEVO+NVO' exhibits earlier blow down, and also undergoes recompression after the exhaust stroke due to advanced exhaust valve closing, resulting in increased pumping loss. The LEVO based strategies incur high pumping losses due to recompression resulting mainly from later exhaust valve closing.

'Modified TM baseline' results in 40°C higher engine outlet temperature with 18% higher fuel consumption than 'TM baseline'. Increase in fuel consumption is accounted to increase in pumping work due to a more restricted EGR valve position, and a decrease in closed cycle efficiency due to fuel quantity modifications. This strategy is representative of the maximum engine outlet temperature obtainable using conventional actuators (without VVA).

'AEEVO+NVO' reached engine outlet temperature in excess of 400°C at a fuel consumption penalty of 42% compared to 'TM baseline'.

Using late exhaust valve opening, 'LEVO1' results in nearly 80°C higher engine outlet temperature than 'TM baseline' with 25% higher fuel consumption. 'LEVO2' uses EVO delayed by 90 crank angle degrees after BDC, resulting in 140°C higher engine outlet temperature than 'TM baseline' with 54% higher fuel consumption. 'LEVO3' uses EVO delayed by 100 crank angle degrees after BDC, resulting in 200°C

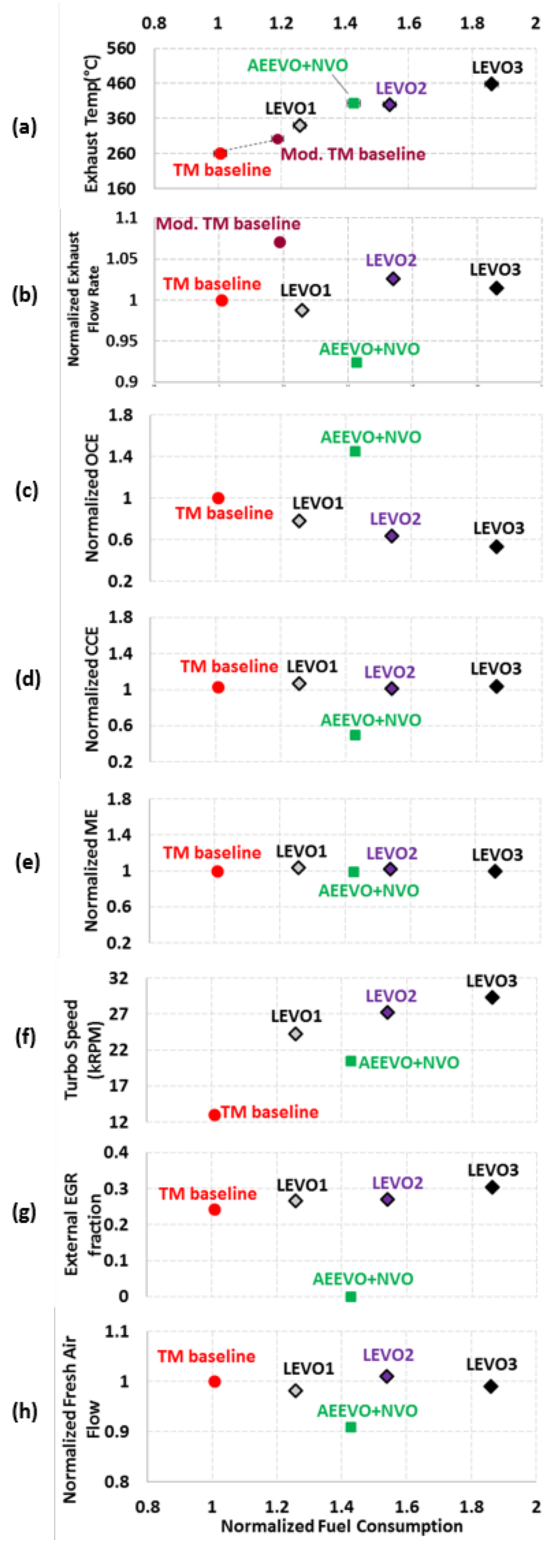

Fig. 3.10. Experimental steady state results at 800 RPM/1.3 bar. Progressively delaying exhaust valve opening leads to increase in fuel consumption, and results in an increase in engine outlet temperature. Due to the effects of LEVO on turbocharger turbine operation, exhaust flow rate is maintained similar to 'TM baseline' in spite of having to use more external EGR.

higher engine outlet temperature than 'TM baseline' with 86% higher fuel consumption. Engine out temperature achieved with 'LEVO 3' is sufficiently elevated for active regeneration of DPF. This plot highlights the trade-off achieved between engine-outlet temperature and fuel consumption by using LEVO. Moving along this trade-off by changing EVO can result in strategies with constrained emissions and superior thermal management compared to 'TM baseline' (example, 'LEVO1'); or strategies with relaxed emission constraints and improved thermal management in comparison to the 'TM baseline' (example, 'LEVO2' and 'LEVO3').

Figure 3.8(b) shows the exhaust flow rates resulting from the above ATS warm-up strategies. Exhaust flow rate decreased in 'AEEVO+NVO' compared to 'TM baseline' due to the use internal EGR for NOx control. As a result of having to use higher quantity of internal EGR, the displaced fresh air flow rate is larger, leading to a lower exhaust flow rate with 'AEEVO+NVO'. An exhaust flow rate similar to 'TM baseline' can be achieved with 'LEVO1'. Higher exhaust rates can be achieved with further delayed EVO, as seen in 'LEVO2' and 'LEVO3'. Higher exhaust flow rates with more delayed EVO are a result of increased turbine speed and higher fuel consumption.

Figures 3.10(c), (d) and (e) show results of cycle efficiency analysis. Higher open cycle efficiency with 'AEEVO+NVO' compared to the other strategies is a result of a less restricted VGT position. Open cycle efficiency progressively decreases with LEVO operation compared to 'TM baseline' due to increased throttling losses via late EVO; and also due to increasingly restrictive VGT positions. Note that 'LEVO1', 'LEVO2' and 'LEVO3' use a less shut VGT position compared to 'TM baseline'. Closed-cycle efficiency decreased with 'AEEVO+NVO' due to use of an early exhaust valve opening and also due to use internal EGR via NVO. CCE remains relatively constant between 'TM baseline' and the LEVO based strategies. Mechanical efficiency remains nearly constant for all strategies as it is primarily a function of engine speed.

Turbine speed for each of the strategies is shown in Figure 3.10(f). Increased turbine speed from 'TM baseline' to 'AEEVO+NVO' results from early exhaust valve opening, which causes increased enthalpy at turbine inlet. The increase in turbine speed for the LEVO-based strategies apparently results from an increase in kinetic energy of the compressed exhaust gases (due to LEVO) as they are expelled from the cylinder through a throttled exhaust valve. Turbine speed is also influenced by fuel consumption. The increase in turbine speed results in higher intake manifold pressure, which allows for exhaust flow rate comparable with 'TM baseline' in spite of having to flow higher amounts of EGR for 'LEVO1', 'LEVO2' and 'LEVO3'.

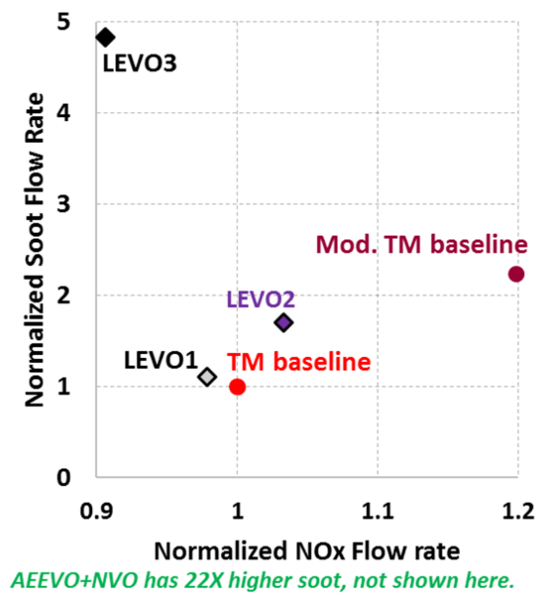

Fig. 3.11. Engine outlet NOx flow rate vs engine outlet soot flow rate for the different strategies. 'AEEVO+NVO' resulted in nearly 22 times higher engine out soot (hence not shown); while LEVO based strategies are able to achieve lower engine out soot than this with similar/improved ATS thermal management performance. 'Modified TM baseline' results in higher engine out emissions than desired.

Higher external EGR fractions for 'LEVO1', 'LEVO2' and 'LEVO3' are required in order to constrain NOx, as these strategies have higher fuel consumption compared to 'TM baseline'. This trend is shown in Figure 3.10(g). Fresh air flow rates consistent with the 'TM baseline' value are a result of increased turbine speed for the LEVO based strategies.

Figure 3.11 shows the trade off between engine outlet NOx and soot. 'AEEVO+NVO' was able to meet engine out NOx constraints by using only internal EGR, but had higher levels of engine-out soot (not shown in Figure 3.11). Similar emissions as 'TM baseline' can be achieved with LEVO (with higher engine-outlet temperatures).

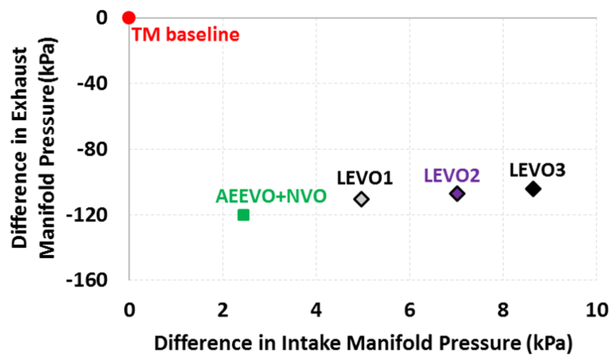

Fig. 3.12. Exhaust manifold pressures are lower for all strategies compared to 'TM baseline' mainly due to maximally shut VGT position in the latter. Intake manifold pressure increases with progressively delayed exhaust valve opening as a result of increasing boost.

The most aggressive LEVO case, 'LEVO3' nevertheless results in 5 times higher engine-out soot than 'TM baseline', while showing significant improvements in thermal management. 'Modified TM baseline' results in higher engine out soot and NOx than 'TM baseline', without ability to use any conventional actuator to control either of these emissions.

As per the plot of exhaust manifold pressure and intake manifold pressure (Figure 3.12), higher exhaust manifold pressure results in 'TM baseline'. The other strategies use a less restricted VGT position, and therefore exhibit lower exhaust manifold pressure. Increases in intake manifold pressure compared to 'TM baseline' are due to increased turbine speed. Turbine speed increments are accountable to reasons discussed earlier.

Normalized heat transfer plots shown in Figure 3.13 indicate that thermal management performance superior to 'TM baseline' can be achieved using exhaust valve profile modulation while using EMP control.

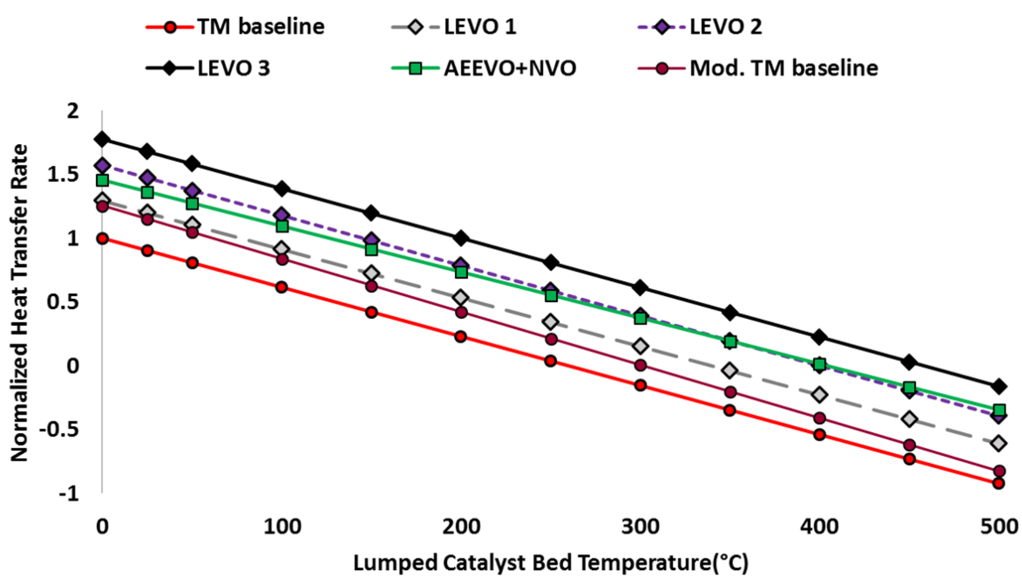

Fig. 3.13. Normalized heat transfer rates for the ATS warm-up strategies discussed earlier. All the strategies show improvements in thermal management compared to 'TM baseline'.

Table 3.4 summarizes the performance of the the different strategies studied in this section.

3.5 Late Exhaust Valve Opening (LEVO) vs Exhaust Throttle Valve (ETV)

Many strategies discussed in this chapter used late exhaust valve opening (LEVO) to increase engine-outlet temperature via increased pumping and throttling losses. A natural question is whether similar performance can be achieved by using an exhaust throttle valve downstream of the turbocharger turbine. A detailed response to this question is beyond the scope of this work, however a few hypothesized differences can be considered based on observations from this study, and are briefly discussed below.

- Soot accumulation on valve – Due to direct contact with the combustion process, soot accumulation on the exhaust valve can be hypothesized to be less concerning if LEVO were used, compared to soot accumulation on an exhaust throttle downstream of the turbocharger turbine. This is because every combustion cycle, the accumulated soot can get oxidized, at least partially.

- Effects on turbocharger turbine speed – LEVO enabled increases in turbine speed. Since an exhaust throttle valve would be downstream of the turbocharger turbine, such an effect cannot be expected to occur.

- Ability to influence external EGR flow – LEVO cannot influence directly the amount of external EGR being recirculated; while, by virtue of being a restriction downstream of the turbocharger turbine, an exhaust throttle valve can potentially influence external EGR flow.

Table 3.4.
Summary of steady state results at 800 RPM/1.3 bar BMEP comparing ATS warm-up, fuel consumption and engine-out emissions of 'TM baseline' with strategies that use exhaust valve profile modulation with EMP control.

Strategy	TM baseline	Modified TM baseline	AEEVO+NVO	LEVO1	LEVO2	LEVO3
Improved A/T warm-up	–	✓	✓	✓	✓	✓
Increase in fuel consumption	–	*18%*	*42%*	*25%*	*54%*	*86%*
Similar/lower Engine out NOx	–	✗	✓	✓	✗	✓
Similar Engine out soot	–	✗	✗	✓	✗	✗
Exh. pressure control not reqd.	✗	✗	✓	✗	✗	✗

3.6 Summary

This chapter demonstrated that in the absence of exhaust manifold pressure control, exhaust valve modulation performs just as well as the conventional thermal management operation, with similar/improved fuel efficiency and similar/better engine out emissions. Late exhaust valve opening with internal EGR via reinduction (LEVO+Reinduction) could reach exhaust temperatures greater than 287°C, while LEVO with internal EGR via NVO (LEVO+NVO) could reach slightly lower temperatures (nearly 240°C) with 15% lower fuel consumption. The latter strategy has increased relevance if newer catalysts with improved conversion efficiency at lower temperatures are considered, and also in the case where close-coupled aftertreatment systems are used. Early exhaust valve opening with internal EGR via NVO (EEVO+NVO) can reach similar exhaust temperature as conventional thermal management, with 8.3% lower fuel consumption, 14% lower engine out NOx and 19% lower engine out soot. This strategy involves modifications to the exhaust profile alone (instead of both intake and exhaust profiles, as is generally observed for NVO).

Late exhaust valve combined with exhaust manifold pressure control can result in superior thermal management than that possible with conventional thermal management operation using conventional, non-VVA actuators. Exhaust temperatures in excess of 450°C were achieved, with a fuel consumption penalty, constrained engine-out NOx and a five fold increase in engine-out soot. This operation has the potential for active DPF regeneration at curb idle, which typically occurs at higher engine speeds and loads.

4. ASSESSMENT OF BENEFITS OF LATE EXHAUST VALVE OPENING FOR AFTERTREATMENT THERMAL MANAGEMENT AT OFF-IDLE OPERATING CONDITIONS

4.1 Motivation for Off-Idle Assessment of LEVO Thermal Management Performance

In the previous chapter, the utility of late exhaust valve opening (LEVO) in achieving desirable aftertreatment thermal management performance without requiring exhaust manifold pressure (EMP) control was demonstrated. The objective of this chapter is to answer the question whether LEVO can be used with equal effectiveness (as curb idle) at other operating conditions in the absence of EMP control.

In this chapter, LEVO is studied at off-idle conditions of 1000 RPM and 1200 RPM, in addition to 800 RPM, at loads between 2.5 bar BMEP and 10 bar BMEP to assess thermal management benefits with emulated fixed geometry turbine (FGT) turbocharger operation. These operating conditions are indicated on the speed-torque space as shown in Figure 4.1. Generated based on an AVL 8 mode analysis [35], this chart shows the fuel consumption of each representative speed-torque bubble for the HD-FTP cycle. The goal of this study is to assess whether LEVO sustains thermal management utility at other operating conditions. At engine speeds below 1600 RPM, the VGT is primarily used for exhaust pressure control for thermal management and to drive sufficient external EGR for NOx control, in addition to boost control. At relatively higher loads within this speed range, in addition to the above two functions, VGT also helps to control fresh air flow and boost. Hence the above mentioned off-idle conditions were selected. At higher speeds and loads (right-half of Figure 4.1), a more critical function played by the VGT is controlling boost, a functionality that

LEVO is hypothesized to not be able to perform as effectively as a VGT. At higher speeds and loads, as seen in Figure 4.1, VGT position is relatively unrestricted - this is done in order to prevent over boosting to maintain in-cylinder pressures below peak cylinder pressure limits, and for EGR fraction control.

The following sections discuss steady state results at 800 RPM, 1000 RPM and 1200 RPM.

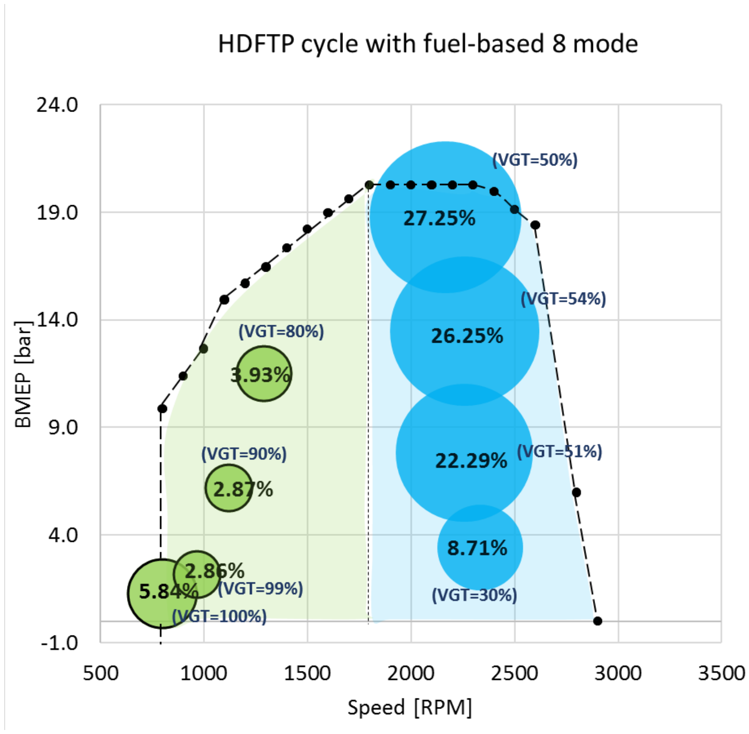

Fig. 4.1. Green bubbles indicate off-idle conditions studied for thermal management benefits of LEVO while using a fixed VGT position to indicate absence of EMP control. VGT positions in parentheses indicate stock values of VGT position during thermal management operation.

4.2 Steady State Results at 800 RPM

Steady state tests were carried out at 800 RPM/2.5 bar BMEP with VGT position set to 60% shut. This was done to emulate operation in the absence of EMP control.

EGR position and rail pressure were modulated to constrain NOx and soot emissions within desired limits. The engine was commanded to operate in thermal management mode and multiple delayed injections were used. EVO position was varied until turbine outlet temperature similar to stock thermal management operation could be achieved. Due to operation with VGT set to 60% shut, loss of back pressure resulted in reduction in amount of external higher pressure EGR that could be achieved (even with a completely open EGR valve). Internal EGR via exhaust reinduction was therefore required for sufficient in-cylinder dilution to achieve desired engine out NOx. At this operating condition, stock VGT position is completely shut. Higher loads than 2.5 bar BMEP were not studied because 2.5 bar BMEP is the maximum load at this speed as represented by the 8 mode analysis of the HD-FTP.

Figure 4.2 shows results for EVO delayed by 100 CAD and 105 CAD. Turbine outlet temperature, exhaust flow rate, turbo speed and cycle efficiency values are compared. Stock thermal management operation is referred to as 'Warm-up 6CF'. Both cases of LEVO are able to reach similar or higher TOT than stock operation, per Figure 4.2(a). Fuel efficiency improved by a maximum of 10% with LEVO, as in case of 'EVO220+reind'. This is due to significant improvement in OCE (Figure 4.2(c)) corresponding to operation with a less restricted VGT position (100% shut vs 60% shut). Exhaust flow rate is observed to increase with delayed EVO, this effect can be attributed to increase in turbo speed (Figure 4.2(f)) along with reduction in external EGR flow. Closed cycle efficiency and mechanical efficiency are nearly equivalent for LEVO and stock operation. Increase in turbo speed with LEVO is a result of increased velocity and enthalpy of the recompressed exhaust gas during exhaust stroke after EVO. LEVO cases require lower EGR fraction than 'Warm-up 6CF' for NOx control on account of lower fuel consumption – this is a contributing factor in increase in exhaust flow rate.

At this operating condition, sensitivity of most parameters to further late EVO is observed to increase (compared to operation at lower loads). With an additional 5 CAD delay in EVO, a 24°C increase in TOT is observed along with 6% higher fuel

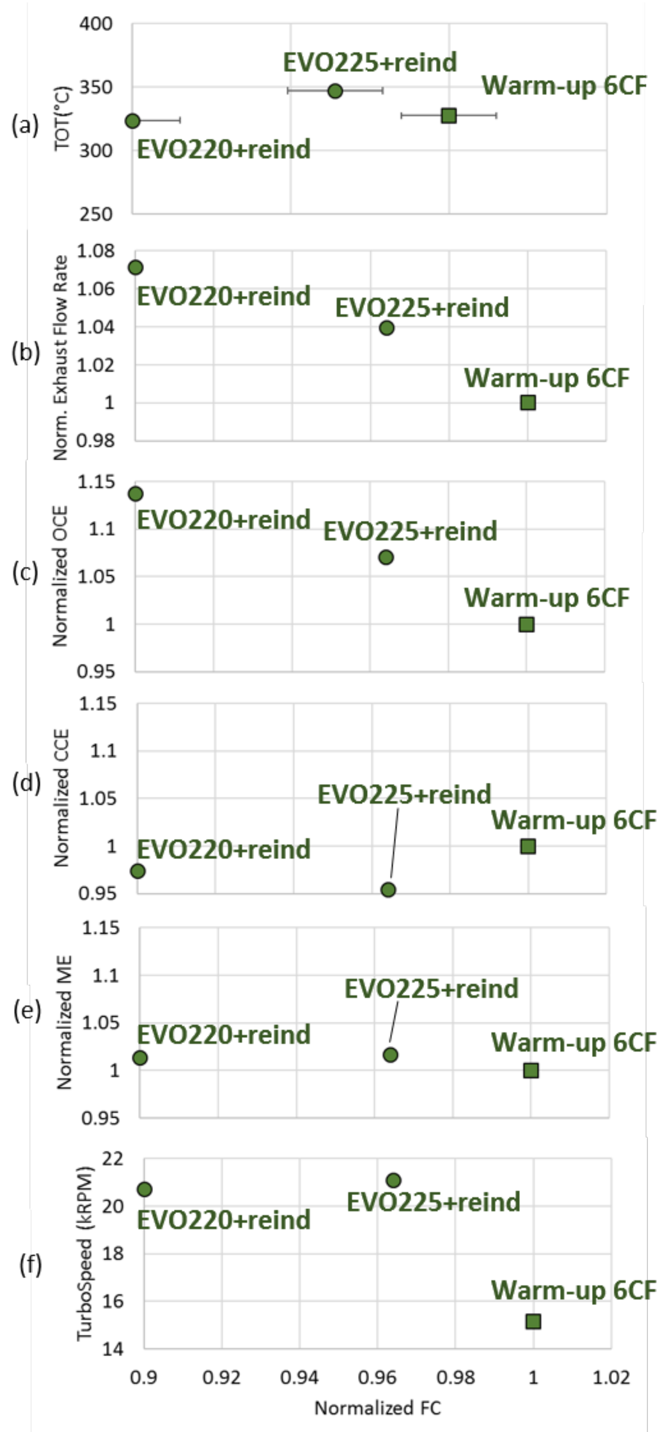

Fig. 4.2. Steady state results at 800 RPM/2.5 bar BMEP, with emulated FGT operation and delayed exhaust valve opening.

consumption. Exhaust flow rate decreases in case of 'EVO225+reind' compared to 'EVO220+reind' because a higher quantity of EGR is required for NOx control in the former.

'EVO220+reinduction' results in improved thermal management performance than stock thermal management operation (which requires EMP control) on account of similar TOT and higher exhaust flow rate. Operation with LEVO highlights the possibility of using earlier injections than those commanded by stock thermal management operation, because LEVO is capable of achieving desired TOT. This can lead to further reduction in fuel consumption and engine out NOx, while addressing (to some extent) concerns of cylinder wall-wetting associated with delayed injections.

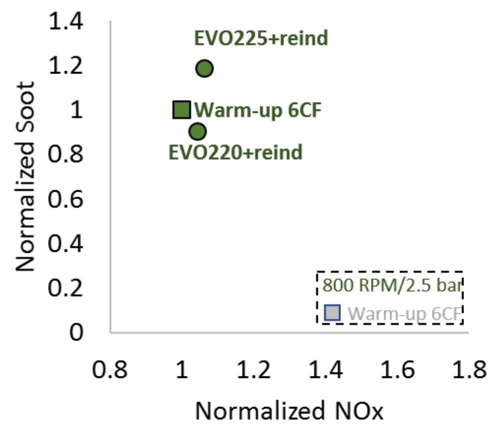

Fig. 4.3. Normalized engine out emissions for LEVO operation at 800 RPM/2.5 bar BMEP.

Figure 4.3 shows the normalized engine out emissions. 'EVO220+reind' is able to meet the desired emission constraints in the absence of EMP control, whereas 'EVO225+reind' results in higher soot because of larger EGR quantity used (as mentioned earlier). Note that LEVO operation also uses internal EGR in addition to external EGR for this operating condition. 'EVO220+reind' results in nearly 10% lower soot, which is a result of a combination of higher air-to-fuel ration and lower fuel consumption.

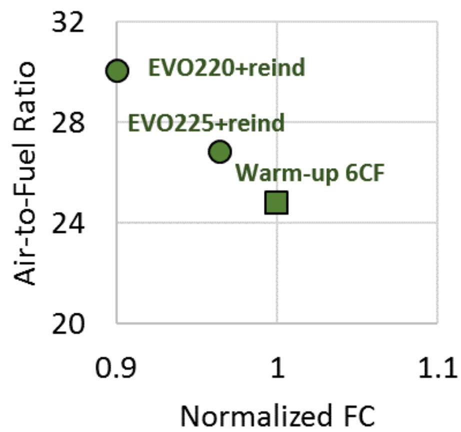

Fig. 4.4. Air to fuel ratio for LEVO operation at 800 RPM/2.5 bar BMEP.

Air-to-fuel ratio (AFR) is shown in Figure 4.4. 'EVO220+reind' has higher AFR than 'EVO225+reind' due to higher exhaust flow rate, while both cases of LEVO operation have higher AFR than stock thermal management operation.

4.3 Steady State Results at 1000 RPM

At 1000 RPM/1.3 bar BMEP, EVO delayed by 103 CAD can achieve similar fuel consumption, TOT and exhaust flow rate as stock thermal management operation, as seen in Figure 4.5(a-b). Exhaust flow rate does not increase as was previously observed, this is an effect of lower turbo speed. Open cycle efficiency improved by 4%, while closed cycle efficiency decreased by nearly 6%, and this result can be attributed to heat loss associated with recompression with LEVO. Mechanical efficiency improved by 2%. OCE improvement is accounted to operation with a less restricted VGT position. Neither 'Warm-up 6CF' or 'EVO223' use external EGR for NOx control, as this operating condition does not lie in the NTE region of the engine [36, 37]. This is also the reason that reinduction does not need to be used in conjunction with absence of EMP control for NOx control. Turbo speed decreases with use of LEVO, this is due to change in VGT position, wherein stock VGT position resulted in boost. Therefore, at 1000 RPM, emulated FGT operation (VGT 60% closed) has a stronger impact on exhaust flow rate than the 'recompress and expel' effect observed with LEVO, or the reduction in amount of external EGR driven.

Steady state results at 1000 RPM/2.5 bar BMEP are also shown in Figure 4.5. A delay of 100 CAD resulted in 13°C increase in TOT, with 4% lower fuel consumption. Exhaust flow rate also decreased. This is an effect of reduction in turbo speed due to change in VGT position. Improvements are observed in open cycle efficiency, while closed cycle efficiency and mechanical efficiency remain nearly unchanged. A greater decrease is observed in turbo speed (compared to 1000 RPM/1.3 bar BMEP), for a similar reason as mentioned earlier. With higher TOT and slightly decreased exhaust flow rate, LEVO can have competitive thermal management benefits compared to stock operation at this operating condition.

Engine out emissions are shown in Figure 4.6 and AFR is shown in figure 4.7. Emission constraints are within desired bounds for both 1.3 bar BMEP and 2.5 bar

BMEP operation at 1000 RPM. Reduction in AFR is consistent with higher load operation.

From this study, it appears that LEVO is able to reach desired elevated TOT for aftertreatment thermal management, however, slight detriments in exhaust flow rate (up to 4%) resulting from an emulated FGT position (and loss of EMP control) is observed. To validate this statement, the study was also carried out at 1200 RPM, and results are discussed in the next section.

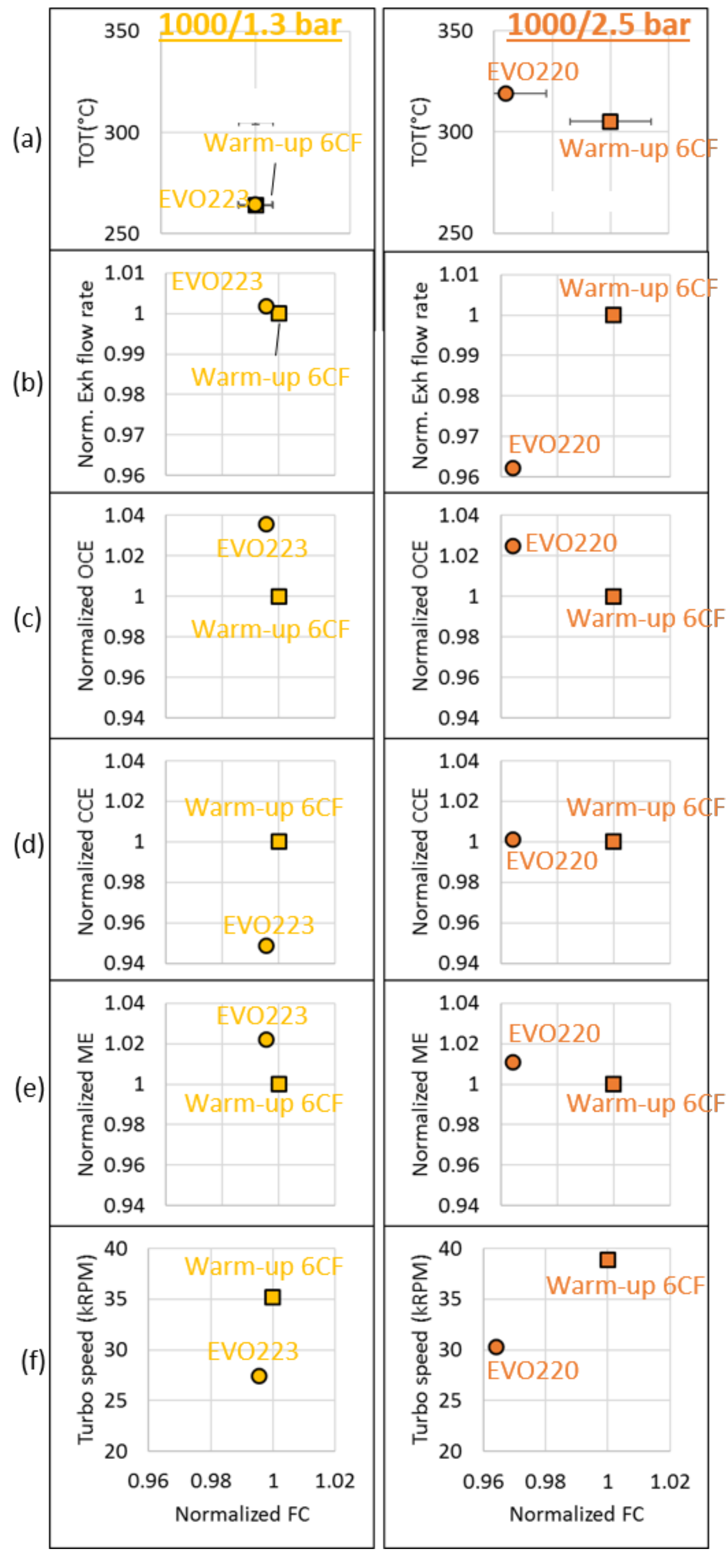

Fig. 4.5. Steady state results at 1000 RPM/1.3 bar BMEP and 1000 RPM/2.5 bar BMEP, with emulated FGT operation and delayed exhaust valve opening.

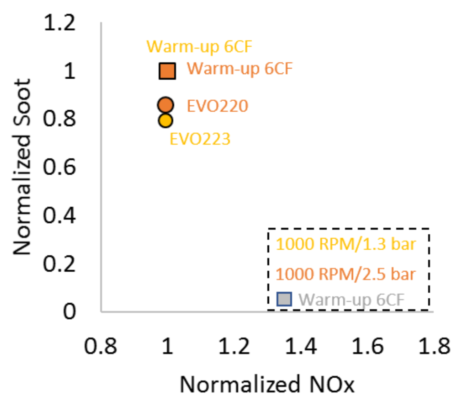

Fig. 4.6. Engine out emissions for LEVO operation at 1000 RPM/1.3 bar BMEP and 1000 RPM/2.5 bar BMEP, without EMP control.

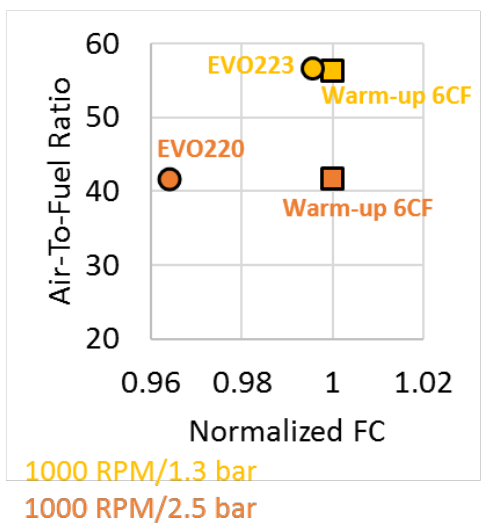

Fig. 4.7. Air-to-fuel ratio for LEVO operation at 1000 RPM.

4.4 Steady State Results at 1200 RPM

Screening at 1200 RPM was carried out at loads of 1.3 bar BMEP, 2.5 bar BMEP, 5 bar BMEP and 10 bar BMEP. Results for TOT, fuel consumption and other parameters are shown in Figure 4.8.

TOT increases as EVO is delayed by 102 CAD at 1200 RPM/1.3 bar BMEP, while fuel consumption and exhaust flow rate decrease. Decrease in exhaust flow rate and turbocharger turbine speed is a result of change in VGT position (and its effects on boost). LEVO cannot compensate for loss in boost associated with use of emulated FGT operation at this operating condition. Similar conclusions apply to results at 1200 RPM/ 2.5 bar BMEP. Operation at 1200 RPM also falls outside of the NTE zone, therefore neither stock thermal management operation or LEVO operation required use of EGR (external or internal).

Figure 4.9 and Figure 4.10 show engine out emissions and AFR, respectively. For operation at 2.5 bar BMEP, desired NOx constraint cannot be achieved. Use of internal EGR can reduce NOx for this case, along with hypothesized further reduction in exhaust flow rate.

Additional results at 5 bar BMEP and 10 bar BMEP are shown in Figure 4.11. Approximately 10% reductions in exhaust flow rate are observed here, albeit with similar TOT and lower fuel consumption. This can be hypothesized to be a concern during transient load changes. It can also be concluded that in the absence of EMP control and a wastegate/supercharger, benefits of using LEVO diminish with increases in load, and at operating conditions closer to the torque curve, LEVO can have a stay-warm utility rather than get-hot utility.

Figure 4.12 and Figure 4.13 show engine out emissions and AFR, respectively. A nearly three-fold increase in engine out soot is observed with LEVO operation at 1200 RPM/10 bar BMEP.

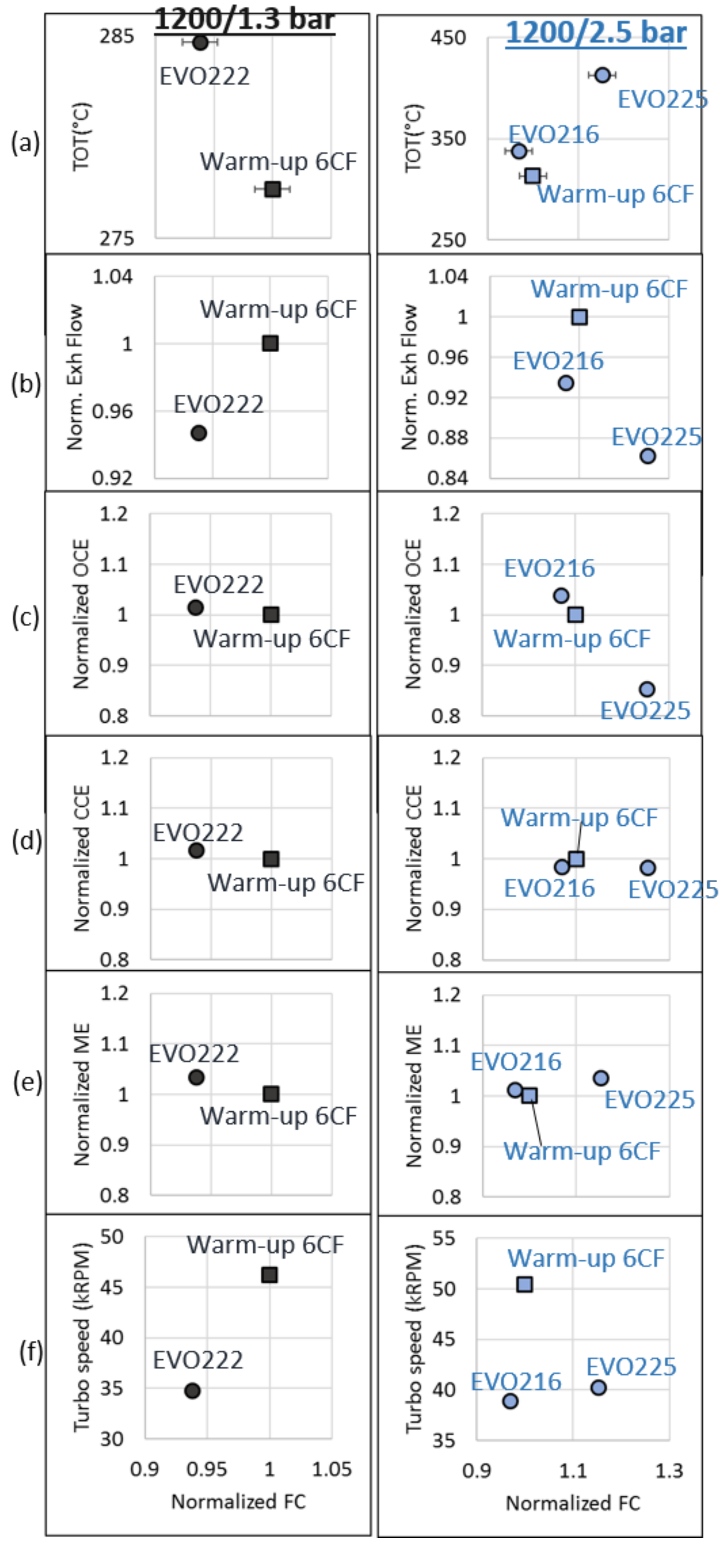

Fig. 4.8. Steady state results at 1200 RPM/1.3 bar BMEP and 1200 RPM/2.5 bar BMEP, with emulated FGT operation and delayed exhaust valve opening.

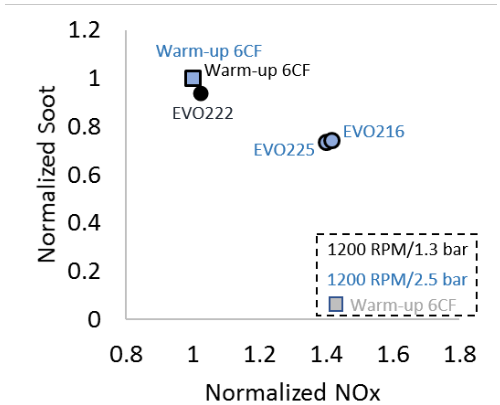

Fig. 4.9. Engine out emissions at 1200 RPM/1.3 bar BMEP and 1200 RPM/2.5 bar BMEP, using LEVO in the absence of EMP control.

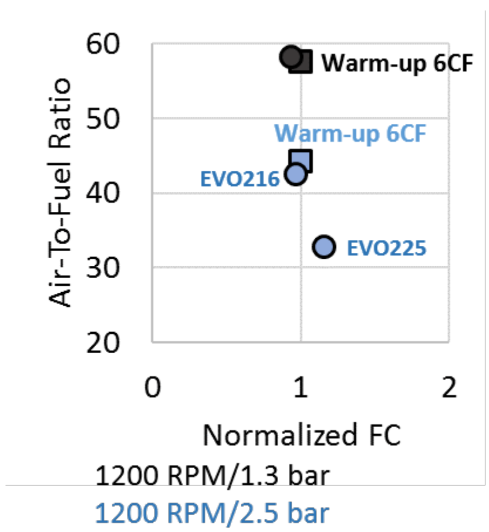

Fig. 4.10. Air-fuel ratio at 1200 RPM/1.3 bar BMEP and 1200 RPM/2.5 bar BMEP, using LEVO in the absence of EMP control.

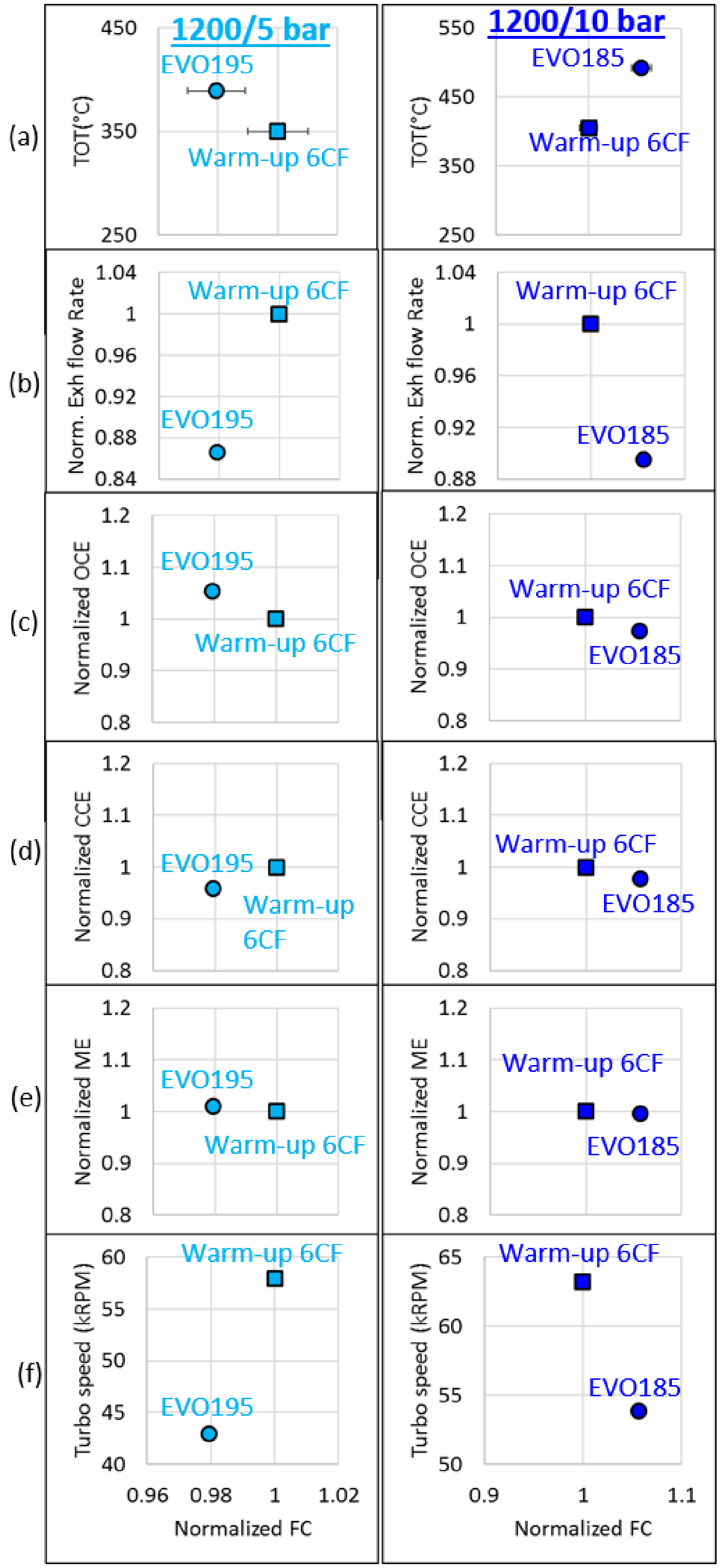

Fig. 4.11. Steady state results at 1200 RPM/5 bar BMEP and 1200 RPM/10 bar BMEP, with emulated FGT operation and delayed exhaust valve opening.

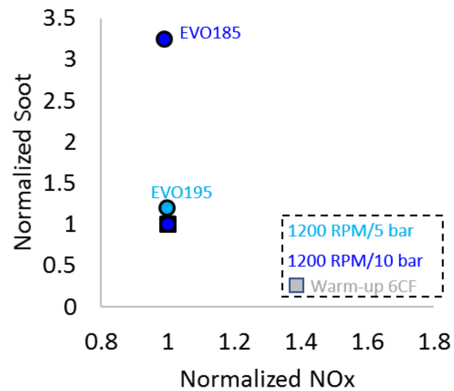

Fig. 4.12. Engine out emissions at 1200 RPM/5 bar BMEP and 1200 RPM/10 bar BMEP, using LEVO in the absence of EMP control.

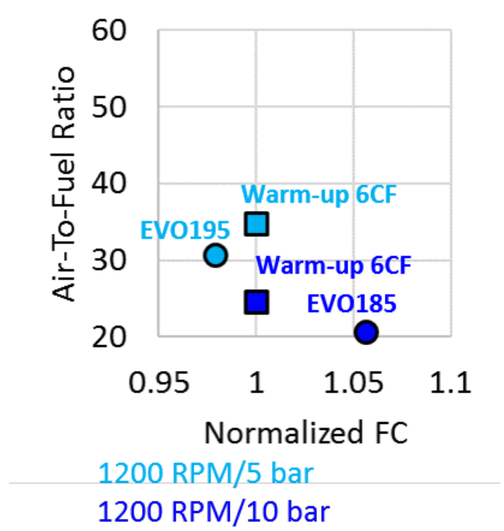

Fig. 4.13. Air-fuel ratio at 1200 RPM/5 bar BMEP and 1200 RPM/10 bar BMEP, using LEVO in the absence of EMP control.

4.5 Summary

A summary of key conclusions is shown in Table 4.1.

Table 4.1.
Summary of results of LEVO operation at off-idle operating conditions in the absence of EMP control.

Condition						
	TOT	Exh FR	FC	Emissions	Get-hot performance	Stay-hot performance
800/50 (EVO 230)	Y	Y	Similar	Y	Better	Similar
800/100 (EVO 225)	Y	Y	10% lower	Y	Better	Similar
1000/50 (EVO 223)	Y	Y	Similar	Y	Similar	Similar
1000/100 (EVO 220)	Y	Y	~3% lower	Y	Similar	Similar
1200/50 (EVO 222)	Y	~6% lower	~6% lower	Y	Similar/slightly lower	Better
1200/100 (EVO 216)	Y	~7% lower	~3% lower	40% higher NOx	Lower	Better
1200/200 (EVO 195)	Y	15% lower	~2% lower	20% higher soot	Lower	Better
1200/400 (EVO 185)	Y	10% lower	6% higher	3X soot	Lower	Better

Late exhaust valve opening with emulated FGT operation is an effective strategy for fuel efficient get-hot operation within a certain range of speed and load. Desired TOT, exhaust flow rate and engine out emissions can be achieved by exhaust valve modulation with possibility of reduced fuel consumption up to 1200 RPM/2.5 bar BMEP. Other potential advantages of LEVO include ability to use earlier injections timings, which can lead to further reduction in fuel consumption. Multiple values of delayed EVO were studied in order to assess whether a narrow range of values for delay in exhaust valve opening can be effective in achieving desired ATS thermal management performance across multiple operating conditions, a consideration which can influence the feasibility of hardware implementation of LEVO. It can be concluded that indeed, LEVO values for the different cases fall within a narrow window of 100 to 120 CAD delay from nominal, strengthening the advantages of implementation of LEVO on hardware.

At 1200 RPM (loads above 2.5 bar BMEP), where the functions of VGT include controlling boost (in addition to ATS thermal management), LEVO cannot compensate for loss of boost mostly associated with emulated FGT operation for the particular design on VGT used here. Desired TOT can be achieved, with lower exhaust flow rates. This implies slower aftertreatment warm-up (albeit more so for conventional ATS layouts than for modern closed coupled ATS layouts) and potentially slower transient load response. However, at these loads, LEVO can be thought to have stay-warm utility, while keeping a warmed-up aftertreatment system at desired temperature while reducing/maintaining fuel consumption. Transient response concerns for LEVO operation in such scenarios can be alleviated by use of FGT with a waste-gate, a clutched supercharger or an electrically driven supercharger.

5. CYLINDER DEACTIVATION WITH VARIABLE VALVE ACTUATION STRATEGIES FOR FUEL EFFICIENT AFTERTREATMENT STAY-WARM OPERATION

5.1 Literature Review

Cylinder deactivation is a popular technology for reducing fuel consumption in IC engines. Deactivating a certain number of cylinders results in an overall reduction in air flow through the engine, reduced pumping losses and is also desirable for fuel efficient thermal management of the ATS. Gasoline engines utilize CDA in order to minimize throttling losses at low to part load operations [38–40] as reduction in air flow rate through the engine enables operation with a more open throttle position. CDA has also been studied in diesel engines. CDA was studied at 800 RPM at a load of 0 bar BMEP and 0.3 bar BMEP to assess increases in exhaust temperature achievable via reduced exhaust flow rate, without consideration for EMP control or use of thermal management approach [41]. Capability of cylinder deactivation to reach temperatures capable of active DPF regeneration at highway cruise was studied in [42]. Transient performance while switching from CDA to six-cylinder operation was studied in [43]. Reduced fuel consumption over the HD-FTP drivecycle while maintaining desired ATS temperatures was demonstrated in [44].

5.2 Three Cylinder Operation With Flexible Valve Train Strategies

This section demonstrates the advantages of utilizing valve train flexibility in the active cylinders in three cylinder operation (3CF) for further improvements in fuel-efficient stay-warm operation. Specifically, following combinations of 3CF operation are considered.

1. 3CF with Late intake valve closing – This strategy uses delayed intake valve closing for the three active cylinders.

2. 3CF with internal EGR – This strategy studies effects of using internal EGR via negative valve overlap for the three active cylinders.

3. 3CF with early exhaust valve opening – The effect of using an early exhaust valve opening for the three active cylinders is considered.

The following subsection reviews the previously-seen results of 3CF without any valve train flexibility. Each of the above strategies is discussed in the following subsections. All the results were experimentally obtained at steady state operation at 800 RPM/1.3 bar BMEP.

5.2.1 Results of Three Cylinder Operation

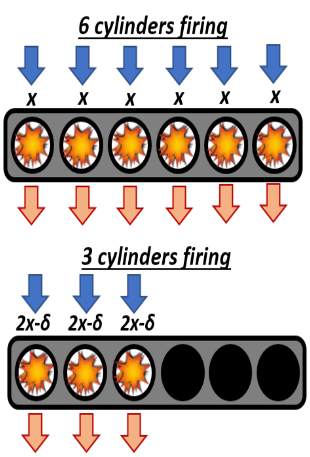

Fig. 5.1. 3CF involves deactivating both fueling and valve motion in the deactivated cylinders.

Figure 5.1 is a schematic for deactivating 3 cylinders. This schematic shows that one bank of cylinders is deactivated by cutting both fueling and valve motion in the inactive cylinders. In this way, only the active cylinders are breathing charge (fresh air+recirculated exhaust gas), which also results in reduction in the net fresh air flow to the engine.

The focus of this section is to review the benefits of 3CF when no other valve train functionality is used for the valve profiles of the active cylinders. Three strategies are compared, and each is described next.

(a) *FE 6CF* – This strategy corresponds to stock ECM calibration at curb idle, which has been optimized by the manufacturer of the engine for fuel efficiency. This operation uses two injections that are close to the TDC. It also relies on the use of a VGT in order to drive sufficient external EGR for NOx control. This strategy is not suitable for ATS thermal management because of lower TOT than desired.

(b) *Warm-up 6CF*– This strategy corresponds to stock thermal management calibration at curb idle. A maximally shut VGT along with delayed, multiple injections are used to achieve TOT and exhaust flow rate that can result in ATS warm-up consistent with meeting 2010 emission targets. A maximally shut VGT serves two purposes here – increasing TOT via increased back pressure, and driving sufficient external EGR.

(c) *Best BSFC 3CF* – This strategy corresponds to 3 cylinder operation optimized for fuel efficiency. Two injections close to the TDC are also used here. This strategy also relies on the use of VGT for driving sufficient external EGR for NOx control. This strategy is not the most suited if the target is ATS thermal management.

(d) *Stay-warm 3CF* – This strategy corresponds to 3 cylinder operation optimized for ATS thermal management. It uses two delayed injections in order to achieve TOT sufficient to maintain temperatures of an already warmed-up ATS. As a result, this strategy is very suitable for maintaining desirable ATS temperatures. An additional feature of this strategy is ultra-low levels of engine-outlet NOx and soot compared to stock operation, which makes this strategy an attractive option to maintain ATS temperature. The desirable reduction in engine-outlet NOx levels is a direct consequence of using delayed injections and reduction in exhaust flow rate.

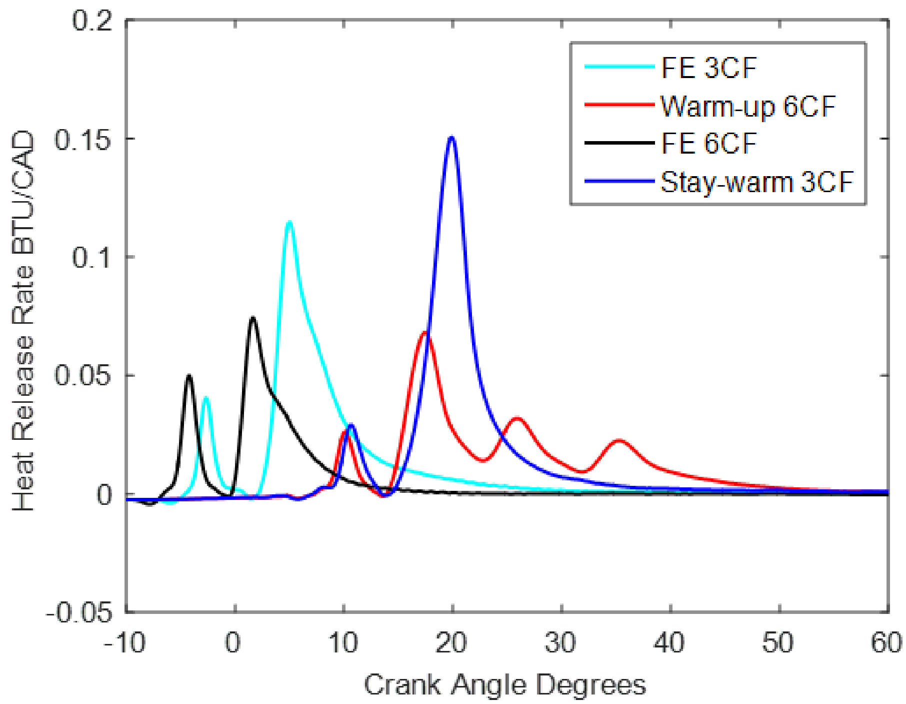

Fig. 5.2. Experimental heat release rates for 3CF and 6CF.

The heat release rate corresponding to three strategies introduced above is shown in Figure 5.2. 'FE 6CF' and 'Best BSFC 3CF' both use injections that are closer to TDC, and hence result in a heat release closer to TDC. 'Warm-up 6CF' shows a delayed heat release rate, along with four peaks as a result of using multiple, delayed injections.

The rate of heat release is higher for 3CF cases compared to the six cylinder operation. This is because the amount of fuel injected in the (active) cylinders with 3CF is twice than that injected in the six cylinder case. The heat release rate for

'Stay-warm 3CF' is more delayed as a result of delayed injections. The peak of the heat release is also higher than 'Best BSFC 3CF' due to higher fuel consumption.

Figure 5.3 shows the plot of in-cylinder pressure against volume for one engine cycle for the three strategies discussed above. 'FE 6CF' shows pressure rise due to combustion close to TDC, while 'Warm-up 6CF' shows pressure rise due to combustion further away. This difference is due to the injection strategy used. The delayed

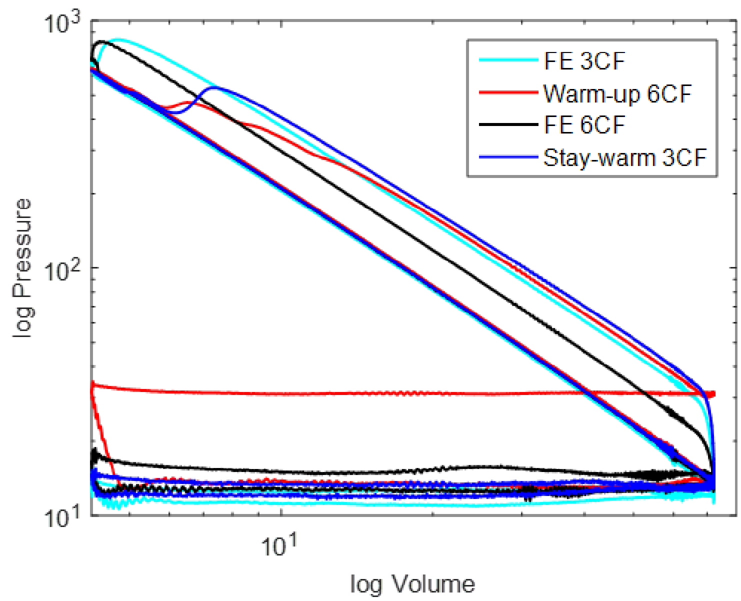

Fig. 5.3. Logarithmic plot of in-cylinder pressure against volume shows that the size of the pumping loop decreases with 3CF.

start of combustion for 'Stay-warm 3CF' is a result of using delayed injections. The area under the closed loop is higher for the 3CF cases compared to the 6CF case, and this due to increased quantity of fueling per cylinder for cylinder deactivation. Higher pressure during the expansion stroke for 'Stay-warm 3CF' compared to 'Best BSFC 3CF' is a result of delayed injections and higher fuel consumption in the former strategy.

A large pumping loop for 'Warm-up 6CF' is a result of using a maximally shut VGT. Such a VGT position leads to increased exhaust back pressure, and results in higher in-cylinder pressure during the exhaust stroke. This plot shows that the size of the pumping loop is significantly decreased for the 3CF cases compared to 6CF operation . The primary reason for this is the reduction in fresh air flow rate on deactivating three cylinders. This results in lower intake and exhaust manifold pressures. A secondary reason for the smaller pumping loop is the VGT position - 3CF cases use a VGT position that is relatively less restricted than VGT position used in 'FE 6CF' operation.

Figure 5.4 shows results the experimental results for TOT, fuel consumption and cycle efficiencies for the above strategies. 'Best BSFC 3CF' corresponds to the most fuel efficient 3CF operation which is optimized for fuel efficiency, while 'Stay-warm 3CF' uses two delayed injections for desired TOT. All results have been normalized with respect to 'FE 6CF'.

Figure 5.4(a) shows that TOT close to 260°C can be reached by using 'Warm-up 6CF', at a 60% fuel consumption penalty. Such elevated TOT is desirable for warming up of a cold ATS to achieve desired conversion efficiency of the ATS catalyst.'Best BSFC 3CF' results in nearly 50°C higher TOT compared to 'FE 6CF' with 15% lower fuel consumption. This is a result of deactivating cylinders. Cylinder deactivation results in reduction in air flow through the engine. Diesel engines usually run lean at low speed/low load conditions, in which the excess air acts as a heat sink. Reducing air flow therefore increases TOT. Decrease in fuel consumption is observed in case of 'Best BSFC 3CF' compared to 'FE 6CF'. This is a result of improved open cycle efficiency as is discussed later. It is important to note that neither 'Best BSFC 3CF' nor 'FE 6CF' have a TOT that is suitable for effective ATS thermal management. This is because ATS systems typically require operating temperature in the range of 200°C-250°C for acceptable conversion efficiency.

'Stay-warm 3CF' results in TOT close to 220°C due to the use of delayed injections. This TOT is favorable for ATS thermal management. Fuel consumption increases from 'Best BSFC 3CF' to 'Stay-warm 3CF' by nearly 10%, and this is due to reduction in closed cycle efficiency on account of delayed injections. Fuel consumption is nevertheless 4% lower than the stock fuel-efficient operation 'FE 6CF'.

Open cycle efficiency for each strategy is shown in Figure 5.4(b). 'Warm-up 6CF' has significantly lower OCE than the other strategies because of the large pumping loop. Both 3CF cases result in higher OCE than 6CF case due to reduction in fresh air flow through the engine.

Closed cycle efficiency for each strategy is shown in Figure 5.4(c). 'Best BSFC 3CF' results in higher CCE than 'FE 6CF' - this is a results of a sharper heat release rate profile, as thermodynamic efficiency of combustion process increases as the energy release process occurs in a shorter CAD duration. CCE decreases in 'Stay-warm 3CF' compared to 'Best BSFC 3CF' due to a delayed heat release profile - this is an effect of using delayed injections. 'Warm-up 6CF' has a low CCE due to a higher EGR fraction.

Mechanical efficiency is higher for 'Best BSFC 3CF' compared to the other cases. This is a combined effect of reduced frictional losses (as only half the number of cylinders are firing) and lower fuel consumption (which results in lower in-cylinder pressure and lower piston ring-to-wall friction).

OCE, CCE and ME contribute to brake thermal efficiency, which is inversely proportional to fuel consumption. As a result of 6% lower CCE, similar OCE and 6% lower ME, 'Stay-warm 3CF' results in higher fuel consumption than 'Best BSFC 3CF'.

Figure 5.5 shows TOT against normalized exhaust flow rate for the above strategies. As expected, 3CF cases result in significant reduction in air flow compared to 6CF case. Decrease in exhaust flow rate for 'Stay-warm 3CF' compared to 'Best BSFC 3CF' can be explained as follows – due to delayed injections, in-cylinder pressure at exhaust valve opening is higher. At a low speed/low load condition aas 800 RPM/1.3 bar BMEP, the boosting effect of the turbocharger is negligible. Therefore, the increased pressure difference between the intake and cylinder leads to increased backflow of exhaust gas, thereby displacing fresh air and resulting in lower fresh air flow rate. Exhaust flow rate is estimated as the summation of fresh air flow and fuel consumption, thus the decrease in fresh air flow rate results in lower exhaust flow rate. Fuel consumption increases, but the increase is still dominated by the decrease in fresh air flow rate.

Higher exhaust flow rate for 'Warm-up 6CF' is a combined result of maximally shut VGT position and higher fuel consumption.

Figure 5.6 shows normalized values of engine outlet soot and NOx. 'Warm-up 6CF' results in higher soot than 'FE 6CF' due lower air-to-fuel ratio. Lower NOx compared to 'FE 6CF' is a result of delayed injections. 'Stay-warm 3CF' results in nearly 60% lower NOx and 50% lower soot than 'FE 6CF'.

Higher engine out soot levels with the stock thermal management calibration 'Warm-up 6CF' (compared to 'FE 6CF') are acceptable because this strategy meets 2010 emission targets. Therefore, here on this work, an effort has been made to constrain engine-out soot to levels similar to or lower than 'Warm-up 6CF'.

The effects of combining intake valve modulation with 3CF operation will be discussed next. All the experimental data is normalized with respect to 'FE 6CF'. Efforts have been to constrain engine out emissions to values below those seen with 'Warm-up 6CF'.

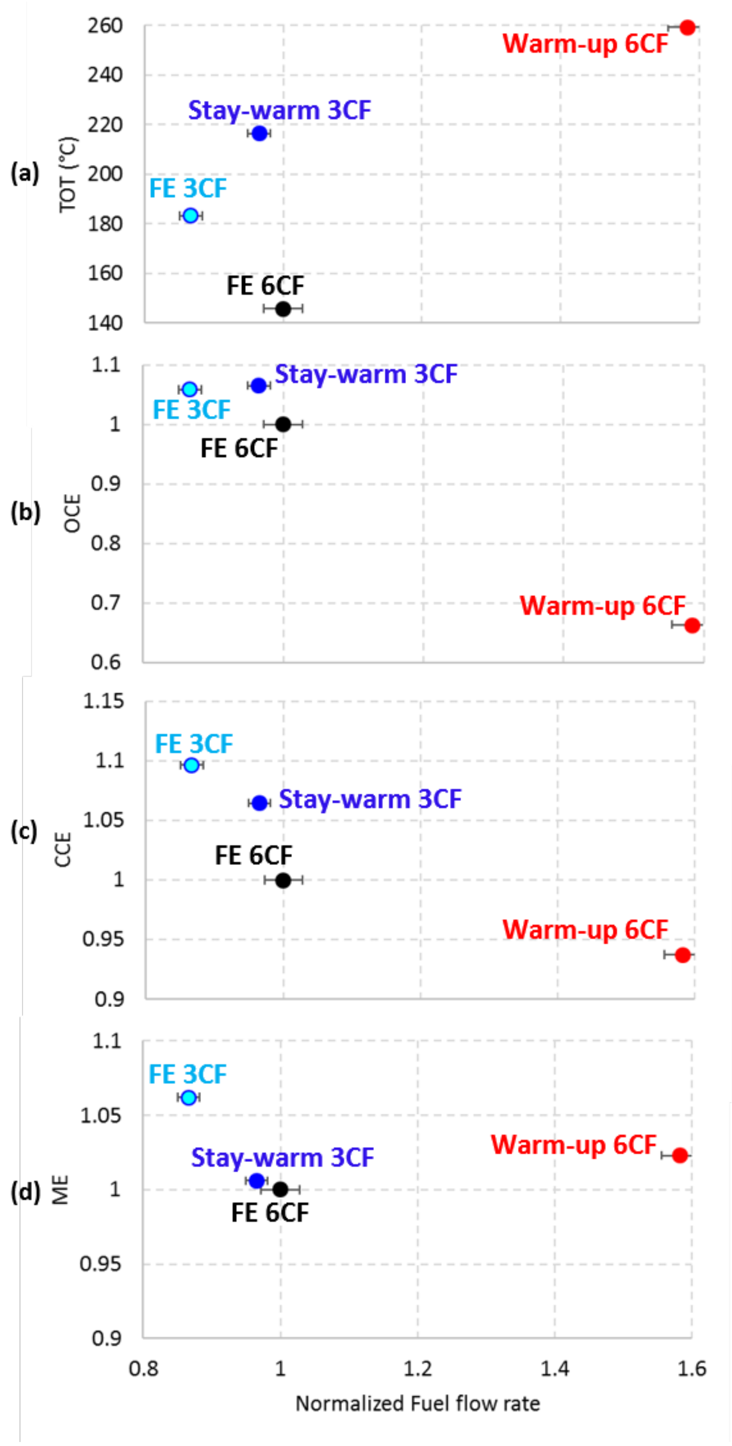

Fig. 5.4. Experimental steady state results at 800 RPM/1.3 bar BMEP for 3CF operation optimized for fuel efficiency, and stay-warm operation.

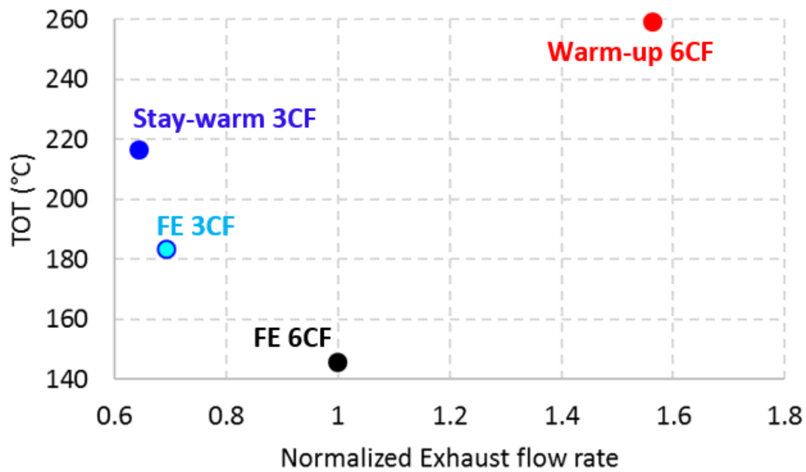

Fig. 5.5. Exhaust flow reduction with 3CF cases is the primary reason for lower fuel consumption compared to six cylinder operation. Data is normalized with respect to 'FE 6CF'.

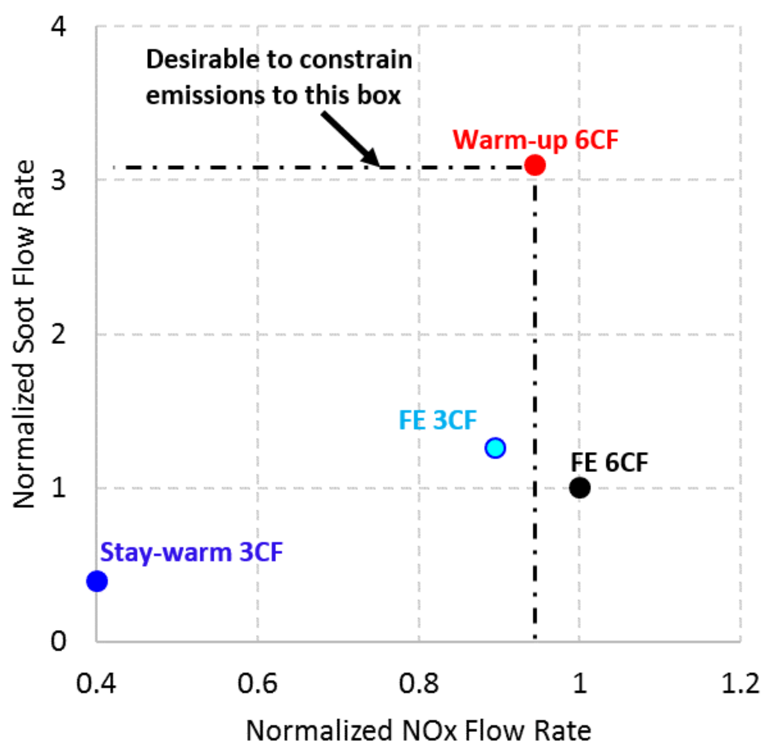

Fig. 5.6. Normalized engine outlet soot vs NOx for the different strategies.

5.2.2 Results of Three Cylinder Operation with LIVC

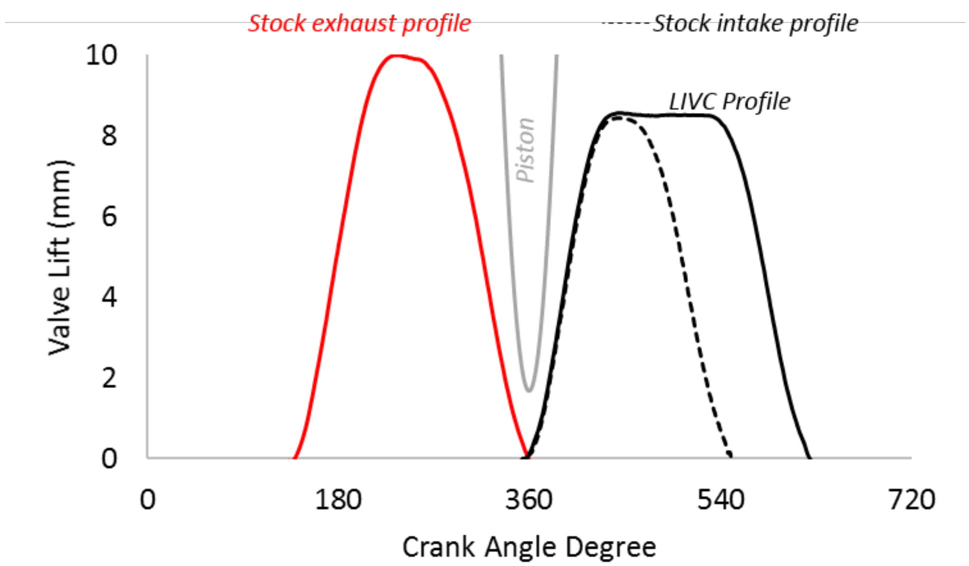

Fig. 5.7. Valve profiles for active cylinders with intake valve closing time delayed past stock values.

Intake valves of the active cylinders were modulated by delaying intake valve closing timing. Figure 5.7 shows the valve profiles for the active cylinders. The purpose of adding LIVC was to understand the effects of LIVC on emissions and thermal management performance.

A description of the strategies that use LIVC is follows next.

(a) *3CF LIVC 1* – This strategy uses a delayed IVC timing, along with a VGT position that is 79% shut, and two injections delayed by 4 CAD after TDC. It also uses external EGR.

(b) *3CF LIVC 2* – This strategy uses similar valve timings and settings as above, with a VGT position that is 45% shut. The goal of this strategy was to understand the effectiveness of reduced ECR (effective compression ratio) for engine-out NOx control without having to drive as much external EGR.

(c) *FE 3CF LIVC* – This is the most fuel efficient 3CF LIVC operation, while using an earlier injection timing (1 CAD after TDC) and VGT position 45% shut.

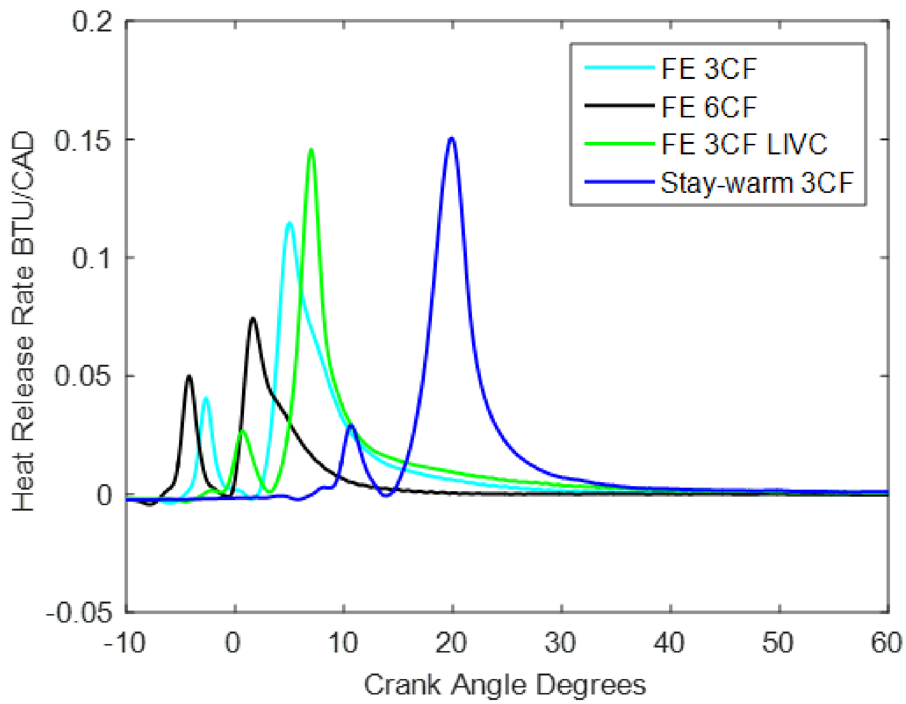

Fig. 5.8. In-cylinder heat release rates for 3CF operation with LIVC.

All the above LIVC strategies use the same delayed IVC timing. The differences arise in injection timings and VGT position, which were used to further optimize fuel consumption while maintaining desired TOT.

Heat release rates in the active cylinder are shown in Figure 5.8. 'FE 3CF LIVC' uses earlier injections compared to 'Stay-warm 3CF'. '3CF LIVC1' and '3CF LIVC2' use slightly delayed injections, and as a result, have delayed heat release rates.

Figure 5.9 shows the in-cylinder pressure for 3 cylinder operation when LIVC is used for the active cylinders. IVC is delayed by 75 CAD compared to stock IVC timing. As a result, the in-cylinder pressure remains similar to intake manifold pressure for some portion of the conventional compression stroke, in spite of the upward motion of the piston. Compression stroke starts much later after BDC, and hence a

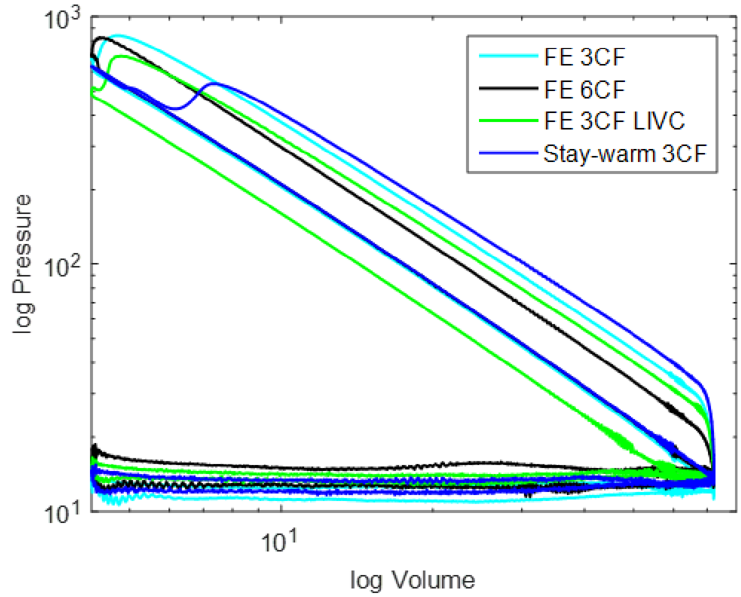

Fig. 5.9. P-V diagram for operation with LIVC results in reduced effective compression ratio.

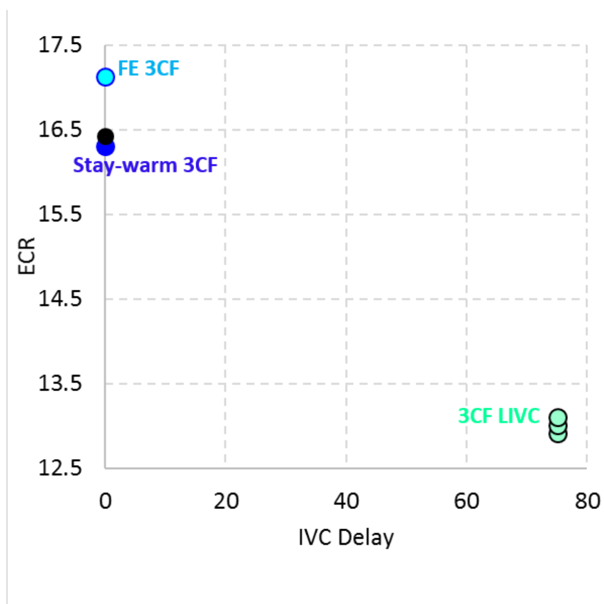

Fig. 5.10. Effective compression ratio decreases due to LIVC operation.

reduction in effective compression ratio can be seen. Figure 5.10 shows the ECR for the cases with LIVC operation, and highlights that ECR was reduced by nearly 3 by using late intake valve closing. Reduction in ECR enables lower engine-outlet NOx, and also allows advancing of injections to improve efficiency.

The experimental results for TOT, fuel, consumption and cycle efficiencies for the LIVC strategies are discussed next. All values are normalized with respect to 'FE 6CF', although data for 'FE 6CF' is not shown. This is done in order to clearly highlight the differences in 3CF and 3CF LIVC operation, which can be observed more effectively on an expanded y-axis scale.

Figure5.11(a) compares TOT and fuel consumption for 3CF LIVC with the other strategies. '3F LIVC1' and '3CF LIVC2' differ only in the VGT position used, with '3CF LIVC2' using a relatively unrestricted VGT position. Increase in TOT is due to less external EGR being driven, and hence reduced heat loss to the EGR cooler. Reduction in external EGR required is due to the ability of reduced ECR to mitigate NOx. The decrease in TOT from 'FE 3CF LIVC' is due to earlier injections in the latter case. 'FE 3CF LIVC' can result in similar TOT as 'Stay-warm 3CF', with 6% lower fuel consumption, while using considerably earlier injection timings.

Figure 5.11(b) shows OCE for the 3CF LIVC cases relative to other strategies. OCE increases by a small amount from '3CF LIVC1' to '3CF LIVC 2' due to the difference between VGT position and the subsequent reduction in air flow rate. OCE remains nearly similar between '3CF LIVC2' and 'FE 3CF LIVC'.

Closed cycle efficiency (Figure5.11(c)) can be said to be very similar for 'Stay-warm 3CF', '3CF LIVC1' and '3CF LIVC2' although the 3CF cases use relatively earlier (7 CAD earlier) injection timing. CCE increases for 'FE 3CF LIVC' as it uses the earliest injection timing among the 3CF LIVC strategies. Mechanical efficiency does not seem to follow any particular trend for the 3CF LIVC cases compared to 'Stay-warm 3CF'.

Exhaust flow rate is the summation of fresh air flow and fuel consumption. Exhaust flow rate increases from '3CF LIVC1' to '3CF LIVC2' due to change in VGT position which reduces the difference between intake and exhaust manifold pressure, and leads to lowered external EGR flow. Exhaust flow rate then decreases when in-

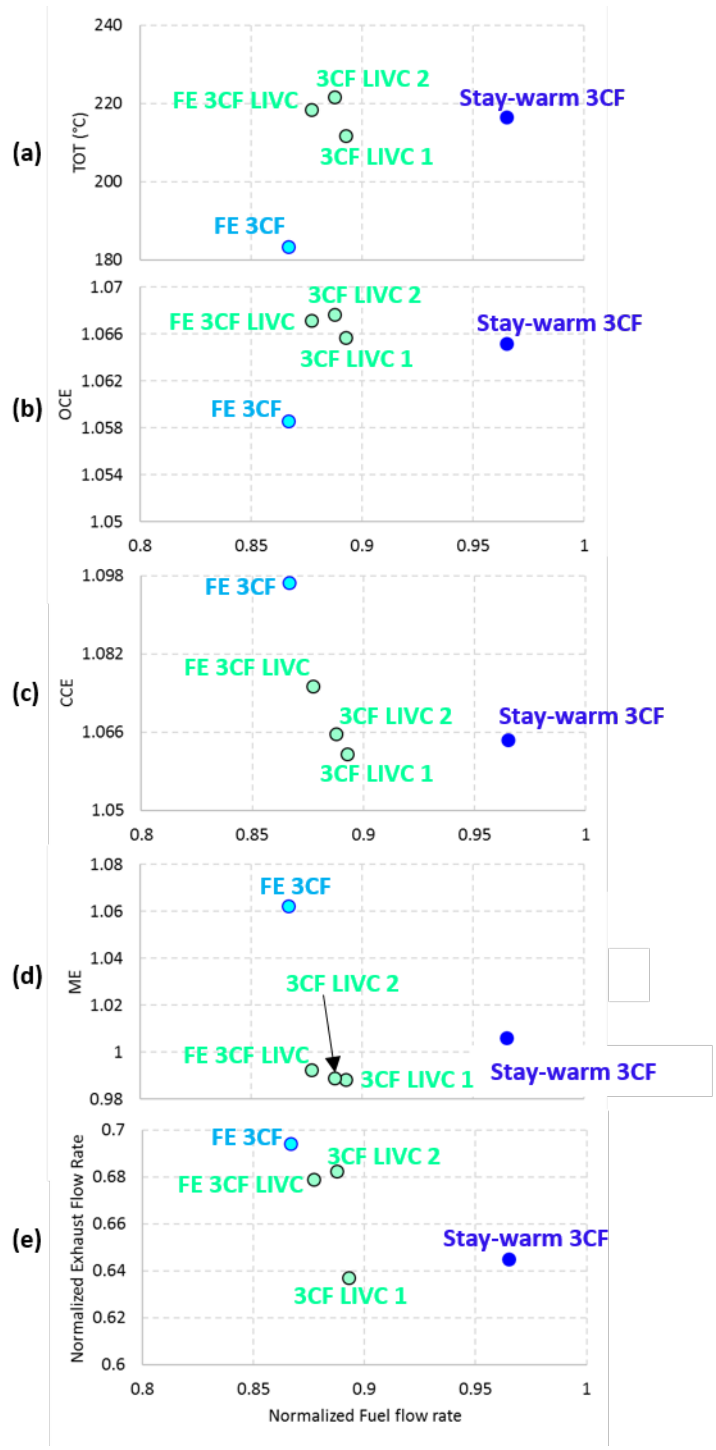

Fig. 5.11. Results of '3CF LIVC' operation. LIVC with 3CF can result in an improved trade off between TOT and fuel consumption. All values are normalized with respect to the stock fuel efficient calibration, which is not shown here.

jection timings is advanced form ‘3CF LIVC2’ to ‘FE 3CF LIVC’ - this is a combined effect of reduction in fuel consumption and reduction in intake manifold pressure.

Engine outlet emissions are shown in Figure 5.12.‘3CF LIVC1’ results in similar NOx, and higher engine outlet soot than ‘Stay-warm 3CF’. ‘3CF LIVC2’ uses a less restricted VGT position than ‘3CF LIVC1’, and hence an increase in NOx is seen. An increase in NOx is seen (10%) when injection timing is advanced as in the case of ‘FE 3CF LIVC’ compared to ‘3CF LIVC2’.

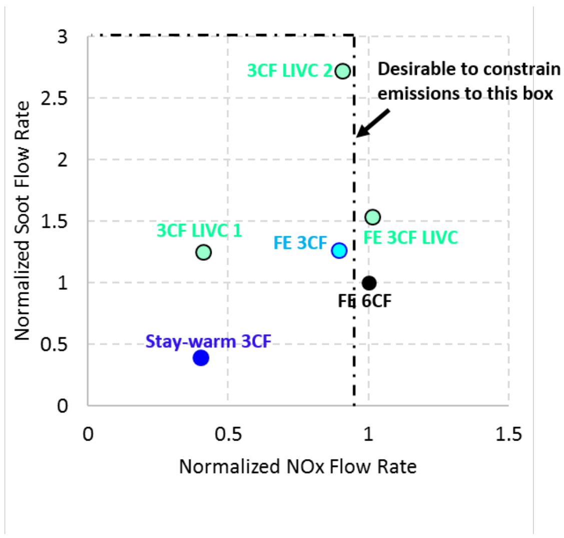

Fig. 5.12. Engine out emissions for 3CF operation with LIVC. LIVC allows lower engine outlet NOx levels, while still using relatively earlier injection timings.

A first law analysis is shown in Figure 5.13. Key comparisons can be made here between ‘FE 3CF’, ‘Stay-warm 3CF’ and 3CF LIVC operation targeting fuel efficiency and stay-warm performance. All the strategies have similar brake power due to equal engine speed and torque. Exhaust heat is lower for ‘FE 3CF’ compared to other strategies due to lower TOT. In-cylinder heat loss is higher for ‘Stay-warm 3CF’ compared to ‘FE 3CF’, potentially due to delayed injections, and hence a delayed heat release. Both instances of 3CF LIVC operation have similar in-cylinder heat loss, albeit slightly higher for the '3CF LIVC' case due to difference in injection timings.

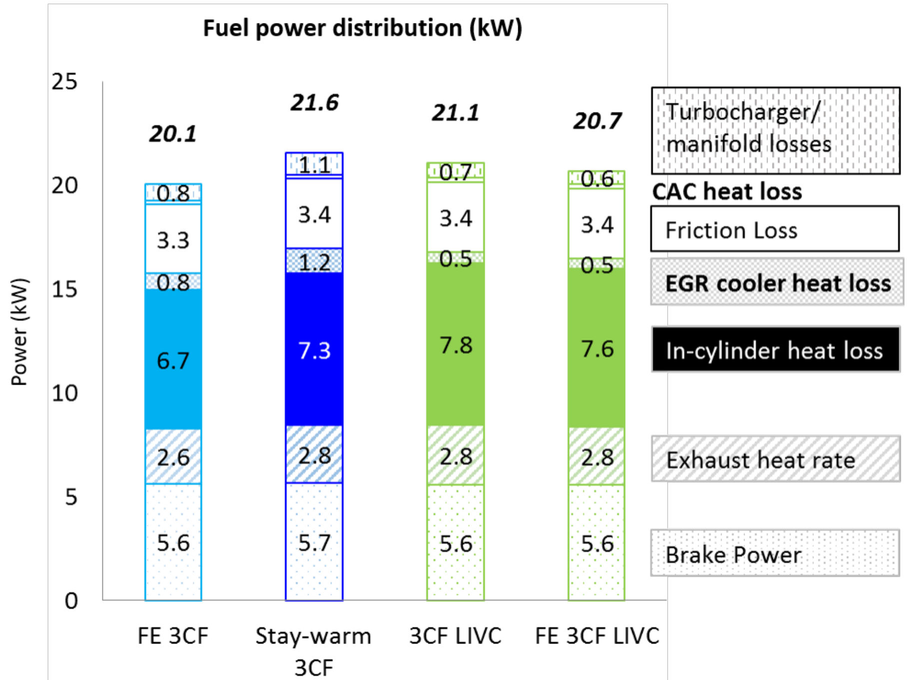

Fig. 5.13. A first law analysis for the various strategies shows the variation of fuel energy is expenditure via different paths.

One explanation for increase in in-cylinder heat loss for the 3CF LIVC cases as compared to 3CF cases without LIVC could be earlier heat release. A key-takeaway from this analysis is that EGR cooler losses decrease for the 3CF LIVC cases as NOx reduction is supplemented (in part) by reduced ECR, and there is reduced need for external EGR.

Summary of 3CF LIVC operation

1. 3CF LIVC can achieve similar TOT as 'Stay-warm 3CF' at 9.6% lower fuel consumption and similar engine out emissions, while using relatively earlier injection timings and reduced dependence on exhaust manifold pressure control.

2. TOT of 3CF LIVC does not decrease when used with a relatively unrestricted VGT position as the elevated TOT is primarily an effect of reduced air flow rate.

5.2.3 Results of Three Cylinder Operation with Internal EGR

The purpose of combining internal EGR operation with the active cylinders in 3CF was to gauge whether stay-warm performance can be improved further by using iEGR. Using internal EGR eliminates heat loss to the EGR cooler, and hence use of iEGR can be hypothesized to result in higher TOT. The challenge with using internal EGR is constraining engine out emissions because internal EGR is 'hotter' than cooled external EGR. Therefore, for equal mass of recirculated gas, internal EGR is less effective in reducing NOx compared to external EGR. Increased in-cylinder dilution leads to reduction in air to fuel ratio, and can lead to increase in engine out soot emissions.

This section investigates effects of using internal EGR and effects of variation in valve timings in order to do so. Effects of stock engine actuators like VGT position, external EGR valve position and injection timing are also studied. The 3CF inernal EGR strategies are broadly categorized as follows:

1. Effect of achieving internal EGR by varying valve timings while maintaining constant VGT position constant

2. Effect of achieving internal EGR by varying valve timings while maintaining injection timing constant

Effect of achieving internal EGR by varying valve timings, while maintaining constant VGT position

The additional strategies studied in this section are described below.

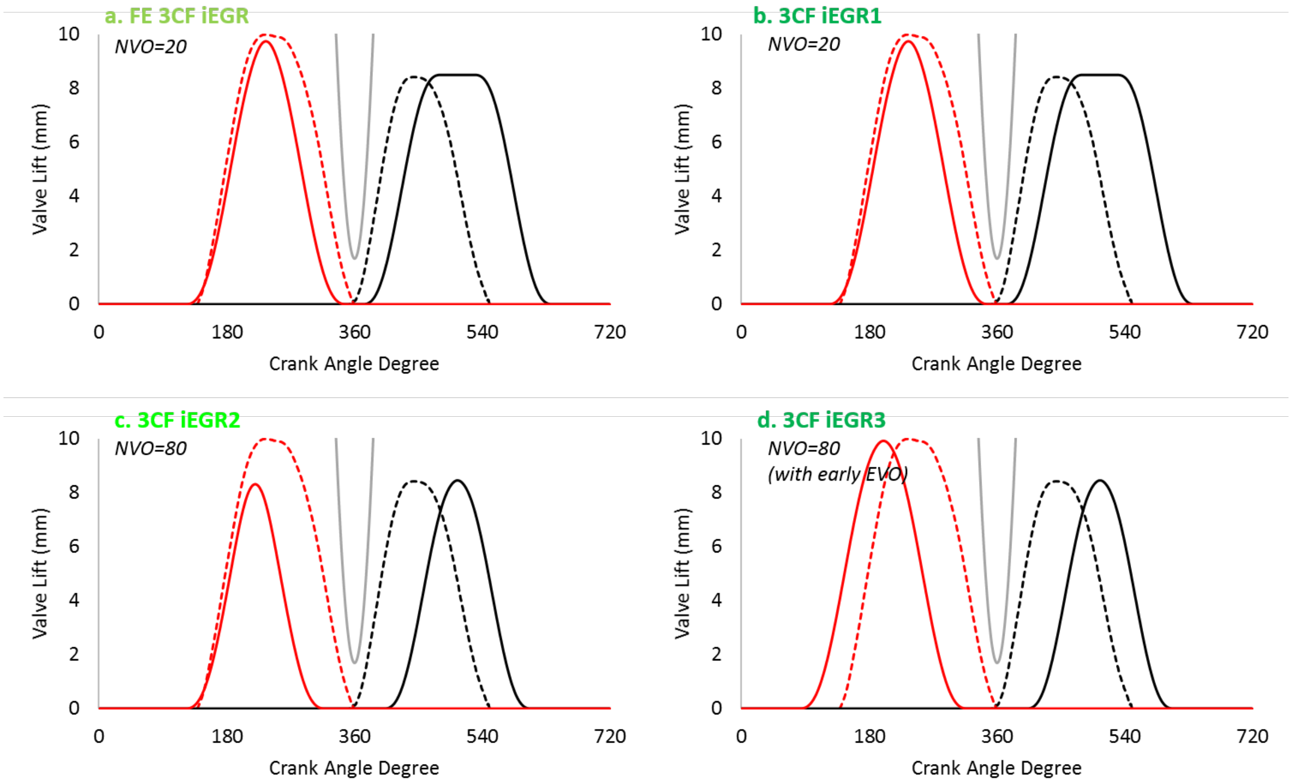

Fig. 5.14. Valve profiles for 3CF iEGR strategies with an unchanging VGT position. Effects of varying amounts of iEGR were studied by varying valve timings. Note that LIVC is also used here. Stock profiles are shown in dotted lines.

(a) *FE 3CF iEGR* – This strategy uses advanced EVC, and a delayed IVO and IVC in order to achive internal EGR via negative valve overlap. There is 20 CAD of negative overlap achieved. Injections relatively closer to the TDC are used (compared to ‘Stay-warm 3CF’), with zero external EGR and a VGT position set to 30% closed. This strategy achieved similar fuel consumption as ‘FE 3CF’, while reaching similar TOT as ‘Stay-warm 3CF’. However, engine out NOx was higher than desired. Valve profiles used are shown in Figure 5.14(a).

(b) *3CF iEGR1* – A variation of 3CF operation with iEGR, this strategy uses the same valve timings as ‘FE 3CF iEGR’. This is the only 3CF iEGR strategy

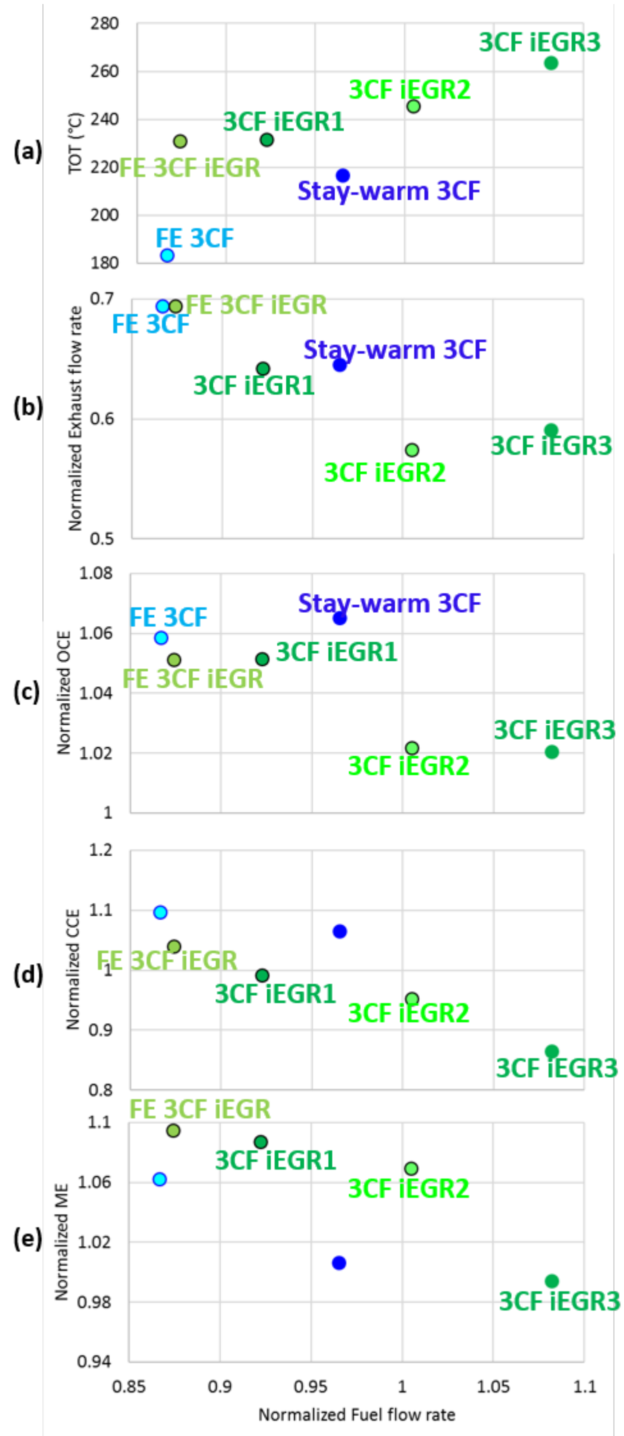

Fig. 5.15. Experimental steady state results for 3CF with internal EGR. Improved TOT than 'Stay-warm 3CF' can be achieved, at lower fuel consumption level.

in this work that also used some amount of external EGR. VGT position was restricted further from 30% closed, just sufficient to drive some amount of external EGR for NOx control. Injection timing was maintained similar to that in ‘FE 3CF’. Valve profiles used are shown in Figure 5.14(b).

(c) *3CF iEGR2* – This strategy used greater amount of NVO between the intake and exhaust vales. VGT position was similar to that in ‘FE 3CF iEGR’. Delayed injections were used - this was another method to constrain engine out NOx. Valve profiles used are shown in Figure 5.14(c).

(d) *3CF iEGR3* – This strategy used similar valve timings as ‘3CF iEGR2’, although with the added difference of an advanced EVO. This was done to achieve higher TOT. Delayed injections were used, along with a VGT position of 30% closed. Valve profiles used are shown in Figure 5.14(d).

Experimental results for TOT, fuel consumption and cycle efficiency are discussed next. Figure 5.15 shows these results, where all values are normalized with respect to ‘FE 6CF’ (the fuel efficient 6 cylinder operation), however ‘FE 6CF’ is not shown in this figure in order to be able to highlight differences between the various 3CF strategies.

Figure 5.15 shows that ‘FE 3CF iEGR’ can result in TOT higher than that achieved in ‘Stay-warm 3CF’, at lower fuel consumption. This strategy, however, also resulted in higher engine out NOx than acceptable, and therefore was combined with external EGR usage to reduce NOx to desired levels. This was done by opening the external EGR valve completely, and closing the VGT in order to drive just the sufficient amount of external EGR. This resulted in ‘3CF iEGR1’. TOT did not change significantly, and an increase in fuel consumption was observed. This increase was due to decreased CCE (as shown later). Note that ‘3CF iEGR1’ is the only point in this dataset to use external as well as internal EGR.

‘3CF iEGR2’ corresponds to similar VGT position as ‘FE 3CF iEGR’, with the added difference of delayed injections. The amount of negative valve overlap is increased to achieve higher recompression (due to earlier EVC) and hence, higher TOT. Injections were delayed in order to reduce engine out NOx. Delayed injections led to increase in TOT and an increase in fuel consumption. Fuel consumption is similar to that of 'FE 6CF' (not shown), with nearly 100°C higher TOT.

'3CF iEGR3' is obtained by using similar settings as '3CF iEGR2', but also with advanced EVO. This is another attempt to understand the TOT ranges that can be reached using 3CF iEGR. In this manner, TOT nearly similar to the stock thermal management calibration can be reached, with 7% higher fuel consumption than stock fuel efficient calibration.

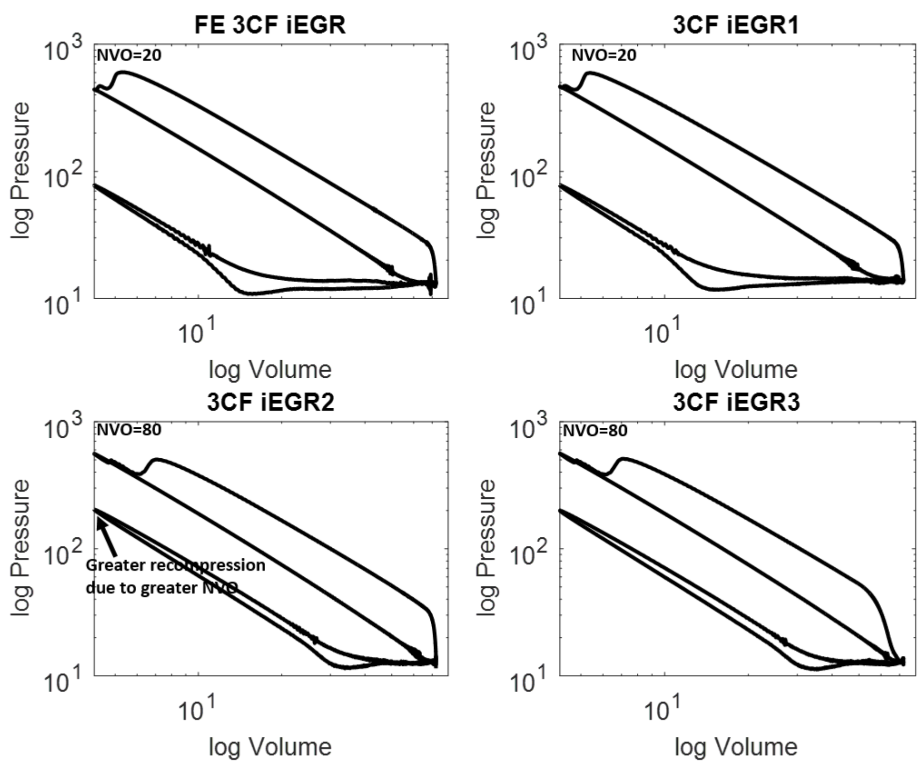

Fig. 5.16. log P-log V diagrams for various 3CF iEGR strategies.

Figure 5.15(b) shows the exhaust flow rates corresponding to each strategy. Exhaust flow decreases from 'FE 3CF iEGR' to '3CF iEGR1' due to increased in-cylinder dilution via use of external EGR in the latter. Further reduction is seen in '3CF iEGR3' as the amount of NVO is increased, which results in higher amount of internally trapped exhaust gas. Exhaust flow rate increases as EEVO is added, this is due to the slight increase in boost which is a result of increased turbine speed due to EEVO.

Figure 5.15(c)-(e) show the normalized values of OCE, CCE and ME for each strategy. CCE is seen to decrease when there is an increase in in-cylinder dilution (either due to increased internal EGR or external EGR). '3CF iEGR2' and '3CF iEGR3' result in lower OCE than the other strategies because of relatively higher amount of negative valve overlap. ME decreases as NVO is increased, potentially due to increased frictional losses associated with recompression of trapped exhaust gas.

Figure 5.16 shows the log P-log V diagrams for each strategy. The decrease in pressure at the end of the second recompression event is due to difference in NVO.

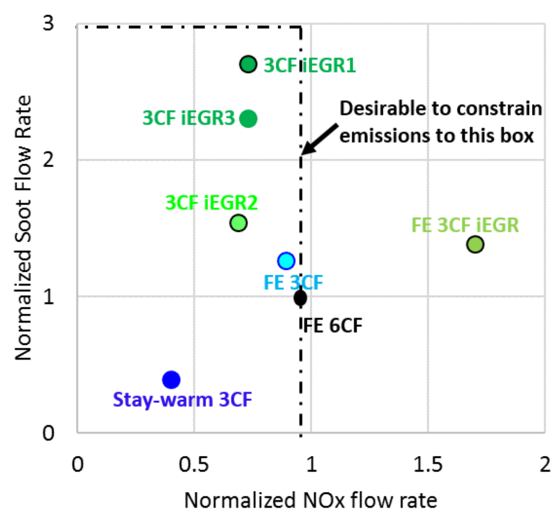

Fig. 5.17. 3CF iEGR strategies can meet desired emission constraints.

Engine out emissions of NOx and soot are shown in Figure 5.17. As was mentioned before, 'FE 3CF iEGR' was not able to meet the desired NOx limits. Using external EGR or increasing the amount of NVO while using late injections helped to constrain NOx to desirable values, while soot was within desired bounds.

Due to the favourable fuel consumption of 'FE 3CF iEGR', and the favorable TOT achieved, a first law analysis was carried out of this strategy. This was compared to a first law analysis for 'FE 3CF', as both these strategies have similar fuel consumption with different stay-warm performance.

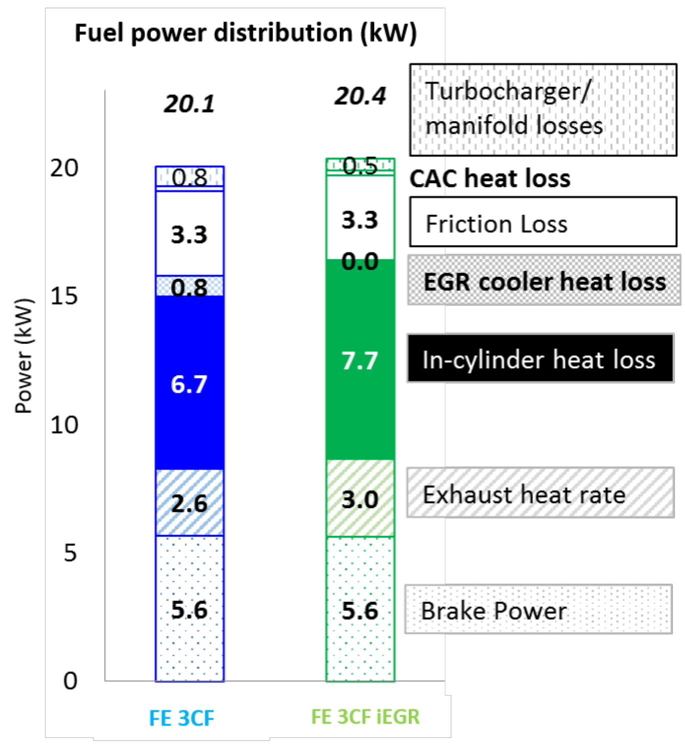

Fig. 5.18. First law analysis of 3CF iEGR shows that iEGR results in higher in-cyl heat loss, while losses to the external EGR cooling loop are eliminated.

Figure 5.18 shows higher exhaust heat rate with 'FE 3CF iEGR', which is due to higher TOT. Increase in in-cylinder heat loss can be accounted to use of internal EGR, where the trapping and recompression of trapped exhaust gas can result in higher heat loss. A crucial difference is that EGR cooler losses are zero for 'FE 3CF iEGR', which is because no external EGR was used. Other losses (turbocharger/manifold) decrease with use of internal EGR.

In summary, the results in this section studied the effect of iEGR on the trade-off between TOT and fuel consumption when VGT position was held constant. Three cylinder operation with iEGR was shown to be capable of resulting in similar fuel consumption as the most fuel efficient 3CF operation, with higher TOT albeit with higher engine out NOx. These 3CF iEGR cases also used LIVC, and the acceptable levels of engine out NOx levels have a contribution of reduced ECR due to LIVC. Therefore, to isolate the effectiveness of NVO in reducing NOx, a new set of strategies was studied, as discussed next.

Effect of achieving internal EGR by varying valve timings while maintaining injection timing constant

This section studies the effects on TOT and fuel consumption when injection timings are held constant. Three cylinder operation is combined with iEGR, with valve timings varied to achieve different levels of internal EGR. Three cases for VGT position are considered for 3CF iEGR operation with constant injection timing. An important difference between these strategies and the ones studied in the previous section is IVC timing. Strategies discussed earlier used both delayed IVO and delayed IVC (similar to intake valve phasing), however, strategies studied in this section use only delayed IVO for achieving internal EGR. Stock IVC timings are used. Figure 5.19 shows the valve profiles used. The strategies are described next.

(a) *3CF iEGR V40* – This corresponds to using delayed injections (similar to 'stay-warm 3CF') with a VGT position of 40% closed. The amount of negative valve overlap between the exhaust and intake valves is 70 crank angle degrees.

(b) *3CF iEGR V80* – This strategy corresponds to a VGT position of 80% closed, with 70 crank angle degrees of NVO. The only difference between this strategy and '3CF iEGR V40' is VGT position.

(c) *3CF iEGR V30* – This strategy differs from the previous two in VGT position, and the amount of NVO. VGT positin is set to 30% closed. The objective of

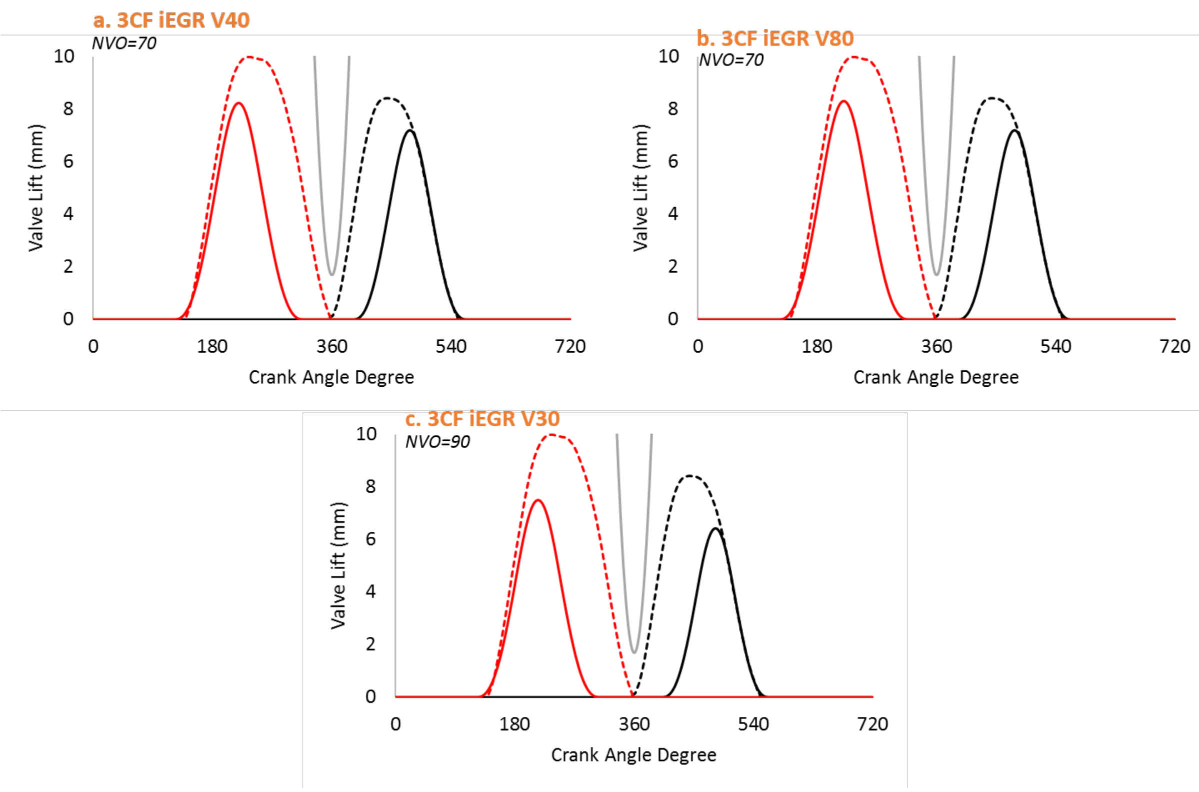

Fig. 5.19. Valve profiles for variations of 3CF iEGR operation studied with injection timing held constant. Stock profiles are shown in dotted lines.

this strategy is to understand the reduction in NOx that can be achieved using only internal EGR.

Figure 5.20 shows the P-V diagrams for these strategies. Increased in-cylinder pressure at the end of the recompression process is an effect of increased mass of trapped exhaust gas. The amount of gas that is trapped is affected by both VGT position, and the amount of NVO.

The results for TOT, fuel consumption, exhaust flow rate and cycle efficiency are discussed next.

Figure 5.21(a) shows that using the same late injections, along with some internal EGR, '3CF iEGR V40' can result in a 20°C increase in TOT without any fuel con-

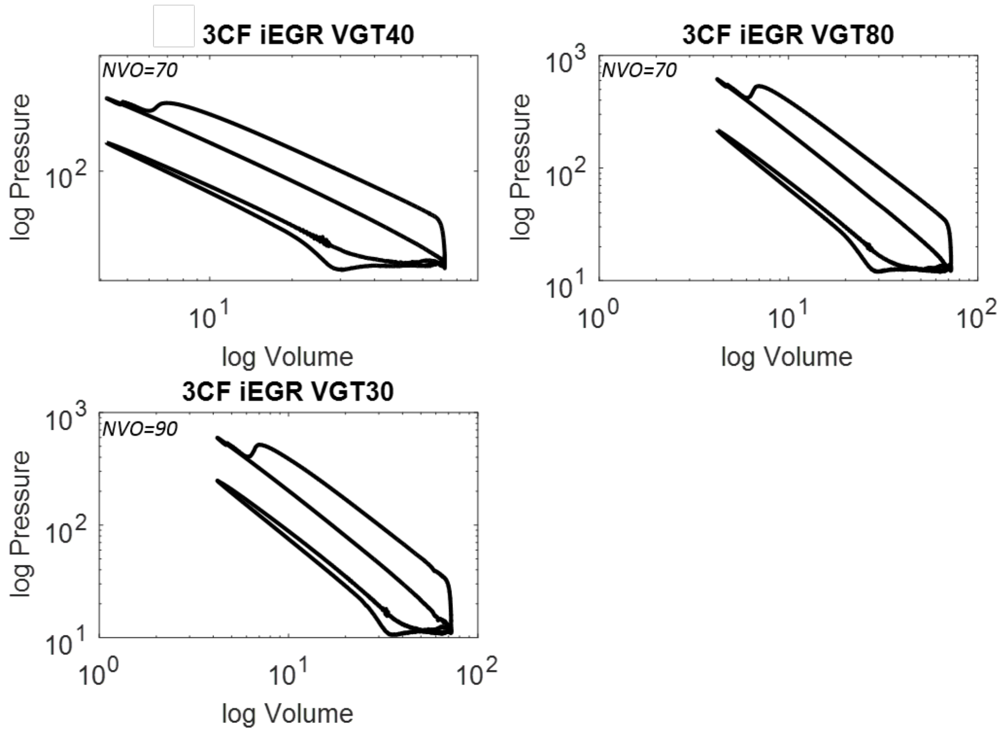

Fig. 5.20. In-cylinder pressure vs volume for the different strategies studied.

sumption penalty. The reason for this is elimination of losses to the EGR cooler, as '3CF iEGR V40' uses only internal EGR for NOx control. On changing VGT position to 80% closed, '3CF iEGR V80' is obtained. TOT reduces, while fuel consumption increases. The reduction in TOT is likely due to an offset balance between in-cylinder heat loss and elimination of EGR cooler loss. This is becasue increased restriction in VGT pathway (via increased VGT position) results in higher exhaust back pressure at EVC, and results in a greater amount of trapped exhaust gas inside the cylinder. Recompression of this gas can lead to heat loss to the surrounding surfaces in the cylinder. '3CF iEGR V30' differs from the other two strategies in both VGT postion and amount of NVO. Greater amount of overlap is used in this case, which leads to a higher TOT and fuel consumption.

Figure 5.21(b) shows that exhaust flow rate increases by a small amount with '3CF iEGR V80' compared to '3CF iEGR V40', in spite of the higher trapped in-cylinder

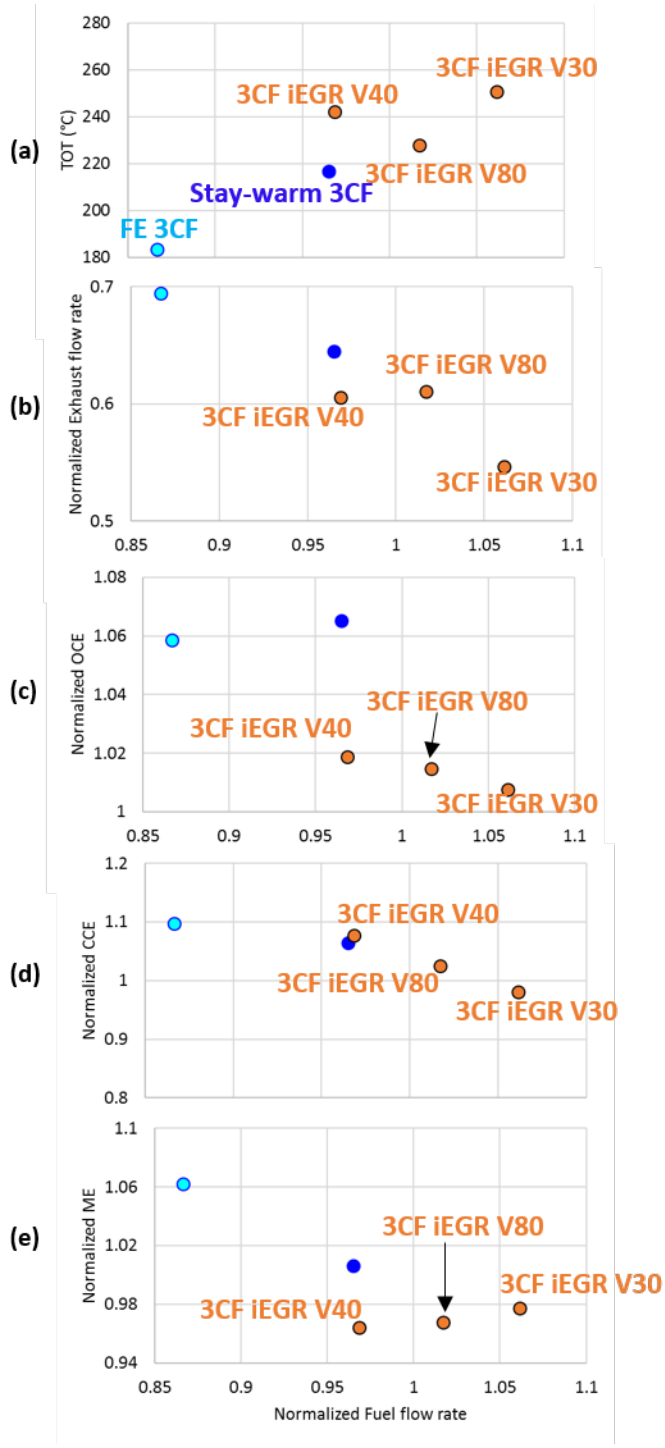

Fig. 5.21. 3CF iEGR can result in 20°C higher TOT than 'Stay-warm 3CF' at no fuel consumption penalty.

mass. This is an effect of higher boost due to increase in turbine speed [45]. Exhaust flow rate decreases with '3CF iEGR V30' due greater amount of trapped mass - here the VGT position is set to 30% shut, which is not suitable for providing boost.

The cycle efficiency values for each strategy are shown in Figure 5.21(c)-(e). A decreasing trend can be seen for OCE for '3CF iEGR V40','3CF iEGR V80' and '3CF iEGR V40'. This is a consequence of increased VGT position (and hence higher exhaust backpressure) for '3CF iEGR V40' to '3CF iEGR V80'. OCE is lowest for '3CF iEGR V30' in spite of a relatively unrestricted VGT position - this is due to increased pumping losses resulting from a greater amount of NVO. CCE decreases from '3CF iEGR V40' to '3CF iEGR V80' due to increased trapped in-cylinder mass due to to the VGT position; while it decreases from '3CF iEGR V80' to '3CF iEGR V30' due to increased trapped in-cylinder mass due to greater NVO. Engine out

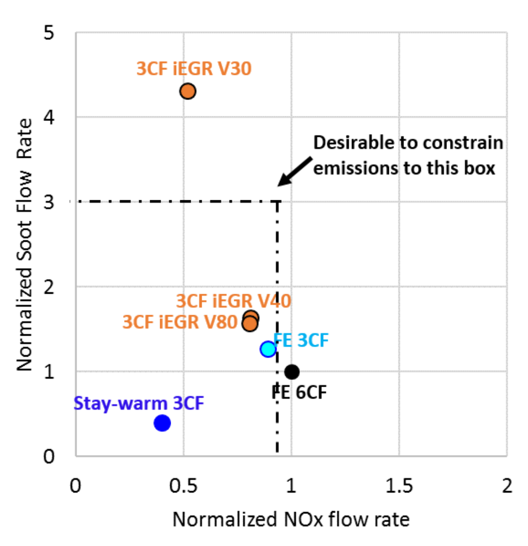

Fig. 5.22. Engine out emissions can be constrained as desired, except in the case of '3CF iEGR VGT30'.

emissions are shown in Figure 5.22. Increased in-cylinder dilution due to NVO in '3CF iEGR V30' led to lower air to fuel ratio, and as a result, led to higher soot levels than acceptable. All other strategies were able to meet desired soot and NOx constraints.

Estimation of internal EGR fraction

A challenge faced with internal EGR operation is determination of the amount of internal EGR. This challenge does not arise for external EGR as there are several established techniques to measure the same. Measuring CO_2 concentration in the intake and exhaust manifolds to determine external EGR fraction is a commonly used technique [46]. EGR flow can be estimated by knowing the parameters related to the EGR valve and using the orifice equation. None of the above methods can be used to estimated internal EGR fraction without using complex and expensive exhaust sampling systems.

An analysis of the in-cylinder contents for the various iEGR strategies was carried out using available measurements of in-cylinder pressure throughout the cycle, and thermocouples placed at appropriate sampling locations. The mass inside the cylinder at IVC consists of fresh air, external EGR and residual exhaust gas which remained in the cylinder from the previous cycle. In cases where internal EGR is not used, the quantity of residual exhaust gas can be expected to be considerably lower (corresponding to pressure at EVC, clearance volume, and exhaust manifold temperature). However, in case of operation with internal EGR, residual amount increases. Internal EGR fraction can therefore be estimated.

Charge flow can be estimated by using estimated external EGR fraction and measured fresh air flow. External EGR fraction is estimated using Equation 5.1.

$$EGR\ Fraction_{external} = \frac{CO_{2,IM} - CO_{2,ambient}}{CO_{2,EM} - CO_{2,ambient}} \tag{5.1}$$

$$Charge\ Flow = \dot{m}_{fresh} + \dot{m}_{fresh} \times EGR\ Fraction_{external} \tag{5.2}$$

$$\dot{m}_{charge} = \dot{m}_{fresh} + \dot{m}_{egr,ex} \tag{5.3}$$

The following equations are used to estimate internal EGR fraction and in-cylinder O_2 by estimating mass of trapped gas inside the cylinder at various instances of the 4 stroke cycle.

$$m_{egr,ex} = m_{charge} - m_{fresh} \tag{5.4}$$

The amount of trapped in-cylinder gas can be estimated using the ideal gas law and in-cylinder pressure at EVC. Temperature of exhaust manifold can be used as equilibrium between cylinder and exhaust manifold can be assumed towards the end of the exhaust stroke (or at EVC).

$$m_{trapped,EVC} = \frac{P_{EVC}V_{EVC}}{RT_{ExhMan}} \tag{5.5}$$

The mass of gas inside the cylinder that participated in the combustion process can similarly be estimated using in-cylinder pressure and volume at EVO, and port temperatures for cylinders.

$$m_{trapped,EVO} = \frac{P_{EVO}V_{EVO}}{RT_{CylPort}} \tag{5.6}$$

The total mass inside the cylinder at EVO is a summation of residue from the previous cycle (which is mass at EVC for the previous cycle), fresh air, fuel and external EGR mass. Therefore, the following equation can be used to estimate fraction of the residue from the total amount.

$$iEGR = 1 - \frac{m_{trapped,EVO} - m_{trapped,EVC}}{m_{trapped,EVC}} \tag{5.7}$$

The oxygen content inside the cylinder can be estimated by knowing the oxygen content in fresh air and in exhaust gas. A stock J1939 lambda sensor measures O_2 fraction of exhaust gas. Oxygen fraction of fresh air can be assumed to be constant at 20.95% by volume. Fuel is assumed to contain no oxygen, and hence is not included in this term.

$$In - cylinder\ O_2 = \frac{v_{air}O_{2,air} + v_{egr,ex}O_{2,exh} + v_{res}O_{2,exh}}{v_{air} + v_{egr,ex} + v_{res}} \tag{5.8}$$

where v_{air}, $v_{egr,ex}$ and v_{res} are volume of fresh air, external EGR and residue gas respectively. $O_{2,air}$ and $O_{2,exh}$ are oxygen fraction (by volume) in fresh air and exhaust, respectively.

Using this estimated in-cylinder O_2 and fuel consumption, and the stoichiometric equation for diesel fuel combustion, excess O_2 can be estimated.

$$Stoich\ O_2 = Fuel\ Injected(mg/st) \times k \tag{5.9}$$

where k is a constant obtained from the stoichiometric combustion equation for oxygen consumed for combustion of one mole of fuel.

$$v_{O_2} = In - cylinder\ O_2 \times (v_{air} + v_{egr,ex} + v_{res}) \tag{5.10}$$

$$mass_{O_2} = \frac{v_{O2} P_{IM}}{RT_{IM}} \tag{5.11}$$

$$Excess\ O_2\ mass = mass_{O_2} - Stoich\ O_2 \tag{5.12}$$

$$Excess\ O_2\ vol = \frac{Excess\ O_2\ mass\ RT_{IM}}{P_{IM}} \tag{5.13}$$

$$Excess\ O_2\ frac = \frac{Excess\ O_2\ vol}{(v_{air} + v_{egr,ex} + v_{res})} \tag{5.14}$$

Above equations were used to estimate mass trapped at EVC, volume of residue, excess O_2 fraction and internal EGR for the 3CF iEGR strategies discussed earlier.

Increased trapped mass is expected in case of '3CF iEGR V80' compared to '3CF iEGR V40' due to higher exhaust back pressure during the exhaust stroke. Increase in trapped mass is also expected from '3CF iEGR V80' to '3CF iEGR V30' due to increase in negative valve overlap. Volume of residue follows a similar trend as trapped mass at EVC. Excess O_2 fraction decreases as in-cylinder dilution increases, while a corresponding increase in internal EGR fraction is observed. Referring to

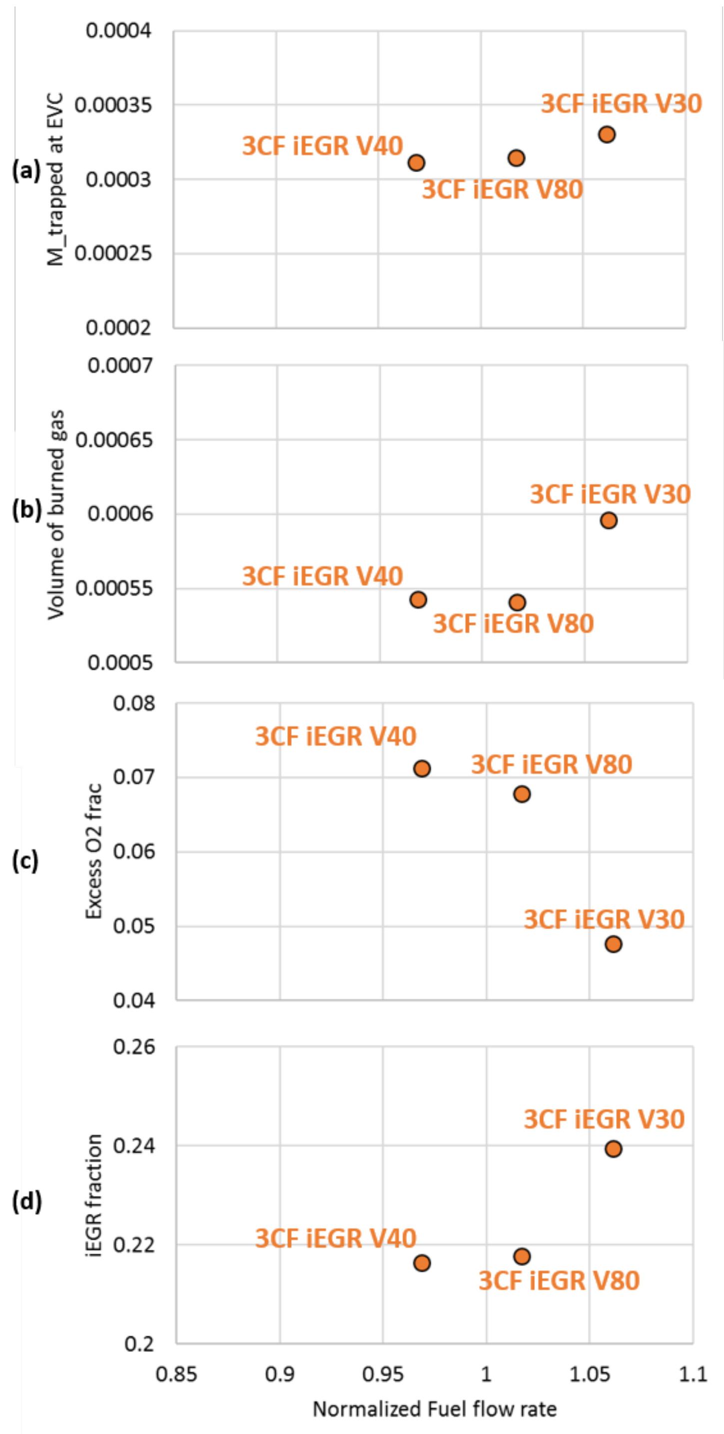

Fig. 5.23. estimated values of certain in-cylinder parameters for the 3CF iEGR strategies follow the trend expected.

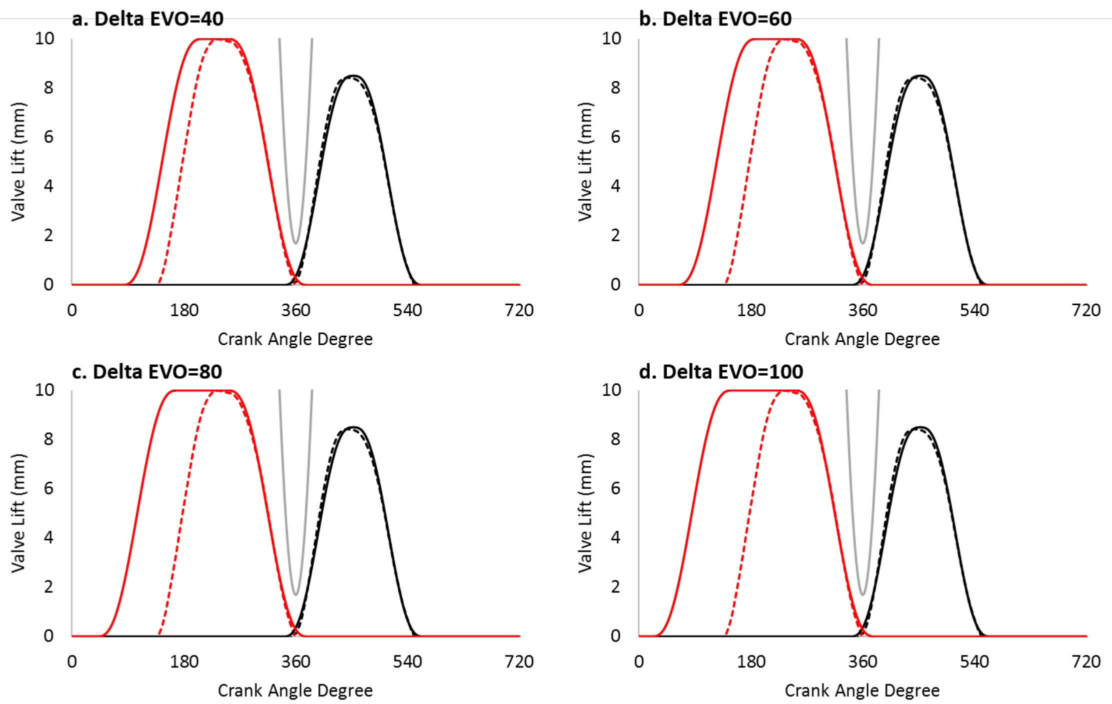

Fig. 5.24. Valve profiles of active cylinders used to study 3CF operation with EEVO. Four cases of EEVO were considered. Stock intake valve profiles were used. Delta EVO corresponds to the amount by which EVO was advanced compared to stock timing. Stock profiles are shown in dotted lines.

engine out emissions for NOx, it can be seen that NOx decreases as internal EGR fraction increases.

5.2.4 Results of Three Cylinder Operation with EEVO

This sections elaborates on steady state experimental results of 3CF operation with EEVO for the active cylinders. Figure 5.24 shows the valve profiles corresponding to four EEVO cases studied.

Exhaust valve opening closer to the combustion TDC results in increased exhaust temperature. The objective of combining 3CF operation with early exhaust valve opening (EEVO) was to achieve higher TOT. Higher TOT obtained in this manner can have benefits for maintaining the temperature of an already warmed-up ATS especially during scenarios of extended idling.

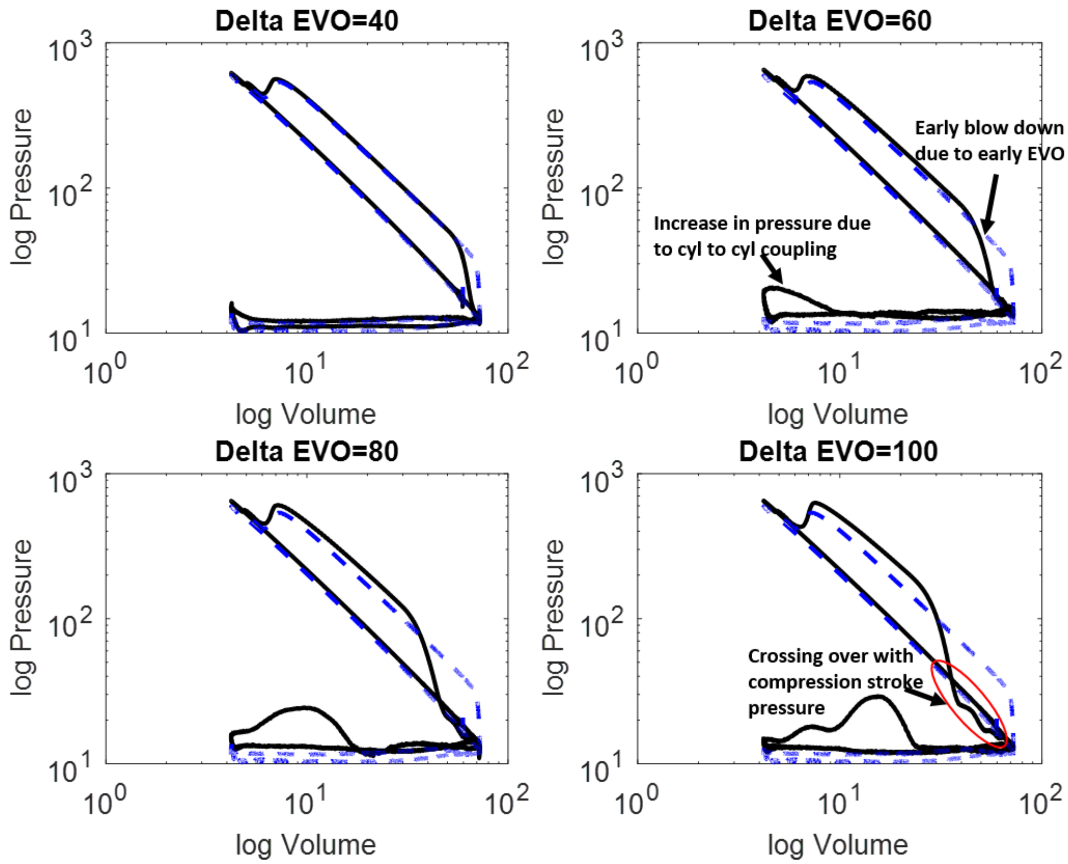

Fig. 5.25. P-V diagrams corresponding to each of the EEVO cases. EEVO results in an earlier blowdown. Cylinder to cylinder coupling becomes more prominent as EVO is advanced further closer to TDC. Dotted blue lines correspond to 3CF operation without EEVO.

P-V diagrams corresponding to each EEVO case are shown in Figure 5.25. Delayed start of combustion is due to the use of delayed injections timings. As exhaust valve opening is advanced, hotter exhaust gas leaves the cylinder resulting in sharper drop in in-cylinder pressure. In cases with the most aggressive EEVO (Delta EVO=100), the in-cylinder pressure is lower than pressure during compression - this is due to large drop in in-cylinder pressure owing to an aggressive blowdown. In-cylinder pressure increases sharply during the exhaust stroke, and location of this rise varies with delta EVO. The increase in pressure is due to coupling between the cylinders, where the exhaust stroke of a cylinder corresponds with EVO of another cylinder. The firing order of the engine is 1-5-3-6-2-4, and the EVO events of two firing cylinders are spaced 120 crank angle degrees apart. However, with 3CF operation, EVO events are spaced 240 crank degrees apart. For example, when cylinder 1 is undergoing the exhaust stroke, EVO of cylinder 3 occurs, resulting in momentary backflow of exhaust gas from cylinder 3 to cylinder 1. This backflow also corresponds to a momentary change in direction of flow which is generally through the manifold into the turbine.

TOT, fuel consumption and cycle efficiency for the EEVO cases are shown in Figure 5.26. Note that 'Warm-up 6CF' has also been plotted as the TOT ranges of 3CF EEVO are similar to that of 'Warm-up 6CF'.

As EVO is advanced, a clear trade-off is observed between TOT and fuel consumption. The most aggressive EEVO results in 340°C TOT, which is 80°C higher than 'Warm-up 6CF'. Figure 5.26(b) shows that exhaust flow rate with EEVO is higher than 3CF cases as EVO is further advanced. 3CF EEVO operation is not capable of reaching similar exhaust flow rates as 'Warm-up 6CF', due to half the total number of cylinders being deactivated. For this reason, in spite of elevated TOT, 3CF EEVO may not be a viable ATS warm-up strategy.

Decrease in OCE as EEVO is further advanced is mostly due to VGT position used - as EEVO was advanced, VGT needed to be closed in order to drive sufficient external EGR for NOx control. VGT position is however not as maximally shut, as in 'Warm-up 6CF'. Closed cycle efficiency decreases with advancing EVO as lower amount of useful piston work is derived from the combusted, expanding gas. Mechanical efficiency fluctuates for the EEVO cases by small amounts.

Another effect of early exhaust valve opening is increase in turbine speed. Figure 5.27 shows that turbine speed increases as EVO is advanced further closer to TDC. This is a result of increased enthalpy of exhaust gas at turbine inlet.

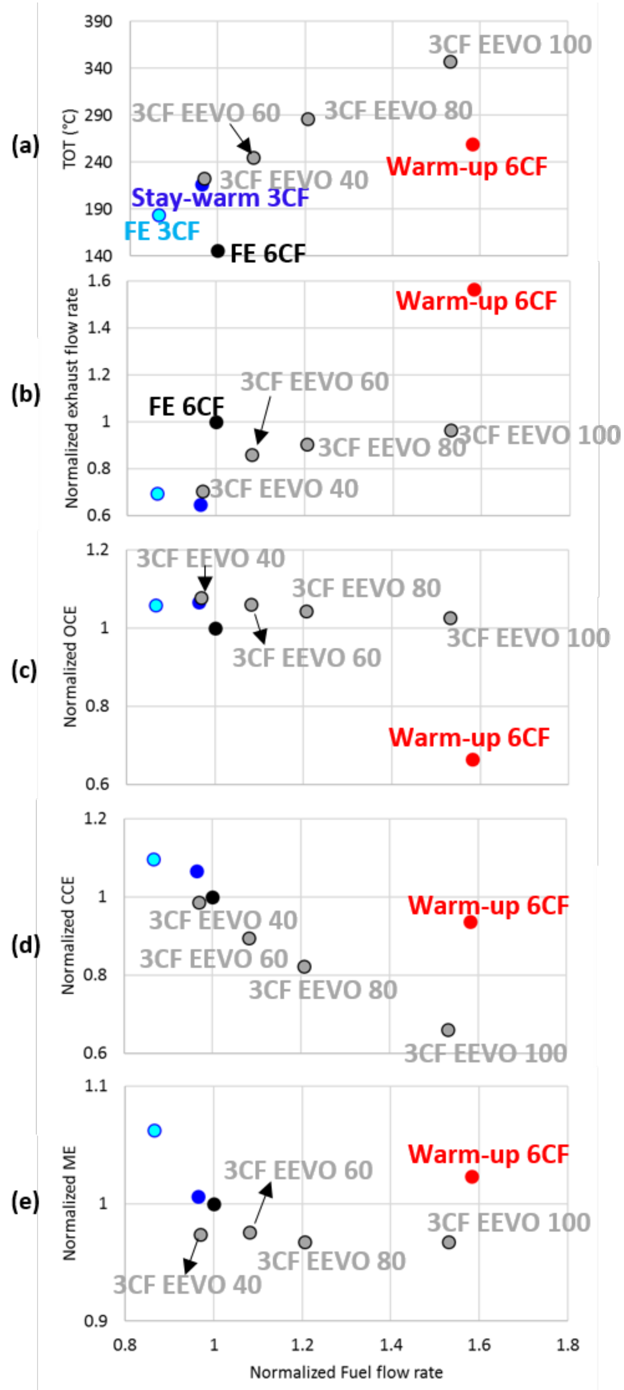

Fig. 5.26. TOT higher than 'Warm-up 6CF' can be achieved with EEVO. EEVO results in lower CCE which is the cause of increased fuel consumption.

The engine outlet emissions for EEVO are shown in Figure. '3CF EEVO 100' is not able to meet either of the emissions constraints, and hence is not shown on the figure. In general, the trade-off between soot and NOx for 3CF becomes challenging to balance as EEVO is a strategy that tends to have higher soot that other strategies. The reason for this occurrence is hypothesized to be insufficient time for post-combustion oxidation of soot.

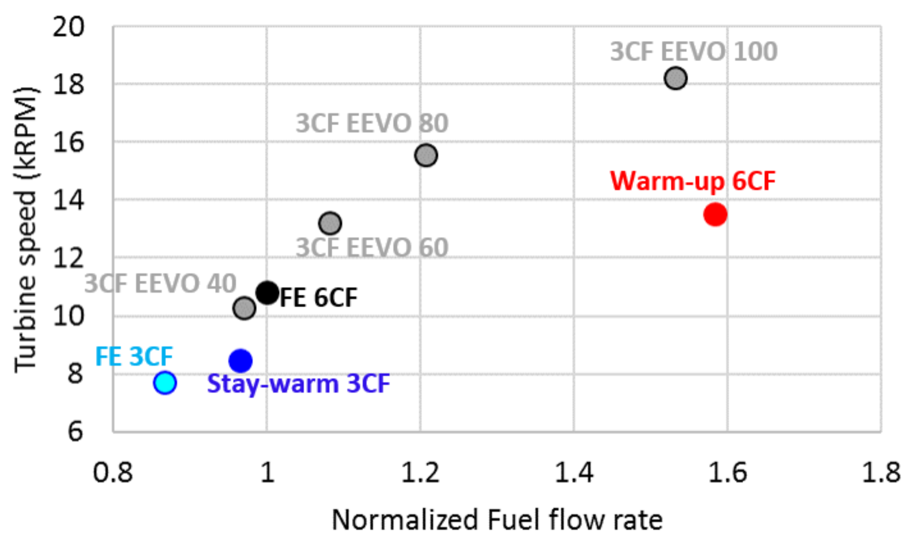

Fig. 5.27. Advanced EVO increases enthalpy at turbine inlet and results in higher turbine speed.

The 3F EEVO strategies studied here used delayed injections. A study was also carried out for 3CF EEVO using early (closer to TDC) injections. The trends for the same, though not shown, were similar to the trends seen in this section. An additional effect of using early injections was NOx constraints, due to which nearly all 3CF EEVO early injection cases resulted in higher NOx levels than desired.

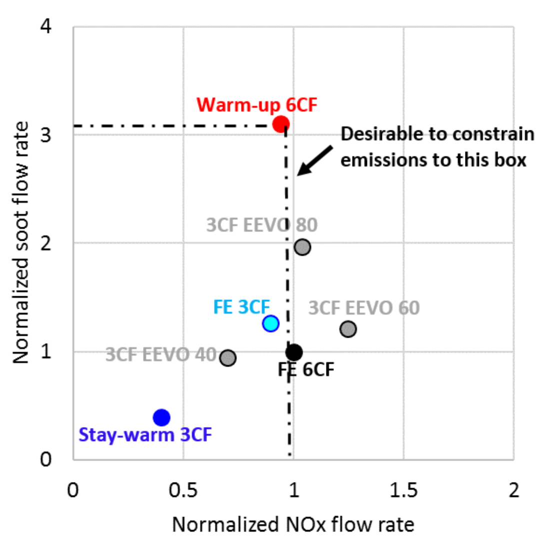

Fig. 5.28. Emissions are within bounds for only two of the four 3CF EEVO cases.

5.3 Two Cylinder Operation with Flexible Valve train Strategies

Deactivating fuel and shutting valve for four cylinders of the total six cylinders results in two cylinder firing (2CF) operation. A schematic of 2CF operation is shown in Figure 5.29. The choice of the cylinders to be deactivated is based on balancing of the firing sequence so generated. Cylinders 3 and 4 firing is an example of one such balanced configuration. This is the configuration that has been used for 2CF results in this section.

The results discussed in this section can be categorized as follows.

(a) *2CF operation* – Operation with 2CF, without using any valvetrain flexibility.

(b) *2CF iEGR* – Operation with 2CF with iEGR via NVO used in the active cylinders

(c) *2CF LIVC* – Operation with 2CF with LIVC in the active cylinders.

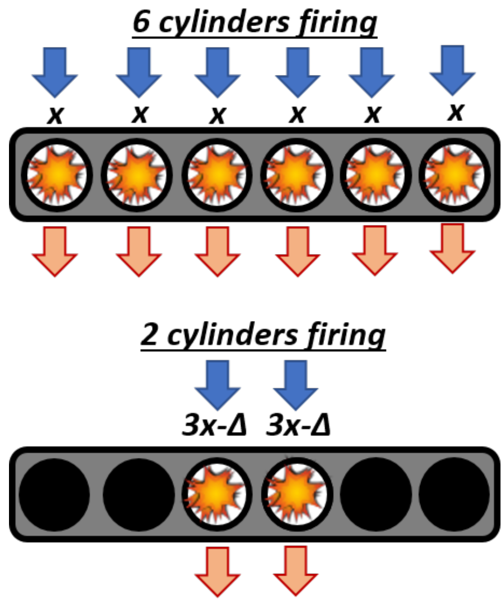

Fig. 5.29. Four cylinders are deactivated by shutting fueling and valves. The fueling quantity in the active cylinders increases to maintain the desired brake torque.

5.3.1 Results of Two Cylinder Operation

Two cases of 2CF operation are considered here, both of which use a constant VGT position of 67% closed.

(a) *FE 2CF* – Fuel efficient 2CF operation with injection timing closer to TDC

(b) *Stay-warm 2CF* – 2CF operation with the objective to achieve high TOT. This strategy uses two delayed injections.

Figure 5.30 shows the heat release rates corresponding to the two cases of 2CF operation. Earlier heat release in 'FE 2CF' is a results of using earlier injections. 'Stay-warm 2CF' has a higher heat release peak due to higher fuel consumption than 'FE 2CF'.

'Stay-warm 2CF' and 'Stay-warm 3CF' use the same two delayed injection timings, but the heat release peak is higher in the former case due to increased amount of fuel injected per cylinder. Heat release is also more 'spread-out' in case of 'Stay-warm

3CF' which affects closed cycle efficiency (as discussed later). A plot of in-cylinder pressure against volume is shown in Figure 5.31.

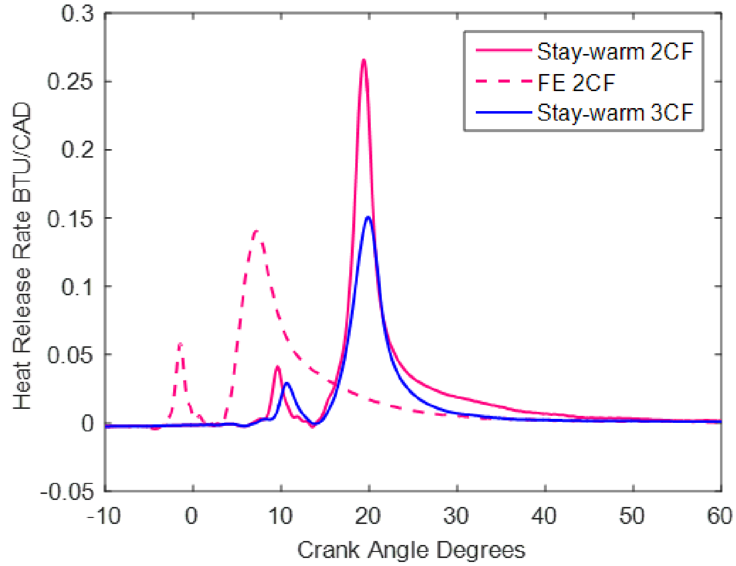

Fig. 5.30. Heat release rate in the active cylinders is higher for 2CF operation due to increased quantity of fuel injected per cylinder. The heat release takes longer to complete for 2CF cases.

The experimental steady state results are shown in Figure 5.32. Figure 5.32(a) shows that 'FE 2CF' uses early injection timing, and results in 20°C higher TOT than 'Stay-warm 3CF', with 5% lower fuel consumption. Delaying injections results in 'Stay-warm 2CF' which achieves similar TOT as 'Warm-up 6CF', while reducing fuel consumption by 40%. compared to 'FE 2CF', TOT increases by nearly 25°C and fuel consumption increases by 7%. Figure 5.32(b) shows the exhaust flow rate for the various strategies. Exhaust flow rate for 'Stay-warm 2CF' remains similar to 'Stay-warm 3CF' due to lower EGR fraction in the former.

Open cycle efficiency is higher for 2CF cases due to the use of a relatively more unrestricted VGT position. Two cylinder operation enabled the use of a more open VGT position because one of the firing cylinders (cylinder 4) is part of the bank that feeds into the EGR loop, and sufficient external EGR could be driven without using

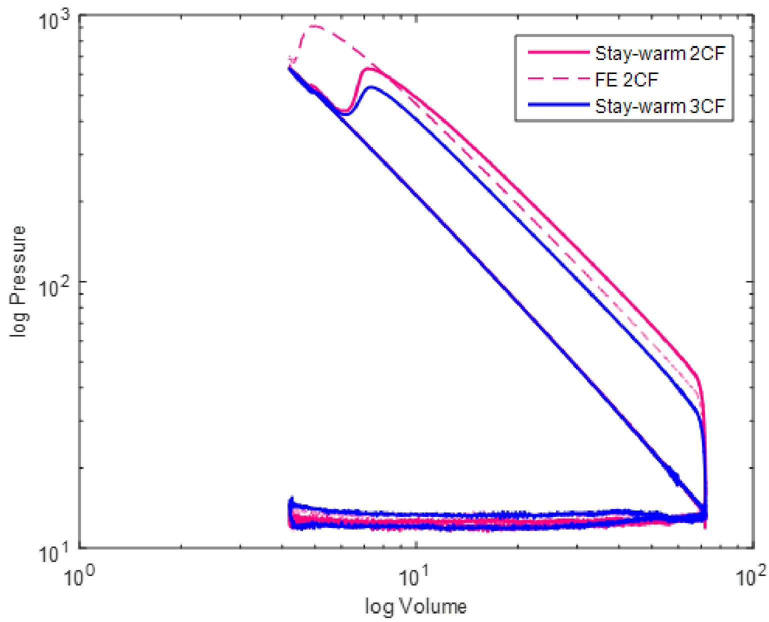

Fig. 5.31. P-V plot for 2CF operation with early and delayed injection timings.

as restricted a VGT position as 'Stay-warm 3CF'. CCE decreases from the 3CF cases to the 2CF cases due to a longer heat release profile. Lower CCE in 'Stay-warm 2CF' compared to 'FE 2CF' is a result of delayed injection timing. Mechanical efficiency also decreases for the 2CF cases due to increased parasitic losses from the inactive cylinders. As a result of higher OCE, lower CCE and lower ME, 2CF cases have higher fuel consumption than 3 CF operation.

Engine out emissions for 2CF cases are shown in Figure 5.33.

A first law analysis was carried out comparing the 2CF and 3CF strategies. Figure 5.34 shows the results of the same.

Since 'Stay-warm 3CF' and 'FE 2CF' have similar fuel consumption, a fair comparison can be made between these two strategies for the break down fuel energy. Brake power remains constant as these results correspond to operation at 800 RPM/1.3 bar BMEP. Higher exhaust heat rate is the result of increased TOT for 'FE 2CF'. In-cylinder heat losses also increase due to the wider heat release rate. EGR cooler

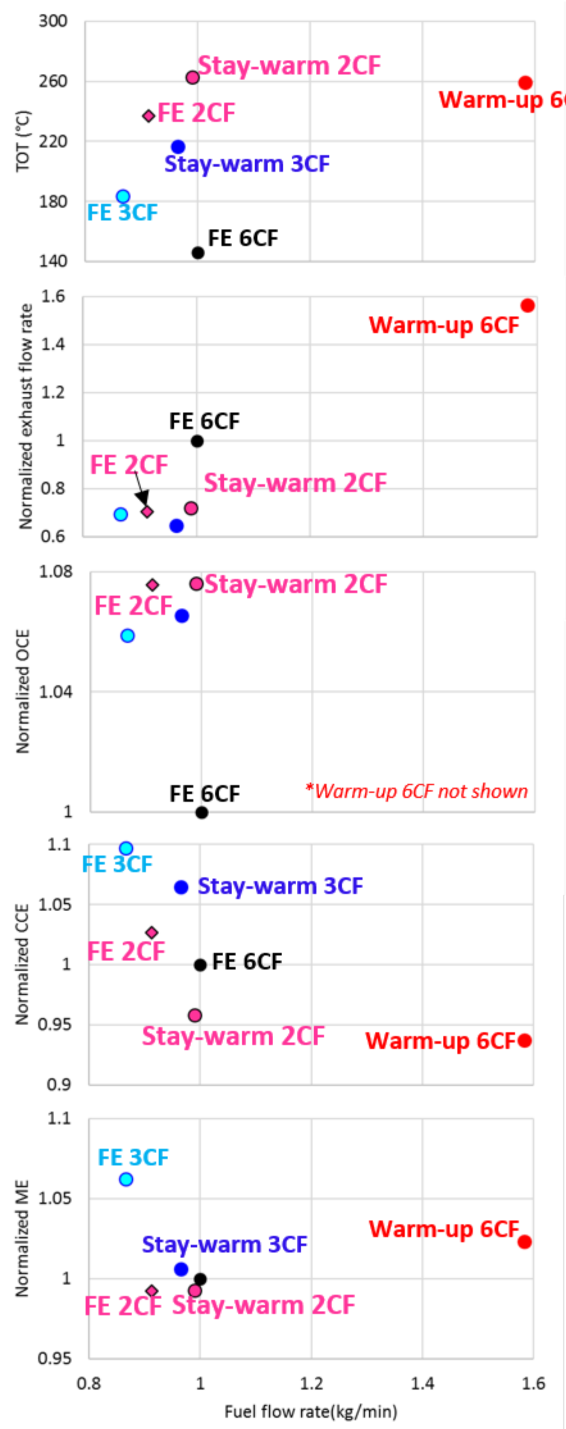

Fig. 5.32. 2CF operation can result in lower exhaust flow rate and similar TOT as 'Warm-up 6CF' with 40% lower fuel consumption. Higher OCE is a result of using an unrestricted VGT position.

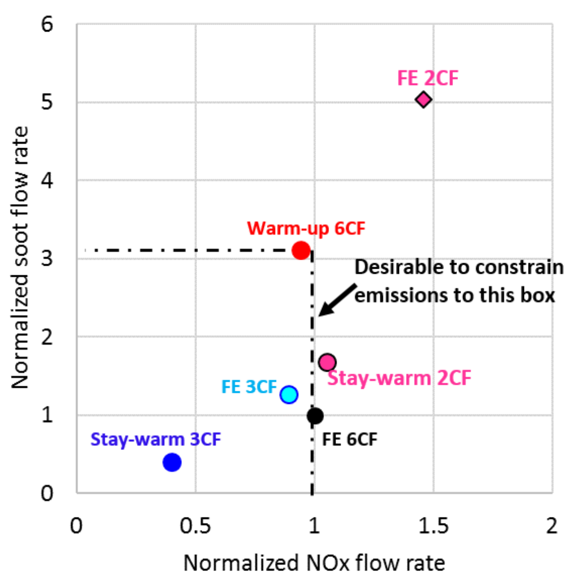

Fig. 5.33. Engine out emissions for 2CF operation calibrated for fuel-efficiency and stay-warm performance.

losses are nearly halved as 'FE 2CF' requires lower external EGR fraction. Decrease in turbocharger/manifold losses can be accounted to a less restrictive VGT position.

In summary, 2CF operation can reach TOT and exhaust flow rate that can be used to maintain ATS temperature at desired values longer during transient operation as well as during extended idling operation.

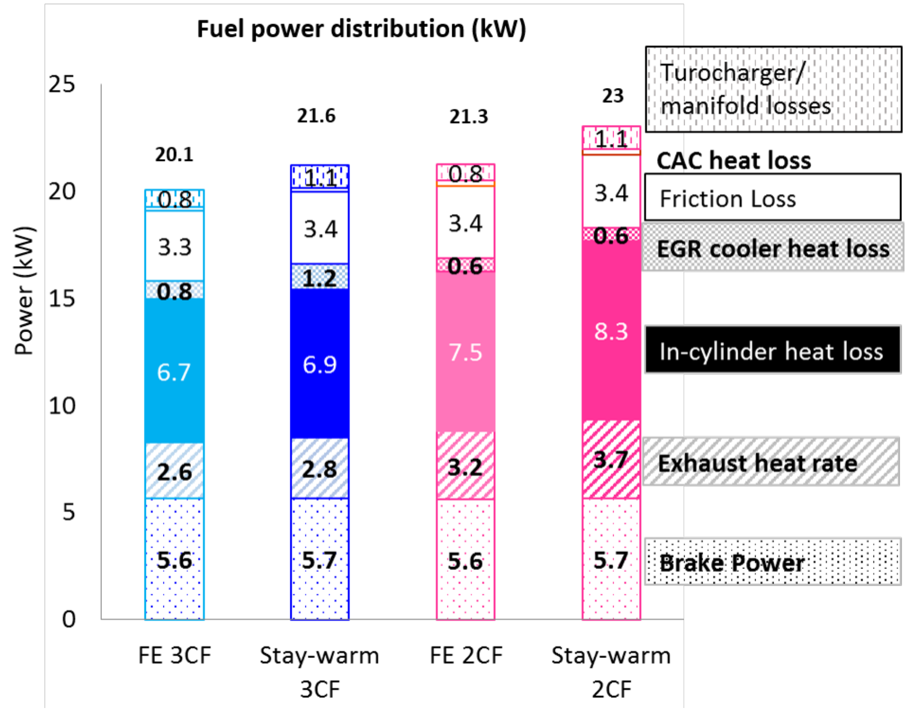

Fig. 5.34. First law analysis comparing distribution of fuel energy for 2CF and 3CF strategies.

5.3.2 Results of Two Cylinder Operation with Internal EGR

Internal EGR combined with 2CF was intended to study the increment in TOT that can be obtained by eliminating EGR cooler losses. Injections timings were similiar to 'Stay-warm 2CF'. Zero external EGR was used. As a result of not having to use external EGR, VGT position was set to a relatively unrestricted value of 30% closed. Valve profiles used are shown in Figure 5.35. Internal EGR is achieved by advancing EVC and delaying IVO. IVC is maintained same as stock values. A negative valve overlap of 40 crank angle degrees is thus achieved.

P-V diagrams for the active cylinders are shown in Figure. The recompression during the conventional exhaust stroke is a result of early EVC which leads to trapped exhaust gas inside the cylinder.

The results for TOT, fuel consumption and other parameters are shown in Figure 5.37. 'Stay-warm 2CF iEGR' results in 22°C higher TOT compared to 'Stay-warm

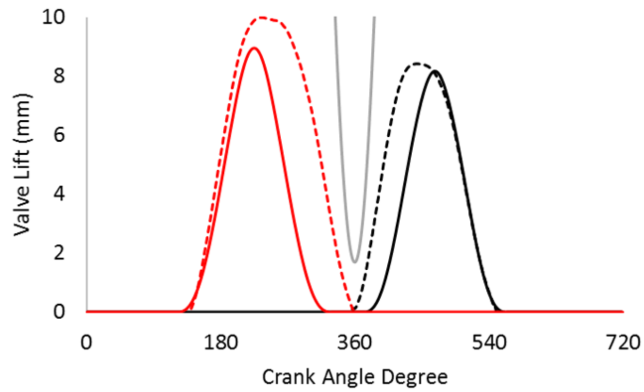

Fig. 5.35. Valve profiles for active cylinders to achieve internal EGR. Dotted lines correspond to stock profiles.

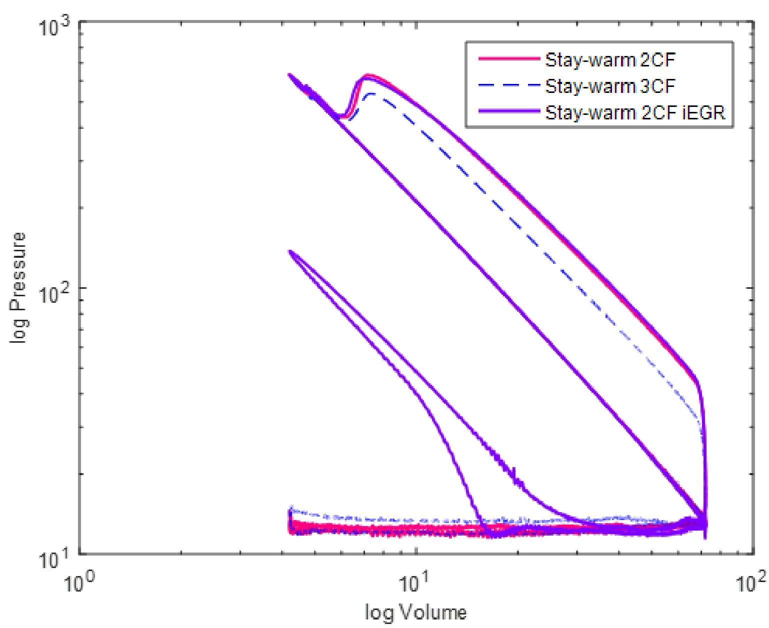

Fig. 5.36. P-V diagram for the active cylinders show the expected recompression due to NVO.

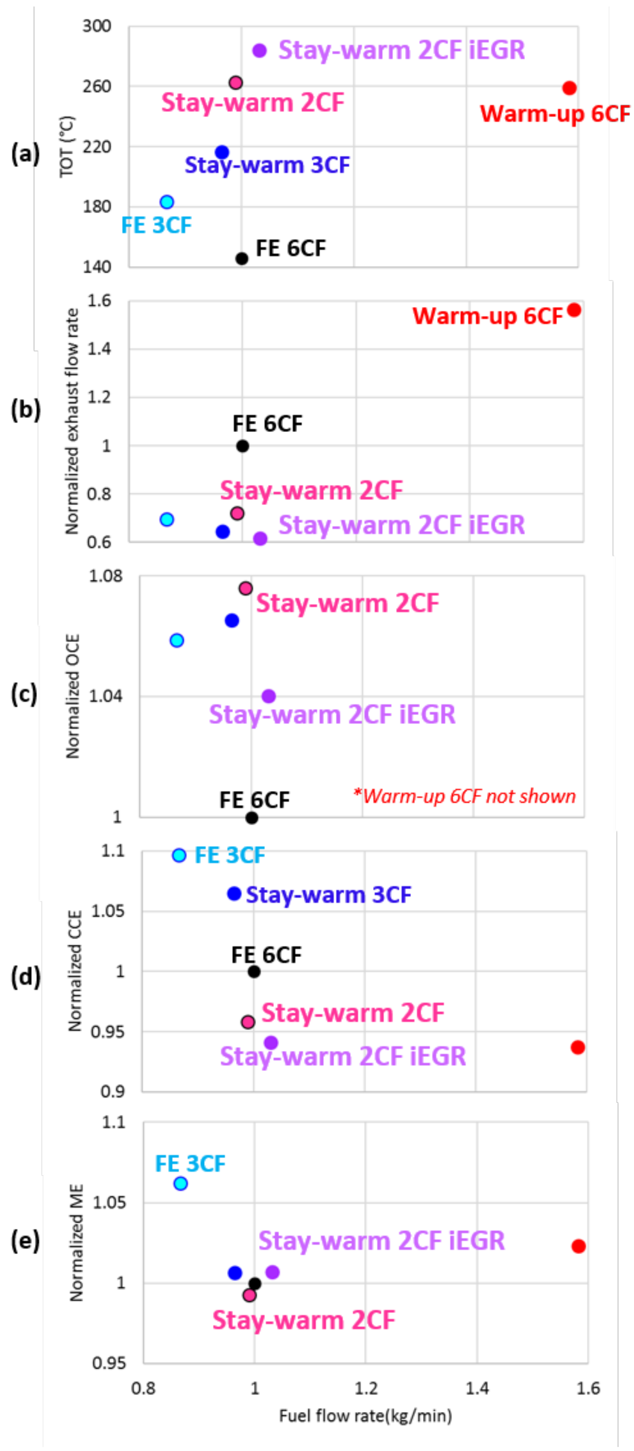

Fig. 5.37. 2CF operation with iEGR can result in nearly 285°C TOT, with lower exhaust flow rate than 'Stay-warm 2CF'.

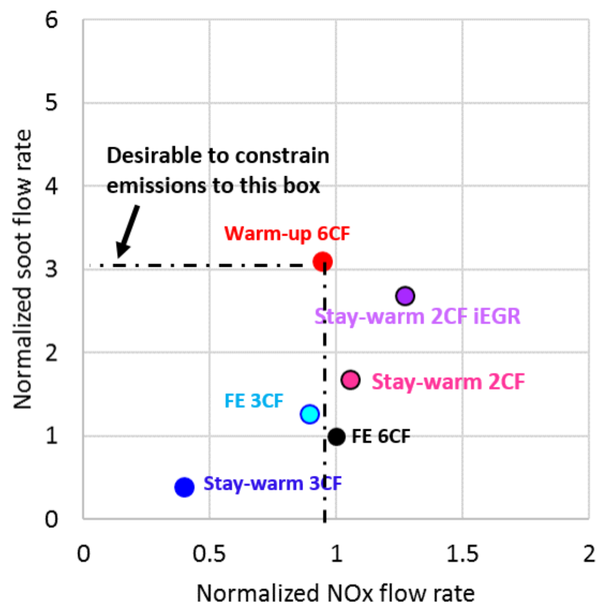

Fig. 5.38. 'Stay-warm 2CF iEGR is not able to completely meet the desired emission limits. Engine out NOx is nearly 20% higher.

2CF iEGR'. Increase in fuel consumption (6%) is in part due to increased pumping losses due to recompression resulting from NVO. Exhaust flow rate decreases as the trapped exhaust gas inside the cylinder displaces fresh air.

Figure 5.37(c) shows that OCE decreases, which is due to increased pumping losses. CCE (Figure 5.37(d)) also decreases due to higher heat loss due to trapping of exhaust gas as well as due to a wider heat release rate. A small improvement is seen in ME.

Engine outlet emissions of NOx and soot are shown in Figure 5.38. 'Stay-warm 2CF iEGR' results in higher engine out NOx, in spite of using delayed injections. Increasing the amount of negative valve overlap (or increasing the internal EGR fraction) can reduce NOx, but not without increasing engine out soot. Thus, balancing the NOx and soot trade-off is a challenge for 2CF iEGR operation on this particular engine set up.

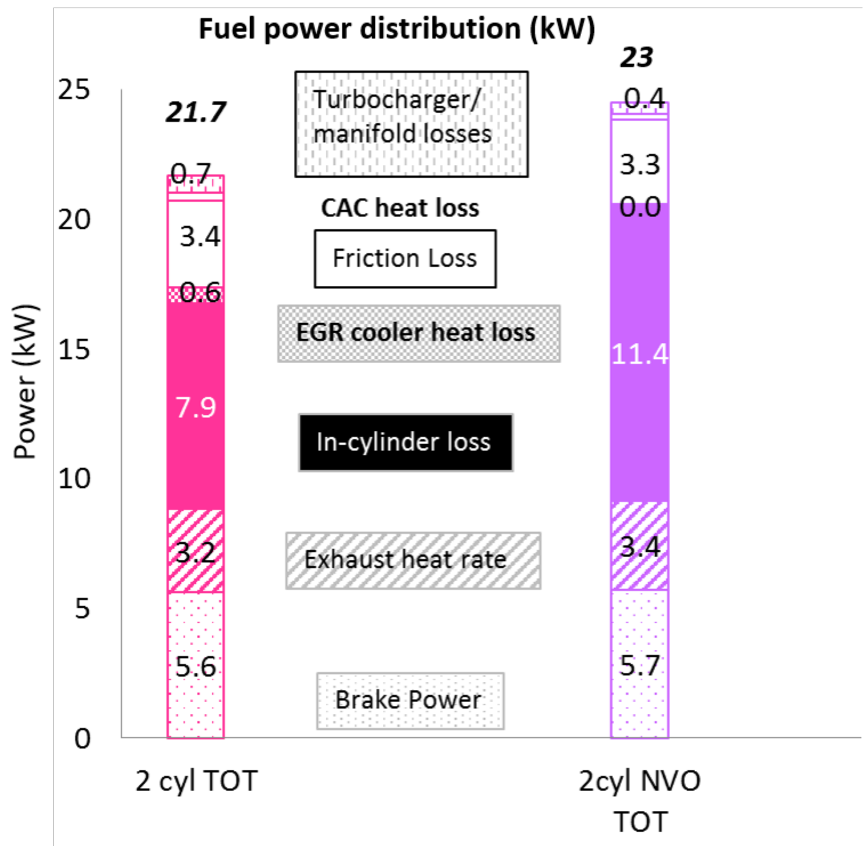

Fig. 5.39. First law analysis comparing ‘Stay-warm 2CF’ and ‘Stay-warm 2CF iEGR’.

The trends seen earlier for iEGR strategies in a first law balance are also seen for 2CF iEGR operation, as per Figure 5.39. In-cylinder heat loss increases due to NVO and wider heat release. EGR cooler losses are eliminated. Reduction in turbocharger/manifold losses can be accounted to a less restrictive VGT position.

Two cylinder operation with internal EGR can achieve elevated TOT, with the challenge of constraining engine out emissions to desired levels without using any external EGR.

5.3.3 Results of Two Cylinder Operation with LIVC

For 2CF operation with LIVC, IVC timing was delayed by 45 crank angle degrees compared to stock IVC timing. Injections close to TDC were used, and VGT position was set to 67% closed. The objective behind using early injections with LIVC was to rely on reduced ECR for NOx control, while improving fuel consumption by using early injections. However, in case of 2CF LIVC too, constraining emissions posed a challenge. Delaying injection timings by an amount sufficient to constrain engine out NOx while using LIVC is not feasible as it led to misfire in the active cylinders. This situation is specific to 2CF operation because of the increased quantity of fuel injected per cylinder. With a higher amount of fuel injected per cylinder, using a very late IVC does not achieve the desired compression for combustion.

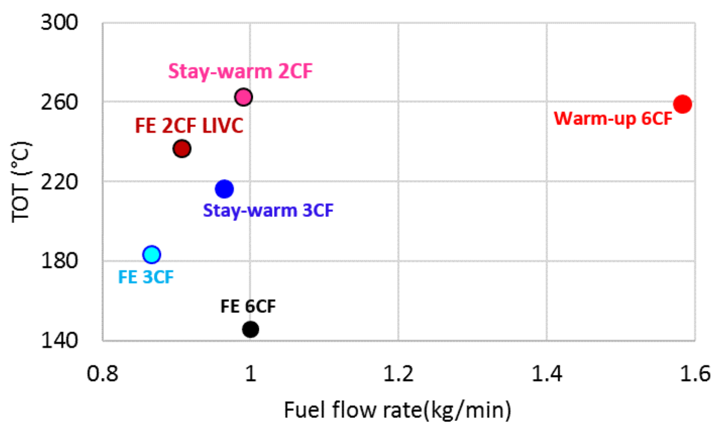

Fig. 5.40. TOT vs fuel consumption for 2CF LIVC operation.

Late IVC also leads to higher engine out soot due to reduction in air fuel ratio via increased fuel consumption. Without using any valvetrain flexibility, 'Stay-warm 2CF' is on the edge of the desired constraints. The most primary effect of adding LIVC to 2CF is then an increase in engine out soot. Two cylinder operation with LIVC results in nearly 250°C TOT, as shown in Figure 5.40, however constraining emission can be challenging due to reasons mentioned above. Emissions are shown in Figure 5.41.

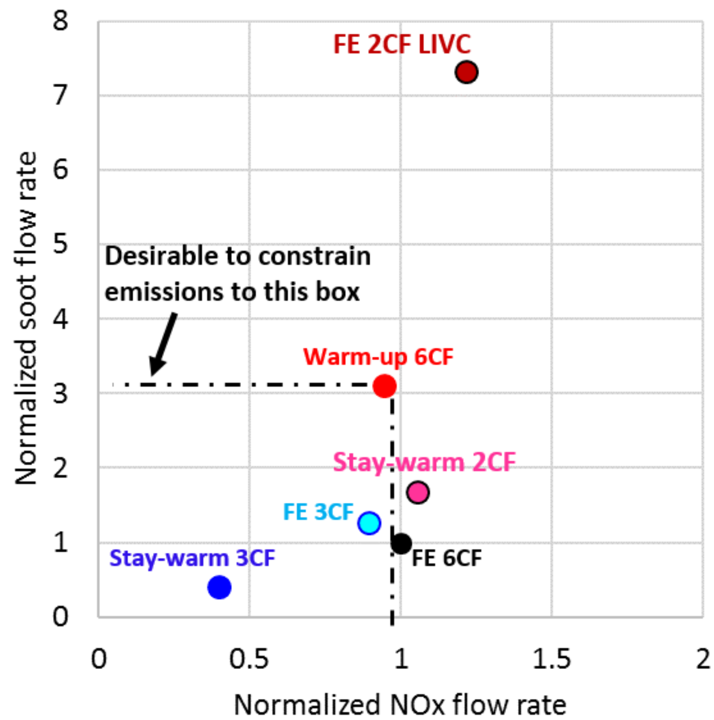

Fig. 5.41. Engine out emissions for 2CF operation with LIVC.

5.4 Comparison of Performance of Key CDA Based Fuel Efficient Stay Warm Strategies

Several of the CDA based stay-warm strategies can be alternatives for maintaining desired ATS temperature while reducing fuel consumption. This section summarizes key CDA based stay-warm strategies. The relative stay-warm performance of these strategies is compared.

Figures 5.42 and 5.43 summarize results of certain strategies. These strategies offer an improved trade-off between TOT and fuel consumption while having other benefits. 'FE 3CF LIVC' obtains desired TOT at lower fuel consumption than 'Stay-warm 3CF', while using early injections and an unrestricted VGT position. 'FE 2CF' offers similar fuel consumption as the most efficient 3CF operation, while using relatively early injections, zero external EGR and unrestricted VGT position. It also

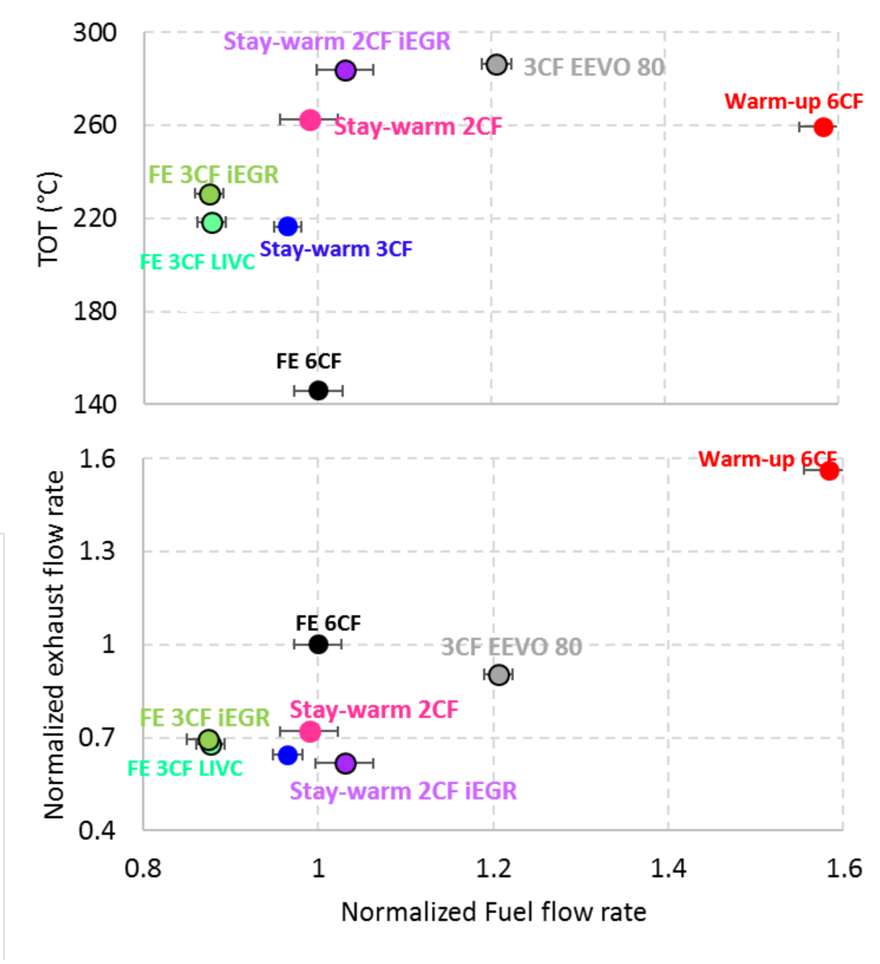

Fig. 5.42. TOT, fuel consumption and exhaust flow rate for key CDA stay-warm strategies.

results in higher TOT than 'Stay-warm 3CF'. 'Stay-warm 2CF' results in similar TOT as 'Warm-up 6CF' with 40% lower fuel consumption. 'Stay-warm 2CF iEGR' can result in higher TOT than 'Warm-up 6CF' without using external EGR or a restricted VGT position. '3CF EEVO 80' can also result in elevated TOT, with higher exhaust flow rate.

'FE 3CF iEGR' has higher engine out NOx, which may not be acceptable at all conditions, but if the ATS is already at an elevated temperature, tail pipe out NOx can be hypothesized to not be drastically higher. A similar argument can be made

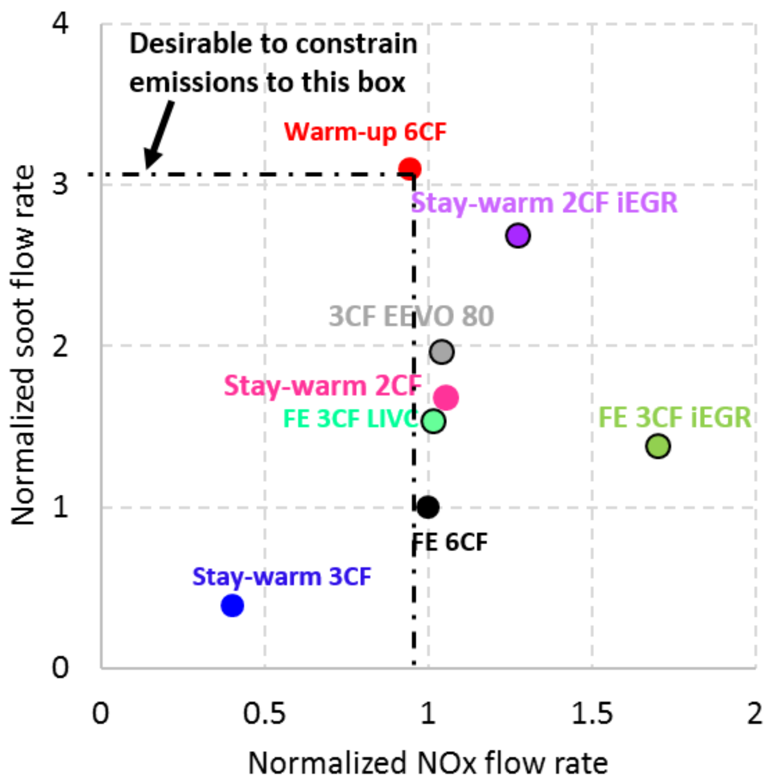

Fig. 5.43. Engine out emissions for key CDA stay-warm strategies.

for 'Stay-warm 2CF iEGR'. All these strategies result in NOx that is lower than the Certified Clean Idle limit of 30 g/hr.

Normalized heat transfer plots for each strategy are shown in Figure 5.44. All CDA strategies outperform 'Warm-up 6CF' for stay-warm performance, primarily due to the reduced flow rate in CDA operation. '3CF EEVO80' also shows some potential for ATS warm-up, although its warm-up performance is not comparable to that of 'Warm-up 6CF'.

A summary of the performance of key CDA based stay-warm strategies is shown in Table 5.1. Comparisons are made with 'Stay-warm 3CF' as this is a strategy that can result in desired ATS thermal management without the need of additional VVA strategies.

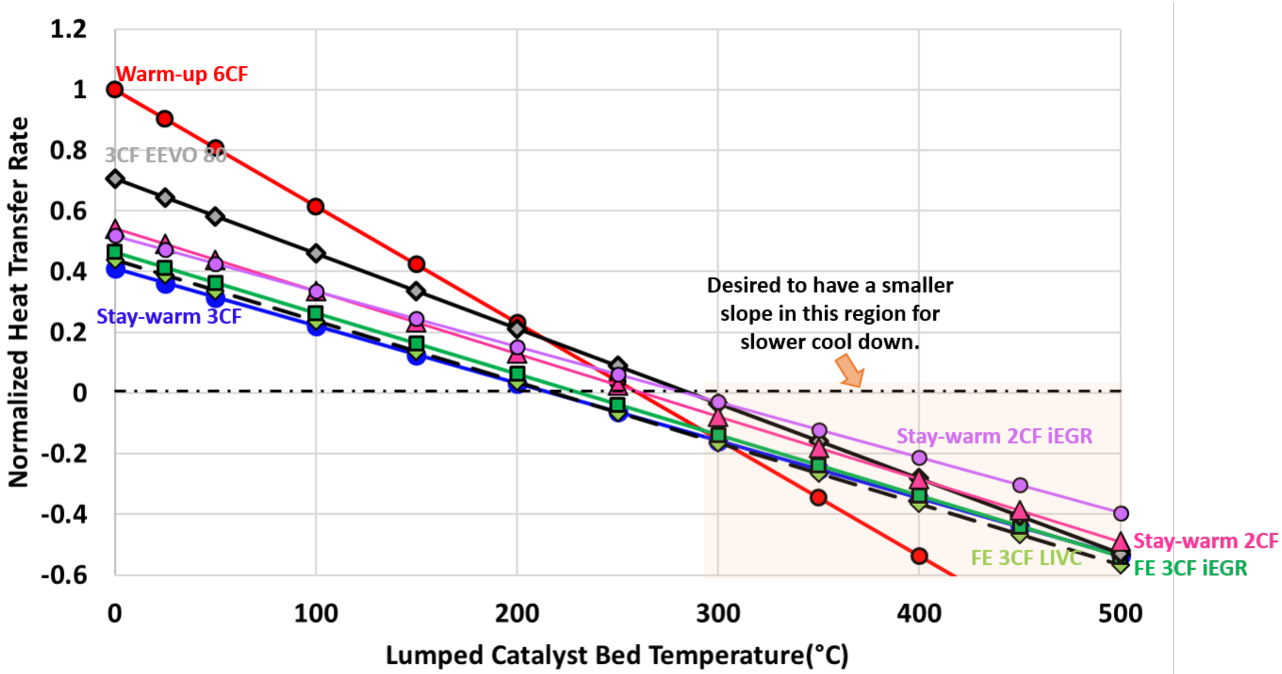

Fig. 5.44. Normalized heat transfer rates show that several of the CDA stay-warm strategies can be considered for a fuel efficient way to maintain ATS temperature.

Table 5.1.
Summary of performance of the key CDA stay-warm strategies compared to 'Stay-warm 3CF'. 'Stay-warm 3CF' is the most competitive CDA based stay-warm strategy which does not use any additional valve train flexibility.

	Comparison with `3CF Stay-warm'				
Strategy	FE 3CF LIVC	FE 3CF iEGR	3CF EEVO 80	Stay-warm 2CF	Stay-warm 2CF iEGR
A/T stay-warm	⬆	⬆	⬆	⬆	⬆
Fuel Consumption	⬇ *(8.8%)*	⬇ *(8.8%)*	⬆ *(24%)*	⬆ *(2%)*	⬆ *(7%)*
Engine out NOx	*Similar*	⬆ *(1.3 times)*	*Within desired limits*	*Within desired limits*	⬆ *(0.87 times)*
Engine out soot	*Within desired limits*	*Within desired limits*	*Within desired limits*	*Within desired limits*	*Within desired limits*
VGT position	*45% closed*	*30% closed*	*84% closed*	*67% closed*	*30% closed*
Injection Timing	*Earlier (at -1 CAD)*	*Earlier (at -4.5 CAD)*	*Similar*	*Similar*	*Similar*

5.5 Summary

Effects of combining VVA strategies with cylinder deactivation were studied here. Using LIVC and iEGR with three cylinder operation resulted in improved trade-off between TOT and fuel consumption. An analysis of in-cylinder content using fundamental equations was used to estimate the amount of internal EGR achieved. Using EEVO with three cylinder operation resulted in TOT that can be useful for ATS temperature maintenance during extended idling. Internal EGR with 2 cylinder operation also resulted in higher TOT without using the VGT or external EGR. It was observed that two cylinder operation with LIVC did not seem viable if engine out emissions were to be constrained while obtaining a stable heat release. The relative stay-warm performance of key strategies was studied, and it was observed that in general, use of VVA with active cylinders in CDA can result in superior fuel-efficient ATS stay-warm performance with advantages such as simplified air handling architecture and use of earlier injections.

6. INTERNAL EGR VIA REINDUCTION AND NEGATIVE VALVE OVERLAP FOR FUEL EFFICIENT AFTERTREATMENT STAY-WARM OPERATION

6.1 Literature Review

Use of internal EGR achieved using various VVA strategies has been studied to a great extent in gasoline engines. Well-established benefits of internal EGR in gasoline engines mostly pertain to improving open cycle efficiency by avoiding intake throttling for air mass control, cold start combustion controllability, charge warm-up and HCCI combustion controllability. A patent filed by Ford [47] describes the effect of phasing the intake and exhaust valves by delaying EVO, EVC, IVO and IVC. A result of delayed EVC is an increase in overlap between intake and exhaust valves, and as the exhaust valve is open during the initial portion of the intake stroke, this results in reinduction of exhaust gases into the cylinder. This operation resulted in NOx emission reduction, reduced dependence on external EGR and improved fuel economy due to reduction of part-load throttling losses. In another study, an oil control valve-based VVA system was developed for a passenger car gasoline engine where internal EGR achieved via negative valve overlap (NVO) was used to heat the cylinder and three-way catalyst during a cold-start. The same study also established the use of exhaust reinduction at part to medium loads to improve intake air swirl and reduce dependence on external EGR [48]. Controls based model development for HCCI in gasoline engines has been studied in [49–52], where residual exhaust gas quantities and properties are controlled (via reinduction or NVO). Other studies for iEGR in gasoline engines has also been described in [53–56]. Use of NVO in gasoline engines has also been studied to enable part fuel injection during the recompression following early EVC to enhance and control the main combustion event [57].

In diesel engines, internal EGR has been studied for improved combustion control for combustion modes like PCCI, HCCI and RCCI [58–62]. Internal EGR was used in an off highway heavy-duty diesel engine to reduce NOx emissions and to supplement external EGR for improved HCCI control [63]. Low load of operation with iEGR for fuel efficiency ATS thermal management has generally not been a focus of past studies in iEGR on diesel engines, with the exception of studies in [64] in which internal EGR via reverse breathing was introduced and studied.

In this chapter, internal EGR via reinduction is studied at 800 RPM/1.3 bar BMEP by presenting comparisons with previously established reference strategies. Further detailed analysis is presented to understand effects of achieving reinduction by different valve timings and lift, and to assist with decisions regarding the most optimal profile to use. Differences between trade-offs achieved in TOT, fuel consumption and emissions are studied. The later half of the chapter presents a comparison of iEGR via NVO and iEGR via reinduction, followed by two short studies involving iEGR via NVO to establish effects of IVO timings and cam phasing on the above mentioned performance parameters. In-cylinder content analysis is used (which was introduced in Chapter 4), to estimate internal EGR fraction and in-cylinder oxygen fraction, thus establishing a simple and representative method for iEGR fraction estimation.

6.2 Motivation for Use of Internal EGR at the Idle Operating Condition

Exhaust gas recirculation is one of the commonly used techniques for in-cylinder control of NOx in IC engines. Recirculated exhaust gas is generally cooled by means of an external cooling circuit before it is re-introduced into the intake manifold. This is done in order to lower temperatures during combustion, thereby slowing down the Zeldovich mechanism and increasing effectiveness of EGR for NOx control. This form of EGR is called external EGR, as recirculated exhaust gas is circulated by means of an external cooling circuit.

Limits on engine out NOx flow rate at the engine idle operating condition are imposed to curb NOx pollution as truck engines spend a significant duration of time at the idle operating condition. In 2008, the California Air Resources Board (CARB) imposed a NOx limit of 30 g/hr for engines intending to idle for more than five minutes at a stretch. The regulation, called the Certified Clean Idle certification, requires engines manufactured in or after 2008 to either shut down after five minutes of idle, or to meet the above limit [34]. Most modern engines certifying to this limit use large quantities of higher pressure external EGR at idle. Certified Clean Idle certification value is expected to decrease further by 67%, resulting in a Certified Clean Idle limit of 10 g/hr [65] in the upcoming updates to CARB regulations.

A positive difference between exhaust manifold pressure and intake manifold pressure is required to drive higher pressure external EGR, along with the ability to regulate this difference between pressure. A commonly used actuator for regulating this difference is the VGT, which at several operating conditions, might also be serving the critical function of ATS thermal management via increasing turbine outlet temperature. In such a scenario, desirable level of control might not be achievable for controlling external EGR fraction using the VGT alone, although the modulation of the EGR valve can provide additional control. Use of the external EGR cooling loop also results in heat loss, which is a critical factor for achieving exhaust temperatures for effective ATS thermal management. EGR cooler fouling due to use of large amounts of cooled external EGR is also a concern [66, 67], especially at idle. Use of internal EGR (iEGR), by virtue of bypassing the external cooling loop, helps to resolve some of the above concerns to varying extents, depending on the technique by which iEGR is achieved.

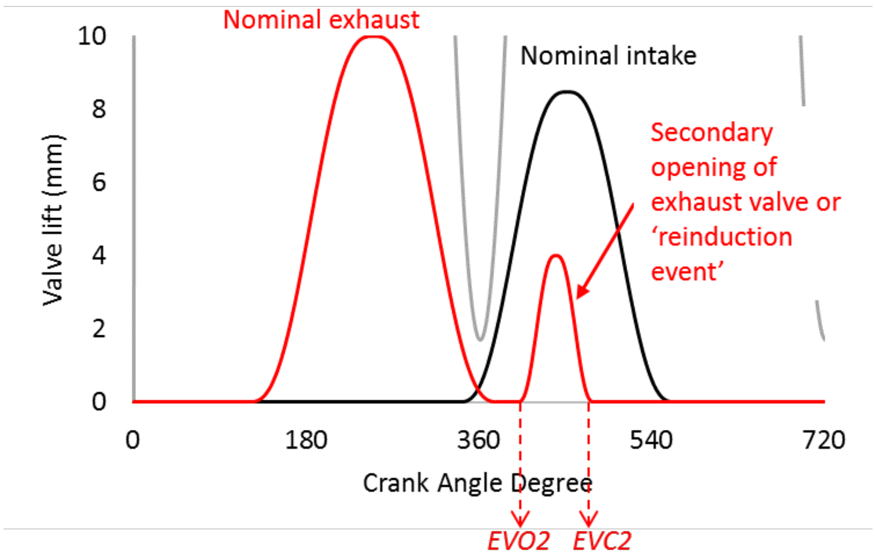

Fig. 6.1. Valve profiles for internal EGR via reinduction.

6.3 Internal EGR via Reinduction

6.3.1 Methodology for Experimental Assessment at 800 RPM/1.3 bar BMEP

Internal EGR via reinduction was studied at 800 RPM/1.3 bar BMEP while using zero external EGR. Performance of iEGR via reinduction for fuel efficient ATS stay-warm was evaluated. Two delayed injections were used, with injection timings maintained constant throughout the study. VGT position was held constant to isolate the effect of reinduction on turbine outlet temperature. Valve profiles for iEGR via reinduction are shown in Figure 6.1. The exhaust valve is opened during the intake stroke to reinduct exhaust gases into the cylinder for providing in-cylinder dilution. The secondary opening of the exhaust valve is called the reinduction event, and EVO2 and EVC2 are used to indicate secondary opening and closing timings respectively.

Internal EGR via reinduction was studied using the following sweeps:

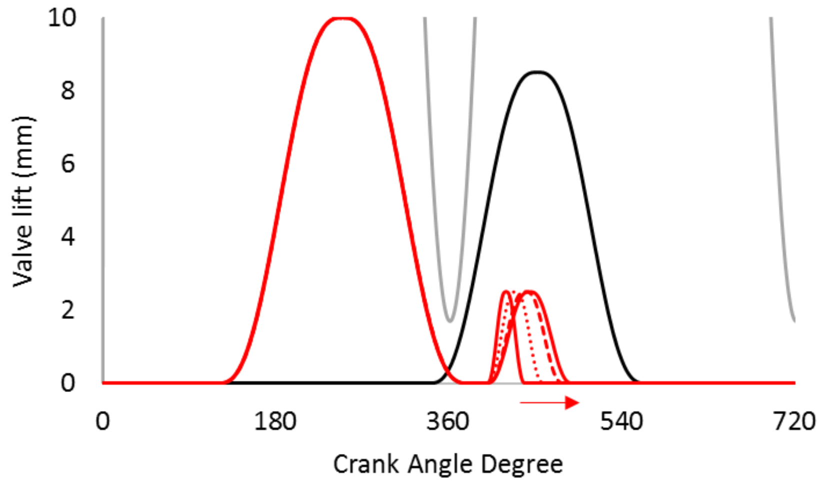

Fig. 6.2. Valve profiles for varied second opening of the exhaust valve during the intake stroke. Primary opening of the exhaust valve, and intake profile are not changed.

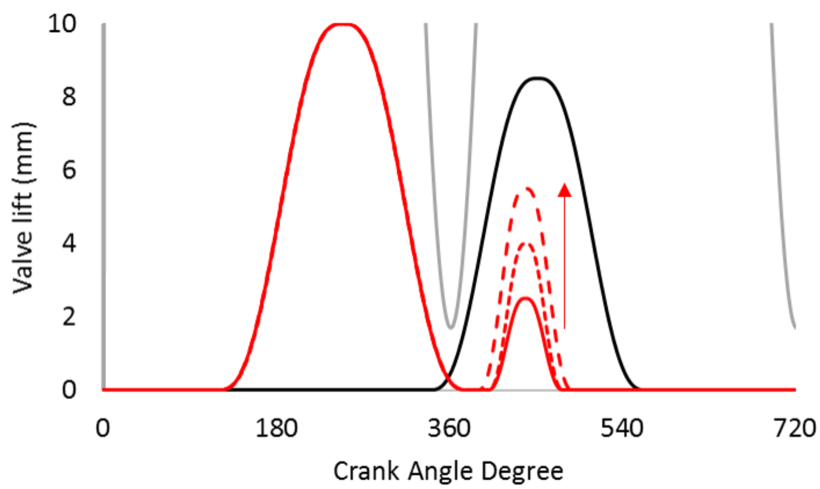

Fig. 6.3. Valve profiles for varied lift of the reinduction event. Primary opening of the exhaust valve and the intake profile are not changed.

1. Secondary closing sweep – EVC2 is varied as shown in Figure 6.2. It was hypothesized that delaying EVC2 will lead to increased amount of reinducted gas.

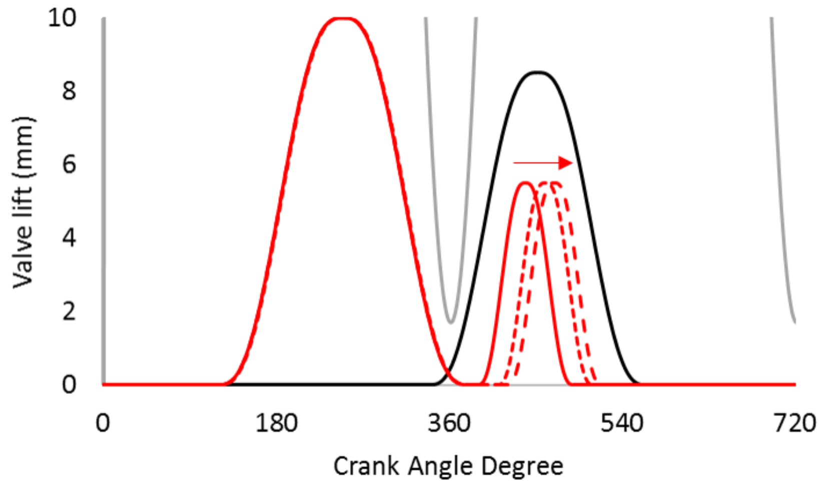

Fig. 6.4. Valve profiles for varied lift of the reinduction event. Primary opening of the exhaust valve and the intake profile are not changed.

2. Secondary lift sweep – Lift of the reinduction event is varied as shown in Figure 6.3.

3. Secondary event phasing sweep – Reinduction event is phased by delaying EVO2 and EVC2 by equal amounts. Valve profiles used are shown in Figure 6.4

The goal of the above sweeps is to help understand the optimum CAD duration for desired fuel efficient stay-warm operation with iEGR via reinduction, while establishing sensitivity of in-cylinder dilution to lift, phase and duration.

Estimation of internal EGR quantity is helpful to achieve the above goal. In-cylinder content analysis is carried out using measurements of thermocouples and in-cylinder pressure. The working fluid, which is assumed to be a homogeneous mixture of fresh air and exhaust gas, is assumed to be an ideal gas. Equations 6.1-6.5 are used for estimating in-cylinder dilution.

$$m_{trapped\,IVC} = m_{fresh\,air} + m_{residual\,gas} + m_{reinducted\,gas} \tag{6.1}$$

Equation 6.1 is a mass balance for the cylinder at IVC, where $m_{fresh\,air}$ is fresh air in the cylinder, $m_{residual\,gas}$ is exhaust gas left over from the previous combustion cycle and $m_{reinducted\,gas}$ is mass of reinducted exhaust gas during the reinduction event. From Equation 6.1, $m_{reinducted\,gas}$ can be estimated by using the following equations and back-substituting in Equation 6.1.

$$m_{trapped,IVC} = \frac{P_{IVC} \times V_{IVC}}{R \times T_{Charge\,Temperature}} \tag{6.2}$$

$$m_{residual\,gas} = \frac{P_{EVC} \times V_{EVC}}{R \times T_{Exhaust\,Temperature}} \tag{6.3}$$

$$m_{fresh\ air} = Fresh\ air\ flow(\frac{kg}{min}) \times \frac{2}{RPM \times No.\ Of\ Active\ Cylinders} \tag{6.4}$$

$Fresh\,air\,flow$ is directly measured using the lab-grade LFE sensor. $T_{Charge\,Temperature}$ and $T_{Exhaust\,Temperature}$ are available as thermocouple measurements. Number of active cylinders is equal to six. Internal EGR fraction can be calculated as

$$internal\ EGR\ fraction = \frac{m_{reinducted\,gas} + m_{residual\ gas}}{m_{trapped\,IVC}} \tag{6.5}$$

In-cylinder oxygen percentage can be calculated in a manner similar to as discussed in Chapter 4. An alternate method to calculate amount of exhaust gas reinducted is by using flow equation for the exhaust valve during the intake stroke, given flow parameters of the exhaust valve and knowledge of in-cylinder and exhaust pressure (not used for results in this work).

6.3.2 Overall steady state results at 800 RPM/1.3 bar BMEP

In this section, the performance of iEGR via reinduction is compared with reference strategies, followed by analysis of effects of parameter variations.

New and prior strategies discussed in this section are briefly described next. Note that strategies 1, 2 and 3 have been introduced in Chapter 4.

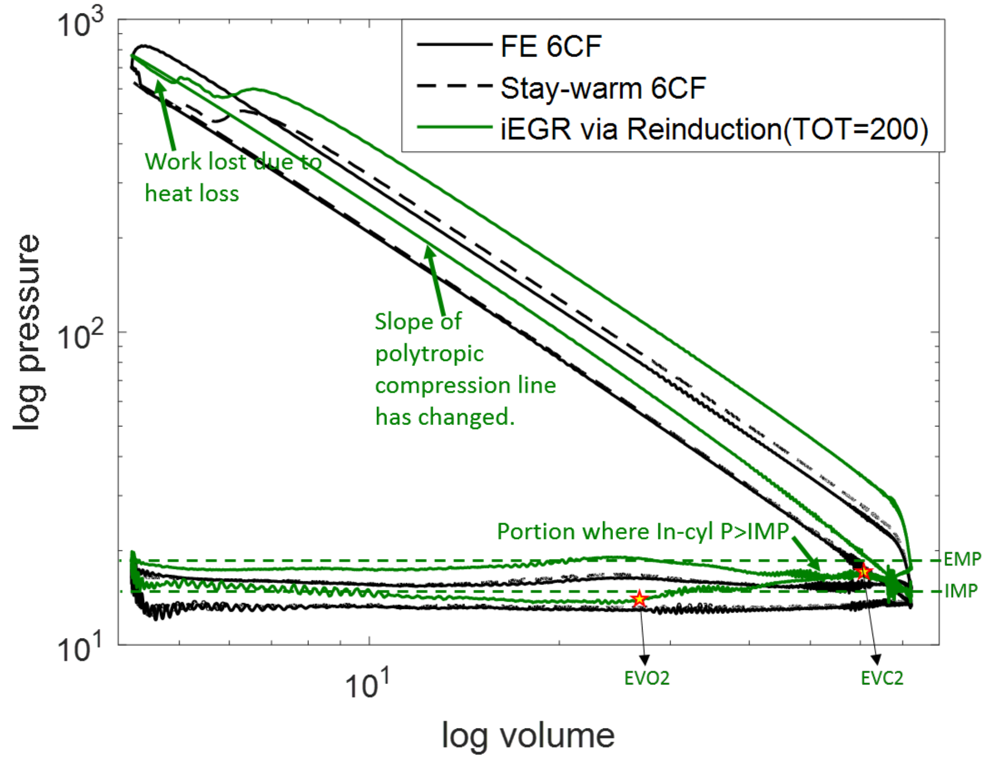

Fig. 6.5. PV diagram for iEGR via renduction shows different slope during compression. In-cylinder pressure becomes equal to exhaust pressure during the reinduction event.

(a) *FE 6CF* – Six cylinder operation with stock calibration optimized for fuel economy at idle. This operation uses two early injections to improve fuel economy. This strategy is not suitable for ATS thermal management on account of lower turbine outlet temperature.

(b) *Warm-up 6CF* – Stock thermal management calibration which uses six cylinder operation with four delayed injections and maximally shut VGT to achieve and maintain desired ATS temperatures.

(c) *Stay-warm 3CF* – Three cylinder operation with two delayed injections and non-maximally shut VGT, a strategy established to maintain desired ATS temperature in a fuel-efficient manner.

(d) *Stay-warm 6CF* – Stock fuel economy calibration with two delayed injections. This strategy demonstrates thermal management capability of six cylinder operation while using two delayed injections, and without VVA functionality. VGT position is close to, but not maximally shut.

(e) *iEGR via Reinduction* – Six cylinder operation with reinduction used on all six cylinders. This strategy uses two delayed injections and zero external EGR. VGT position is maintained similar to ‘FE 6CF’. Steady state points for the sweeps described earlier are shown.

Figure 6.5 shows a logarithmic plot of in-cylinder pressure versus volume for a particular case of iEGR via Reinduction. Plots for ‘FE 6CF’ and ’Stay-warm 6CF’ are shown for reference. EVO2 and EVC2 are marked on the plot. Steady state averaged values of exhaust and intake manifold pressure for ‘iEGR via reinduction’ are also marked.

‘FE 6CF’ uses two early injections (closer to TDC) while ‘Stay-warm 6CF’ and ‘iEGR via Reinduction (TOT=200)’ use two delayed injections. ‘FE 6CF’ and ‘Stay-warm 6CF’ have similar open loop area as these two strategies use the same VGT position, and have similar exhaust flow rate (as shown later).

For ‘iEGR via Reinduction(TOT=200)’, differences are observed in both the closed and open loops of the P-V diagram. Differences between slope of the polytropic compression line can be explained by considering the differences in gas composition. Due to relatively larger amount of in-cylinder dilution (or iEGR), it can be hypothesized that ‘iEGR via Reinduction(TOT=200)’ has a larger ratio of specific heats (gamma) than ‘FE 6CF’, where the gas being compressed does not have as much EGR. The compression ratio does not change as IVC timing remains constant between different strategies. Towards the end of compression, there is less piston work in the form of heat loss. In-cylinder pressure after EVO2 is greater than intake manifold pressure (but lower than exhaust manifold pressure), as expected, because the cylinder is exposed to exhaust manifold due to the open exhaust valve during the intake stroke. In-cylinder pressure remains at this intermediate value throughout the reinduction event, and drops down to another intermediate pressure between intake and exhaust manifold pressure.

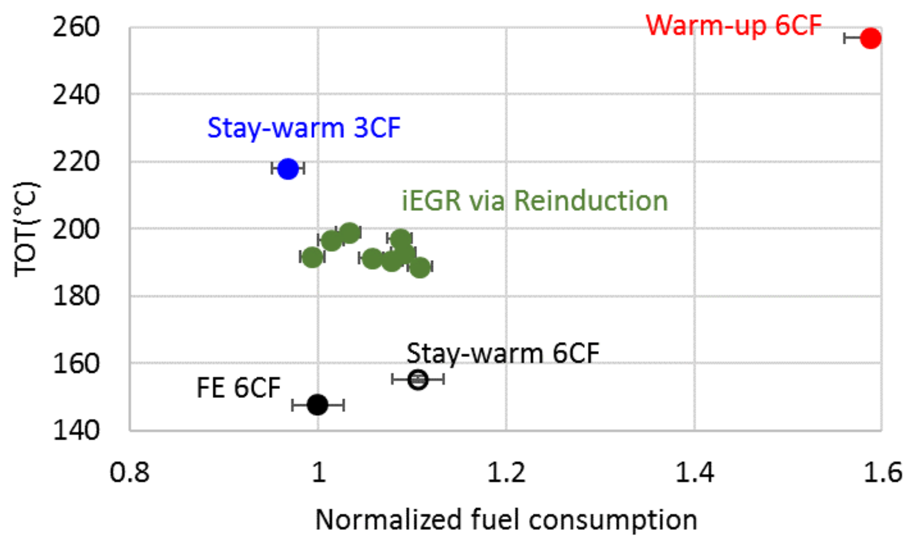

Fig. 6.6. Reinduction results in higher TOT than 'FE 6CF', with fuel consumption varying from 10% increase to 1% decrease depending on the type of reinduction event used.

Figure 6.6 shows the trade-off between fuel consumption and turbine outlet temperature for the strategies described above. Figure 6.7 shows a plot of TOT vs exhaust flow rate. As was discussed in Chapter 4, 'Warm-up 6CF' results in nearly 60% higher fuel consumption compared to 'FE 6CF', and is conventionally used for effective ATS thermal management at idle. 'Stay-warm 3CF' offers an improved solution to maintain ATS temperatures, while reducing fuel consumption by 4% (compared to 'FE 6CF').

'Stay-warm 6CF' is obtained by delaying injection timings, and results in 11% higher fuel consumption than 'FE 6CF' with 7°C higher TOT.

Points labeled as 'iEGR via Reinduction' represent variations obtained by sweeping EVO2, EVC2 and lift of the reinduction event. These points indicate the FC vs TOT space that can be traversed with such variations of the reinduction event.

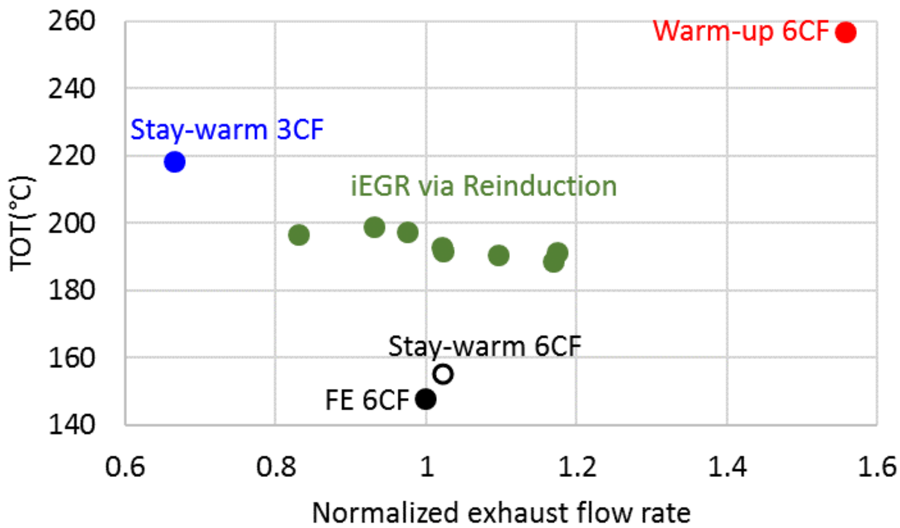

Fig. 6.7. Reinduction can result in upto 20% lower exhaust flow rate compared to 'FE 6CF'; albeit reductions in exhaust flow rate comparable to 'Stay-warm 3CF' are not possible (within emission constraints).

It is observed, in general, that use of reinduction (with zero external EGR) results in higher TOT than 'FE 6CF' with fuel consumption ranging from an increase of 10% to a decrease of 1%. Increase in TOT is primarily due to reduction in exhaust flow rate, as shown in Figure 6.7. Eliminating heat loss to the external EGR cooler is another reason for higher TOT than 'FE 6CF'. Reduction in exhaust flow rate is achieved by using relatively higher quantities of in-cylinder dilution (or iEGR), which displaces fresh air. Exhaust flow rates are however greater than 'Stay-warm 3CF' operation indicating that even with use of large quantities of internal EGR (with soot emissions constrained), six cylinder operation cannot reach exhaust flow rates comparable to three cylinder operation. 'iEGR via Reinduction' is able to achieve 200°C TOT, with 1% lower fuel consumption and nearly 20% lower exhaust flow rate than 'FE 6CF' operation. A maximally shut VGT is not required and neither is external EGR. 'Stay-warm 6CF' cannot achieve elevated TOT even with the use of delayed injections.

Engine out NOx and soot emissions for above strategies are shown in Figure 6.8.

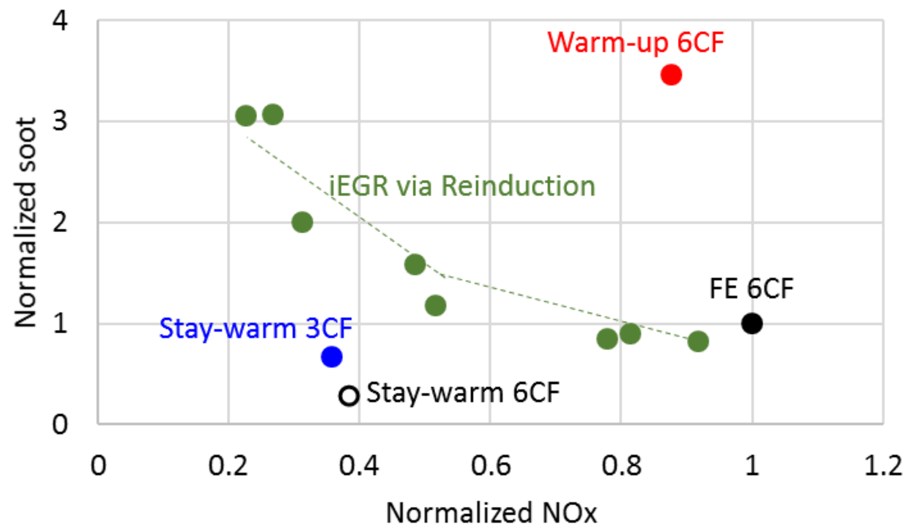

Fig. 6.8. iEGR via Reinduction results in upto 80% lower engine out NOx, with soot emissions constrained to desired values.

Reinduction is able to achieve emissions equivalent to or lower than 'Warm-up 6CF' (which is the stock calibration that corresponds to meeting 2010 emission norms). Decrease in NOx from 'FE 6CF' to 'Stay-warm 6CF' is due to the use of delayed injections in 'Stay-warm 6CF'. Upto 80% lower NOx is achieved using reinduction as a result of using delayed injections and increased in-cylinder dilution via iEGR. Reinduction shows the trend of increasing soot emissions as NOx decreases - this is due to increasing quantity of internal EGR. For approximately similar engine out NOx, reinduction results in higher soot than 'Stay-warm 3CF'. One significant reason for this is the fact that reductions in engine out NOx flow rate for the latter are also attributed to lower exhaust flow rate. Engine out concentration of NOx, however, shows a different trend as seen in Figure 6.9. Reinduction results in lower NOx concentration in parts per million compared to 'Stay-warm 3CF'. Lower NOx concentration can be attributed to relatively higher in-cylinder dilution along with hypothesized lower temperatures for the Zeldovich mechanism as the quantity of fuel combusted per cylinder per cycle is lower compared to 'Stay-warm 3CF'.

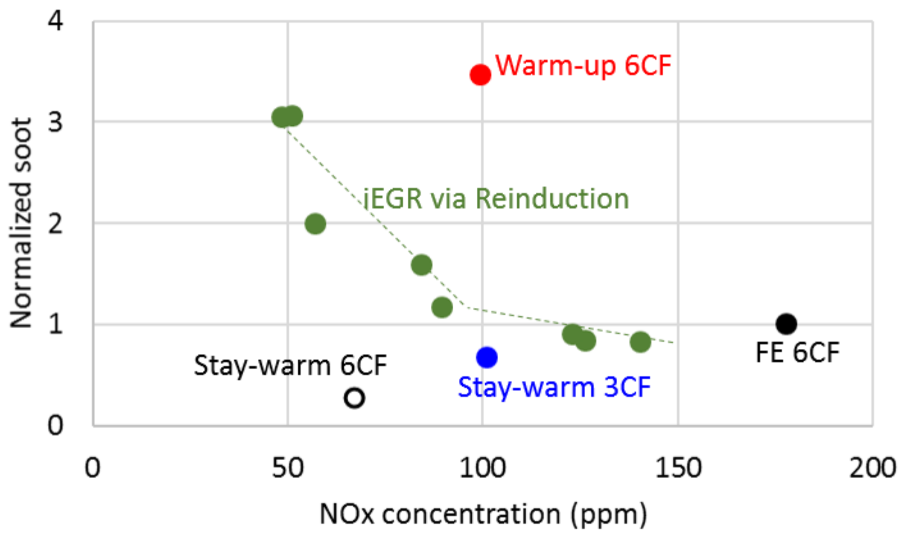

Fig. 6.9. An interesting trend can be observed from engine out NOx concentration of reinduction compared to other strategies.

6.3.3 Results of Varying Exhaust Valve Closing of Secondary Reinduction Event

Valve profiles for this sweep are shown in Figure 6.2. Steady state results are normalized with respect to 'FE 6CF'. 'Warm-up 6CF' is not shown in these plots. Exhaust valve closing for the reinduction event is varied from 440 CAD to 490 CAD, while exhaust valve opening is maintained constant at 400 CAD with a constant lift. No external EGR is used. Quantity of reinducted exhaust gas is expected to increase with increasing duration of the reinduction event i.e. with delay in EVC2.

Figure 6.10 shows that the effect of increased reinduction via delaying EVC2 is primarily seen as differences in the pumping loop. Note that EVO2 is maintained constant for all cases. As shown in the zoomed in portion, slightly higher exhaust manifold pressure is observed with the earliest EVC2, and decreases with delayed EVC2. These differences, albeit not significant, can be attributed to difference between exhaust flow rate. This observation is also a reason for the slower rate of rise

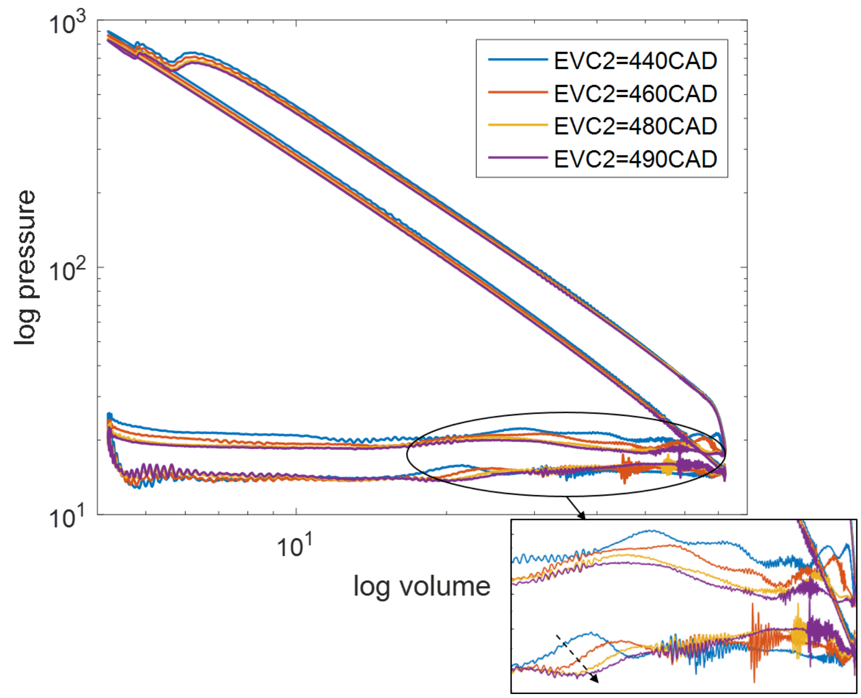

Fig. 6.10. PV diagrams for various (delayed) values of EVC2. Dotted arrow in offset shows direction of increasing reinduction.

of in-cylinder pressure during the reinduction event, as shown by the dotted arrow in offset.

Comparison of other key parameters in Figure 6.11(a) shows that nearly 10°C increase in TOT is obtained with a 50 CAD delay in EVC2. This is partly an effect of reduction in exhaust flow rate, as seen in Figure 6.11(b). Reduction in exhaust flow rate is expected as EVC2 is delayed due to increased amount of reinducted exhaust gas. Open cycle efficiency increases due to a smaller pumping loop as a consequence of reduction in fresh air flow rate. Closed cycle efficiency decreases as EVC2 is delayed, however rises back to similar values as 'FE 6CF', possibly due to reduction of in-cylinder heat loss. It is interesting to note that 'Stay-warm 6CF' has lower closed cycle efficiency than the reinduction points in spite of similar injections timings - this is due an advanced heat release (and smaller CA50) with reinduction points. This can

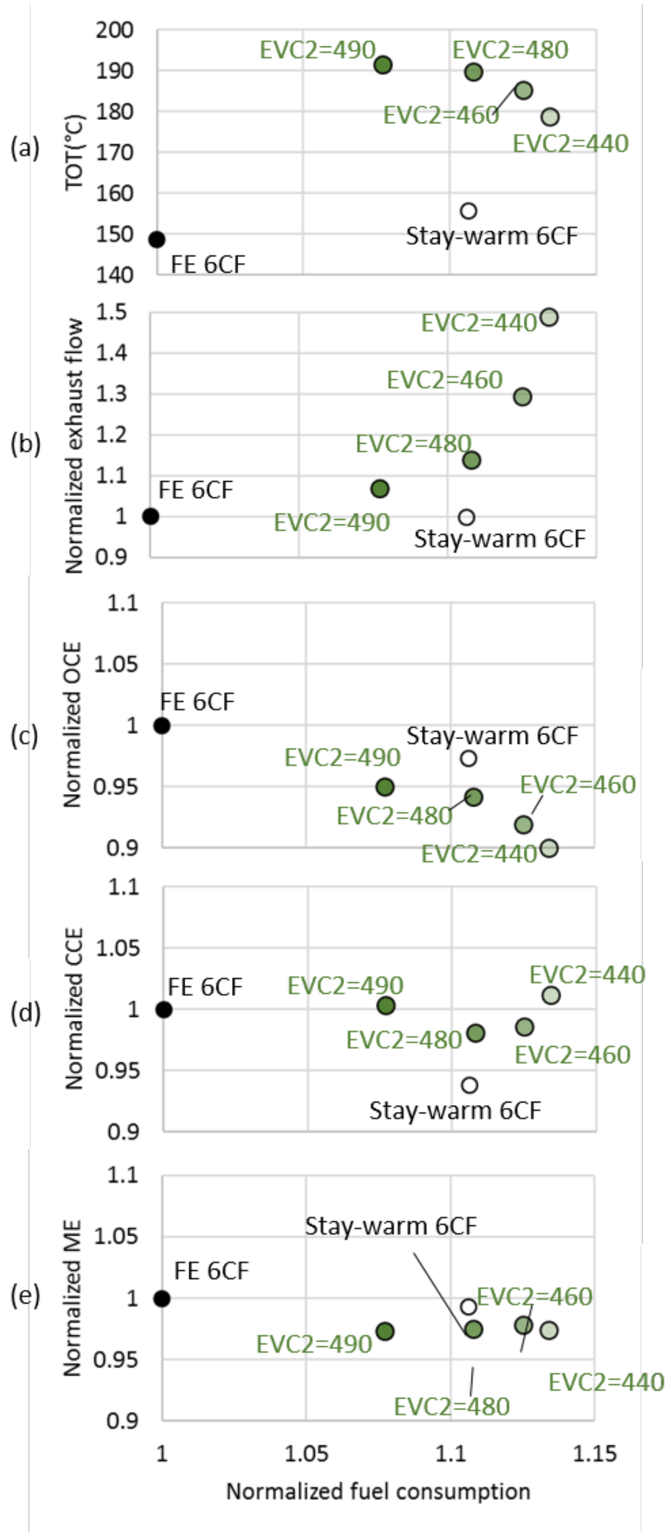

Fig. 6.11. TOT, exhaust flow rate and cycle efficiency values for varying EVC2 in study of iEGR via reinduction are compared.

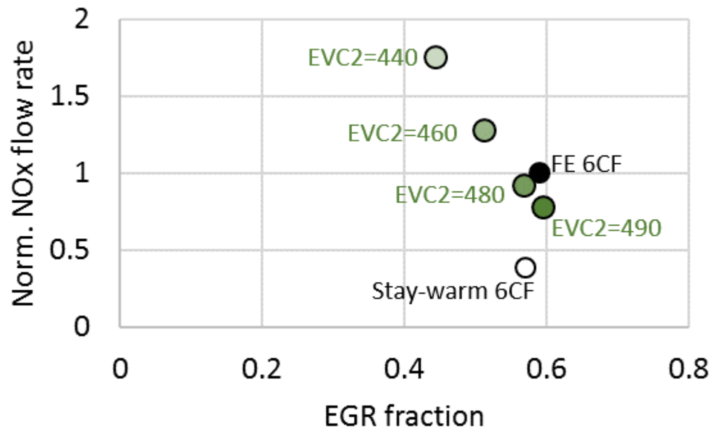

Fig. 6.12. Engine out NOx as a function of computed EGR fraction.

also be thought of as an effect of higher gamma with the reinduction case. Mechanical efficiency is similar for 'FE 6CF', 'Stay-warm 6CF' and reinduction.

A plot of EGR fraction as computed by the equations described earlier is shown in Figure 6.12. Increasing EGR fraction for reinduction cases corresponds to delayed EVC2. It appears from this plot that beyond a certain value, further delay in EVC2 has diminishing effect on iEGR fraction. This figure shows that in spite of similar value of computed EGR fraction for the cases shown in this figure, NOx values show greater variation – this is an effect of delayed injection timings while comparing 'FE 6CF' and 'Stay-warm 6CF'; and an effect of using colder EGR in case of 'Stay-warm 6CF' compared to the reinduction points. 'Stay-warm 6CF' uses cooled external EGR. Note that the method used here for estimating EGR fraction (even for 'FE 6CF' and 'Stay-warm 6CF') is different than CO2-concentration based estimation of EGR fraction.

Figure 6.13 shows the dependence of engine out NOx on estimated in-cylinder oxygen fraction. Finally, Figure 6.14 shows engine out emissions of NOx and soot, along with dotted lines indicating corresponding desired constraints.

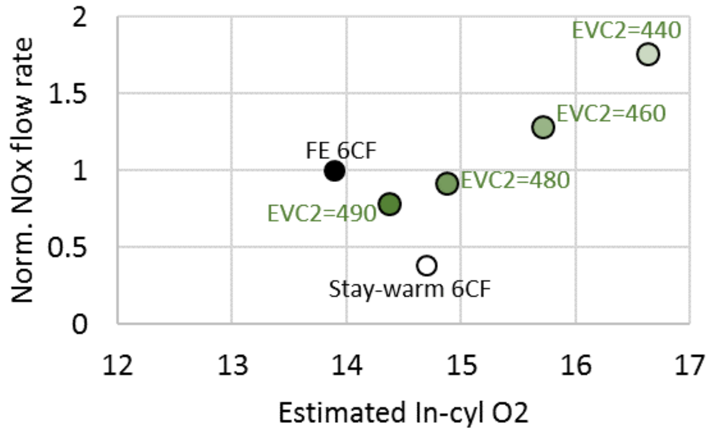

Fig. 6.13. Estimated in-cylinder oxygen fraction decreases with delay in EVC2.

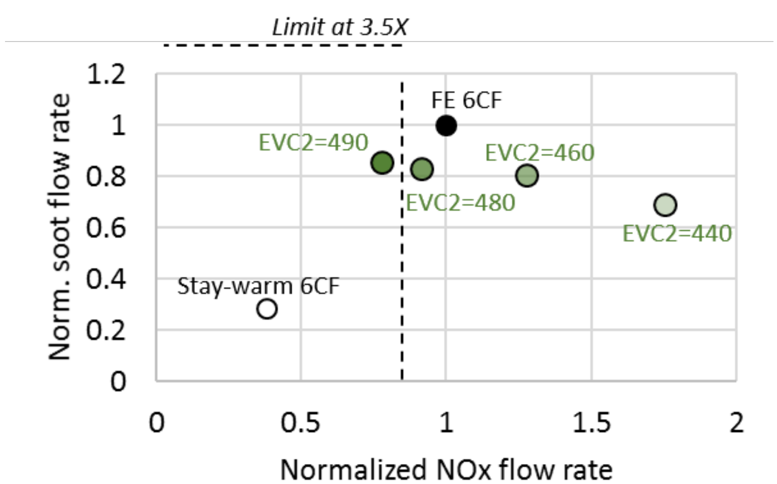

Fig. 6.14. Engine out soot vs NOx flow for EVC2 sweep

6.3.4 Results of Varying Lift of Secondary Reinduction Event

Experimental steady state results of varying the lift of reinduction event are discussed in this section. Valve profiles used are shown in Figure 6.3. Duration of the reinduction event is maintained constant. It is expected that increasing lift will lead to greater amount of in-cylinder dilution via internal EGR. Results for TOT, exhaust flow rate and cycle efficiency are shown in Figure 6.15.

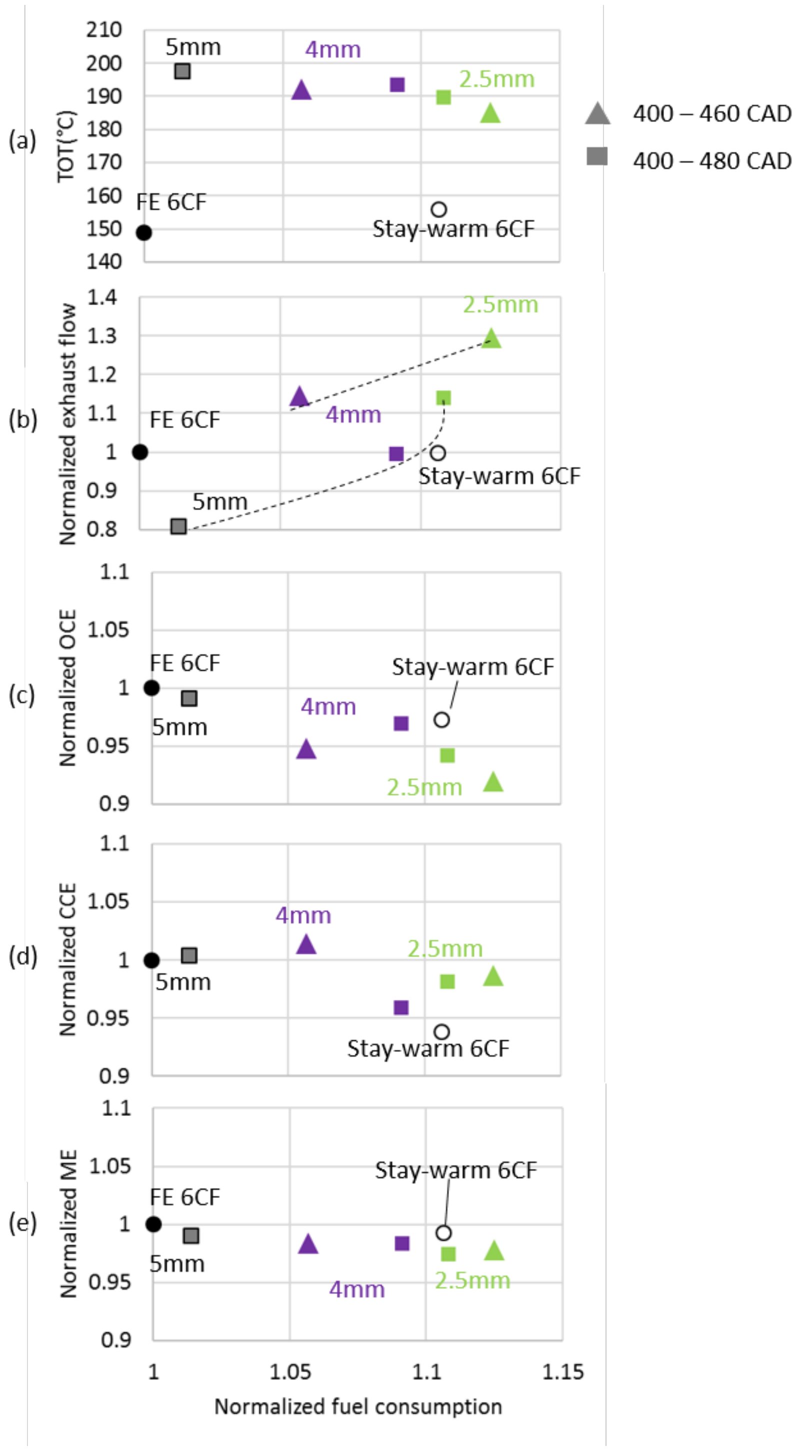

Fig. 6.15. For the same duration, increasing lift of the reinduction event leads to lower exhaust flow rate and hence increases in TOT are observed.

In Figure 6.15, data points represented using similar shapes have constant duration of reinduction event. As lift increases, exhaust flow rate decreases and TOT increases, amounting to 10°C for the case of 400-480 CAD duration. Figure 6.15(b) shows a sharper trade-off between reduction in exhaust flow rate and increasing duration for the 400-480 CAD than for the duration of 400-460 CAD. This implies greater effects of lift on gas flow dynamics for larger duration of reinduction event.

Open cycle efficiency, as shown in Figure 6.15(c) follows a trend correlated with exhaust flow rate : decrease in exhaust flow rate corresponds to improving open cycle efficiency.

In conventional operation, generally, closed cycle efficiency is observed to decrease with introduction of EGR due to additional heat loss and delayed heat release. On the other hand, Figure 6.15(d) shows that cases with 5mm lift and 2.5mm lift have similar closed cycle efficiency. In the case of 400-460 CAD duration, the 4mm lift case shows higher closed cycle efficiency than the 2.5mm lift case. This can be explained by considering the ratio of specific heats (gamma) for the different cases. A plot of closed cycle efficiency versus gamma is shown in Figure 6.16. In the case with 400-460 CAD duration, 2.5mm and 4mm lift cases have the same closed cycle efficiency, in spite of expected higher amount of internal EGR (and hypothesized heat loss) for 4mm lift case. However, gamma is higher for the 4mm lift case, and this fact can be used to explain the observed trend in closed cycle efficiency. For cases where relatively larger amount of in-cylinder dilution is used (via internal EGR or external EGR or both), closed cycle efficiency will be affected more strongly by mixture properties like gamma. Increase in gamma can be attributed to increasing temperature of the combustion mixture and to mixture composition. For the above cases, gamma was calculated using measured in-cylinder pressure and volume data, and the fact that $PV^{\gamma} = constant$ for a polytropic process.

A mathematical relation between closed cycle efficiency and gamma for the Diesel cycle is given by Equation 6.6 [68].

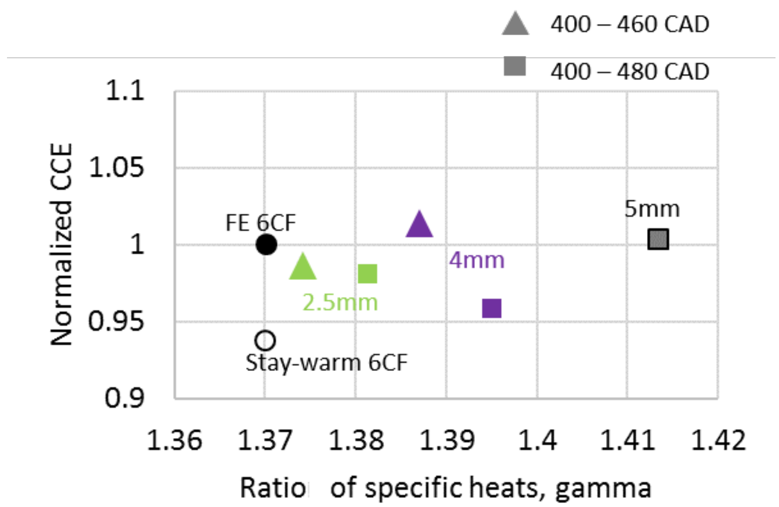

Fig. 6.16. Closed cycle efficiency for cases with large amounts of internal EGR is also influenced by gamma of the combustion mixture.

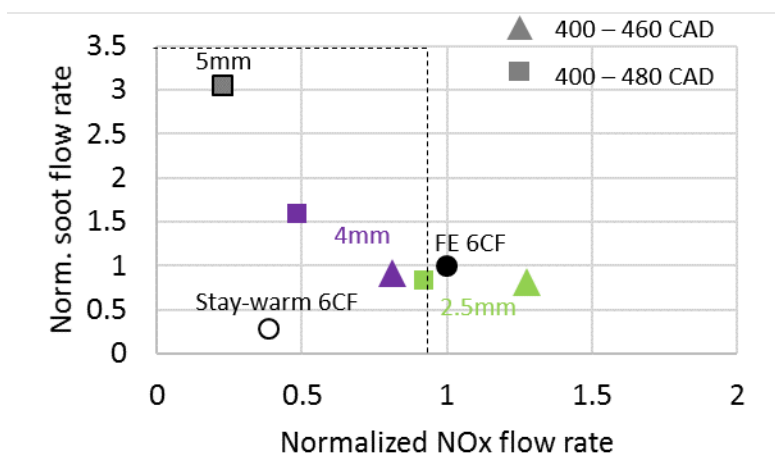

Fig. 6.17. Engine out NOx and soot are within desired constraints.

$$\eta_{closed\ cycle} = 1 - \frac{1}{r^{\gamma-1}} \times \frac{\alpha^{\gamma} - 1}{\gamma(\alpha - 1)} \tag{6.6}$$

where r is the compression ratio (generally, geometric; more accurately, effective), α is the cut-off ratio i.e. ratio of end and start volume during combustion phase and γ is the ratio of specific heats for the combustion mixture.

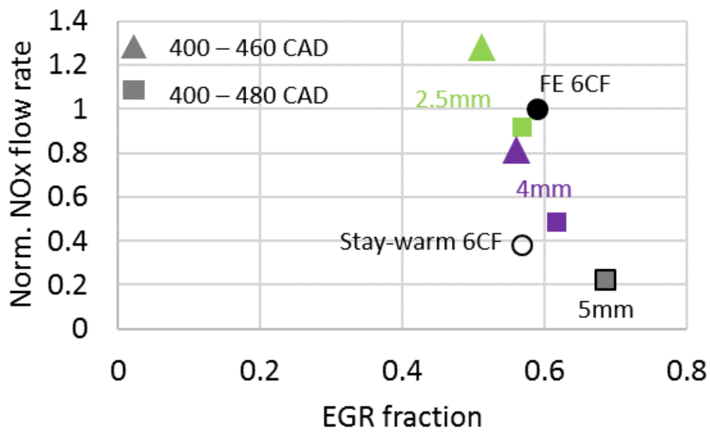

Fig. 6.18. Engine out NOx as a function of calculated EGR fraction.

Mechanical efficiency, per Figure 6.15(e) is nearly equivalent across the different cases, albeit being lower for the reinduction cases : this can be attributed to frictional losses associated with the reinduction event.

Engine out emissions are shown in Figure 6.17. The desired emission constraints (as set by 'Warm-up 6CF') are shown by dotted lines. Significant reduction in engine out NOx is achievable by using internal EGR. NOx emissions as a function of calculated EGR fraction are shown in Figure 6.18.

Figure 6.19 shows the PV diagrams for both reinduction durations. In-cylinder pressure during exhaust stroke decreases as lift increases, which is a direct consequence of reduction in air flow rate.

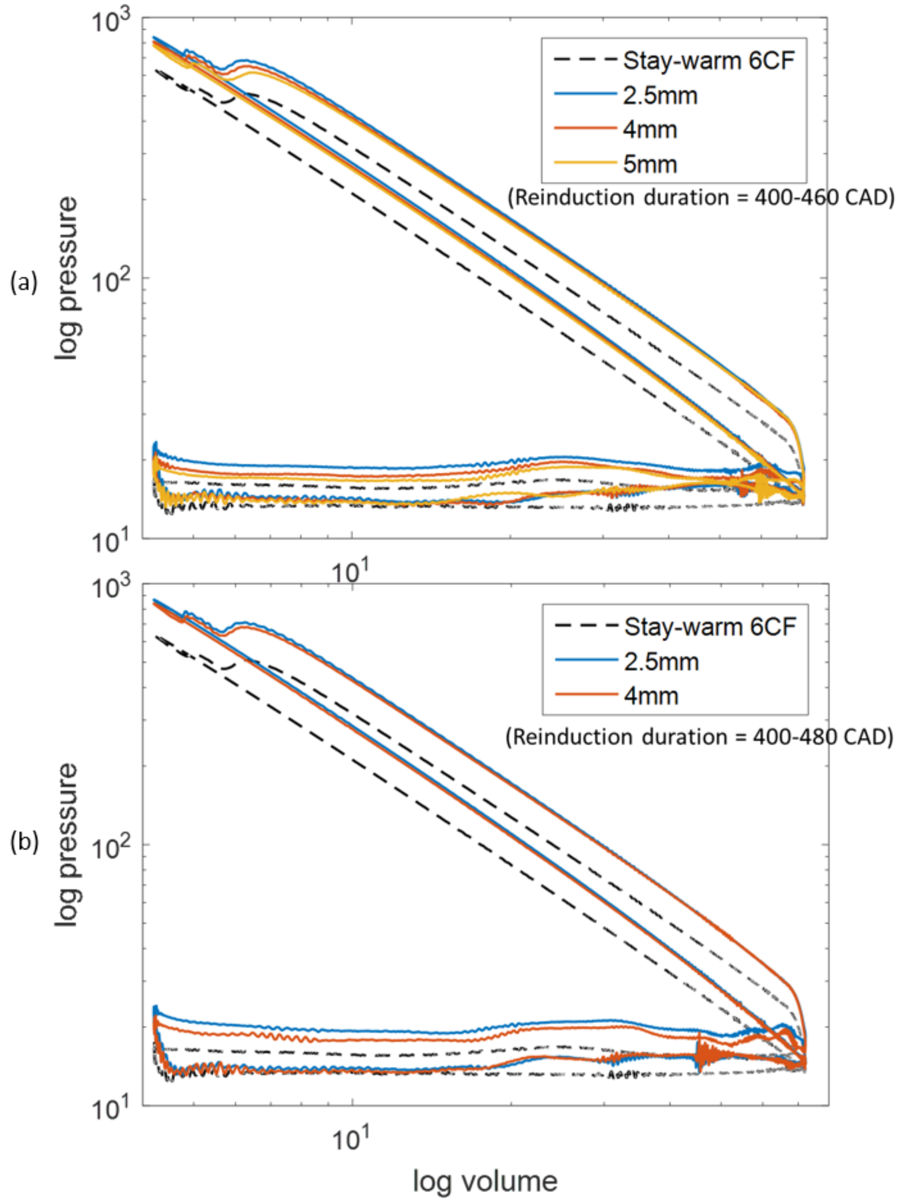

Fig. 6.19. PV diagram for the various lift cases shows effect of increasing lift on in-cylinder pressure, however this has more sensitivity to duration than lift.

6.3.5 Results of Phasing of Secondary Reinduction Event

This section presents a study in the effects of phasing the reinduction event to assess impact on mass of reinducted gas. Secondary exhaust valve opening and closing timings were varied. Lift was maintained constant at 5.5 mm. Duration of the reinduction event was maintained constant. Valve profiles are shown in Figure 6.4.

The turbine outlet temperature, exhaust flow rate and values for cycle efficiencies are shown in Figure 6.20. Phasing the reinduction profile does not indicate a significant change in TOT, as seen in Figure 6.20(a). This trend can be explained by studying the trend in exhaust flow rate and fuel consumption. The '420-520CAD' duration case has highest exhaust flow rate amongst the cases with iEGR via reinduction. In this case, it would be expected to have lower TOT due to higher AFR, however this is not the case because the '420-520CAD' duration case also has higher fuel consumption on account of lower open and closed cycle efficiencies. All the cases with iEGR have higher TOT than 'FE 6CF', although TOT is lower than that observed with 'Stay-warm 6CF' (circa 220°C). Figure 6.20(b) shows that as the reinduction profile is phased further away from (intake) TDC, exhaust flow rate increases. This phenomenon is examined more closely in a later subsection using GT-Power simulations. Trends in open cycle efficiency are consistent with trends in exhaust flow rate, where it is observed for the reinduction cases that OCE decreases as exhaust flow rate increases. Reduction in CCE for the 420-520CAD case can be accounted to higher in-cylinder heat loss on account of higher mass of fresh air during combustion. Mechanical efficiency is lower for the cases with reinduction. As a result of lower OCE, CCE and ME the case with reinduction event 420-520 CAD has lower fuel efficiency than 'FE 6CF'.

Engine out emissions are shown in Figure 6.21. Desired emission constraints are indicated by dotted lines. It can be noted that for nearly equivalent value of engine out NOx, case with 420-520 CAD has lower soot than the case with 410-510 CAD. This is due to higher fresh air flow rate with the latter. Higher soot with the former

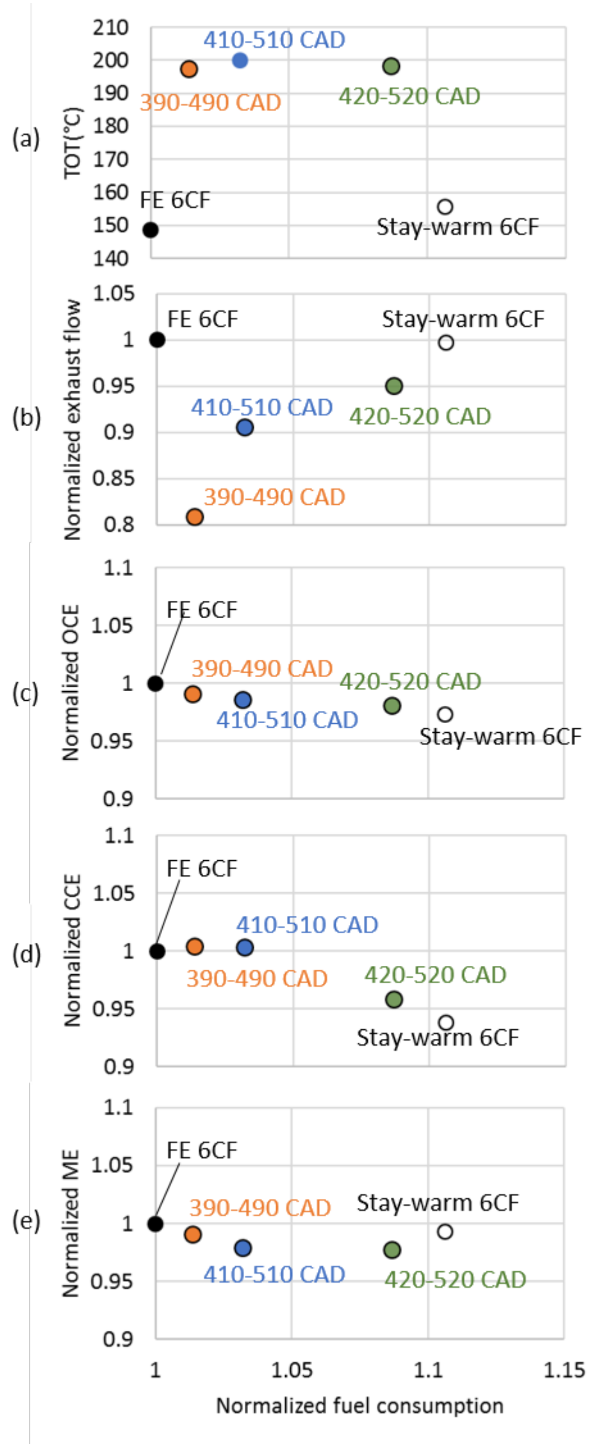

Fig. 6.20. TOT, exhaust flow rate and cycle efficiency comparisons for phased reinduction event. Exhaust flow rate increases as the profile is phased further away from TDC.

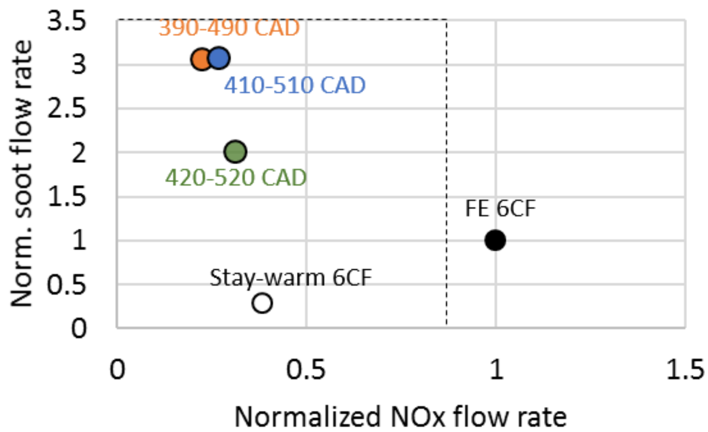

Fig. 6.21. Emissions are within desired constraints for phased reinduction sweep.

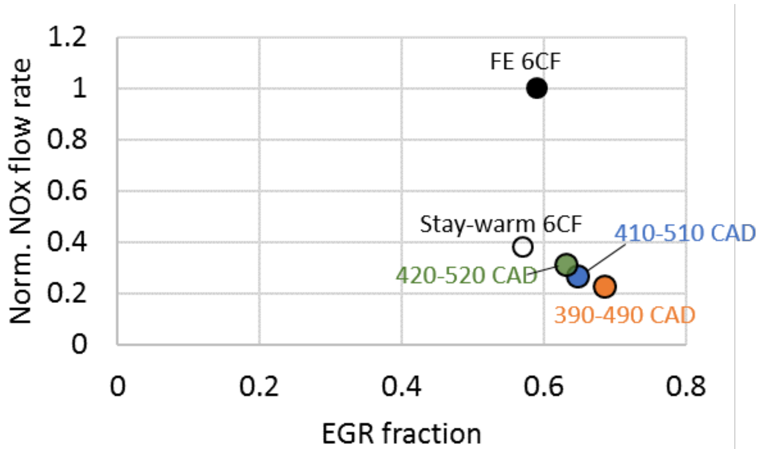

Fig. 6.22. Engine out NOx as a function of calculated EGR fraction.

can be attributed to larger quantity of hot internal EGR. 'Stay-warm 6CF' has lower engine out NOx as well as soot, however it is not a preferred strategy for fuel-efficient stay-warm operation on account of its higher exhaust flow rate, fuel consumption and lower TOT. Engine out NOx as a function on calculated EGR fraction is shown in Figure 6.22. EGR fraction reduces as the reinduction event is phased, and this is an effect of reduced amount of reinducted gas for a larger quantity of fresh air. Variation in EGR fraction is relatively small compared to variation in engine out NOx.

Effect of phased reinduction profile on exhaust flow rate

Increased exhaust flow rate with phased profile can be explained by examining the interaction between the following (primarily) significant flows: exhaust gas flowing into the cylinder from the exhaust manifold (with piston moving down), intake gas (fresh air) flowing into the cylinder from the intake manifold and exhaust gas flowing from the exhaust manifold to the intake manifold via the cylinder. Figure 6.23 is a schematic highlighting these flows. A positive difference between exhaust and intake manifold pressure is assumed, as is the generally the case for most operating points of a turbocharged diesel engine.

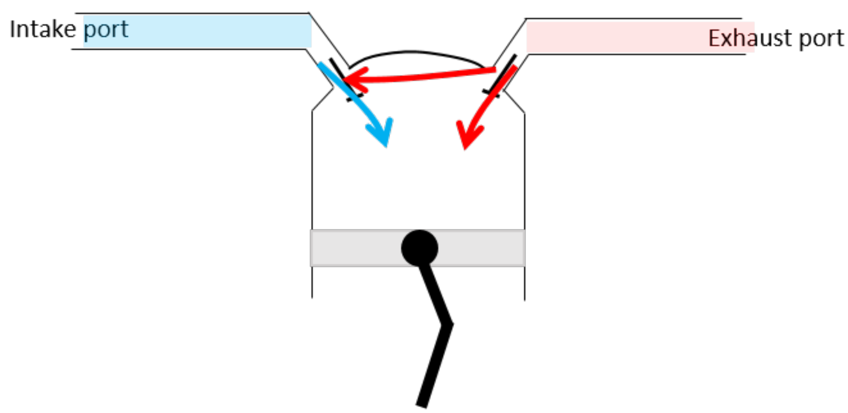

Fig. 6.23. Flows into and out of the cylinder during a reinduction event, where the exhaust valve is opened during the intake stroke. Mass of reinducted exhaust gas is determined by the dynamic interactions between the various flows.

GT-power simulations were utilized to better understand the reduction in exhaust flow rate based on gas flows during the reinduction event by studying instantaneous flows across the valves. Reinduction profiles simulated are shown in Table 6.1. Valve profiles simulated are shown in Figure 6.24. Fresh air flow rate as predicted by GT-power is shown in Figure 6.25 for the above profiles. Note that EVO2 values lower than 390 CAD are not recommended for experimental implementation (due to nominal EVC being 380 CAD, which prevents the valve from closing completely).

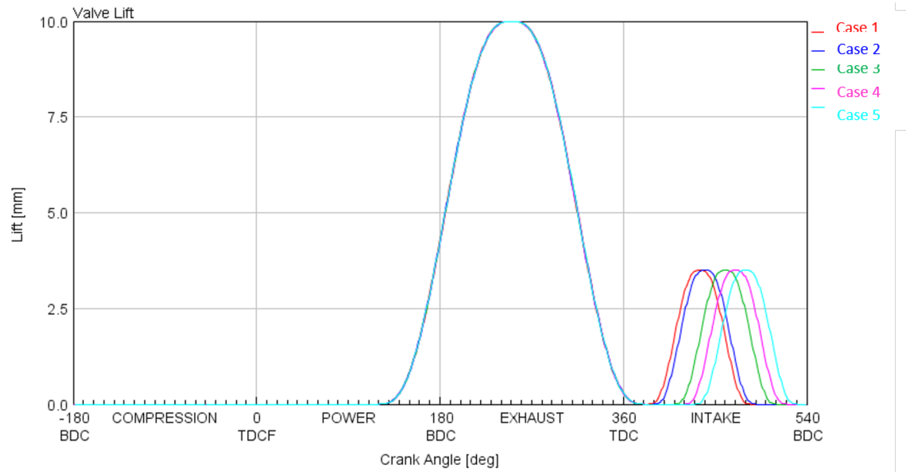

Fig. 6.24. Valve profiles simulated in GT-Power at 800 RPM/1.3 bar BMEP.

The goal of these simulations is to understand gas-exchange behaviour, and hence simulation settings were modulated to enable the simulations to converge without laying as much emphasis on absolute values of fuel consumption, fresh air flow and emissions.

Table 6.1.
Reinduction event phase timings simulated in GT-Power. As a reference, intake valve is open from 340-565 CAD during the intake stroke.

Label	EVO2	EVC2
Case 1	385	485
Case 2	390	490
Case 3	410	510
Case 4	420	520
Case 5	430	530

In order to familiarize with plots of mass flow rate across the intake and exhaust valves, Figure 6.26 can be referred. These results correspond to stock fuel efficient operation. In portion (a), exhaust gases from the exhaust manifold enter the cylinder

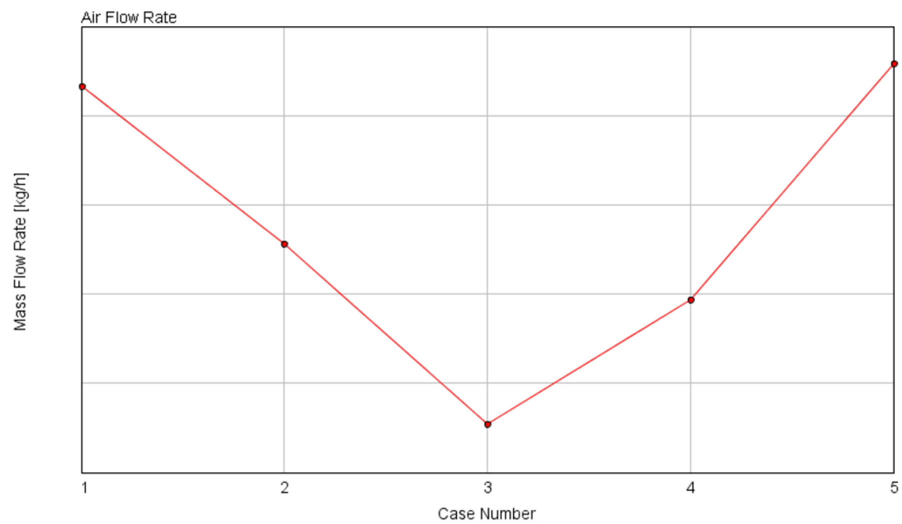

Fig. 6.25. Air flow rate first decreases, then increases as the reinduction profile is phased. Simulation at 800 RPM/1.3 bar BMEP.

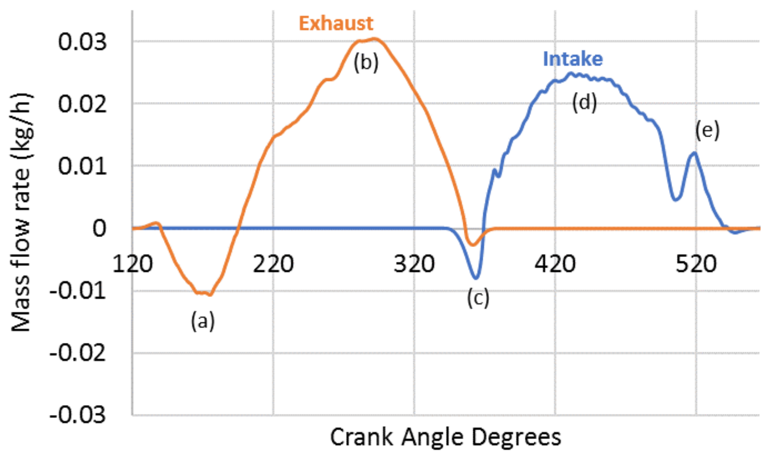

Fig. 6.26. Mass flow rates across the exhaust and intake valves for baseline operation. Simulation at 800 RPM/1.3 bar BMEP.

during the expansion stroke. In portion (b), as the exhaust stroke is underway, combustion products are expelled into the exhaust manifold. During portion (c), where both intake and exhaust valves are open at low lift, some exhaust gases enter the intake manifold via the intake valve (hence the negative flow rate). Intake stroke begins at TDC (or 360 CAD), and during portion (d), charge (fresh air + EGR) flows into the cylinder via the intake valve. This flow rate has a peak value at nearly 445 CAD, which is close to mid-way through the intake stroke (360 CAD to 540 CAD). Although intake valve closes (nominally) at 565 CAD, there is no significant flow through the valve after 540 CAD at this operating condition (mostly unboosted). Next, valve flow rate results for each of the phased reinduction cases (in Table 6.1) are shown.

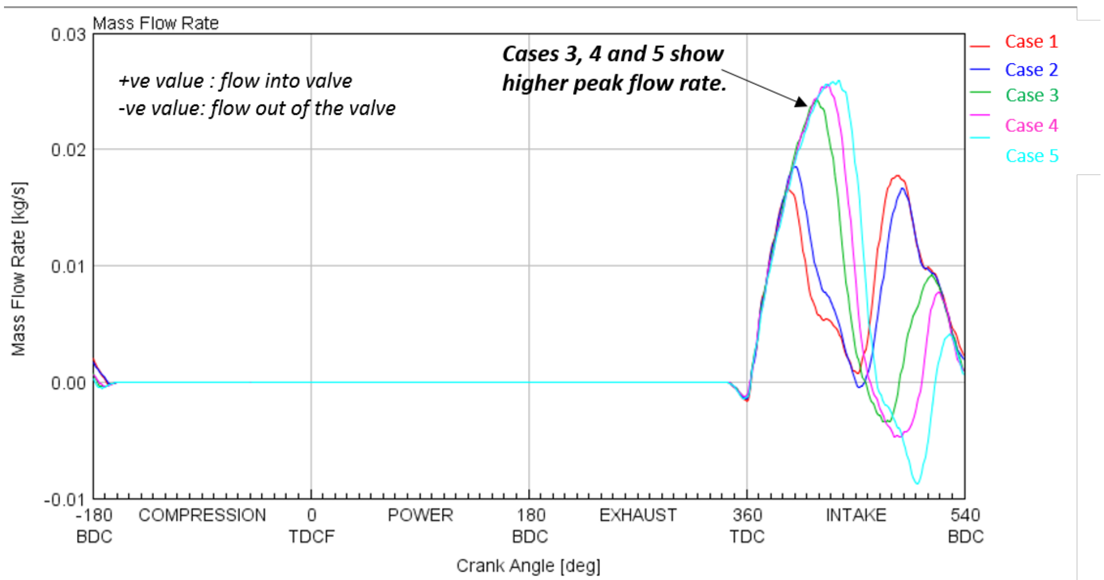

Fig. 6.27. Mass flow rates across the intake valve include positive and negative flows, of both fresh air and reinducted exhaust gas. Simulation at 800 RPM/1.3 bar BMEP.

Mass flow rates across the intake valve for each case are shown in Figure 6.27. A sharp decrease in flow rate across the intake valve is observed at EVO2 (EVO2 values used are stated in Table 6.1). Flow rate drops to near-zero values, then increases again after EVC2. For Cases 1 and 2, only positive values of flow rate across the intake valve are observed, indicating that only fresh air is flowing in from the intake valve, and that the reinducted exhaust gas flows from exhaust manifold to cylinder via the exhaust valve. Cases 3, 4 and 5 show higher peak value of flow rate across the valve - this can be accounted to the fact that the suction created due to the downward motion of the piston becomes weaker after a certain mid-way CAD position as the piston moves downwards. Therefore, with delay in EVO2, the cylinder is drawing charge (fresh air) from the intake manifold for a longer duration, leading to higher fresh air flow rate. These cases also show negative flow rate across the valve for some duration of the reinduction event, which indicates flow back into the intake manifold. This is because the intake and exhaust manifolds are effectively 'shorted' during the reinduction event, and a mixture of fresh air (incoming from the intake manifold) and exhaust gases (from exhaust manifold) flow from exhaust manifold to intake manifold via the cylinder due to difference between pressure.

It is also interesting to note that the magnitude of the 'back-flow' through the intake valve increases with more phasing - this is because the difference between pressure between exhaust manifold and cylinder decreases later on in the intake stroke, while difference between exhaust and intake manifold pressure remains constant; thus causing reinducted exhaust gases to flow into the intake manifold. After EVC2, flow becomes positive again, indicating flow of gases (fresh air + reinducted exhaust gas) back into the cylinder from the intake manifold. It would not be possible at this point to guarantee that all the reinducted gas that flowed back into the intake manifold would re-occupy the cylinder during the final portion of the intake stroke.

Mass flow rates across the exhaust valve for each case are shown in Figure 6.28. An observation can be made from Figure 6.28, i.e. the magnitude of flow rate across the exhaust valve (and hence mass of reinducted gas) is nearly independent of the EVO2 and EVC2 timings, implying that the mass of reinducted gas is a primarily a function of exhaust manifold pressure (and VGT position) at the operating condition of 800 RPM/1.3 bar BMEP. An important conclusion from this study is that a reinduction event earlier on in the intake stroke (preferably in the duration from TDC to mid-stroke) is more effective in obtaining in-cylinder dilution via internal EGR. Delayed reinduction events lead to lower dilution, increase in exhaust flow rate and hence performance that is not desired for fuel efficient stay-warm operation.

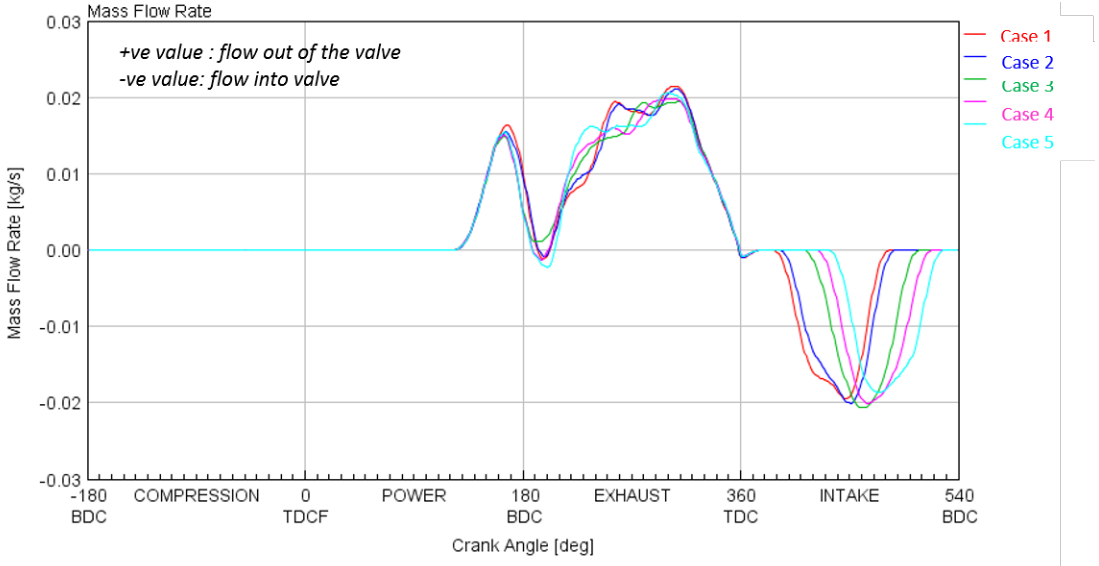

Fig. 6.28. Magnitude of flow rate across the exhaust valve is observed to have small variations with phasing of reinduction profile. Simulation at 800 RPM/1.3 bar BMEP.

6.4 Internal EGR via Negative Valve Overlap

Negative valve overlap (NVO) entails advancing exhaust valve closing time from nominal value such that some amount of exhaust gas can be trapped inside the cylinder. The trapped gas then acts as internal EGR for the next cycle.

Internal EGR via NVO for fuel-efficient aftertreatment system (ATS) stay-warm is studied in this section. Reduction in exhaust flow rate is expected with use of increasing quantities of internal EGR which will lead to lower fuel consumption while keeping a warmed-up ATS at desirable temperatures for a longer duration. Use of internal EGR will also eliminate heat loss to the external EGR cooler, thereby assisting to achieve desirable turbine outlet temperature. Following two parameter sweeps were carried out:

1. Advancing EVC, with and without delayed IVO – Valve profiles used are shown in Figure 6.29. The goal of this study is to discern the effect of advancing EVC with and without delay in IVO, to establish the effect of IVO on the amount

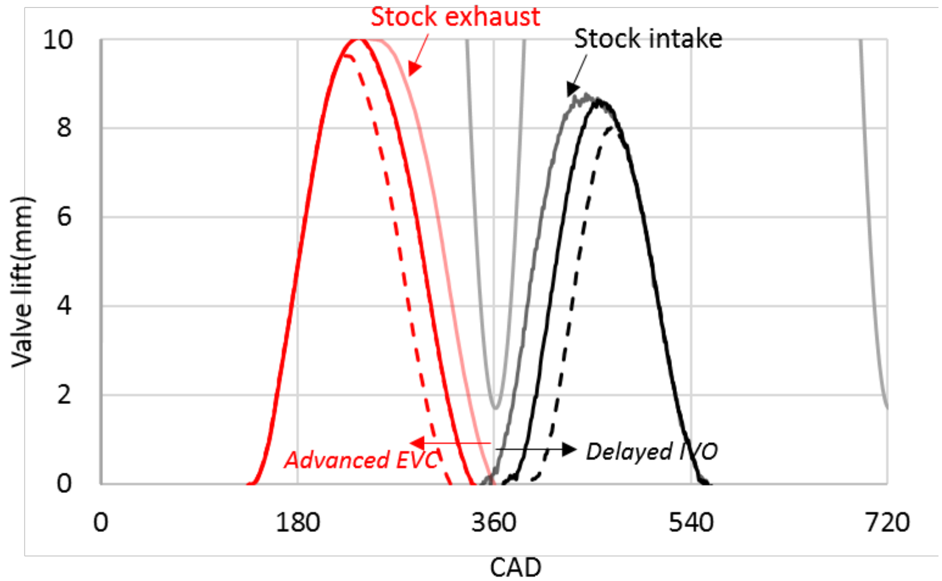

Fig. 6.29. Valve profiles to study effect of advancing EVC with and without delayed IVO for internal EGR via NVO.

of trapped gas and fresh air flow rate. For practical implementation of NVO, this study will provide a basis for design/selection of exhaust and intake valve phasers.

2. Phasing of exhaust and intake profiles – Valve profiles used are shown in Figure 6.30. In this sweep, EVC and IVO are varied by equivalent crank angle degrees i.e. exhaust and intake valves are phased.

Steady state results at 800 RPM/1.3 bar BMEP are discussed next, followed by further analysis of each of the above two parameter sweeps.

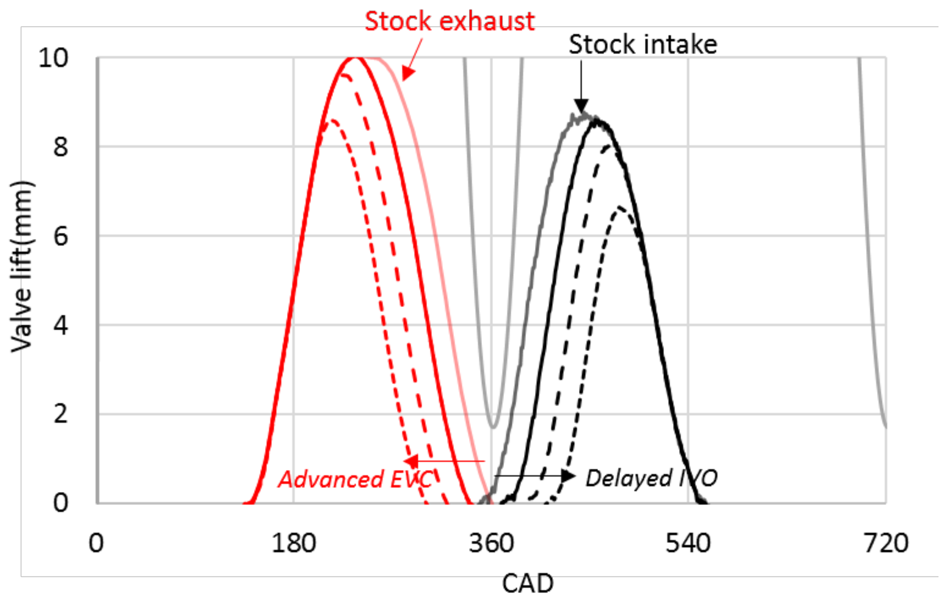

Fig. 6.30. Valve profiles to study effect of cam phasing on iEGR via NVO.

6.4.1 Overall Steady State Results at 800 RPM/1.3 bar BMEP

This section will present a comparison of iEGR via NVO with previously established reference operating modes. Strategies compared include:

(a) *FE 6CF*

(b) *Warm-up 6CF*

(c) *Stay-warm 6CF*

(d) *Stay-warm 3CF*

(e) *iEGR via reinduction* – Best case of reinduction study, corresponding to reinduction event from 410 CAD to 510 CAD, with lift of 5.5 mm. This corresponds to highest TOT achieved with reinduction in this study, along with 3% higher fuel consumption than 'FE 6CF'.

(f) *iEGR via NVO* – Best case of NVO study, with EVC2 = 295 CAD and IVO2 = 425 CAD. These valve timings correspond to the maximum value of TOT seen in the study while targeting similar/lower fuel consumption than 'FE 6CF'.

Steady state cases with iEGR do not use any external EGR. VGT position and rail pressure are modified to obtain the best possible trade-off between TOT and emissions. VGT position for 'iEGR via reinduction' is more restricted than that for 'iEGR via NVO'. Two delayed injections are used in both 'iEGR via Reinduction' and 'iEGR via NVO'. Except for 'Stay-warm 3CF', all other cases correspond to six cylinder operation.

In-cylinder pressure as a function of volume is shown in the PV plot in Figure 6.31. All three cases shown on this plot use equivalent injection timings. Exhaust valve opening and intake valve opening for 'iEGR via NVO' are marked on the plot. Early EVC in 'iEGR via NVO' leads to recompression of trapped exhaust gas, and a rise in in-cylinder pressure after EVC. Due to heat loss, frictional loss and other losses, negative pumping work is incurred during the recompression-expansion process, as indicated by directions of arrows on the PV plot. Comparing the pumping loops for 'iEGR via Reinduction' and 'iEGR via NVO' shows that similar in-cylinder pressure and exhaust manifold pressure towards BDC with 'iEGR via reinduction' yields an advantage in terms of lower pumping work, however, the NVO case incurs additional pumping work after IVO. Therefore, in spite of using a less restricted VGT position, NVO incurs a higher pumping penalty than reinduction.

Figure 6.32 compares TOT, exhaust flow rate, fuel consumption and cycle efficiencies for the different strategies. 'iEGR via NVO' results in nearly 20% higher fuel consumption than 'FE 6CF', and 16% higher fuel consumption than 'iEGR via Reinduction' with 20°C lower TOT, as shown in Figure 6.32(a). 'iEGR via NVO' results in nearly similar exhaust flow rate as 'iEGR via Reinduction', although exhaust flow rate is significantly higher compared to 'Stay-warm 3CF'. In spite of very similar exhaust flow rate, higher TOT is seen with 'iEGR via reinduction' than 'iEGR via NVO' – this is because of larger quantity of iEGR used in reinduction (as shown

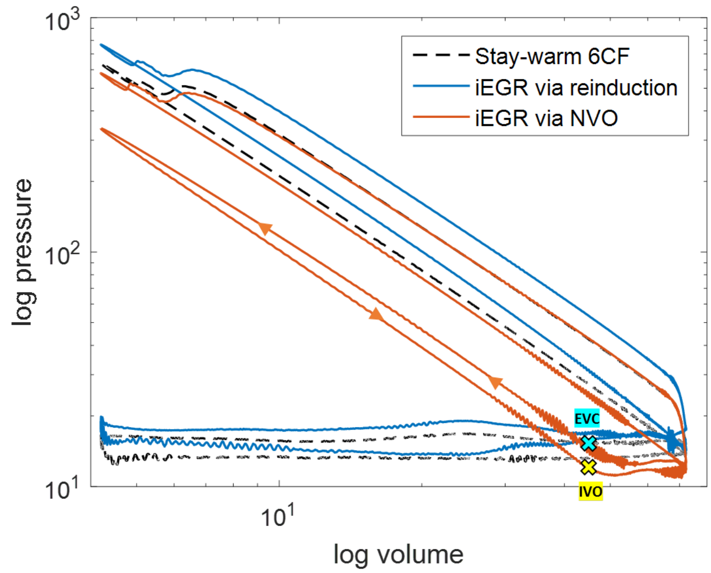

Fig. 6.31. PV diagram comparing two different methods of obtaining internal EGR.

later in the section), which leads to higher charge temperature before and after combustion i.e. heat addition (considering T-s diagram for an ideal diesel cycle) occurs at a higher temperature resulting in higher temperature during isentropic expansion phase. This observation is an instance of increase in TOT due to difference between charge composition rather than air to fuel ratio. Slight differences observed in exhaust flow rate between 'iEGR via Reinduction' and 'iEGR via NVO' are accounted to different amounts of internal EGR obtained, which is mainly influenced by valve positions and VGT position. Trends in OCE, CCE and ME can be used to explain the differences in fuel consumption. Figure 6.32(c) shows reduction in open cycle efficiency for 'iEGR via NVO', this is due to pumping loss associated with recompression of trapped exhaust gas after EVC, as was discussed earlier in context of the PV diagram. Closed cycle efficiency is also lower with use of NVO, this can be accounted to greater in-cylinder heat loss due to use of hotter iEGR. Trapped and recompressed exhaust gas (in case of 'iEGR via NVO') is expected to have higher temperature than exhaust gas which is expelled from the cylinder, comes in contact with cylinder ports (and exhaust manifold walls, thereby losing heat) and is then reinducted back (as in the case of ‘iEGR via Reinduction’). As a note, higher CCE (compared to any other case) with ‘iEGR via Reinduction’ was attributed to a shifted trade-off between effects of higher ratio of specific heats and in-cylinder heat losses on closed cycle efficiency. Figure 6.32(e) shows that mechanical efficiency is nearly similar across the various cases, albeit showing lower values for ‘iEGR via Reinduction’, potentially due to additional piston friction losses associated with reinduction of exhaust gas back into the cylinder.

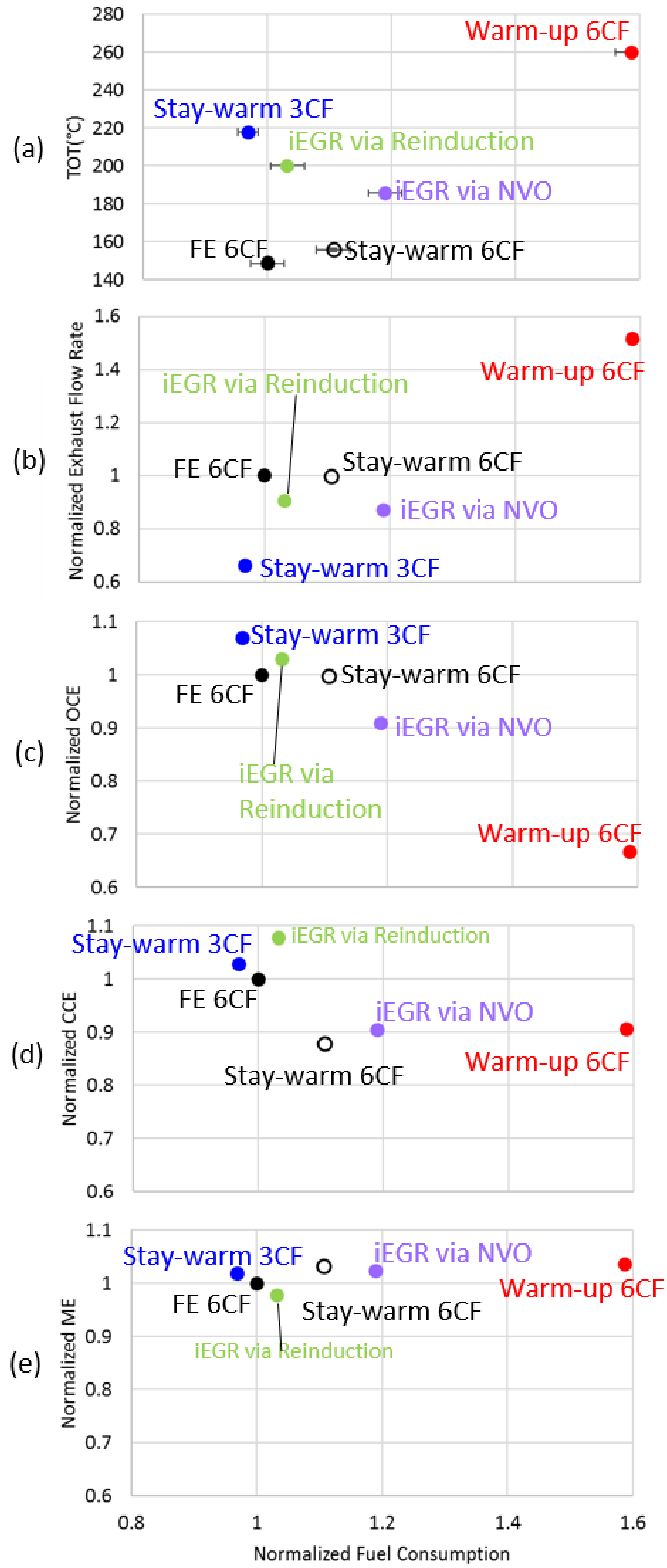

Fig. 6.32. Steady state results at 800 RPM/1.3 bar BMEP comparing iEGR via Reinduction and iEGR via NVO.

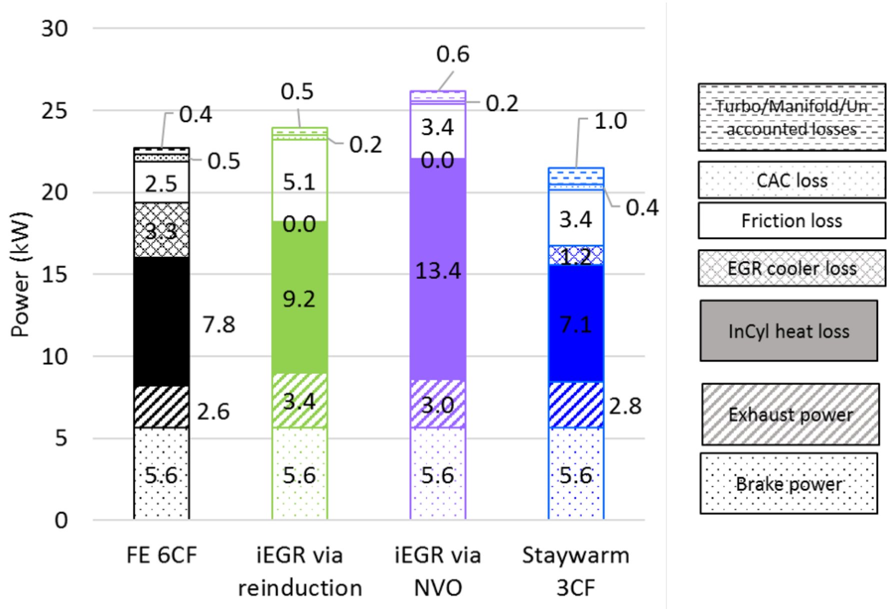

Fig. 6.33. First law analysis to compare distribution of fuel power for iEGR via reinduction and NVO.

Figure 6.33 shows a comparison of distribution of fuel power for 'iEGR via Reinduction', 'iEGR via NVO', 'FE 6CF' and 'Stay-warm 3CF'. Brake power is equal for all cases, due to operation at 800 RPM/1.3 bar BMEP. 'FE 6CF' has lower exhaust power than other cases due to lower TOT. 'iEGR via Reinduction' results in higher exhaust power than 'iEGR via NVO' due to higher TOT, in spite of lower exhaust flow rate. 'Stay-warm 6CF' results in lower exhaust power than the iEGR cases due to significantly lower exhaust flow rate. In-cylinder heat loss is comparable for 'FE 6CF' and 'Stay-warm 3CF', however, cases with iEGR show higher values. This is partly due to use of uncooled EGR, and partly due to heat losses incurred during the recompression event after EVC. As was expected earlier, 'iEGR via NVO' indeed shows higher in-cylinder heat loss than 'iEGR via Reinduction'. This is due to use of hotter iEGR. EGR cooler heat losses are zero in cases where zero external EGR is used. Frictional losses are comparable for 'Stay-warm 3CF' and 'iEGR via NVO', while increasing for 'iEGR via reinduction'.

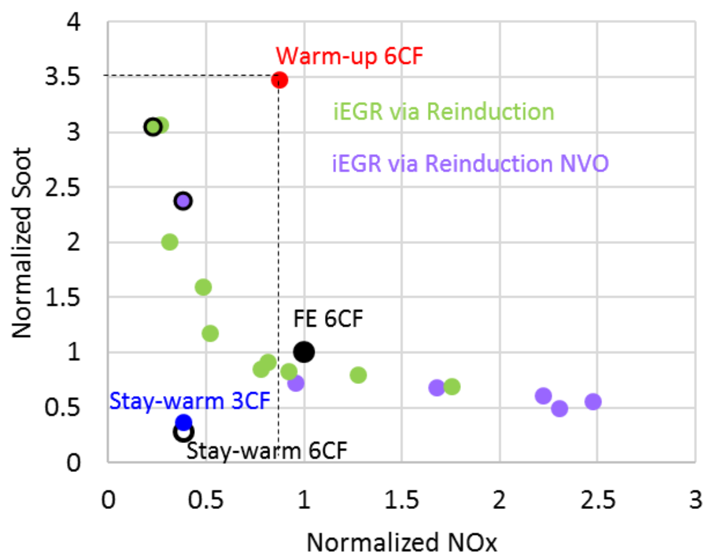

Fig. 6.34. Normalized engine out emissions.

Engine out NOx and soot emissions are shown in Figure 6.34. Note that all data points for both reinduction and NVO are shown, to clearly highlight trade-offs between emissions for each method of obtaining iEGR. Best case reinduction and NVO data points are highlighted as black-outlined symbols. Differences in engine out emissions are primarily attributed to difference between quantity of internal EGR used. Since each of 'iEGR via Reinduction' and 'iEGR via NVO' correspond to screened results for best possible fuel efficient stay-warm operation, it can be concluded that lower engine out NOx is achievable with reinduction, albeit with higher soot. Soot emissions are higher due to lower exhaust flow rate, which leads to lower air to fuel ratio. Lower exhaust flow rate is due to use of relatively larger quantity of internal EGR.

Correlation between NOx emissions and EGR fraction can also be studied from Figure 6.35, which indeed shows higher EGR fraction for 'iEGR via Reinduction'. Internal EGR cases shown here correspond to the best performance cases, which were shown in Figure 6.32. Values in brackets correspond to calculated mass of internal EGR per cylinder. 'iEGR via reinduction' has a greater EGR fraction (by nearly

12%), and results in 30% lower NOx – an observation that can be correlated to the fact that larger fraction of 'colder' iEGR (as in case of 'iEGR via Reinduction') is more effective in NOx reduction than lower quantity of 'hotter' iEGR (as in case of 'iEGR via NVO').

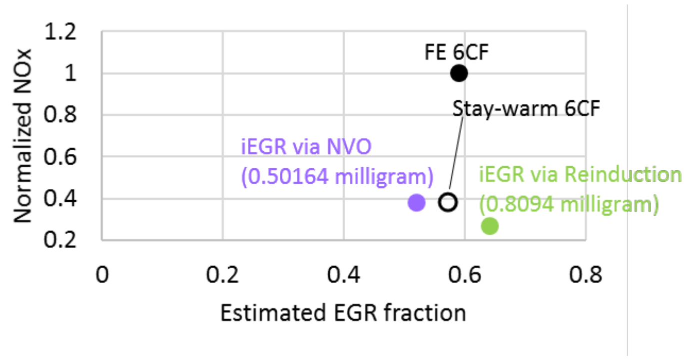

Fig. 6.35. Correlation between computed EGR fraction and engine out NOx for iEGR via Reinduction and NVO.

Another correlation can be drawn between in-cylinder oxygen content and NOx, as seen in Figure 6.36. In-cylinder oxygen content is estimated using the equations and methodology discussed in Chapter 4. Engine out NOx is directly influenced by amount of oxygen present in the pre-combustion charge. This trend is reflected here for both reinduction and NVO with almost exact similarity. In other words, this observation supports the theory that irrespective of nature of obtaining in-cylinder dilution, NOx decreases as in-cylinder oxygen decreases. Another interesting observation is that for same engine out NOx, 'Stay-warm 3CF' has higher in-cyl oxygen content, implying dependence of NOx on other factors such as temperatures during NOx formation by Zeldovich mechanism.

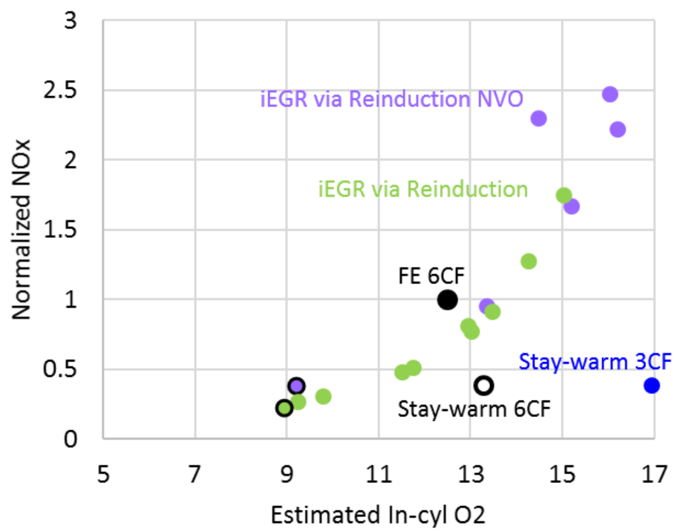

Fig. 6.36. NOx as a function of estimated in-cylinder oxygen.

6.4.2 Results for Achieving NVO by Varying Exhaust Valve Closing With and Without Modulation of Intake Valve Opening Timing

This study aims to validate the hypothesis that IVO has a significant impact on both fuel efficiency and amount of internal EGR obtained for a study of iEGR via NVO. Valve profiles used are shown in Figure 6.29, where two cases of EVC are considered : EVC = 360 CAD and EVC = 340 CAD, with IVO timing held equal to stock value, and delayed for each EVC timing.

The logarithmic PV plot in Figure 6.37 shows that using a nominal IVO timing with advanced EVC results in a large pumping loop during the intake stroke, resulting in decreased open cycle efficiency. This pumping loop is an indicator of the loss in recompression work which was done by the piston on the trapped exhaust gas after EVC. Using delayed IVO along with advanced EVC helps to recover a portion of the recompression work (in spite of heat losses and friction), and is a more fuel-efficient manner to implement NVO. A plot comparing other key performance parameters is shown in Figure 6.38. For the case with EVC = 340, the effect of delayed IVO on fuel efficiency is as hypothesized, i.e. efficiency improves with delayed IVO, primarily

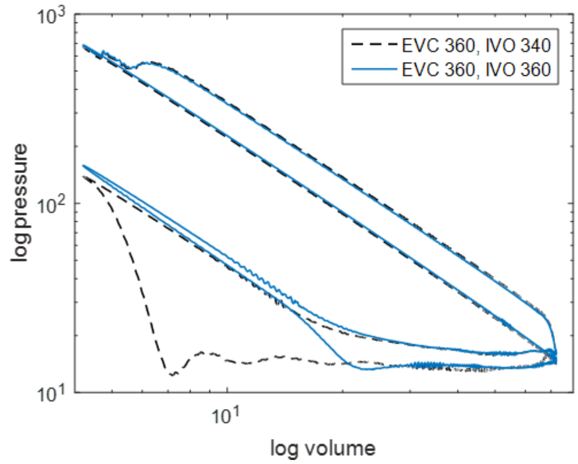

Fig. 6.37. PV diagram comparing effect of IVO timing for a given advanced EVC timing.

due to an improvement in OCE (Figure 6.38(b)). Closed cycle efficiency decreased by a slight value, while mechanical efficiency remained nearly equivalent. However, in the case with EVC = 360, the observed trend in fuel consumption is opposite to expectations based on the hypothesis that delayed IVO can improve fuel efficiency. This is because of an increase in OCE accompanied by decrease in CCE, where the two effects interact to result in lower brake thermal efficiency. As shown in Figure 6.38(b), OCE does improve (as expected), however CCE decreases due to increase in amount of internal EGR (which leads to increased in-cylinder heat loss, delayed heat release). Figure 6.38(e) shows PMEP values for each case, where lower PMEP corresponds to higher open cycle efficiency.

Figure 6.39 establishes the dependence of iEGR quantity on IVO timing. It can be seen that delayed IVO leads to higher trapped EGR mass (at start of combustion). This is a direct impact of the phenomenon that opening the intake valve further away from TDC leads to a stronger 'suction' force, increasing the retainment of the trapped exhaust gas and preventing it from escaping into the intake manifold (without

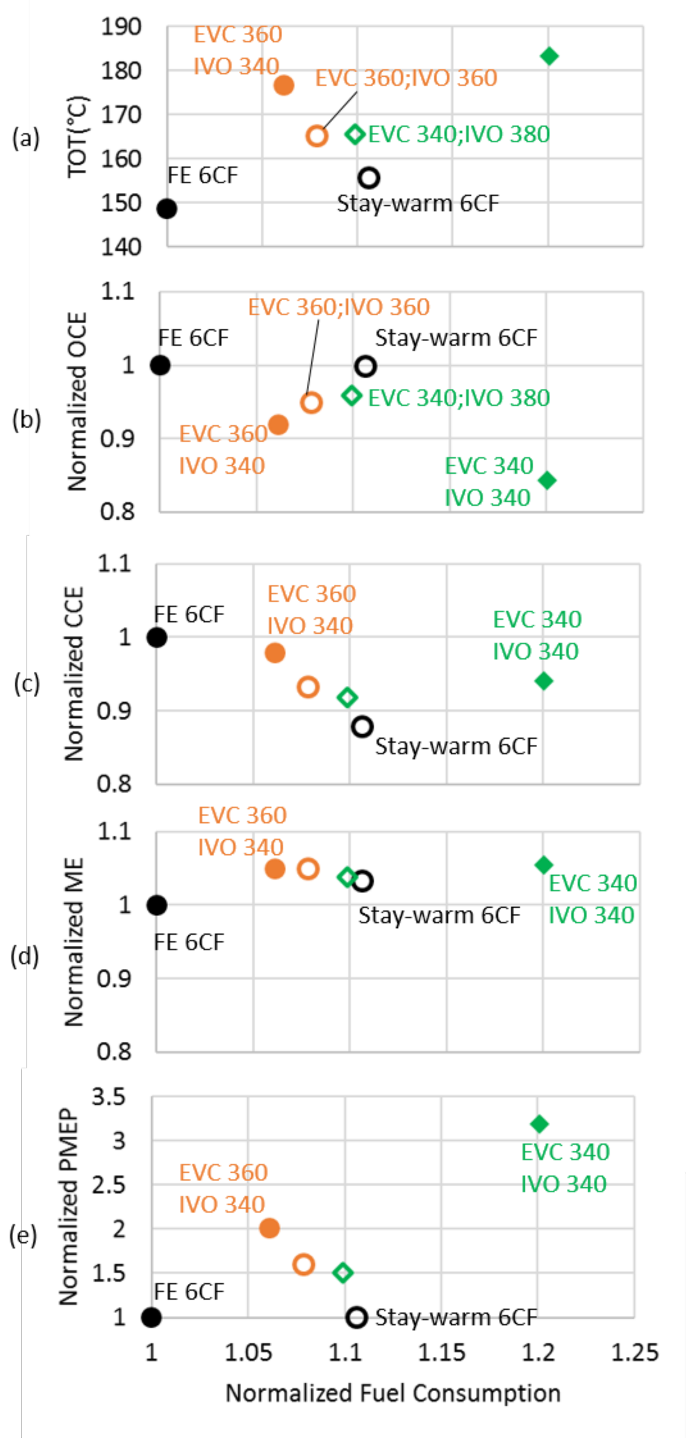

Fig. 6.38. Comparison of key performance parameters for NVO operation with and without delayed IVO.

certainty that the entirety of it will be reintroduced in the cylinder during the intake stroke). Mass of trapped exhaust gas is calculated as follows.

$$m_{trapped\ IVC} = m_{trapped\ iEGR\ at\ EVC} + m_{fresh\ air} \tag{6.7}$$

$$m_{trapped\ iEGR\ at\ EVC} = m_{trapped\ ivc} - m_{fresh\ air} \tag{6.8}$$

where $m_{trapped\ IVC}$ is total mass (exhaust gas as well as fresh air) at IVC, calculated using the ideal gas law and measurements of in-cylinder pressure, volume and intake manifold temperature at IVC; $m_{fresh\ air}$ is the mass of fresh air inducted into a cylinder per cycle, calculated using measurement of LFE; and $m_{trapped\ iEGR\ at\ EVC}$ is the mass of trapped exhaust gas in the cylinder assuming that at EVC, cylinder content is primarily composed of trapped exhaust gas (ignoring small amounts of residue from the previous cycle).

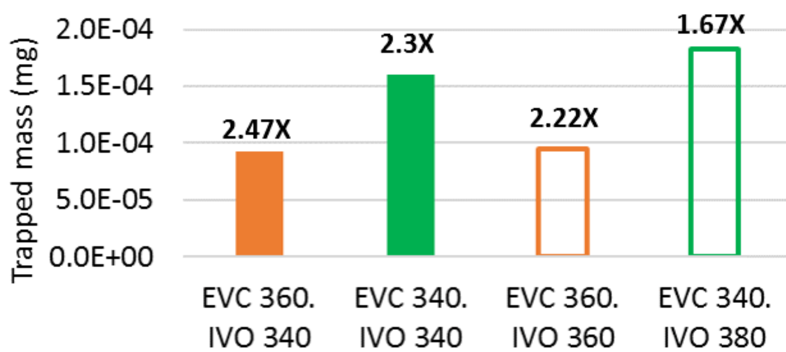

Fig. 6.39. Mass of trapped exhaust gas increases with delayed IVO.

Values displayed above each bar chart in Figure 6.39 show values of engine out NOx normalized by stock fuel efficient operation ('FE 6CF'). NOx decreases as amount of iEGR increases.

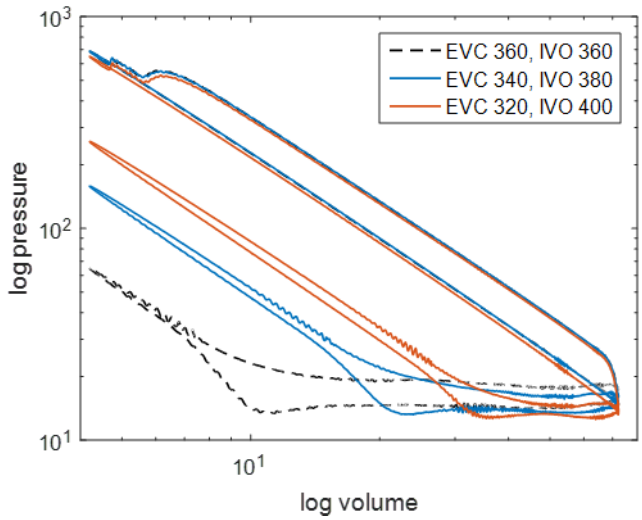

Fig. 6.40. PV diagram comparing effect of phasing of intake and exhaust valves for iEGR via NVO.

6.4.3 Results for Achieving NVO via Variable Intake and Exhaust Valve Phasing

The goal of this study is to establish a trend for fuel consumption, emissions and TOT for iEGR via NVO using cam phasing. This study will present a comparison to the corresponding trends observed with use of iEGR via reinduction. Valve profiles studied are shown in Figure 6.30. Three cases of phased profiles are considered, with both (intake and exhaust) valves phased away from nominal timings by 20 CAD, 40 CAD and 60 CAD. The best case 'iEGR via NVO' is also shown for comparison, which used 85 CAD phasing.

A PV plot for the above cases is shown in Figure 6.40. The closed loop remains significantly similar for the different cases, which is primarily due to use of equivalent injection timings. As EVC is advanced, recompression of a larger amount of trapped exhaust gas occurs, leading to higher in-cylinder pressure. Corresponding delay in IVO assists with decreasing size of the pumping loop (by allowing recovery of recompression work) and with greater retainment of trapped exhaust gas. Figure 6.41 shows the trapped mass as a function of phasing for a cylinder in one cycle, calculated using

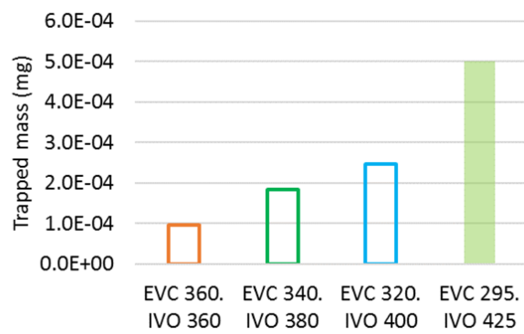

Fig. 6.41. Quantity of trapped exhaust gas for phased intake and exhaust profiles.

Equation 6.7 and Equation 6.8. Quantity of internal EGR increases, as expected, with advanced EVC. Increase in trapped mass quantity appears to be non-linearly varying with phasing. Therefore, smaller changes in intake and exhaust phasing at relatively advanced EVC will lead to greater in-cylinder dilution than larger changes at later EVC timings.

Engine out emissions corresponding to these cases are shown in Figure 6.43. A sharp increase in engine out soot, and a corresponding decrease in NOx is observed, aligning with the trend observed in trapped mass. This plot also indicates that a minimum phasing amount of 60 CAD is required to meet desired emission constraints at 800 RPM/1.3 bar BMEP. Increase in soot is accounted to reduction in air to fuel ratio due to decrease in fresh air flow rate.

Turbine outlet temperature, fuel consumption and cycle efficiency values are shown in Figure 6.42. Fuel consumption increases as the profiles are increasingly phased, in general. This trend corresponds to decrease in closed cycle efficiency as amount of iEGR increases. Open cycle efficiency remains nearly constant, except in the case with 85 CAD where OCE decreases. The cause of this observation is higher PMEP, as seen in Figure 6.42(e). Mechanical efficiency remains nearly equivalent across the different cases.

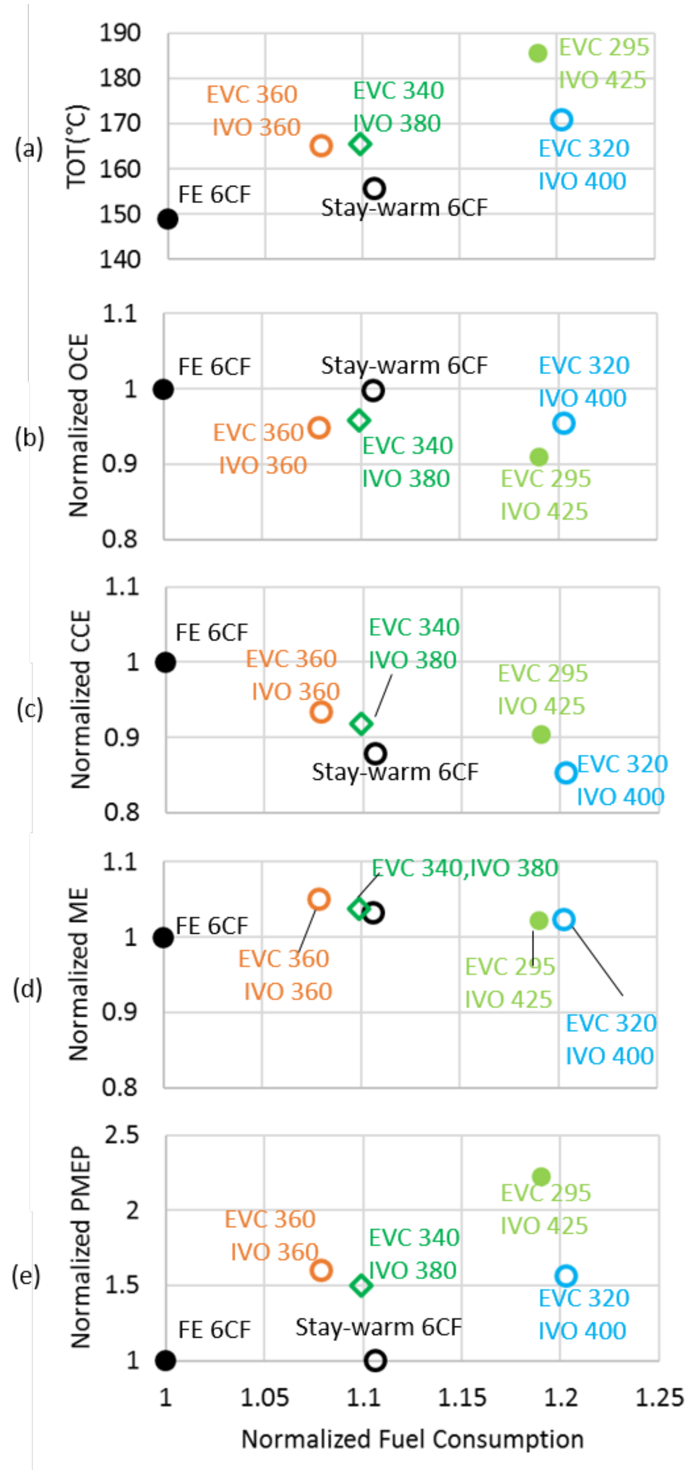

Fig. 6.42. TOT, exhaust flow rate and fuel efficiency for study of phased NVO profiles.

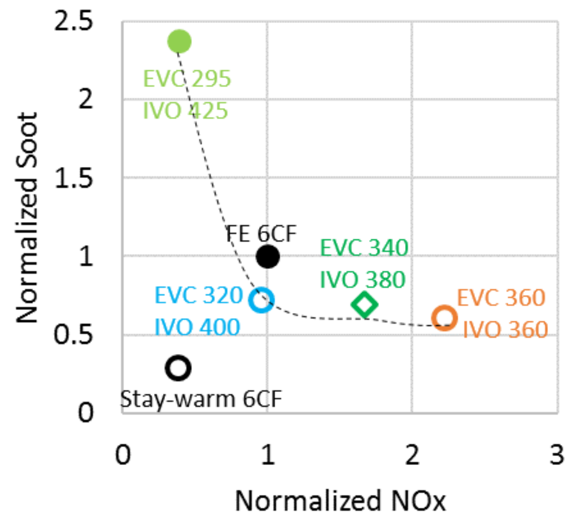

Fig. 6.43. Engine out NOx and soot emissions.

6.5 Summary

This chapter compared two methods of achieving internal EGR i.e. reinduction and negative valve overlap for fuel efficient ATS stay-warm operation at 800 RPM/1.3 bar BMEP. Further parameter sweeps and analysis were carried out for each method to establish relative merits of using certain valve profiles over others. Internal EGR via reinduction was studied by carrying out sweeps of EVC2, lift and reinduction event phase. Internal EGR via NVO was studied by cam phasing and IVO sweep. Key conclusions from this chapter are summarized below, and are also shown in Table 6.2. Figure 6.44 and Figure 6.45 compare the performance of these strategies.

1. Reinduction involves use of colder internal EGR than NVO. Since colder EGR is more effective in NOx control, greater reductions in engine out NOx can be achieved using reinduction than using NVO, for nearly equivalent air to fuel ratio (or soot).

2. Use of reinduction is more fuel efficient at 800 RPM/1.3 bar BMEP. Open cycle efficiency improvements compared to NVO are possible, mainly due to absence

Table 6.2.
Summary of effects of varying different parameters for study of iEGR via NVO and reinduction.

	Negative valve overlap		Reinduction		
Valve profile varied→ / Parameter	*Delayed intake valve opening (for given advanced EVC)*	*Cam phasing*	*Delayed EVC2*	*Increased Lift*	*Phased profile*
iEGR quantity	↑	↑	↑	↑	↓
Fresh air flow	↓	↓	↓	↓	↑
Fuel consumption	↓	↑	↓	↓	↑
Engine out NOx	↓	↓	↓	↓	↑
Engine out soot	↑	↑	↑	↑	↓

of pumping losses associated with recompression in NVO. Closed cycle efficiency improvements were observed, typically at higher levels of internal EGR and this was attributed to higher ratio of specific heats.

3. Internal EGR via reinduction results in better stay-warm performance than internal EGR via NVO, along with improved fuel efficiency. 'Stay-warm 3CF' nevertheless outperforms both 'iEGR via Reinduction' and 'iEGR via NVO' in terms of fuel efficient stay-warm performance, because reductions in exhaust flow rate that are achievable with cylinder deactivation cannot be achieved in six cylinder operation even with use of large amounts of EGR.

4. Internal EGR via reinduction results in more effective increases in in-cylinder dilution for reinduction events prior to mid-stroke rather than afterwards. For constant EVO2 and EVC2, increasing lift has the expected impact of increasing dilution, although sensitivity to lift is largely affected by EVO2 and EVC2. Therefore, it is optimal to place a reinduction event prior to mid-stroke CAD during the intake stroke.

5. Internal EGR via NVO with delayed IVO results in improved fuel efficiency and trapped gas retainment than use of stock (earlier) IVO. Phasing intake and

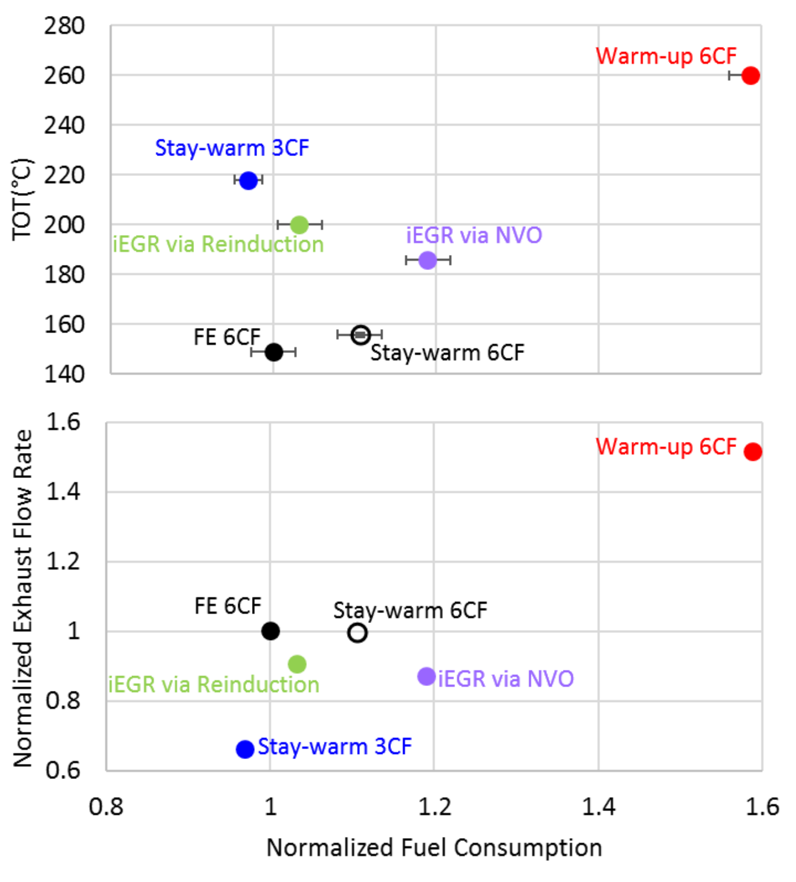

Fig. 6.44. Summary of results: Comparison of TOT, fuel consumption and exhaust flow rate for iEGR via reinduction and iEGR via NVO.

exhaust valves away from each other has an almost parabolic impact on trapped gas quantity, with a minimum of 60 CAD phasing required to achieve desired emission constraints at this particular speed and load.

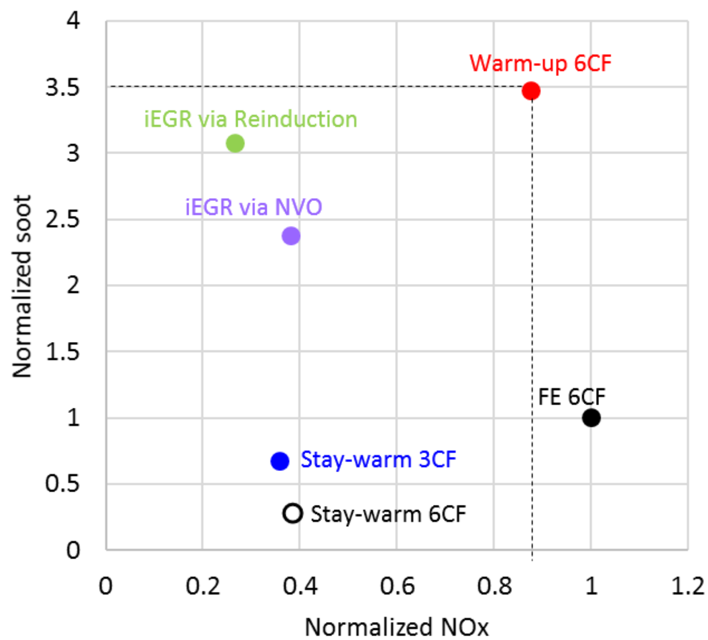

Fig. 6.45. Summary of results: Engine out emissions for iEGR via reinduction and iEGR via NVO.

7. DISSERTATION SUMMARY

Valvetrain flexibility in a modern medium-duty diesel engine has the potential to significantly improve aftertreatment system (ATS) thermal management performance by enabling implementation of non-conventional valve profiles. Primarily through modifications to the gas-exchange process, valvetrain flexibility enables improved fuel economy, lower engine out emissions and other advantages such as simplified air handling architectures. This chapter presents a summary of the work in this dissertation.

Chapter 1 motivated the study of cleaner and fuel efficient medium/heavy duty diesel engines in the backdrop of environmental concerns associated with exhaust emissions from the transportation industry. Chapter 2 described the experimental test-bed, instrumentation and measurement techniques used for the experimental data presented in this work. Data analysis methodologies used throughout this work were discussed.

Chapter 3 demonstrated the ability of exhaust valve modulation to reach exhaust temperatures and flow rates consistent with desired aftertreatment thermal management in the absence of exhaust manifold pressure control, an instance of valvetrain flexibility enabling desired performance with simplified air handling architecture. Late exhaust valve opening with reinduction and early exhaust valve opening with negative valve overlap were studied. When combined with EMP control, LEVO could reach exhaust temperatures greater than 450°C, capable of DPF regen at idle. Chapter 4 presented a study of LEVO operation at off-idle conditions in the absence of EMP control, demonstrating thermal management benefits.

Chapter 5 presented an evaluation of CDA combined with other flexible valvetrain strategies such as LIVC, iEGR and EEVO. These strategies improved fuel-efficient stay-warm operation for ATS thermal management idle and extended idle operation.

Other potential benefits such as reduced dependence on EMP control, use of earlier injections or elimination of external EGR were observed.

Chapter 6 was a study comparing the performance of internal EGR via reinduction and negative valve overlap to establish the reasons for selecting the optimal strategy. Sensitivity of performance and in-cylinder dilution to valve positions and lift was studied by carrying out an analysis of in-cylinder contents. This study also presented an analysis of in-cylinder contents to estimate iEGR fraction.

8. RECOMMENDATIONS FOR FUTURE WORK

Future work for this study could involve the experimental implementation of some novel stay-warm strategies introduced in Chapter 1. These would include on-engine testing of exhaust-stroke based intake re-filling (intake valve is opened during the exhaust stroke) and half-bank variable compression ratio (VCR) operation, where half the cylinders operate with delayed IVC and injections timings, along with large EGR quantities being used. This strategy has been shown (via GT-Power simulations) to possess potential to parallel the performance of the most optimal three cylinder stay-warm operation. VCR across the engine along with ability to run certain cylinders at different air to fuel ratios than others (considering location of cylinders relative to the EGR loop) can be effective in achieving further lower engine out NOx emissions.

For faster aftertreatment warm-up, use of 2 stroke operation with combustion in the 2-stroking cylinders is a potential future step.

Assessment of thermal management performance of the strategies discussed in this document for new advanced aftertreatment systems, such as close-coupled ATS, or SCR on DPF system, or ATS systems with improved low temperature catalyst conversion efficiency will be valuable.

Finally, VVA-controlled gas-exchange behaviours can be studied and applied for engine operation with alternative fuels such as biodiesel and natural gas to improve fuel efficiency, emissions and torque response.

REFERENCES

REFERENCES

[1] NASA, 2017. [Online]. Available: https://climate.nasa.gov/evidence/

[2] EIA, "Annual energy outlook 2018 with projections to 2050," 2018. [Online]. Available: https://www.eia.gov/outlooks/aeo/pdf/AEO2018.pdf

[3] EPA, "Federal register," vol. 76, 2011. [Online]. Available: https://www.gpo.gov/fdsys/pkg/FR-2011-09-15/pdf/2011-20740.pdf

[4] E. P. Agency, "Phase 2 greenhouse gas emissions and fuel efficiency standards for medium and heavy duty engines and vehicles," 2018. [Online]. Available: https://fas.org/sgp/crs/misc/IF10927.pdf

[5] EPA, "Heavy-duty highway compression-ignition engines and urban buses: Exhaust emission standards," 2016. [Online]. Available: https://nepis.epa.gov/Exe/ZyPDF.cgi?Dockey=P100O9ZZ.pdf

[6] S. Charlton, T. Dollmeyer, and T. Grana, "Meeting the us heavy-duty epa 2010 standards and providing increased value for the customer," *SAE International Journal of Commercial Vehicles*, vol. 3, no. 1, pp. 101–110, oct 2010. [Online]. Available: https://doi.org/10.4271/2010-01-1934

[7] W. R. Wade, J. E. White, and J. J. Florek, "Diesel particulate trap regeneration techniques," in *SAE International Congress and Exposition*. SAE International, feb 1981. [Online]. Available: https://doi.org/10.4271/810118

[8] D. J. Stanton, "Systematic development of highly efficient and clean engines to meet future commercial vehicle greenhouse gas regulations," 2013.

[9] M. Koebel, M. Elsener, and M. Kleemann, "Urea-scr: A promising technique to reduce nox emissions from automotive diesel engines," *Catalysis Today*, vol. 59, pp. 335–345, 06 2000.

[10] J. Girard, G. Cavataio, R. Snow, and C. Lambert, "Combined fe-cu scr systems with optimized ammonia to nox ratio for diesel nox control," *SAE International Journal of Fuels and Lubricants*, vol. 1, no. 1, pp. 603–610, apr 2008. [Online]. Available: https://doi.org/10.4271/2008-01-1185

[11] D. A. Pierpont and R. D. Reitz, "Effects of injection pressure and nozzle geometry on d.i. diesel emissions and performance," *SAE Transactions*, vol. 104, pp. 1041–1050, 1995. [Online]. Available: http://www.jstor.org/stable/44633277

[12] E. Mancaruso, S. S. Merola, and B. M. Vaglieco, "Study of the multi-injection combustion process in a transparent direct injection common rail diesel engine by means of optical techniques," *International Journal of Engine Research*, vol. 9, no. 6, pp. 483–498, 2008. [Online]. Available: https://doi.org/10.1243/14680874JER01308

[13] M. Dürnholz, G. Eifler, and H. Endres, "Exhaust-gas recirculation - a measure to reduce exhaust emissions of di diesel engines," in *International Congress & Exposition*. SAE International, feb 1992. [Online]. Available: https://doi.org/10.4271/920725

[14] Z. Han, A. Uludogan, G. J. Hampson, and R. D. Reitz, "Mechanism of soot and nox emission reduction using multiple-injection in a diesel engine," in *International Congress & Exposition*. SAE International, feb 1996. [Online]. Available: https://doi.org/10.4271/960633

[15] O. Maiwald, R. Brück, S. Rohrer, M. Zaki, A. Schatz, and F. Atzler, "Optimised diesel combustion and scr exhaust aftertreatment combined with a 48 v system for lowest emissions and fuel consumption in rde," *25th Aachen Colloquium Automobile and Engine Technology*, 2010. [Online]. Available: {http://www.emitec.com/fileadmin/user_upload/Presse/Paper_Vortraege/2016_Aachen_Conti_Super_Clean_Diesel_V10.pdf}

[16] Cummins, "Cummins unveils the future of diesel with low nox and low co2 emissions technology during iaa commercial vehicles show." [Online]. Available: https://www.cummins.com/news/releases/2018/09/19/cummins-unveils-future-diesel-low-nox-and-low-co2-emissions-technology

[17] M. Sellnau, "Advancement of gasoline direct injection compression ignition (gdci) for high efficiency and us tier3 emissions," *ERC2017, University of Wisconsin*, 2017.

[18] D. B. Gosala, A. K. Ramesh, C. M. Allen, M. C. Joshi, A. H. Taylor, M. V. Voorhis, G. M. Shaver, L. Farrell, E. Koeberlein, J. James McCarthy, and D. Stretch, "Diesel engine aftertreatment warm-up through early exhaust valve opening and internal exhaust gas recirculation during idle operation," *International Journal of Engine Research*, vol. 19, no. 7, pp. 758–773, 2018. [Online]. Available: https://doi.org/10.1177/1468087417730240

[19] L. Roberts, M. Magee, G. Shaver, A. Garg, J. McCarthy, E. Koeberlein, E. Holloway, R. Shute, D. Koeberlein, and D. Nielsen, "Modeling the impact of early exhaust valve opening on exhaust aftertreatment thermal management and efficiency for compression ignition engines," *International Journal of Engine Research*, vol. 16, no. 6, pp. 773–794, 2015. [Online]. Available: https://doi.org/10.1177/1468087414551616

[20] R. G. Silver, T. Paulson, and J. Martin, "Scr on filter based aftertreatment for high efficiency engine systems." [Online]. Available: https://www.erc.wisc.edu/documents/symp17/2010_Cat_Paulson.pdf

[21] James McCarthy Jr., "Driving automotive innovation - cylinder deactivation." [Online]. Available: https://www.theicct.org/sites/default/files/Panel20120-20Jim20McCarthy_Cyl20Deac.pdf

[22] J.-P. Zammit, M. J. McGhee, P. J. Shayler, and I. Pegg, "The influence of cylinder deactivation on the emissions and fuel economy of a four-cylinder direct-injection diesel engine," *Proceedings of the Institution of Mechanical Engineers, Part D: Journal of Automobile Engineering*, vol. 228, no. 2, pp. 206–217, 2014. [Online]. Available: https://doi.org/10.1177/0954407013506182

[23] S. Gehrke, D. Kovács, P. Eilts, A. Rempel, and P. Eckert, "Investigation of vva-based exhaust management strategies by means of a hd single cylinder research engine and rapid prototyping systems," *SAE International Journal of Commercial Vehicles*, vol. 6, no. 1, pp. 47–61, apr 2013. [Online]. Available: https://doi.org/10.4271/2013-01-0587

[24] A. Mayer, T. Lutz, C. Lämmle, M. Wyser, and F. Legerer, "Engine intake throttling for active regeneration of diesel particle filters," in *SAE 2003 World Congress & Exhibition*. SAE International, mar 2003. [Online]. Available: https://doi.org/10.4271/2003-01-0381

[25] J. Zammit, M. McGhee, P. Shayler, T. Law, and I. Pegg, "The effects of early inlet valve closing and cylinder disablement on fuel economy and emissions of a direct injection diesel engine," *Energy*, vol. 79, pp. 100 – 110, 2015. [Online]. Available: http://www.sciencedirect.com/science/article/pii/S0360544214012158

[26] A. Garg, M. Magee, C. Ding, L. Roberts, G. Shaver, E. Koeberlein, R. Shute, D. Koeberlein, J. James McCarthy, and D. Nielsen, "Fuel-efficient exhaust thermal management using cylinder throttling via intake valve closing timing modulation," *Proceedings of the Institution of Mechanical Engineers, Part D: Journal of Automobile Engineering*, vol. 230, no. 4, pp. 470–478, 2016. [Online]. Available: https://doi.org/10.1177/0954407015586896

[27] U. S. D. of Energy", "Idle reduction." [Online]. Available: https://afdc.energy.gov/conserve/idle_reduction_basics.html

[28] T. L. Linda Gaines, "Idling: Cruising the fuel inefficiency expressway," *DOE*, 2009.

[29] B. T. Incropera. P., DeWitt. D. and L. A, *Fundamentals of Heat and Mass Transfer*. John Wiley and Sons, 2007.

[30] B. A. Makartchouk, A. and A. Lack, "Exhaust throttle valve system and method for diesel particulate filter regeneration," 2011, uS Patent, US20110252765A1. [Online]. Available: https://patentimages.storage.googleapis.com/98/e1/6d/771817bd7ca1c3/US20110252765A1.pdf

[31] G. B. Parvate-Patil, H. Hong, and B. Gordon, "An assessment of intake and exhaust philosophies for variable valve timing," *SAE Transactions*, vol. 112, pp. 2174–2189, 2003. [Online]. Available: http://www.jstor.org/stable/44741433

[32] "Method and system for engine braking in an internal combustion engine using a stroke limited high pressure engine brake," Patent, 2005. [Online]. Available: https://patentimages.storage.googleapis.com/07/18/a2/2a00931eb4c385/US6866017.pdf

[33] T. Dollmeyer, J. Rumsey, L. Brackney, and L. LaPointe, "Method for controlling turbine outlet temperatures in a diesel engine at idle and light load conditions," 2007, uS Patent, US20070186538A1. [Online]. Available: https://patents.google.com/patent/US20070186538A1/en

[34] C. A. R. Board, "Heavy-duty vehicle idling emission reduction program." [Online]. Available: https://ww3.arb.ca.gov/msprog/truck-idling/truck-idling.htm

[35] [Online]. Available: https://www.dieselnet.com/standards/cycles/avl_8mode.php

[36] [Online]. Available: https://www.dieselnet.com/standards/cycles/nte.phphd

[37] [Online]. Available: https://www.law.cornell.edu/cfr/text/40/86.1370

[38] T. G. Leone and M. Pozar, "Fuel economy benefit of cylinder deactivation - sensitivity to vehicle application and operating constraints," in *SAE International Fall Fuels & Lubricants Meeting & Exhibition*. SAE International, sep 2001. [Online]. Available: https://doi.org/10.4271/2001-01-3591

[39] A. Falkowski, M. McElwee, and M. Bonne, "Design and development of the daimlerchrysler 5.7l hemi® engine multi-displacement cylinder deactivation system," in *Non-Conference Specific Technical Papers - 2004*. SAE International, may 2004. [Online]. Available: https://doi.org/10.4271/2004-01-2106

[40] C. Kuruppu, A. Pesiridis, and S. Rajoo, "Investigation of cylinder deactivation and variable valve actuation on gasoline engine performance," in *SAE 2014 World Congress & Exhibition*. SAE International, apr 2014. [Online]. Available: https://doi.org/10.4271/2014-01-1170

[41] C. Ding, L. Roberts, D. J. Fain, A. K. Ramesh, G. M. Shaver, J. James McCarthy, M. Ruth, E. Koeberlein, E. A. Holloway, and D. Nielsen, "Fuel efficient exhaust thermal management for compression ignition engines during idle via cylinder deactivation and flexible valve actuation," *International Journal of Engine Research*, vol. 17, no. 6, pp. 619–630, 2016. [Online]. Available: https://doi.org/10.1177/1468087415597413

[42] X. Lu, C. Ding, A. K. Ramesh, G. M. Shaver, E. Holloway, J. McCarthy, M. Ruth, E. Koeberlein, and D. Nielsen, "Impact of cylinder deactivation on active diesel particulate filter regeneration at highway cruise conditions," *Frontiers in Mechanical Engineering*, vol. 1, p. 9, 2015. [Online]. Available: https://www.frontiersin.org/article/10.3389/fmech.2015.00009

[43] D. B. Gosala, C. M. Allen, A. K. Ramesh, G. M. Shaver, J. James McCarthy, D. Stretch, E. Koeberlein, and L. Farrell, "Cylinder deactivation during dynamic diesel engine operation," *International Journal of Engine Research*, vol. 18, no. 10, pp. 991–1004, 2017. [Online]. Available: https://doi.org/10.1177/1468087417694000

[44] M. C. Joshi, D. B. Gosala, C. M. Allen, K. Vos, M. Van Voorhis, A. Taylor, G. M. Shaver, J. McCarthy, D. Stretch, E. Koeberlein, and L. Farrell, "Reducing diesel engine drive cycle fuel consumption through use of cylinder deactivation to maintain aftertreatment component temperature during idle and low load operating conditions," *Frontiers in Mechanical Engineering*, vol. 3, p. 8, 2017. [Online]. Available: https://www.frontiersin.org/article/10.3389/fmech.2017.00008

[45] Diesel˙Net, "Variable geomtery turbochargers." [Online]. Available: https://www.dieselnet.com/tech/air_turbo_vgt.php

[46] Cambustion, "Ndir 500 fast co and co2 analyzer." [Online]. Available: https://www.cambustion.com/products/ndir500

[47] S. Russ and R. Stein, "Engine control strategy using dual equal cam phasing combined with exhaust gas recirculation," 2000, US Patent, US6321731B1. [Online]. Available: https://patentimages.storage.googleapis.com/ad/27/3a/de6d0f1bd0c30c/US6321731.pdf

[48] C. Sellanu, M and P. Dingle, "Method and apparatus for combustion optimization in an ic engine utilizing hcci and vva," 2006, US Patent, US2006/0144356A1. [Online]. Available: https://patentimages.storage.googleapis.com/1c/25/22/675d7e77ba5f83/US20060144356A1.pdf

[49] P. A. Caton, H. H. Song, N. B. Kaahaaina, and C. F. Edwards, "Strategies for achieving residual-effected homogeneous charge compression ignition using variable valve actuation," *SAE Transactions*, vol. 114, pp. 364–381, 2005. [Online]. Available: http://www.jstor.org/stable/44722007

[50] A. M. Kulkarni, G. H. Adi, and G. M. Shaver, "Modeling Cylinder-to-Cylinder Coupling in Multi-Cylinder HCCI Engines Incorporating Reinduction," vol. Volume 9: Mechanical Systems and Control, Parts A, B, and C, pp. 1597–1604, 11 2007. [Online]. Available: https://doi.org/10.1115/IMECE2007-42487

[51] N. B. Kaahaaina, A. J. Simon, P. A. Caton, and C. F. Edwards, "Use of dynamic valving to achieve residual-affected combustion," *SAE Transactions*, vol. 110, pp. 508–519, 2001. [Online]. Available: http://www.jstor.org/stable/44724326

[52] G. M. Shaver, J. C. Gerdes, and M. J. Roelle, "Physics-based modeling and control of residual-affected hcci engines," *Journal of Dynamic Systems, Measurement, and Control*, 2013. [Online]. Available: https://pdfs.semanticscholar.org/72ee/753a37c211928a47f7d4c3c97aeea5b988e3.pdf

[53] J. F. Rodriguez and W. K. Cheng, "Reduction of cold-start emissions through valve timing in a gdi engine," *SAE International Journal of Engines*, vol. 9, no. 2, pp. 1220–1229, 2016. [Online]. Available: http://www.jstor.org/stable/26284891

[54] "Engine warm-up of a hcci engine," Patent, 2010. [Online]. Available: https://patentimages.storage.googleapis.com/4a/32/97/33b6dcae3b483f/US7684925.pdf

[55] J. F. Rodriguez and W. K. Cheng, "Analysis of nox emissions during crank-start and cold fast-idle in a gdi engine," *SAE International Journal of Engines*, vol. 10, no. 2, pp. 646–655, 2017. [Online]. Available: https://www.jstor.org/stable/26285073

[56] G. Almkvist, H. Sandguist, and H. Hakansson, "Method of reducing exhaus gas emissions during cold start conditions and an internal combustion engine in which the method is used," Patent, 2006. [Online]. Available: https://patentimages.storage.googleapis.com/c1/2c/a3/2161bcc188983d/US7124734.pdf

[57] R. R. Steeper and M. L. Davisson, "Analysis of gasoline negative-valve-overlap fueling via dump sampling." 10 2013. [Online]. Available: https://www.osti.gov/servlets/purl/1095938

[58] B. Kinkhabwala, S. S, A. Raaj, K. Sadagopan, and S. Pandey, "Feasibility of employing negative valve overlap for enhanced charge homogeneity in pcci diesel engine using 1d thermodynamic simulation and 3d cfd study," in *Symposium on International Automotive Technology 2019*. SAE International, jan 2019. [Online]. Available: https://doi.org/10.4271/2019-26-0135

[59] M. Mikulski, P. R. Balakrishnan, and J. Hunicz, "Natural gas-diesel reactivity controlled compression ignition with negative valve overlap and in-cylinder fuel reforming," *Applied Energy*, vol. 254, p. 113638, 2019. [Online]. Available: http://www.sciencedirect.com/science/article/pii/S030626191931325X

[60] H. K. H. T. H. C. Kohei Kuzuoka, Takashi Kondo and K. Hashimoto, "Controlling combustion with negative valve overlap in a gasoline-diesel dual fuel compression ignition engine," *International Journal of Engine Research*, vol. 17, no. 3, pp. 354–365, 2019. [Online]. Available: https://journals.sagepub.com/doi/pdf/10.1177/1468087415580216

[61] L. Shi, K. Deng, Y. Cui, S. Qu, and W. Hu, "Study on knocking combustion in a diesel hcci engine with fuel injection in negative valve overlap," *Fuel*, vol. 106, pp. 478 – 483, 2013. [Online]. Available: http://www.sciencedirect.com/science/article/pii/S001623611200868X

[62] L. Shi, K. Deng, and Y. Cui, "Study of diesel-fuelled homogeneous charge compression ignition combustion by in-cylinder early fuel injection and negative valve overlap," *Proceedings of the Institution of Mechanical Engineers, Part D: Journal of Automobile Engineering*, vol. 219, no. 10, pp. 1193–1201, 2005. [Online]. Available: https://doi.org/10.1243/095440705X34847

[63] J. Schwoerer, S. Dodi, M. Fox, S. Huang, and Z. Yang, "Internal egr systems for nox emission reduction in heavy-duty diesel engines," mar 2004. [Online]. Available: https://doi.org/10.4271/2004-01-1315

[64] A. K. Ramesh, T. E. Odstrcil, D. B. Gosala, G. M. Shaver, S. Nayyar, E. Koeberlein, and J. James McCarthy, "Reverse breathing in diesel engines for aftertreatment thermal management," *International Journal of Engine Research*, vol. 20, no. 8-9, pp. 862–876, 2019. [Online]. Available: https://doi.org/10.1177/1468087418783118

[65] C. A. R. Board, "Carb staff current assessment of the technical feasibility of lower nox standards and associated test procedures for 2022 and subsequent model year." [Online]. Available: https://ww3.arb.ca.gov/msprog/hdlownox/white_paper_04182019a.pdf

[66] M. J. Lance, Z. G. Mills, J. C. Seylar, J. M. E. Storey, and C. S. Sluder, "The effect of engine operating conditions on exhaust gas recirculation cooler fouling," *International Journal of Heat and Mass Transfer*, vol. 126, 5 2018.

[67] S.-H. Jang, S.-J. Hwang, S.-K. Park, K.-S. Choi, and H.-M. Kim, "Effects of pm fouling on the heat exchange effectiveness of wave fin type egr cooler for diesel engine use," *Heat and Mass Transfer*, vol. 48, no. 6, pp. 1081–1087, Jun 2012. [Online]. Available: https://doi.org/10.1007/s00231-011-0950-1

[68] J. B. Heywood, *Internal Combustion Engine Fundamentals*. McGraw Hill, 1988.

VITA

VITA

Education

Ph.D., Mechanical Engineering *May 2020*

Purdue University, West Lafayette, IN

Dissertation: Opportunities to improve aftertreatment thermal management and simplify the air handling architectures of highly efficient diesel engines incorporating valvetrain flexibility.

MS, Mechanical Engineering *August 2017*

Purdue University, West Lafayette, IN

Thesis: Diesel engine cylinder deactivation for improved system efficiency while maintaining elevated aftertreatment temperatures.

B.E., Electronics and Telecommunication *August 2015*

Cummins College of Engineering for Women (University of Pune), India

Project: Compact battery health monitoring system.

Employment

Research assistant, Herrick Labs (August 2015 – December 2019)

Powertrain Modeling Intern, Tesla (June 2019 – August 2019)

Teaching assistant, ME540 (Internal Combustion Engines) (August 2018 – December 2018)

CPE intern, Cummins Inc. (May 2016 – July 2016)

Electronics group intern, Cummins India Ltd. (May 2014 – June 2014)

Achievements

Invited panelist - Powertrain, SAE COMVEC, Indianapolis, September 2019

SAE John Johnson award for Outstanding Research in Diesel Engines, 2018

Cummins - Purdue Fellowship, 2015

Publications

- **Mrunal Joshi**, Dheeraj B Gosala, Cody M Allen, Kalen Vos, Matthew VanVoorhis, Alexander Taylor, Gregory M Shaver, James McCarthy, Jr., Dale Stretch, Edward Koeberlein and Lisa Farrell, **Reducing Diesel Engine Drive Cycle Fuel Consumption through Use of Cylinder Deactivation to Maintain Aftertreatment Component Temperature During Idle and Low Load Operating Conditions**, Frontiers In Mechanical Engineering, 2017
- Dheeraj B Gosala, Aswin K Ramesh, Cody M Allen, **Mrunal C Joshi**, Alexander H Taylor, Matthew VanVoorhis, Gregory M Shaver, Lisa Farrell, Edward Koeberlein, James McCarthy Jr. and Dale Stretch, **Diesel engine aftertreatment warm-up through early exhaust valve opening and internal exhaust gas recirculation during idle operation**, International Journal of Engine Research, 2017
- **Mrunal Joshi**, Dheeraj B Gosala, Cody M Allen, Sirish Srinivasan, Matthew VanVoorhis, Alexander Taylor, Kalen Vos, Gregory Shaver, James McCarthy, Jr., Lisa Farrell and Edward Koeberlein, **Diesel Engine Cylinder Deactivation for Improved System Performance over Transient Real World Drive Cycles**, SAE Technical Paper 2018-01-0880, 2018
- Aswin K Ramesh, Dheeraj B Gosala, Cody M Allen, **Mrunal Joshi**, Lisa Farrell, Edward Koeberlein, James McCarthy, Jr. and Gregory M Shaver, **Cylinder Deactivation for Increased Engine Efficiency and Aftertreatment Thermal Management in Diesel Engines**, SAE Technical Paper 2018-01-0384, 2018
- Cody M Allen, **Mrunal C Joshi**, Dheeraj B Gosala, Gregory M Shaver, Lisa Farrell, James McCarthy, Jr., **Experimental assessment of diesel engine**

cylinder deactivation performance during low-load transient operations, IJER 2019

- Kalen Vos, Gregory M Shaver, **Mrunal Joshi**, James McCarthy, Jr., **Implementing Variable Valve Actuation on a Diesel Engine at High-Speed Idle Operation for Improved Aftertreatment Warm-Up**, IJER 2019
- Kalen Vos, Aswin K Ramesh, Gregory M Shaver, **Mrunal Joshi**, James McCarthy, Jr., **Strategies for Using Valvetrain Flexibility Instead of Exhaust Manifold Pressure Modulation for Diesel Engine Gas Exchange and Thermal Management Control**, IJER, 2019
- **Mrunal C Joshi**, Dheeraj B Gosala, Gregory M Shaver, James McCarthy, Jr. and Lisa Farrell, **Exhaust valve profile modulation for improved diesel engine curb idle aftertreatment thermal management**, under review by sponsors, 2019
- **Mrunal C Joshi**, Gregory M Shaver, James McCarthy, Jr. and Lisa Farrell, **Comparison of internal exhaust gas recirculation via reinduction and negative valve overlap for fuel-efficient aftertreatment thermal management at idle in a diesel engine**, in process, 2019